

Towards real-world biomechanical analysis of performance and functional capacity using wearable sensors

Présentée le 27 octobre 2022

Faculté des sciences et techniques de l'ingénieur
Laboratoire de mesure et d'analyse des mouvements
Programme doctoral en robotique, contrôle et systèmes intelligents

pour l'obtention du grade de Docteur ès Sciences

par

Salil APTE

Acceptée sur proposition du jury

Prof. A. M. Alahi, président du jury
Prof. K. Aminian, Prof. V. Gremeaux, directeurs de thèse
Prof. B. Eskofier, rapporteur
Prof. P. Bonato, rapporteur
Dr S. Lorenzetti, rapporteur

As you prepare your breakfast, think of others
(do not forget the pigeon's food).
As you conduct your wars, think of others
(do not forget those who seek peace).
As you pay your water bill, think of others
(those who are nursed by clouds).
As you return home, to your home, think of others
(do not forget the people of the camps).
As you sleep and count the stars, think of others
(those who have nowhere to sleep).
As you liberate yourself in metaphor, think of others
(those who have lost the right to speak).
As you think of others far away, think of yourself
(say: "If only I were a candle in the dark").
— Mahmoud Darwish, *Almond Blossoms and Beyond*

ACKNOWLEDGEMENTS

First and foremost, I would like to thank my advisor, Prof. Kamiar Aminian, for his guidance and support throughout the last four years. His clarity of thought and rigor has helped improve my skills to analyze a problem more deeply, while never losing sight of the bigger picture. I appreciate the openness of communication that we maintained throughout and the feedback I received. Thanks to his immense experience, we managed to achieve a good balance between working independently and receiving his guidance. Dr. Vincent Gremeaux, my co-advisor, has always been available whenever I needed his advice, despite his extremely busy schedule. I am thankful to my thesis committee members for the discussion and evaluation, Prof. Alexandre Alahi, Prof. Bjoern Eskofier, Prof. Paulo Bonato, and Dr. Silvio Lorenzetti. It is an honor to have them preside over my thesis defense. I also want to thank Dr. Purbasha Sarkar, Prof. David Braun, Prof. Heike Vallery, and Dr. Michiel Plooi for their mentorship and support during my academic research journey.

Beyond the thesis, I am thankful to Prof. Aminian for providing me the opportunity to join the beautiful LMAM family. From welcoming me to Switzerland and allowing me to enter the lab without the camipro on the first day, everyone at LMAM has continued to be supportive and have helped me grow into my role as a doctoral candidate. The lab atmosphere has always been congenial, prioritized sharing of knowledge and experience, and everyone has been together during the difficult times (and coffee breaks). I feel honoured to be part of this community and appreciate my colleagues and friends here: Mrs Francine Eglese, Mr. Pascal Morel, Dr. Arash Atrsaei, Ms. Gaelle Prigent, Mr. Mahdi Hamidirad, Dr. Abolfazl Soltani, Dr. Anisoara Ionescu, Ms. Yasaman Izadmehr, Dr. Mina Baniasad, Dr. Mathieu Falbriard, Dr. Pritish Chakravarty, Mr. Hojjat Karami, Mr. Guido Mascia, Ms. Sara Pagnamenta, Dr. Dario Alimonti, Mr. Tom Bertrand, Mr. Martin Savary, Mr. Joaquin Cabeza, Dr. Lena Carcreff, Dr. Matteo Mancuso, Dr. Wei Zhang, Dr. Hooman Dejnabadi, Dr. Majid Yousefsani, and Dr. Benedikt Fasel. I would also like to thank my collaborators, students, and everyone who gladly participated in all the studies conducted as a part of thesis.

I would like to thank my friends, whether here or elsewhere, with whom I have shared moments of happiness, connection, and fun. Although the thesis occupied a large space in my life, I owe some of the most cherished highlights of it to my friends and colocs in Switzerland - Sagar, Prakhar, Harshal, Rhythima, Harshit, Anjali, Saurabh, Tejal, Mahendra, Sai, Simran, Vivek, Anna, Manon, Laura, Felipe, and countless others. Sagar and Prakhar helped me create a feeling of home in Lausanne. Along the way from Nagpur to Lausanne, I have been fortunate to cultivate some wonderful companionships – Saurabh, Saheel, Shreyas, Ajinkya, Anurag, Aparajita, Pallav, Ravi, Vicky, Madhura, Anindo, Ajinkya, Himanshu, Rupinder, Jay, Atul, Sejal, Valentina, Petros, Geetank, Abdullah, Robert, Manyu, Vibhas, Chiara, Aviral, Kjartan, Klaas, Milan,

Mathieu, Alessandro, and many others. I am grateful for your rock-solid support and the shared memories. Elodie, the last year I have spent with you has been full of beautiful moments and I deeply cherish your company. Thank you for your warmth, your courage, and your support.

This work is a tribute to my parents, Shivangi and Shripad Apte, whose past decades have been dedicated to ensuring that me and my brother, Anuj, have the best quality of life that they could provide. They instilled my love of learning, fostered my curiosity, and inspired me by being exemplary members of the community. Words cannot express the impact they have had on my life and how much I appreciate their support, encouragement, and love. My grandparents, Vasudha and Madhukar, have always been there for me, and I will always be immensely grateful for having their presence in my life. Last but not the least, I want to thank my younger brother, Anuj, for being a constant source of inspiration, support, and dark humor. To everyone above and others who have been a part of my life, thank you for believing in me, supporting me, and making me who I am today.

This research work has been supported by the EPFLinnovators fellowship awarded under the Marie Skłodowska-Curie grant of the European Union's Horizon 2020 research and innovation programme.

Lausanne, the 27th of October 2022
Salil Apte

ABSTRACT

In the last hundred years, the record for completing a marathon has dropped from nearly 3 hours in 1908 to 2 hours and 1 minute in 2018. This monumental improvement is due to advances in the understanding of human physiology, biomechanics of movement, and the collaboration of physicians, coaches, scientists, and engineers in the field of human performance. With advances in microelectronics and computation, the devices used to measure physiological signals and analyze motion have evolved from large-scale devices in the laboratory to portable devices in the field. Today, wearable heart rate monitors are an integral part of runners' training sessions, with heart rate data routinely used to assess effort intensity and stress on the body. As athletes translate their physical capacity into performance on the field through their movement, biomechanical assessment can provide valuable information that complements physiological assessment. However, the potential of using biomechanical information in the evaluation of training sessions and standardized tests in practice remains largely untapped, partly because the assessment devices remain cumbersome to use and often require long post-processing, as well as programming skills. The proposed work aims to realize this potential by developing field methods for performance and capacity evaluation using portable inertial measurement units (IMUs) and Global Navigation Satellite System (GNSS) receivers.

Running performance can be characterized by the ability to maintain appropriate running technique despite fatigue, while keeping the effort intensity prescribed by the coach, or planned as a pacing strategy. In this work, a systematic review was conducted to examine and synthesize the results of fatigue protocols in running, followed by continuous measurements during a competition to confirm the trends obtained from the review with data from the field and to measure the changes in running technique due to fatigue. In addition, models were developed to accurately estimate running power using foot-worn IMU over a range of speeds and inclines and validated using gold standard methods in the laboratory, to better characterize running intensity. The second part of this work consisted of investigating the ability of IMUs and GNSS to improve the evaluation of athletes in standardized tests, referred to as their functional capacity. Functional capacity is typically used by coaches to develop appropriate training loads for athletes. This work presented validated methods to instrument common functional tests with wearable sensors to measure the speed, agility, and endurance of athletes in the field. In addition, these methods enable the extraction and a deeper analysis of relevant biomechanical parameters that contribute to the measured capacity and help the sporting staff understand athletes' strengths and weaknesses in detail.

All the research conducted, and methods developed in this thesis are based on various combinations of a minimal body-worn sensor setup with foot-worn IMUs and a single trunk-worn IMU-GNSS unit. The signal processing algorithms and models developed

in this work allow the recorded signals to be translated into easily interpretable and actionable information. Based on this information, coaches and physical therapists can develop customized training programs that target the relevant parameters. The proposed sensor setups and methods have been used and validated in a variety of situations, such as pre-season testing of a professional soccer team, training sessions of elite sprinters, the Lausanne half-marathon race, etc., highlighting their potential for real-world application. I believe that this work will help pave the way towards a deeper understanding of the biomechanical contributions to performance in running and provide new tools for the development of personalized training and rehabilitation programs, with the aim of optimizing positive adaptation to training stimuli, thereby reducing the incidence of injury, and help the return to sport process for injured athletes.

Keywords

wearable sensors, movement analysis, real-world, sensor fusion, signal processing, machine learning, human data collection, running, marathon, sprinting, fatigue, power, agility, endurance, training

RÉSUMÉ

Au cours des cent dernières années, le record pour terminer un marathon est passé de près de 3 heures en 1908 à 2 heures et 1 minute en 2018. Cette amélioration monumentale est due aux progrès dans la compréhension de la physiologie humaine, de la biomécanique du mouvement et à la collaboration de médecins, d'entraîneurs, de scientifiques et d'ingénieurs dans le domaine de la performance humaine. Avec les progrès de la microélectronique et de l'informatique, les appareils utilisés pour mesurer les signaux physiologiques et analyser le mouvement sont passés d'appareils à grande échelle en laboratoire à des appareils portables sur le terrain. Aujourd'hui, les moniteurs portables de fréquence cardiaque font partie intégrante des séances d'entraînement des coureurs, les données de fréquence cardiaque étant régulièrement utilisées pour évaluer l'intensité de l'effort et le stress sur le corps. Puisque les athlètes traduisent leur capacité physique en performances sur le terrain à travers leurs mouvements, l'évaluation biomécanique peut fournir des informations précieuses qui complètent l'évaluation physiologique. Cependant, le potentiel d'utilisation des informations biomécaniques dans l'évaluation des séances d'entraînement et des tests standardisés dans la pratique reste largement inexploité, en partie parce que les dispositifs d'évaluation restent difficiles à utiliser et nécessitent souvent un long post-traitement, ainsi que des compétences en programmation. Le travail proposé vise à exploiter ce potentiel en développant des méthodes de terrain pour l'évaluation des performances et de la capacité à l'aide d'unités de mesure inertielle portables (IMU) et de récepteurs du système mondial de navigation par satellite (GNSS).

La performance de course peut être caractérisée par la capacité à maintenir une technique de course appropriée malgré la fatigue, tout en gardant l'intensité d'effort prescrite par l'entraîneur, ou planifiée selon une stratégie de course. Dans ce travail, une revue systématique a été menée pour examiner et synthétiser les résultats des protocoles de fatigue dans la course à pied, suivis de mesures en continu lors d'une compétition pour confirmer les tendances obtenues à partir de la revue avec des données de terrain et pour mesurer les changements dans la technique de course à cause de la fatigue. De plus, des modèles ont été développés pour estimer avec précision la puissance de course à l'aide d'IMU portés aux pieds sur une gamme de vitesses et d'inclinaisons et validés à l'aide de méthodes de référence en laboratoire, afin de mieux caractériser l'intensité de course. La deuxième partie de ce travail a consisté à étudier la capacité des IMU et du GNSS à améliorer l'évaluation des athlètes dans des tests standardisés, appelée leur capacité fonctionnelle. La capacité fonctionnelle est généralement utilisée par les entraîneurs pour développer des charges d'entraînement appropriées pour les athlètes. Ce travail présente des méthodes validées pour instrumenter des tests fonctionnels communs avec des capteurs portables pour mesurer la vitesse, l'agilité et l'endurance des athlètes sur le terrain. De plus, ces méthodes permettent l'extraction et une analyse plus approfondie des paramètres biomécaniques appro-

priés qui contribuent à la capacité mesurée et aident le personnel sportif à comprendre en détail les forces et les faiblesses des athlètes.

Toutes les recherches menées et les méthodes développées dans cette thèse sont basées sur diverses combinaisons d'une configuration minimale de capteur porté sur le corps avec des IMU portés aux pieds et une seule unité IMU-GNSS portée sur le tronc. Les algorithmes et les modèles de traitement du signal développés dans ce travail permettent de traduire les signaux enregistrés en informations facilement interprétables et exploitables. Sur la base de ces informations, les entraîneurs et les kinésithérapeutes peuvent développer des programmes d'entraînement personnalisés qui ciblent les paramètres appropriés. Cette configuration et ces méthodes ont été utilisées et validées dans diverses situations, telles que les tests de pré-saison d'une équipe de football professionnelle, les séances d'entraînement de sprinteurs d'élite, le semi-marathon de Lausanne, etc., mettant en évidence leur potentiel pour l'application dans le monde réel. Je crois que ce travail contribuera à ouvrir la voie vers une compréhension plus approfondie des contributions biomécaniques à la performance en course à pied et fournira de nouveaux outils pour le développement de programmes d'entraînement et de rééducation personnalisés, dans le but d'optimiser l'adaptation positive aux stimuli d'entraînement, réduisant ainsi l'incidence des blessures, et aider au processus de retour au sport des athlètes blessés.

Mots clés

capteurs portables, analyse du mouvement, fusion de capteurs, le monde réel, traitement du signal, apprentissage automatique, collecte de données humaines, course à pied, marathon, sprint, fatigue, puissance, agilité, endurance, entraînement

Contents

Acknowledgements	i
Abstract	iii
Résumé.....	v
List of figures	xi
List of tables.....	xiii
I. Introduction	1
1 Background and motivation	3
1.1 Training paradigm for running	3
1.1.1 Role of training	3
1.1.2 Quantification of training	5
1.1.3 A typical training framework	6
1.1.4 Going beyond training load	7
1.1.5 Potential of biomechanical assessment	8
1.2 Running biomechanics and its assessment	10
1.2.1 Biomechanics of running gait	10
1.2.2 Objective assessment of gait biomechanics	14
1.3 Evaluation of functional capacity	21
1.3.1 Speed.....	21
1.3.2 Change-of-direction ability	22
1.3.3 Endurance.....	23
1.4 Thesis objectives and outline	25
II. Biomechanical assessment for performance and fatigue analysis	29
2 Biomechanical response of lower extremities to acute fatigue	31
2.1 Introduction	32
2.2 Methods.....	33
2.2.1 Search strategy and sources	33
2.2.2 Eligibility criteria	34
2.2.3 Study classification and data extraction	35
2.2.4 Parameter definition	36
2.2.5 Data synthesis	37

2.3	Results	37
2.3.1	Study selection.....	37
2.3.2	Characteristics of selected literature	38
2.3.3	Parameters for analysis.....	41
2.3.1	Parameter trends	41
2.4	Discussion	43
2.4.1	Response to fatigue	43
2.4.2	Role of functional tests	45
2.4.3	Influence of protocols	45
2.4.4	Recommendations for an IMU-based wearable sensor setup	46
2.4.5	On study protocols.....	48
2.4.6	Limitations	49
2.5	Conclusion	49
2.6	Appendix	50
2.6.1	Eligibility criteria	50
2.6.2	Study appraisal.....	51
2.6.3	Parameter definition	52
2.6.4	Data synthesis	52
3	Concurrent evolution of biomechanical parameters with perceived fatigue	55
3.1	Introduction.....	56
3.2	Materials and equipment	57
3.3	Methods	58
3.3.1	Preprocessing.....	58
3.3.2	Feature extraction	59
3.3.3	Statistical analysis	61
3.4	Results	63
3.4.1	Evolution with race and ROF values.....	63
3.4.2	Onset of change	65
3.4.3	Differences according to performance	67
3.5	Discussion	69
3.5.1	Gait spatiotemporal parameters and perceived fatigue.....	69
3.5.2	Secondary gait parameters	70
3.5.3	Progression of the trunk motion.....	70
3.5.4	Limitations	71
3.6	Conclusion	72
4	Estimation of running power with foot-worn IMUs	73
4.1	Introduction.....	74
4.2	Materials and protocol.....	76
4.3	Methods	77

4.3.1	Reference power estimation	77
4.3.2	IMU data processing.....	78
4.3.3	Feature development	79
4.3.4	Feature selection	81
4.3.5	Model development	82
4.4	Results.....	83
4.5	Discussion and conclusion	87
III.	Augmentation of in-field functional capacity testing	91
5	Sprint velocity estimation using GNSS-IMU sensor fusion.....	93
5.1	Introduction	94
5.2	Materials and equipment.....	95
5.3	Methods.....	96
5.3.1	Velocity and duration estimation algorithm.....	96
5.3.2	Estimation of profiles – velocity, force, and power	98
5.3.3	Validation process	99
5.4	Results.....	100
5.4.1	Velocity estimation.....	100
5.4.2	Validity of estimated velocity	100
5.4.3	Validity of exponential fitting	102
5.5	Discussion	103
5.5.1	Validity of the proposed method	103
5.5.2	Exponential fitting and athlete profiles	104
5.5.3	Limitations and future work	105
5.6	Conclusion.....	106
5.7	Appendix	106
6	Development of an instrumented Change-of-Direction field test.....	109
6.1	Introduction	110
6.2	Materials and equipment.....	112
6.3	Methods.....	113
6.3.1	Labelling of video data	113
6.3.2	Algorithm development	114
6.3.3	Metrics for performance in COD test	118
6.4	Results.....	119
6.4.1	Labelling of video data	119
6.4.2	Detection and duration of COD	119
6.4.3	Performance metrics	121
6.5	Discussion	123
6.5.1	Validity of the proposed method	123
6.5.2	Performance metrics	125

6.5.3	Limitations and future work.....	127
6.6	Conclusion	128
6.7	Appendix	129
7	Biomechanical contributions to performance in a Cooper test	131
7.1	Introduction.....	132
7.2	Materials and Equipment	133
7.2.1	Participants and study design	133
7.2.2	Laboratory test.....	134
7.2.3	Field test	135
7.3	Methods	135
7.3.1	Preprocessing and parameter estimation.....	135
7.3.2	Extraction of metrics.....	136
7.3.3	Selection of metrics	138
7.3.4	Distance estimation	140
7.4	Results	141
7.4.1	Distance and speed estimation.....	142
7.4.2	Selection of metrics	142
7.5	Discussion	145
7.5.1	Distance and speed estimation.....	145
7.5.2	Selection of metrics	146
7.5.3	Limitations and recommendations	149
7.6	Conclusion	150
7.7	APPENDIX: Results for estimation with wrist-worn IMU	150
IV.	Conclusion and recommendations for future work	151
8	Conclusion and discussion.....	153
8.1	Contributions.....	153
8.1.1	Part I: Biomechanical assessment for performance and fatigue analysis	154
8.1.2	Part II: Augmentation of in-field functional capacity testing	156
8.1.3	Potential application to training	157
8.2	Limitations.....	159
8.2.1	Protocol.....	159
8.2.2	Algorithm development and analysis.....	160
8.3	Future development.....	161
8.3.1	A more inclusive study population.....	161
8.3.2	Methodological development.....	162
8.3.3	Augmenting training prescription	163
	Bibliography	165
	Curriculum Vitae.....	188

LIST OF FIGURES

Figure 1.1 Summary of the different aspects of training in sports.....	4
Figure 1.2 Predominant framework for one training session.....	6
Figure 1.3 Overtraining and its adverse effects.....	7
Figure 1.4 Extended framework for estimation and monitoring of training load	8
Figure 1.5 Gait phases and temporal events of the running gait cycle.	11
Figure 1.6 Relationship between gait parameters	12
Figure 1.7 Vertical, anteroposterior (AP), and mediolateral (ML) GRF profiles for runners.....	13
Figure 1.8 An example of investigation of foot strike patterns using video footage.....	15
Figure 1.9 Stages of the optoelectronic motion capture process	17
Figure 1.10 Typical setup and protocol for a 40-m sprint test	21
Figure 1.11 Typical setup for a T-test to evaluate the change-of-direction capacity	23
Figure 1.12 Tests for estimating the maximum oxygen uptake	24
Figure 1.13 Outline of thesis	27
Figure 2.1 Study selection and categorization process	38
Figure 2.2 Number of studies according to the different aspects of a fatigue protocol	39
Figure 2.3 Number of studies per parameters category	40
Figure 2.4 Number of studies utilizing wearable and stationary measurement systems.....	40
Figure 2.5 Parameters that show a consistent trend in response to acute fatigue and a potential wearable sensor setup to measure them in field	48
Figure 2.6 Flowchart for the extraction of the summary trends for different parameters	53
Figure 3.1 Sensor configuration used for the measurement.....	58
Figure 3.2 Flowchart for the overall procedure	59
Figure 3.3 Flowchart for the estimation of secondary gait metrics	60
Figure 3.4 Flowchart of the trunk movement characterization process	61
Figure 3.5 Statistical analysis procedure where the biomechanical parameters and the ROF values are used as inputs	61
Figure 3.6 Parameters with a significant change with the race segments (in blue) and/or rating of fatigue (in green)	64
Figure 3.7 Evolution of the secondary gait parameters with race progression.....	64
Figure 3.8 Evolution of stability and smoothness with race progression.	65
Figure 3.9 Change in perceived fatigability (ROF) with race progression.....	67
Figure 3.10 Results of the LME models for the response of the gait parameters	67
Figure 3.11 Evolution of the secondary gait parameters with perceived fatigability.....	68
Figure 3.12 Evolution of stability and smoothness with perceived fatigability.	68
Figure 4.1 Measurement systems and data collection protocol.	76
Figure 4.2 Estimation of reference power.....	77

Figure 4.3 Flowchart for the proposed power estimation method.	79
Figure 4.4 Relationship between the reference power and the treadmill speed	84
Figure 4.5 Cumulative distribution of ϵ_{100} , ϵ_{50} , ϵ_0 (%) of the proposed method	84
Figure 4.6 Illustration of reference and predicted power for level running	84
Figure 4.7 Bland–Altman analysis for power estimation with maximum noise (ϵ_{100})	85
Figure 4.8 Estimation error (%) for all speeds and slopes.....	85
Figure 5.1 Sensor setup and measurement protocol	96
Figure 5.2 Flowchart for the sprint velocity estimation algorithm	97
Figure 5.3 Scenario illustrating the estimated velocity profile	100
Figure 5.4 Validation of estimated velocity profile.....	101
Figure 5.5 Bland-Altman plots for sprint parameters	102
Figure 5.6 Modelling of the sprint velocity profile	102
Figure 5.7 Force-velocity and power-velocity profiles.....	105
Figure 5.8 Change in the percentage of RMS error	107
Figure 6.1 Conventional T-test for COD performance assessment.....	110
Figure 6.2 Sensor setup and the nine phases of the Agility T-test.....	113
Figure 6.3 Event labels for each COD segment to be used as reference data	114
Figure 6.4 Start of motion (dashed green lines) and first step (black line) detection.....	115
Figure 6.5 Segmentation of one test sample using reconstructed AP acceleration signal	116
Figure 6.6 Segmentation of the T-test based on video labelling for 8 of the 23 athletes.....	119
Figure 6.7 Error between video-based duration and photocell duration	119
Figure 6.8 Time of event from video and from algorithm for four T-tests	120
Figure 6.9 Box plot of ϵ_s and ϵ_e for COD detection for each micro analysis method	120
Figure 6.10 Bland-Altman plot for detected COD start/end events	121
Figure 6.11 Mean (solid line) and S.D. (dashed lines) for the velocity during the T-test.	122
Figure 6.12 Correlation between total cutting time for each COD and the total completion time of the T-test.....	123
Figure 6.13 Comparison between the five best (red) and worst (blue) participants.....	123
Figure 6.14 Velocity profile during the T-test for two fastest and slowest athletes.....	129
Figure 7.1 Protocol and sensor setup for the 12-minute field test.....	134
Figure 7.2 Flowchart of the overall procedure for selection of metrics	136
Figure 7.3 Procedure for selection of performance metrics for the biomechanical profile	139
Figure 7.4 Methods for the estimation of distance covered over the 12-minute run	141
Figure 7.5 Performance of participants grouped according to D_{ref} and GNSS tracking	141
Figure 7.6 Profile for the biomechanical parameters during the Cooper test	143
Figure 7.7 Selected metrics and their categories.....	144
Figure 8.1 Profile for runners based on the biomechanical parameters	158

LIST OF TABLES

Table 1.1 Non-exhaustive list of biomechanical metrics estimated using body-worn IMUs.....	20
Table 2.1 Details of the PiCO strategy used to conceptualize search terms	33
Table 2.2 Parameter trends in response to acute fatigue	41
Table 2.3 Adapted MINOR scale (Slim et al., 2003b) used for scoring the studies.....	52
Table 3.1 Effect size results for the statistical analysis.....	66
Table 4.1 Statistical features (X_s) extracted for each stride	80
Table 4.2 Bias (median), precision (IQR) and mean absolute error (MAE) of the power estimation algorithm.....	86
Table 4.3 Labels and coefficients for the 15 most important features of the EN models	86
Table 5.1 Median (IQR) values of the RMS error.....	101
Table 5.2 RMS error for the modelled velocity profile.	103
Table 6.1 Mean \pm S.D. of estimation error and (%) for each displacement phase and COD	120
Table 6.2 mean \pm S.D. for performance metrics across all four COD segments	122
Table 7.1 List of biomechanical parameters (units) extracted	137
Table 7.2 Error rates for the five distance estimation methods.....	142
Table 7.3 Biomechanical metrics selected through LASSO regression and statistical testing	144

I. INTRODUCTION

1 BACKGROUND AND MOTIVATION

1.1 TRAINING PARADIGM FOR RUNNING

1.1.1 *Role of training*

Training denotes the process of preparation for a specific task and sports training refers more specifically to the preparation of athletes for the highest level of fitness and performance (Kasper, 2019). Training involves the exposure of body to higher than accustomed training stress or stimulus, thereby inducing compensatory improvements in performance capacity (Madden et al., 2013). For example, an endurance runner is trained to run for a distance longer than their typical running distance or speeds higher than their comfortable speed, to improve their endurance. The amount of stimulus should be personalized by acknowledging the individual differences between athletes' adaptation to prior training, which is affected by their unique psychological (motivation, pain, confidence, etc.), physiological (fitness, training background, injury history, age, height, weight, etc.), environmental (lifestyle, nutrition, role within the team, etc.), and genetic profile (O'Connor, 2013). The personalized training stimulus should be planned systematically i.e., periodized to create an appropriate progression in stress, to maintain continued positive adaptation to training. Furthermore, this planning should aim at introducing variations in training types (intensity, duration, volume, activity, contraction mode, work/rest ratio, etc.) to avoid burnout, injury, soreness, illness and ensure optimal physical condition for competitions (Drew & Finch, 2016; Gabbett, 2020). In general, a training program comprises of different aspects of athlete's performance (Figure 1.1). For instance, neuromuscular training is typically aimed at improving the proprioceptive, balance, flexibility, and sensorimotor skills of the athletes and reduce the instances of injuries (Emery et al., 2005; Hübscher et al., 2010). Neuromuscular training can consist of multi-intervention programs with a combination of plyometric, weight, agility, balance, and sport-specific exercises (Engelbrechtsen et al., 2008). This type of training can be particularly beneficial for young athletes to develop fundamental motor skills and improve movement biomechanics, thereby reducing sports-related injury risk (Myer et al., 2011).

The aim of physical conditioning programs is to improve the athlete's strength, endurance, and ability to exert power. Development of muscular strength and power is associated with improved general athletic ability (e.g., jumping, sprinting, and change of direction) and force-time characteristics (e.g., speed of force development and external mechanical power) (Suchomel et al., 2016). Resistance training of both limbs simultaneously, a combination of heavier and lighter loads, and eccentric training are generally recommended to produce the highest improvements in muscular strength (Suchomel et al., 2018). Similarly, higher endurance usually leads to an improvement in sporting performance, though there are conflicting results for concurrent training for

endurance and strength (Leveritt et al., 1999). Various modalities exist for enhancing athlete's endurance, such as training in an hypoxic (low oxygen) environment (artificial or at high altitudes) (Sinex & Chapman, 2015), polarized training ($\geq 80\%$ of training volume at an intensity below first ventilatory threshold) (K. S. Seiler & Kjerland, 2006), high volume moderate intensity (60 – 70 % peak power output) training, low volume high intensity ($\geq 80\%$ peak power output) training, etc. (Flueck & Eilers, 2010). Endurance training enhances the important parameters of aerobic fitness, such as maximal oxygen uptake ($\dot{V}O_{2max}$), exercise economy (energy cost for per unit of exercise), the lactate/ventilatory threshold and oxygen uptake kinetics (C. M. Jones et al., 2017).

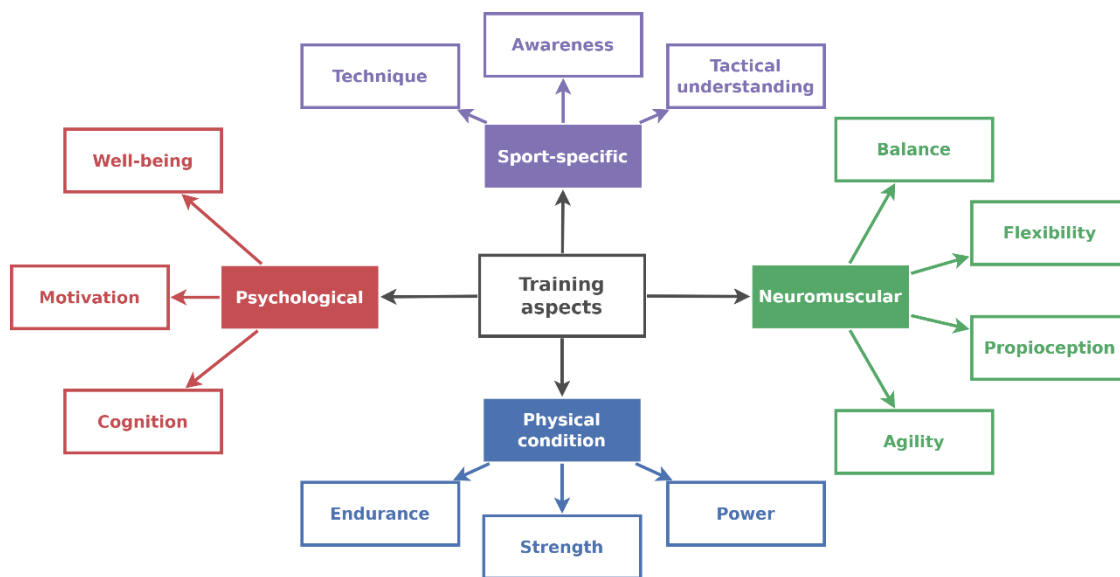


Figure 1.1 Summary of the different aspects of training in sports

Along with the neuromuscular and conditioning programs, training in sports also encompasses the monitoring of athletes for their mood states, anxiety and stress about performance, feeling of fatigue, cognitive abilities, etc (Raglin, 2001). Subjective questionnaires such as the profile of mood states (POMS) (Curran et al., 1995), rating-of-fatigue (ROF) scale (Micklewright et al., 2017), etc. are generally used to assess these factors. Based on the these assessment, cognitive, behavioral, relaxation-based interventions can be provided to the athletes (Weinberg & Comar, 1994) with the aim of developing arousal regulation skills, volition skills, goal-setting skills, etc. (Birrer & Morgan, 2010) and learning interest enhancing strategies to improve motivation (Green-Demers et al., 1998). Development of these skills has shown improvement in athlete's performance and their ability to reach and maintain peak performance conditions (Harmison, 2006). In addition to this, such training and assessment can help athletes to improve their psychological readiness for return to sports after a major injury or incident (Glazer, 2009). Finally, to develop expert performance for particular motor skills, it is pertinent for athletes to devote a substantial amount of time for practicing the specific movements and responses (Starkes et al., 2014). Examples of such movements are the kicking a ball in soccer, serving in tennis, foot placement in running, etc. Technique can be defined a specific sequence of movements performance to achieve a specific task, and has strong implications not only on the sporting

performance, but also on the likelihood of developing chronic injuries (Lees, 2002). These movements are typically practised under the supervision of coaches, in an environment which is similar to the one for the sporting competition. However, with the advent of virtual reality systems which reproduce environments with high fidelity and can track body movement, athletes can also train these movements based on feedback in a virtual environment (Miles et al., 2012).

Apart from technique, athletes are also trained to improve their visual awareness, especially in case on team sports wherein the players need to be aware of the entire playing field (Appelbaum & Erickson, 2018). This can be complemented by tactical training for team sports, wherein the athletes are trained to improve their decision making in response to in-game situations (Rein & Memmert, 2016). This work mainly focuses on training aimed towards improving the athlete's technique, endurance, agility, and speed. Running presents a unique scenario where all three aspects can be trained simultaneously, since speed drills have shown to enhance endurance, agility, and speed in runners and soccer players (Iaia & Bangsbo, 2010; Lupo et al., 2019). Performed under the guidance of a coach, these running drills can be shortened and repeated multiple times in order to improve a particular aspect of running technique.

1.1.2 *Quantification of training*

To ensure positive adaptation to training and minimize injury risk, it is essential to accurately evaluate sport and non-sport training load (TL), and optimize it based on the on-field performance, functional capacity, physical and psychological status of an athlete (Soligard et al., 2016). TL is generally quantified as the product of the intensity of training (running speed, lifted/pushed weight resistance, etc.) and the volume of training (duration/distance of run, number of repetitions and sets, etc.) and classified as external and/or internal load, wherein, the former refers to the training stimulus provided to athletes and is evaluated independently of their personal physiology (Borresen & Lambert, 2009; Mujika, 2017). External training load is usually measured via training time, training repetitions, power output measurement devices, time motion analysis through the study of movement pattern and GPS, and neuromuscular function testing through jump tests and sprint performance (Halsen, 2014). External TL has been the basis of the traditional training prescription and load monitoring systems, but it does not always reflect the internal load accurately, as individual responses to training stimulus differ from one athlete to another. These responses which are both physiological and psychological are represented by internal training load.

Typical measures for internal TL include subjective metrics such as rating of perceived exertion (RPE) and other inventories, and objective metrics based on heart rate (HR), blood lactate, training impulse, etc. (Borresen & Lambert, 2009). Subjective and objective metrics can also be used together (HR – RPE ratio) for evaluation of internal load (Halsen, 2014). Monitoring both, external and internal TL, is crucial in evaluating the optimal training stimulus for an individual athlete. Recent advances in wearable technology have led to the use of portable global navigation satellite system (GNSS) devices and accelerometers in external TL measurement during competitions and training, especially in team sports (Aughey, 2011; Camomilla et al., 2018). Portable heart rate

monitors have enabled the seamless monitoring of heart rate (HR) and heart rate variability (HRV) in sports, and resting HRV has been used to monitor the physiological response and adaptation of athletes to training stimuli (Kiviniemi et al., 2007). External load derived from runs and training evaluated with GPS and accelerometer consistently show positive associations with metrics of internal load derived from perceived exertion and heart rate (McLaren et al., 2018).

1.1.3 A typical training framework

A typical training framework (Figure 1.2) for runners involves setting the initial external training load (TL) based on the functional capacity of the athlete, while subsequent loads are based on coaching heuristics and competition schedule. The training plan is usually adjusted based on the physical condition of the athlete, especially the presence of pain, illness, or injury. Internal TL is generally estimated using subjective metrics like RPE. Current practices in sports mainly involve the use of external TL, complemented by HR-RPE based internal TL, for training load monitoring and estimation during the season (Halsen, 2014). Traditionally, coaches used only the results from functional capacity tests to determine the initial TL and its progression throughout the season (Figure 1). However, recent ideas such as Acute:Chronic work ratio (ACWR) have provided an important heuristic method for determining the sequence of loads (Hulin et al., 2016). The goal in such a case is to design TL progression such that the ACWR is maintained close to 1, wherein the acute work is the load during 1-week and the chronic work is the average chronic load during 4-weeks (Hulin et al., 2016). Proliferation of wearable GPS devices and heart rate monitors has provided an ease of monitoring TL objectively in team sports, further spreading the use of above-mentioned monitoring methods (Aughey, 2011).

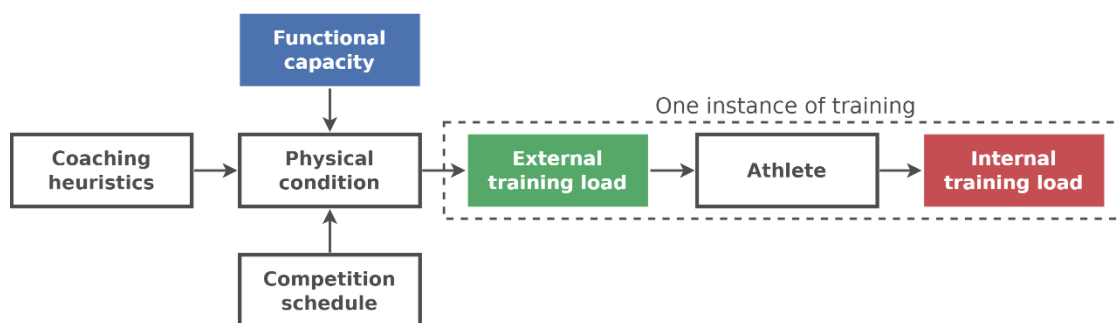


Figure 1.2 Predominant framework for one training session, as a part of a prescribed program. Results from the functional tests are used to set initial external TL, while subsequent loads are based on heuristic ideas such as acute-chronic work ratio (ACWR) (Hulin et al., 2016), etc. Internal TL is generally estimated using subjective metrics like RPE.

Though these practices provide ease-of-use, they suffer from some important limitations while personalizing the TL to an individual. Each athlete has their own specific physiology and movement technique, and adapts to a training program in a different way (Pickering & Kiely, 2019). The design and implementation of TL schemes without considering the personalized context of adaptation can lead to the issue of overtraining (Lehmann et al., 1997). Overtraining is a major factor leading to muscle injuries, especially in non-contact and endurance sports (Budgett et al., 2000). Overtraining is typi-

cally a consequence of inappropriate training load management and results in long-term performance decrement. Furthermore, overtraining (Figure 1.3) can result in other adverse effects such as decreased immunity, increased likelihood of chronic fatigue, mood disorders, etc. (Kreher & Schwartz, 2012).

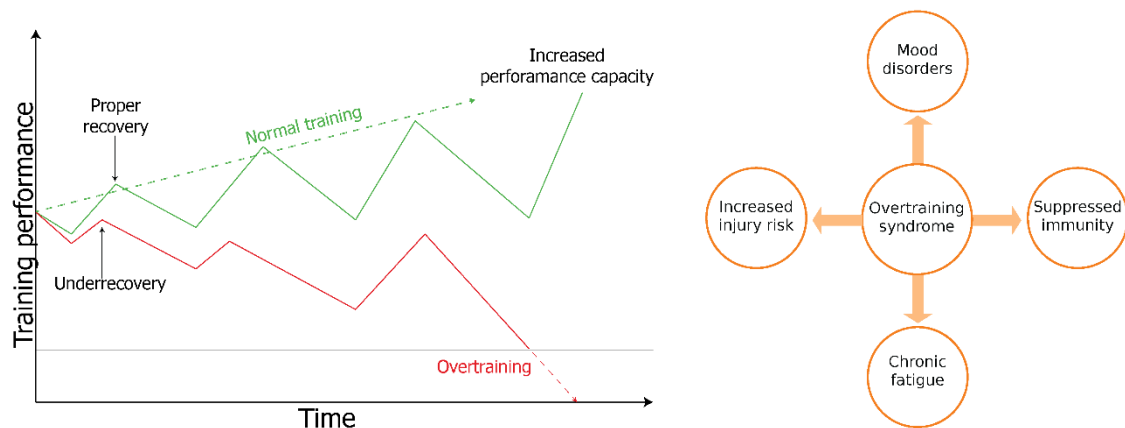


Figure 1.3 Overtraining and its adverse effects, based on (Budgett et al., 2000)

In this context, current TL estimation practices have following limitations: 1) It is difficult for coaches to observe the athlete movement in training, particularly in the context of team sports. External and internal TL do not provide information about the technique. 2) Functional tests used to assess capacity typically use the overall group trends to model participant response. While these representative values can resemble actual athlete behaviour to a certain extent, they can be personalized further with instrumenting the in-field tests with wearable sensors. Furthermore, the sensor data can provide additional metrics to understand the movement better. 3) Internal TL from the exercise mainly encapsulates the physiological response and the subjective feeling of exertion and does not inform the coach about the technique of the athlete during a training session.

1.1.4 Going beyond training load

An extended framework (Figure 1.4) for the training of runners, based on the conceptual suggestions in (Impellizzeri et al., n.d.; C. M. Jones et al., 2017; Vanrenterghem et al., 2017), can overcome the above-mentioned limitations using a personalized physical profile of an athlete as a foundation for the customization of training. This physical profile contains two main components: i) accurate functional capacity of an athlete based on instrumented tests to measure speed, agility, and endurance ii) the training history containing the prior external and internal loads experienced, and the performance during training sessions. By focusing on both, performance and overall internal TL, this physical profile can capture the effects of individual external TL on both physiological and neuromuscular adaptations. Thus, it considers the physical response of athletes for each training session and allows the coaching staff to take better-informed decisions.

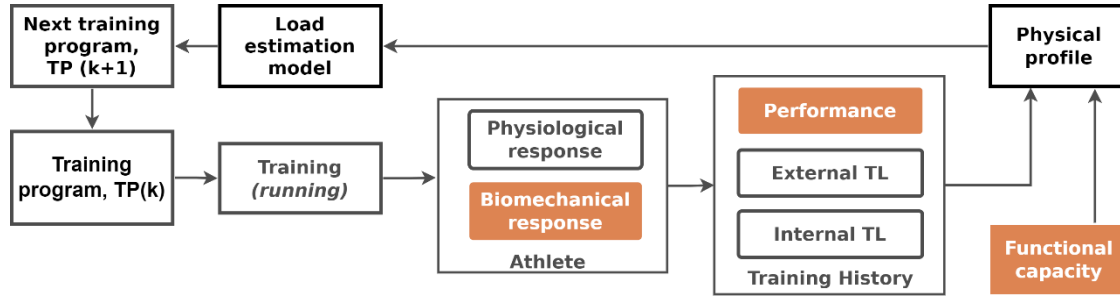


Figure 1.4 Extended framework for estimation and monitoring of training load, which considers the physical profile of the athlete to personalize the load. This profile is based on the training load (TL), biomechanical performance in training, and the functional capacity of the athlete. Based on the physical profile generated from one training program, the load estimation model can estimate an optimal set of loads for the subsequent training program.

The orange blocks are the focus of this thesis and are explained in detail in the following sub-sections.

This physical profile can serve as an input to a load estimation model, which can compute optimal training progression based on the constraints set by the coaching staff like a specific ACWR, minimum training performance, etc. Pilot studies of such estimation models, based on constrained optimization (Carey et al., 2018) and artificial neural networks (Bartlett et al., 2017) approaches, have already shown promising results. While these models mainly consider external TL and RPE (internal TL), they could serve as templates for models considering the proposed physical profiles. For example, in the case of an athlete preparing for a marathon, the physical profile will contain: i) functional capacity from speed and endurance tests performed before start of the current training program TP(k) and ii) measured external TL, internal TL, and performance during the running training sessions. This profile will then serve as an input to load estimation model which will predict an optimal training program TP(k+1) to prepare for the next marathon. Thus, this extended framework will enable assessment of intra-individual changes after training programs and post-injury rehabilitation, and further develop a tailored training program. The thesis targets this extended framework (personalized training program) by investigation of the main components of this framework: biomechanical response, performance, and functional capacity. It is, however, important to note that this extended training framework does not alone provide a complete solution to the optimization of training loads. There are multiple factors affecting the relationship of training to performance and injury (Coyne et al., 2018), and thus subjective questionnaires and tests about emotional well-being, recovery, and physiological status are also necessary to create a holistic monitoring program.

1.1.5 Potential of biomechanical assessment

Performance during training can be characterized by the magnitude of a particular metric such as speed, cadence (steps per minute), mechanical power, etc., and the inability to maintain the prescribed intensity can be assessed as a decrease in performance (Passfield et al., 2022). Internal factors such as fatigue, stress, hydration, etc., or environmental factors such as humidity, temperature, the presence of competitors, etc., may influence the perception of internal load and heart rate response (Halsen, 2014). Because these factors do not directly affect measured running power or speed, they can

serve as a useful supplementary measures to monitor training load during exercise (Paquette et al., 2020). Running speed and power can also provide complementary information about performance; for example, a decrease in running power while running speed remains constant indicates a reduction in the energy cost for that running speed (Cerezuela-Espejo et al., 2018; Taboga et al., 2021).

Running performance depends not only on the maximal capacity and the proportion of that capacity that is constantly used, but also on running economy (RE). RE is the volume of oxygen (VO_2) consumed per kilogram of body weight per kilometer; the less oxygen consumed, the better RE and the more efficient the run (Folland et al., 2017; Foster & Lucia, 2007). In runners with similar endurance capacity, RE can vary by up to 30% (J. T. Daniels, 1985; Morgan et al., 1989). Running mechanics determine the energy absorbed and the propulsive forces generated during ground contact, thus influencing RE. Running mechanics, particularly during the propulsion phase, show a strong correlation with RE during treadmill running (Beattie et al., 2014; Moore, 2016; Saunders et al., 2004). In addition, an increase in the variability of the temporal parameters of gait is associated with an increase in the cost of running, which worsens the RE (Candau et al., 1998). Measurement of RE in the field requires the use of portable gas analyzers, which makes measurement during regular training sessions cumbersome and expensive. However, running biomechanics, i.e., running technique can be accurately and conveniently assessed during training sessions (Willy, 2018).

The biomechanics of running can be altered through specific training and adopting an economical running technique can improve RE and thus performance (Moore, 2016; Saunders et al., 2004). For example, in a longitudinal endurance training program, a reduction in stride rate variability (for example, achieved through a metronome sound) and an improvement RE were reported as outcomes, although there was limited change in the oxygen capacity of the participants (Slawinski et al., 2001). In addition to its influence on performance, a running technique tailored to the athlete also ensures appropriate limb and joint loading, and is thus linked to running related injuries (Paquette et al., 2020; Willy, 2018). At a similar running speed, loading forces and moments are influenced by the body mass index (BMI), length of the steps, foot angle at ground contact, running shoes, running surface, etc. (Bertelsen et al., 2017). A conventional training framework (Figure 1.2) does not consider all these factors and can therefore benefit from the performance assessment provided by the analysis of running biomechanics during training and functional capacity testing.

The assessment of biomechanics in the field is crucial for understanding the strengths and weaknesses of athletes and tailoring the training to achieve an appropriate technique and performance capacity. A single proper or good technique does not necessarily exist, but it varies from one athlete to another, depending on anthropometry, experience, past injuries, and sometimes it is more the discrepancies between these factors and running style that indicates an improper running technique. In the following two sections, we will explore in detail the biomechanics of running and the various functional tests, and their evaluation in the laboratory and in the field. The biomechanics of running form the basis of the first part of this thesis, which aims to evaluate the athlete

in the field by his ability to maintain a better running technique despite increasing fatigue and to reach the prescribed intensity (measured by running power). Augmentation of field tests by an accurate estimation of the functional capacity and the evaluation of the biomechanical contributions to this capacity form the main objective of the second part of the work.

1.2 RUNNING BIOMECHANICS AND ITS ASSESSMENT

1.2.1 *Biomechanics of running gait*

Endurance running, understood as extended periods of running using aerobic metabolism, is unique to humans among all primates (Bramble & Lieberman, 2004). While nonhuman primates can sprint rapidly, their endurance running capacity is exceptionally lower than that of humans (Hunt, 1991). When adjusted for body mass and size, human running speeds are relatively higher, compared to those for trotting in quadrupeds (Heglund & Taylor, 1988). Compared to nonhuman primates, human legs have long elastic tendons and human feet contain elastic structures in the plantar arch. These rocspring-like structures allow up to 50% savings in metabolic costs due to the elastic function of the Achilles tendon and up to 17% due to the elastic arch of the foot (Ker et al., 1987; Thorpe et al., 1999). It is suggested that endurance running capability played an important role in the evolution of the Homo species, as it helped hominids exploit protein rich resources such as marrow, meat, etc. through scavenging and hunting and these food sources, in turn, may have made it possible for our unique combination of large bodies, small guts, big brains and small teeth (Aiello & Wheeler, 1995; Semaw et al., 2003; Wrangham et al., 1999). Running evolved from its role in human evolution to becoming an important training activity for competitive athletes in track and field clubs, university programs, etc. (Bale, 2004) in the early twentieth century. In the last half of 20th century, endurance running has become one of the most popular recreational sporting activities, and more than 10% of people in the United States, England, and the Netherlands, and other European countries report habitually jogging (or running several kilometers) daily (Dai et al., 2015; Deelen et al., 2019; England, 2019; Scheerder et al., 2015). Thus, the biomechanical assessment of running is relevant to a large segment of the population, far beyond competitive athletes.

1.2.1.1 *Spatiotemporal parameters of gait*

The basic unit of analysis of running is the gait cycle (Figure 1.5), which describes the continuous and repetitive pattern of movement of the body during running (Dugan & Bhat, 2005). The duration of a gait cycle is called cycle time, with the stride frequency representing the number of strides taken within a second or minute. The cycle begins when a foot strikes the ground and ends when the same foot strikes the ground again. The phase when the foot contacts the ground is called the stance phase, and its total duration is called the contact time (t_c). It begins when the foot touches the ground (initial contact or IC) and continues until the toe leaves the ground (toe-off TO). The stance phase is divided into two sub-segments depending on the function: the braking phase, in which the leg absorbs landing forces and supports fall in the position of the body's center of mass (CoM), and the push-off phase, in which forward acceleration is generated to propel the body forward (Divert et al., 2005). Depending on the speed, the land-

ing forces can be 2 to 5 times the body weight and this can cause significant braking impulse, unless the athlete has the required muscle strength to repel this force (Weyand et al., 2000). The athlete can store these contact forces as elastic energy within the leg muscle-tendon complex and use it to propel the body in the push-off phase. Acute fatigue can lead to reduction in the ability of muscles to absorb and recycle the impact energy (Darch et al., 2022), needing an increase in the duration of t_g to store and release the same impulse. The duration of t_c is directly correlated to the step frequency, and thus, the running speed (Weyand et al., 2000). The ratio of t_c to the t_g is known as the duty factor (d_f). A lower t_c and d_f have been linked to a better performance in terms of RE (Folland et al., 2017; Moore et al., 2019; Mooses et al., 2021; Nummela et al., 2007).

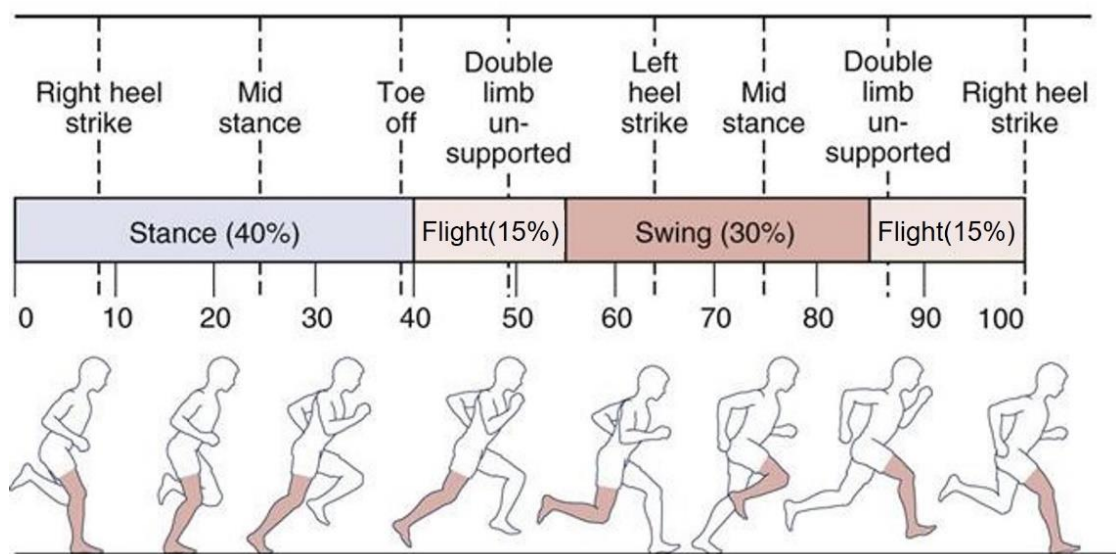


Figure 1.5 Gait phases and temporal events of the running gait cycle. The relative proportion of the different phases relative to cycle time is indicative of the typical values during jogging (Dugan & Bhat, 2005). The events are marked according to the ipsilateral leg, i.e., the leg highlighted in color. Adapted from (Magee, 2014)

The interval of the gait cycle from the toe-off to the next initial contact is referred to as the swing phase, and its duration is referred to as swing time (t_s). The stance and swing phases are also known as terrestrial and aerial phases due to the presence and absence of ground contact, respectively (Novacheck, 1998). As the swing phase begins for one leg, the other leg approaches the end of its swing phase, resulting in a period where neither foot touches the ground, the flight phase. The flight phase begins with the final contact of the ipsilateral leg and ends with the initial contact of the contralateral leg. The ipsilateral leg is highlighted in color, while the contralateral leg is shown in gray in Figure 1.5. Thus, a swing phase is composed of a flight phase, the stance phase of the contralateral leg, and a second flight phase (Novacheck, 1998). The duration of flight phase is known as flight time (t_f) and can be considered for each step separately. Although t_f is less correlated with cadence compared to t_c , their durations relative to t_g have been used to classify runners into terrestrial/aerial (Gindre et al., 2015). Since the foot is not in contact with the ground during the flight phase, speed cannot be increased, and the athlete must move the leg cyclically in preparation for the next foot strike.

Stance, swing, and flight phases constitute the framework within which other kinetic and kinematic features are studied. For these studies, it is therefore imperative to detect and differentiate the different temporal parameters of gait and their relative proportions, accurately and precisely. The most used spatial parameter of gait is the stride length (SL), which refers to the distance between the successive foot contacts for the same leg. In contrast, step length refers to the distance between the successive foot contacts of the right and left legs.

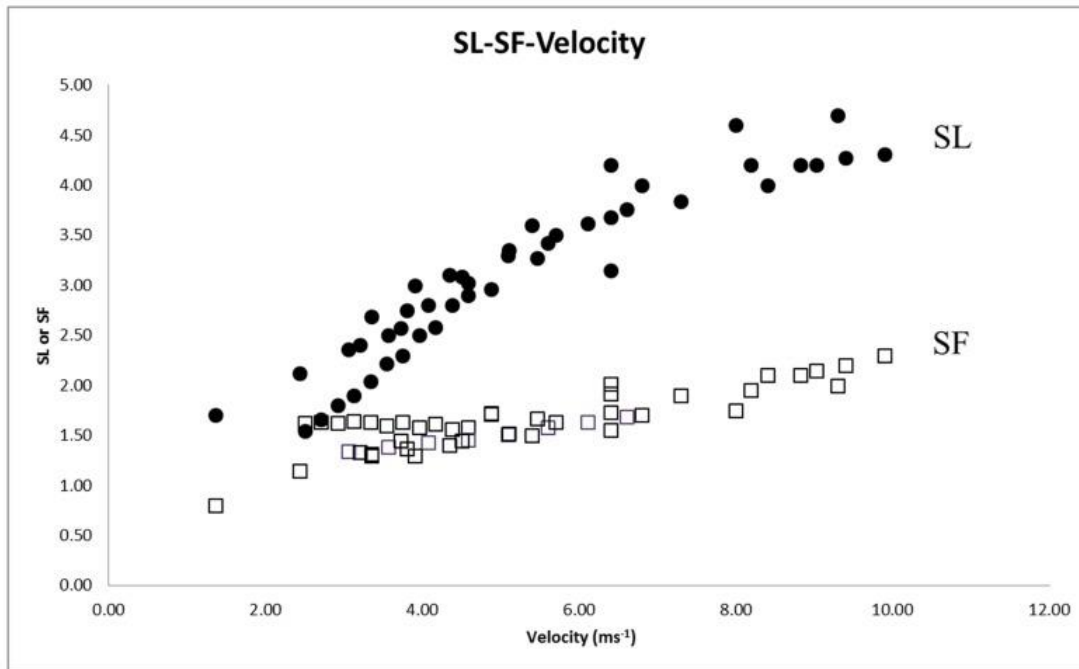


Figure 1.6 Relationship between gait parameters, the stride length (SL) in m, stride frequency (SF) in Hz, and the running velocity in ms⁻¹. Adapted from (J. Bailey et al., 2017)

One can estimate the running speed based on the knowledge of the stride length and stride frequency (SF) or cadence corresponding to twice stride frequency. Both parameters show a particular association with speed, with stride length increases substantially together with the speed at endurance running speeds (Figure 1.6) up to approximately 6 ms⁻¹. Due to this relationship, an increase in SL at a constant SF can lead to an increase in running speeds. However, too much increase in SL can cause the runners to place their foot beyond their CoM position (in sagittal plane), leading to an increased loading of the knee joint due to the impact forces (Lenhart et al., 2014). Instead, to increase the speed, the runner can train to maintain an appropriate SL and try to improve the SF. Even a 10% increase in step rate can lead to a considerable reduction in loading in the knee and hip joints and improvement in the RE due to reduced muscle work (Heiderscheit et al., 2011; Quinn et al., 2021).

1.2.1.2 Kinematics and kinetics of gait

Running is one of the main modes of bipedal locomotion for humans, alongside walking and sprinting. Transition from walking to running happens when periods of double support (both feet simultaneously maintain contact with ground) are replaced by periods of flight (both feet are in air). Unlike walking, the body maintains a forward

lean through the gait cycle during running. To reduce the vertical excursion of the CoM caused by the higher impact forces (due to higher velocities) during running, the lower extremity joints exhibit a greater range of motion (ROM) during the gait cycle (R. A. Mann & Hagy, 1980; Williams, 1985). During the stance phase, the knee flexes to approximately 40° at the initial contact, followed by a flexion up to 60° during the loading phase and back to 40° at the end of the push-off phase. Knee flexion during the stance phase allows the leg to act as an elastic element to store and release the impact energy (Novacheck, 1998). Similarly, the hip is also flexed to approximately 50° at initial contact and extends throughout the stance phase, achieving a slight overextension at toe-off. The knee and hip reach their maximum flexion angle (approximately 125° for the knee and 55° for the hip) during the swing phase (mid-swing), while the ankle joint has its maximum plantarflexion angle at the beginning of the swing phase (Novacheck, 1998). While sagittal motion is the primary basis of the running movement, there is also a rotational component, as the joints of the leg lock to support the body on each side during the stance phase. During the forward motion of the ipsilateral leg, there is a forward motion of the contralateral arm, resulting in a rotation of the rib cage. This counter pelvic rotation is modulated by the spine and helps to dissipate the impact forces during the braking phase (Pontzer et al., 2009). The coordinated movement from the lower limbs to the lumbar-pelvic-hip complex is sometimes referred to as the kinematic chain (larger movement composed of series of joint movements), and its analysis may be crucial to the study of upper limb RRI (Schache et al., 1999).

The kinematics and kinetics of foot contact play a crucial role in running stride, as all the forces and moments are transmitted to the surface through the foot. These contact forces experienced by the foot are known as ground reaction forces (GRFs), and the shape of the force-time curve for GRF has been extensively studied in the literature as it contains information about the forces experienced by the CoM of the body (Hamill et al., 1983; Keller et al., 1996; Munro et al., 1987). The shape of the GRF force profiles is related to the running technique, body mass, speed, and foot strike angle, and has been linked to the RE (Jewell et al., 2017; Moore et al., 2016). The shape of the GRF profile is strongly related to the foot strike angle, with runners with rearfoot strike (RFS) exhibiting a characteristic impact peak in the VGRF profile (Figure 1.7).

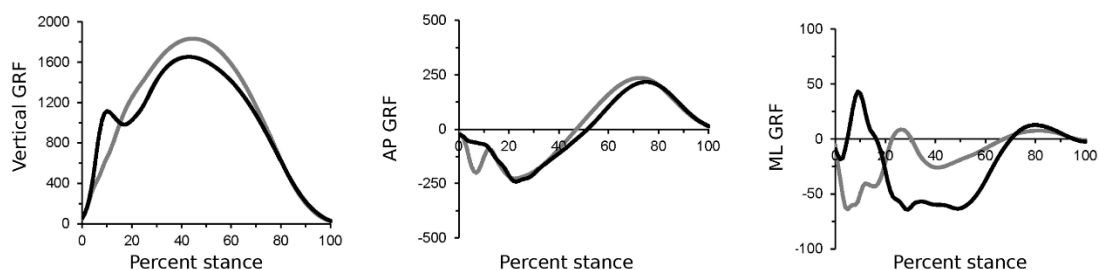


Figure 1.7 Vertical, anteroposterior (AP), and mediolateral (ML) GRF profiles for runners with rearfoot (black line) and non-rearfoot (grey line) strike, with a characteristic impact peak in the VGRF for rearfoot strikers (RFS). VGRF has been of particular interest in literature due to its high magnitude and role in support the CoM of the body. Adapted from (Gruber et al., 2017) with permission from Elsevier.

The anteroposterior GRF (Figure 1.7) are linked to the braking and propulsive sub-segments in the stance phase, where a negative AP GRF impulse slows down the run-

ner and a positive AP GRF impulse lead to an increase in speed. Although AP GRF has not been used to characterize runner populations in the same way as VRGF, it has been linked to the production of mechanical power and used for to study the biomechanics of sprinting (Rabita et al., 2015; Samozino et al., 2016). Compared to VRGF and APGRF, mediolateral GRF is understudied. The loading rate, calculated by dividing the maximal vertical force by the time to the maximal vertical force and measured in terms of defined as bodyweight per second (Bauer et al., 2001), is generally used to characterize differences in the weight acceptance phase of VGRF profiles for different athlete populations (Hamill et al., 1983). For example, due to a reduced loading rate, the time course of the impact force is likely to be delayed runners with mid foot strike (MFS) or fore foot strike (FFS) compared to those with a rearfoot strike (RFS) (Boyer et al., 2014; Gruber et al., 2017). MFS and RFS also result in different forces and moments in the lower extremities, with lower loading in the knee joint for MFS and the ankle joint for RFS (Knorz et al., 2017). In addition to joint loading, the transition to MFS and FFS is easier at higher SF than RFS, thus increasing the likelihood of MFS (or FFS) at higher speeds (Huang et al., 2019). Similarly, FFS and MFS result in greater activation of the tendon springs during the weight acceptance phase (braking phase), allowing for a greater storage of impact energy and improved running efficiency (Alexander, 1991; Lieberman et al., 2010). As foot strike angle directly depends on the muscular activation of the calf muscles, so does the rest of lower limb motion. The common method for measuring muscle activation is surface electromyography (sEMG), and the use of sEMG in biomechanical research has led to extensive studies and results (Luca, 1997). However, an overview of the muscle activity has not been provided here due to the focus of this thesis on the biomechanical assessment in terms of kinematics and kinetics. The following section provides a brief overview of the methods and technologies used for biomechanical assessment in the laboratory and in the field.

1.2.2 *Objective assessment of gait biomechanics*

The goal of gait analysis usually depends on the nature of the research question. Lower limb kinematics, such as the knee flexion angle and the foot strike angle, especially during the stance phase, have been extensively studied in the literature (Dugan & Bhat, 2005). The nature and magnitude of impact forces and their relationship to running speed and injury likelihood are another important area of gait analysis (Darch et al., 2022; Weyand et al., 2000). Finally, the influence of the running environment, such as the use of a treadmill or running track, the speed of the treadmill, the slope of the surface, the type of shoes, the presence of competition, etc., and the condition of the athlete (feeling of fatigue, pain, etc.) also comprise a well-studied field of research (Bon-temps et al., 2020; Halson, 2014; Hamill et al., 1983; Lieberman et al., 2010). Objective instrumented gait analysis using metrological techniques began in nineteen (1872) century with innovations of Marey and Carlet, who combined shoes with air chambers to record the pressure differential generated by foot impact forces and a pneumatic recording system (Baker, 2007; Carlet, 1892; Marey, 1890). These pioneering efforts were followed few years later by photographic techniques developed independently by Muybridge and Demeny (Muybridge, 1882; Pociello, 1999). Braune and Fischer extended this to 3D analysis of gait kinematics and CoM motion in 1895, which was followed by the recording of 3D GRF during walking by an early force plate prototype devel-

oped by Amar in 1916 (Baker, 2007; Braune & Fischer, 1895). The advent of high-speed visible and infrared spectrum still and video cameras, the development of high-sensitivity sensor technology, and its miniaturization with the MEMS paradigm have ushered in the modern era of objective gait analysis. The modality used for gait analysis usually depends on research question, athlete population, and running conditions (Higginson, 2009).

1.2.2.1 Video cameras

Video cameras are typically set up to record gait biomechanics from one of three anatomical planes of motion: sagittal, frontal, and transverse. The cameras are convenient to set up and can provide recordings at a high frame rate (≥ 240 Hz). Because no pre-processing and special software are needed to view the resulting footage, video cameras are also used for subjective observation of gait. They can help physicians, physical therapists, and coaches to identify the presence of abnormalities in running technique such as overstriding, overpronation during stance phase, improper trunk posture, restricted hip and knee flexion, etc., and develop appropriate training and treatment strategies (Souza, 2016). Cameras allow observation of running technique in the form of foot strike patterns (Figure 1.8), lower extremity joint angles, stance foot motion, and near-objective analysis of lower extremity joint angles (Souza, 2016).



Figure 1.8 An example of investigation of foot strike patterns using video footage, where front foot (A), mid foot (B), and rear foot (C) strike can be observed. Figure adapted from (Souza, 2016) with permission from Elsevier.

While automated techniques have been developed to detect and classify human gait (Goffredo et al., 2010; van Mastrigt et al., 2018), accurately investigating the temporal gait parameters using video cameras requires the labelling of different events of the gait cycle (Figure 1.5), such as initial contact (IC) and toe-off (TO). This labelling can be done using video analysis software such as Kinovea¹ (open source), Adobe Premiere Pro² (proprietary), Dartfish³, etc., with the accuracy of estimate depending on the resolution of the temporal parameters and the frame rate of the cameras. Video cameras have also served as reference devices for assessment of motion with other measurement devices in a variety of use-cases, such as running, swimming, and even tracking animal behaviors in the wild (Chakravarty et al., 2019; Hamidi Rad et al., 2021; Lee,

¹ <https://www.kinovea.org/>

² <https://www.adobe.com/uk/products/premiere.html>

³ <https://www.dartfish.com/>

Sutter, et al., 2010). Because of their convenience, cameras can also be utilized in the field to observe a specific section of the race or a portion of the running tracks. For example, video cameras have been used to observe foot strike patterns during marathons and other long-distance running competitions (Larson et al., 2011; Peltonen et al., 2012; Ruder et al., 2019), and on a 400-m running track (Di Michele & Merni, 2014). Video cameras can complement more sophisticated measurement devices such as motion tracking cameras, force plates, and wearable sensors during protocols to check for causes of abnormalities in the recorded data.

1.2.2.2 *Optical motion tracking*

Optical motion tracking systems use infrared camera systems and stereophotogrammetry to record the motion of specific markers attached to the body in a 3D volume (Guerra-filho, 2005). These systems are typically used as gold standard reference for 3D motion quantification during running. Due to the ability of the cameras to record the position of the markers with a resolution of 10^{-3} m, they provide high accuracy and precision (Eichelberger et al., 2016). Markers can be passive, reflecting incident infrared light, or electrically powered to allow the camera system to record their unique labels. Passive markers, which are extremely lightweight and easy to attach, represent the majority of motion capture tracking systems used in running analysis (Higginson, 2009). However, these markers must be attached to specific bony landmarks on the body to reconstruct the skeletal motion and limit errors caused by the muscle stretching/contraction during running motion (Blache et al., 2017). These errors are known as soft tissue artefacts and can be of a large magnitude (2.5 to 10 cm and 8° for orientation) during highly dynamic movements depending on the placement of the marker (Barré et al., 2015; Peters et al., 2010). New methods such as OpenPose and PoseNet have been proposed to make motion capture ‘markerless’ (Cao et al., 2021; Kendall et al., 2015) and avoid the soft tissue artefacts. However, they still need to be improved to replace the widespread use of marker-based systems as the gold standard (Nakano et al., 2020).

The placement of markers on body segments depends on the objectives of the study. a full-body configuration of markers (Figure 1.9a) is typically used to assess both the upper and lower limbs during running (Folland et al., 2017), while a specific marker configuration on the foot can be used to study the foot strike angle (Falbriard et al., 2020). Marker locations obtained through the footage (Figure 1.9b) are usually labelled to specify the location of the bony landmarks (where the markers are attached) and create a 3D representation of the body (Figure 1.9c) using appropriate links between the markers (links between markers provide motion constraints). The links are refined using a skeletal model of the body to obtain the final 3D representation (Figure 1.9d). Predefined configurations for marker attachment have been proposed in literature (R. B. Davis et al., 1991) and some of these have been implemented in commercially available optoelectronic motion capture systems to automatically recognize marker labels (positions on the body), such as the plug-in gait⁴ of Vicon systems. Predefined configu-

⁴ <https://docs.vicon.com/display/Nexus213/About+the+Plug-in+Gait+model>

rations can automate the process of marker labelling, reducing errors and the time required for the process.

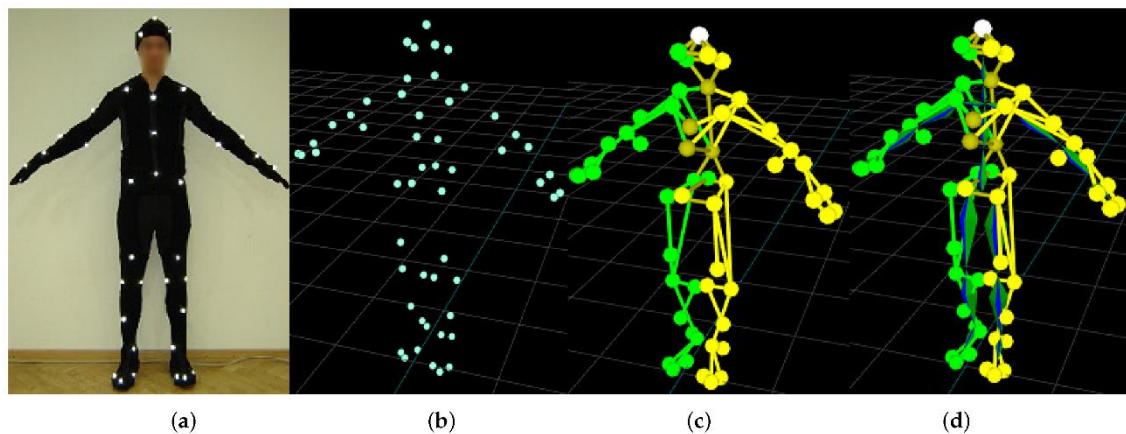


Figure 1.9 Stages of the optoelectronic motion capture process with participant fitted with markers (a), markers registered on camera (b), body mesh (c), and mesh matched skeleton (d). Adapted from (Skurowski & Pawlyta, 2021)

The configuration of the infrared cameras generally depends on the study environment and the volume of motion to be studied, with the cameras usually placed around the periphery of the laboratory. Because of the limitations of the captured volume covered by the cameras and the need to fix the position and orientation of the cameras during and after calibration, running protocols are generally performed on a treadmill (Adams et al., 2016; Folland et al., 2017; Hamner et al., 2010; R. Mann et al., 2014; Maurer et al., 2012; Napier et al., 2019). However, some markers may not be detected or recorded by some cameras because limb movement obstructs the cameras' line of sight. This phenomenon is referred to as occlusion and can affect the accuracy of measurements, along with soft tissue artefacts. Despite these problems, motion capture systems are widely used to accurately measure joint angles, CoM motion, translational and rotational velocities of body segments, and even temporal parameters of gait based on accelerations of foot markers (Handsaker et al., 2016). The latter can be useful in the absence of treadmills or running tracks with force plates.

1.2.2.3 Force plates

Force plate systems are rigid plates supported by three-dimensional force transducers that measure force based on piezoelectric or strain gauge sensors (Wardoyo et al., 2016). By placing a transducer at each corner of a rigid plate, the system can record the reaction forces that the running surface exerts on the runner during the stance phase. These systems are the gold standard method for estimating the force-time profile for vertical ground reaction forces (VGRF); this profile is used to estimate loading rate, understand foot strike pattern, peak force, center of pressure (CoP) trajectory, and push-off and braking impulses (R. Cross, 1999; Dugan & Bhat, 2005; Novacheck, 1998). By establishing appropriate thresholds for the VGRF force-time profile, the initial contact and toe-off events of the stance phase can be identified, which can then be used to estimate the temporal parameters of gait (Falbriard et al., 2018). However, there is no consensus on the magnitude of these thresholds, as some studies have used fixed thresholds (in N) (J. B. Cronin & Rumpf, 2014; Leitch et al., 2011), whereas others have

used threshold dependent on the runner's body weight and/or the recorded value of the peak force (J. B. Cronin & Rumpf, 2014; Falbriard et al., 2018; Williams & Cavanagh, 1987). Force estimated from the force plates, the limb parameters (mass, length, inertia), and the limb kinematics and CoM motion obtained from the motion capture systems, can be combined to estimate the net joint moments and forces using an inverse dynamics approach (Alkjaer et al., 2001; Riemer et al., 2008). This approach utilizes the knowledge of limb kinematics (motion capture data used as reference) obtained using a mathematical gait model to estimate gait kinetics (force plate data used as reference). Thus, the motion capture and force plate approaches together provide a deeper insight into the joint loading caused by a particular running technique (Oh et al., 2013; Skals et al., 2017; Van Hulle et al., 2020).

For gait analysis, the force plate is usually integrated into the track used for running protocols. However, the distinct appearance of the force plate may cause runners to unconsciously adjust their gait to step precisely on the plate. This problem is referred to as 'targeting' and is known to lead to biases in the timing and magnitude of the peak values in the VGRF force-time profile (Challis, 2001). To overcome this problem, the force plates can be camouflaged to visually look like the track, or they can be integrated into a treadmill. The latter solution allows laboratory measurements to control the running speeds and gradients and can be used to study their effects on running biomechanics. However, the dynamics of the treadmill (motor vibrations and resonant frequency of the treadmill) can introduce noise into the signals recorded by the force plates. This necessitates specific signal processing steps to improve the accuracy of the obtained force-time profile (Garofolini et al., 2019; Lieberman et al., 2010; Weyand et al., 2000). The kinematics of running on the treadmill are largely comparable to those of running overground. However, some differences have been observed particularly in the foot strikes angle in the sagittal plane, leads to caution about ecological validity (Van Hooren et al., 2020). In contrast, wearable sensor systems offer the possibility to measure the biomechanics of walking in the field, and therefore a brief overview of some use cases is provided in the following section.

1.2.2.4 *Wearable systems*

Inertial measurement units (IMUs) and global navigation satellite systems (GNSS, often incorrectly referred to as GPS systems in common parlance) have been traditionally utilized for designing inertial navigation systems in vehicles and projectiles (Groves, 2015; King, 1998). However, advances in the micro-electro-mechanical systems (MEMS) technology have led to miniaturization of the IMU and GNSS receiver and reduction in their power consumption and cost, thus enabling their widespread use in commercial wearable devices. As a wearable, the GNSS receiver provides a global position of the user, which can then be used to track the trajectory and speed of movement by athletes. Today, the GNSS sensor is widely used by amateur and professional athletes for winter sports, team sports, running, cycling, etc. and forms the basis of commercial fitness trackers along with heart rate monitors (Sperlich et al., 2020). GNSS receiver is mainly used outdoor as a feedback tool to manage pacing during competitions, depending on the nature of the competition route (Gløersen et al., 2018). During running, the system can be used to maintain a specific speed, which has been set as a target according to the prescribed external load (Halsen, 2014). On training completion, the system can be

used to analyze the variation in speed and evaluate the performance of the athlete during training. The GNSS receivers, however, cannot provide information about the biomechanics of running, thus limiting its potential for analysis of running technique.

IMUs, with their ability to measure acceleration (using a 3-D accelerometer) and angular velocity (using a 3-D gyroscope), have the potential to provide information about limb dynamics during running when attached to a specific limb. While the use of gyroscopes for measurement of spatiotemporal parameters of gait began with their use in walking (Aminian et al., 2002), today IMUs are widely used to analyze running biomechanics in the laboratory and field (Benson et al., 2022; Moore & Willy, 2019). Foot-worn have been used to estimate contact time (t_c), swing time (t_s), flight time (t_f), and gait cycle time (t_g) with an inter-trial median \pm IQR bias less than 12 ± 10 ms and a precision less than 4 ± 3 ms (Falbriard et al., 2018). Furthermore, foot-worn IMUs can also provide an accurate estimation of running speed (0.00 ± 0.11 m/s accuracy and 0.11 ± 0.05 m/s precision), which, in combination with t_g can be used to assess the step length (Falbriard et al., 2021). Inertial sensors, using artificial neural networks, have been used to produce an accurate estimate of knee flexion/extension angles (mean root mean square error $<5^\circ$) and vertical ground reaction forces (root mean square error < 0.27 times the bodyweight) (Wouda et al., 2018). The VRGF profile can subsequently be used to estimate the loading rate and peak VRGF force. Wearable IMUs have shown potential for analysis of lower limb kinematics, with an accurate assessment of foot strike angle, pitch angle at mid-stance, pronation angle before initial contact, heel lift during swing phase, and orientation of the shank (Falbriard et al., 2020; Strohrmann et al., 2011; Zandbergen et al., 2022).

A large number of studies have used an accelerometer attached to the shank to measure the tibial loading and an accelerometer on the head to measure shock attenuation produced by the body between the tibia and the head (Benson et al., 2022). In addition to the spatiotemporal, kinematic, and kinetic parameters of gait, trunk-worn IMU offers an opportunity to measure the movement quality in terms of stability and smoothness (Kiely et al., 2019; Schütte et al., 2018). These metrics characterize proficiency of coordinated movements during running and a reduction in their value has implication for increased energy cost of running. Moreover, inertial sensors can provide continuous analysis of running biomechanics throughout the training or competition (Meyer et al., 2021b). It also enables investigation into variability of the gait cycles and their long-range correlation (complexity). Measurement of these metrics can be useful for the runners due to their relationship to running technique. For example, cycle time variability and its long-range correlations (complexity) are an indicator of running technique, and a potential predictor of running related injuries (RRIs) (Gruber et al., 2021; Meardon et al., 2011), with trained runners showing lower variability and higher complexity (Nakayama et al., 2010). Furthermore, use of IMUs on both feet simultaneously can provide insight into the symmetry running of running gait. Measurement of symmetry during running can help evaluate the risk of overuse injury for a particular limb and test the athlete's readiness to resume training after rehabilitation (Zifchock et al., 2008). Symmetry of gait is also related to the energy cost of running and thus to the RE. 10% increase in the asymmetry in step time and contact time can lead to increased metabolic costs of running, up to 3.5% and 7.8%, respectively (Beck et al., 2018).

While foot-worn IMUs cannot provide direct information about the CoM motion and the vertical stiffness, temporal parameters of gait and running speed can be used to indirectly estimate these parameters. The most common method is through the use of the spring-mass model (Blickhan, 1989), which considers the runner as a point mass and the supporting leg as a linear spring, with the vertical stiffness characterizing the motion of the center of mass (COM) in response to the vertical GRF. By some geometric consideration and modeling the VGRF by a sine-wave (Farley & González, 1996; J.-B. Morin et al., 2005), this model enables an understanding of the storage and return of elastic energy and allows the computation of the vertical stiffness (k_v), maximum vertical excursion of the CoM, and the maximum VGRF. Equations 1.1 to 1.3 detail the computation, with g and m being the gravitational acceleration and the runner's mass respectively. Furthermore, to understand the positive and negative work during running, the duty factor (d_f) of the gait (Alexander 1991) can be estimated using equation (1.4) and the temporal parameters of gait (t_g , t_c , and t_f):

$$k_v = \frac{F_m}{\Delta z} \text{ (kN} \cdot \text{m}^{-1}) \text{ (1.1)}$$

$$F_m = \frac{\pi}{2} m g \left(\frac{t_f}{t_c} + 1 \right) \text{ (N) (1.2)}$$

$$\Delta z = t_c^2 \left(\frac{g}{8} - \frac{F_m}{m \pi^2} \right) \text{ (m) (1.3)}$$

$$d_f = \frac{t_c}{t_g} \text{ (1.4)}$$

Thus, wearable IMUs can provide an accurate description of running gait and the associated movement quality. Table 1.1 provides a non-exhaustive list of biomechanical metrics estimated using wearable IMUs and validated using reference systems. Details into the estimation methods have not provided for the sake of brevity and keeping in line with the broad nature of the overview provided in this chapter. Combined with their cheap cost, unobtrusive nature, wearable inertial sensors and GNSS receiver provide an immense opportunity for the analysis of running biomechanics and performance during in-field training and competition. However, they can also be used during field tests of functional capacity, to improve the capacity estimation and provide additional insights into the biomechanical contributions to the said capacity.

Table 1.1 Non-exhaustive list of biomechanical metrics estimated using body-worn IMUs, based on literature (Clansey et al., 2012; Falbriard et al., 2018, 2020, 2021; Soltani et al., 2020; Strohrmann et al., 2011; S. C. Winter, 2018; Wouda et al., 2018). Metrics shown in *italics* were estimated using IMU on feet and/or trunk

Spatiotemporal	Kinematic	Kinetic
<i>Contact time</i>	Foot strike angle	VGRF peaks
<i>Flight time</i>	Pitch angle at mid-stance	<i>Vertical stiffness¹</i>
<i>Swing time</i>	Pronation angle before IC	Loading rate
<i>Cycle time</i>	Knee sagittal angles	Tibial acceleration
<i>Stride length</i>	Heel lift	Sacral acceleration
<i>Speed</i>	CoM motion	

¹Estimated indirectly using the spring-mass model

1.3 EVALUATION OF FUNCTIONAL CAPACITY

This section provides a short overview of the field tests used to determine the functional capacity of athletes, in terms of their speed, ability to rapidly change direction, and endurance. The importance of each of these capacities, the most common method assessment, and the potential benefits of instrumenting the test with wearable sensors are presented briefly.

1.3.1 Speed

Speed ability is primarily assessed through straight-line sprints or track-based time trials, where the total time taken to cover a specific distance, while running with a maximal effort, is assessed (J.-B. Morin et al., 2012; Peserico & Machado, 2014). The runner usually starts from a crouched position with both hands (Figure 1.10) and one knee touching the ground, while in 'flying' sprint the athlete is already sprinting for 30 m before the start time is recorded. The former is more commonly used and performance in the sprint test is an indication of the ability of the athletes to produce and apply high amount contact force with the ground in the horizontal direction (J.-B. Morin et al., 2011). This ability is important in the context of various sports, due to the need for rapid acceleration from a stationary position (Mendiguchia et al., 2014).

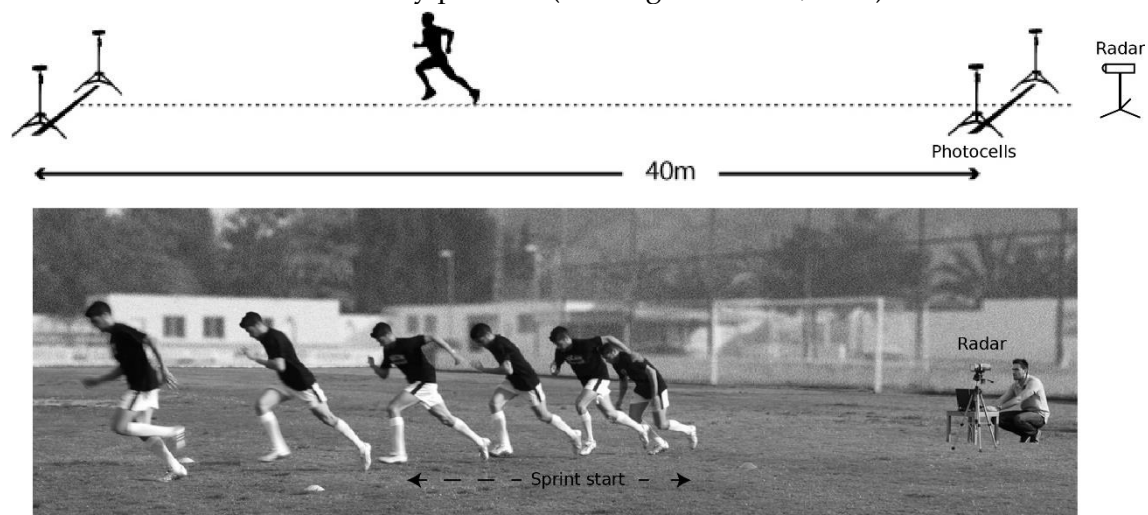


Figure 1.10 Typical setup and protocol for a 40-m sprint test, with a start based on a crouched position. Adapted from (Mendiguchia et al., 2014) with permission from Georg Thieme Verlag KG

Velocity profile obtained during the sprint test is used to create the horizontal force-velocity (F-V) and horizontal power-velocity (P-V) plots for athletes. The relationship between the external horizontal force generation and increasing running velocity can be characterized by the F-V relationship. The extrema of the F-V plot can provide information about the theoretical maximal velocity of the treadmill belt the legs could produce under zero load and theoretical maximal horizontal force the legs could produce over one contact phase at null velocity (J.-B. Morin et al., 2012). The F-V and P-V plots characterize the theoretical mechanical limits of the athlete in terms of individual muscle strength, neuromuscular control, morphological factors, etc. (Cormie et al., 2011). These profiles can thus be crucial for understanding factors limiting performance and designing personalized training programs and evaluating injury risks (J.-B.

Morin & Samozino, 2016). These parameters and the force-power-velocity profiles can be ascertained using the velocity profile during sprint. The prominent model of estimating instantaneous sprint velocity ($v_{mdl}(t)$) is based on the use of a Doppler radar (Furusawa et al., 1927; Samozino et al., 2016) to measure the maximum velocity in combination with the equation below:

$$v_{mdl}(t) = v_{max}(1 - e^{\{-\frac{t}{\tau}\}}) \quad (1.5)$$

where v_{max} is the maximum horizontal velocity during the sprint and τ is a constant, estimated using ensemble experimental data. Obtained velocity profile ($v_{mdl}(t)$) is differentiated to obtain horizontal acceleration, and subsequently the F-V and P-V profiles. Since the Doppler radar requires a skilled operator and can only record one sprinter at a time, instrumenting the sprint test with wearable sensors can aid in widening its application to larger cohorts of runners. While straight line speed is critical for sprinters and endurance runners, the ability for a quick change of direction (COD) is also critical for practitioners of other sports, such as team sports. Following section presents a brief overview of the field test used to evaluate the capacity for COD.

1.3.2 *Change-of-direction ability*

The ability for change of direction (COD) at high speeds is crucial for performance in range of terrestrial sports such as soccer, basketball, tennis, etc. and winter sports like alpine skiing (Sheppard & Young, 2006). The most important factors affecting the technical execution of COD are the angle between the approach direction before and after the COD and speed with which COD is approached. This approach movement can be a combination of forward/backward sprint, shuffle, slalom run, etc. Therefore, these tests can take different forms depending on the COD and the approach movement. A "T" shape of ten yards has been used in many sports such as soccer, basketball, rugby, etc. (Semenick, 1990). A smaller size can be used for combat sports or court games like badminton, etc. (Kamuk, 2020; Sekulic et al., 2017), while a cross shape is used in alpine skiing performance test (Vogt, 2017). Amongst these, the T-test is one of the most commonly used tests for assessing the capacity to quickly change direction (Pauole et al., 2000). It involves five sequential movements: i) Sprint forward (A to B) ii) Shuffle left (B to C) iii) Shuffle right (C to D) iv) iv) Shuffle left (D to B) v) Sprint backwards (B to A), as illustrated in Figure 1.11. The test is scored based on the total completion time, typically measured through photocells positioned at the starting line; a lower timing indicates better performance and a better capacity of athletes to rapidly change direction without losing speed and balance. T-test performance can also provide an insight into the readiness of athlete to return to sport after an Anterior Cruciate Ligament injury (Paterno et al., 2010), due to the role of knee loading in the change of direction.

The COD T-test results have shown poor correlation with other tests such as vertical jump, straight sprint, leg power and leg speed, or lower limb strength (Chaouachi et al., 2009; Pauole et al., 2000; Sassi et al., 2009). It was concluded that a fast COD implied not only strength in the legs or speed, but also coordination, technique, balance, or other physical capabilities that have yet to be defined (Baechle et al., 2008; Young et al., 2015). The athlete needs to aggressively plant their foot on the ground and quickly accelerate off the ground to achieve shorter COD time. To aid this ability, the athlete re-

quires high muscle strength, primarily eccentric, in the knee extensors, hip extensors, plantar flexors, hip adductors and abductors (Spiteri et al., 2013). Eccentric braking capabilities enable the athlete to reduce momentum in current direction of motion, before the accelerating into the new direction of motion (Delaney et al., 2015). This change of momentum makes it crucial to distinguish between the 180° COD (at points D and C in Figure 1.11) and 90° COD (at point B in Figure 1.11).

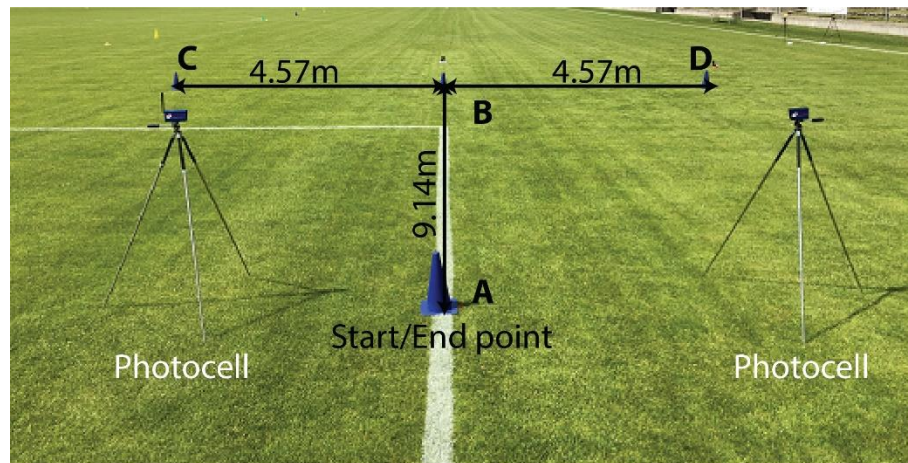


Figure 1.11 Typical setup for a T-test to evaluate the change-of-direction capacity

Evaluation of total completion time does not provide information about these COD, and thus force plates and motion capture systems have been used to investigate the braking/propulsion dynamics at the COD (Havens & Sigward, 2015; McBurnie et al., 2021). To extend these methods in the field, wearable IMUs have been used in conjunction with machine learning methods to estimate the sagittal planes components of the ground reaction force, detect different types of COD movements, and assess the symmetry of bilateral movement between the injured and healthy limb during COD (Gurchiek et al., 2017; McGinnis et al., 2017; Meghji et al., 2019; Stetter et al., 2019). However, these recent advances have led to the presence of many metrics to evaluate the COD performance. This makes the interpretation of the results challenging for the coaches and the athlete, who prefer a system that reduce the total amount of information to the most relevant facts (Roos et al., 2013). Thus, instrumenting the T-test to strike a balance between the amount and usability of information can be valuable.

1.3.3 Endurance

Individual values of physiological variables, especially the endurance capacity, are generally used to prescribe training intensities for runners (Cerezuela-Espejo et al., 2018). Common methods to prescribe exercise intensity use percentage of various markers of endurance capacity such as maximal oxygen uptake ($\dot{V}O_{2max}$) or maximum heart rate (HR_{max}). To enable easier use of $\dot{V}O_{2max}$ for training prescription, it can be translated into a parameter easy to use on the field, such as speed (Berthoin et al., 1994). Consequently, Maximal Aerobic Speed (MAS), i.e., the lowest running speed at which maximal oxygen uptake ($\dot{V}O_{2max}$) occurs (Hill & Rowell, 1996), is commonly used to prescribe training intensities (Bellenger et al., 2015; Berthoin et al., 1994). However, at the same percentage of $\dot{V}O_{2max}$, athletes can exhibit different levels of lactate accumu-

lation (T. Mann et al., 2013). Therefore, it can also be beneficial to prescribe training intensity in zones close to ventilatory (VT) or lactate thresholds (LT), as they represent sub-maximal individual metabolic response (Vago et al., 1987). Like MAS, the speed at the second VT (sVT2) can be used to make it easier to measure threshold-based training intensity in the field, and speed at first ventilatory threshold (VT1) is a fundamental to ensure pure aerobic stimulus, especially in the polarized training model (Muñoz et al., 2014). Gold standard for MAS and sVT2 estimation remains laboratory treadmill test, which involves the measurement of breath composition using a gas analyzer while the speed of treadmill is slowly increased (Figure 1.12A)

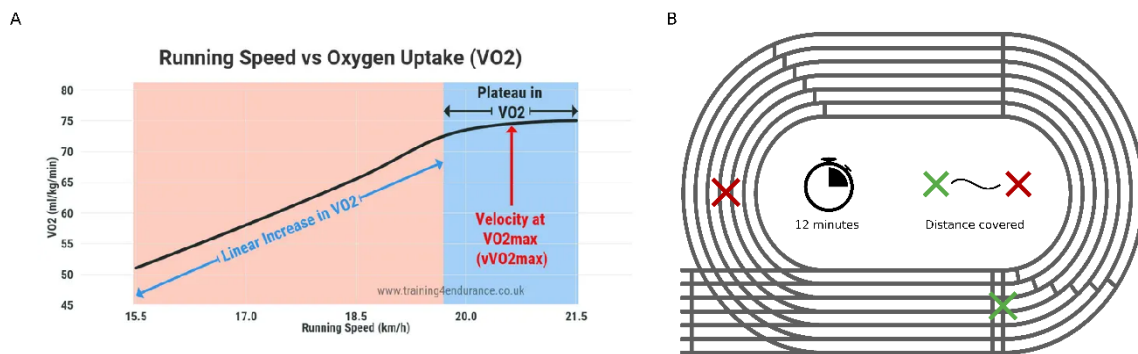


Figure 1.12 Tests for estimating the maximum oxygen uptake A. Change in the oxygen uptake ($\dot{V}O_2$) during an incremental speed test on a treadmill, the velocity reached at the maximum oxygen uptake ($\dot{V}O_{2max}$) is known as the $v\dot{V}O_{2max}$ or the maximum aerobic speed (MAS) B. Typical setup for a 12-minute Cooper test in the field, the distance includes the number of laps times 400 m plus the remaining distance on the last lap. Adapted from training-endurance.co.uk

The gold standard test, however, requires trained personnel, expensive equipment and can only be performed with/for one runner at a time (Bellenger et al., 2015; Paradisis et al., 2014). To overcome this problem, field tests have been developed which are simple, cost effective, and do not require specialized instrumentation (O'gorman et al., 2000). This allows them to be incorporated within routine training programs, with possible repetitions through the season. Some important field tests for endurance capacity are the Université de Montréal track test, the 20-m shuttle run test, the 12-minute running test, and time-trials over a set distance from 1200 and 2200 m, with 2000 m being optimal (Bellenger et al., 2015; Cooper, 1968; L. A. Léger et al., 1988; L. Léger & Boucher, 1980). First two tests involve audio cues that indicate the athlete to increase speed whereas the third assumes maximum effort at self-selected running speed, making it easier to implement with a large cohort in parallel. For motivated young runners, the 12-minute Cooper test provides an accurate estimation of the VO_{2max} (Bandyopadhyay, 2015; Cooper, 1968) using the following equation:

$$\dot{V}O_{2max} = 22.351 \times d - 11.288 \quad (1.6)$$

where VO_{2max} is measured in $ml \cdot kg^{-1} \cdot min^{-1}$ and d is the distance covered in kilometers during the 12 minutes. The VO_{2max} values obtained using equation (1.6) provide a good prediction of half-marathon finishing times and are correlated well with the race performance (Alvero-Cruz et al., 2019). However, the race performance also depends on the RE, which, in turn, is influenced by the running biomechanics (Moore, 2016).

Therefore, it can be worthwhile to investigate the biomechanics during the 12-minute Cooper test and understand their contributions to endurance performance.

1.4 THESIS OBJECTIVES AND OUTLINE

Running technique is one of the crucial factors that explain the variance in performance and economy between runners of varied skills levels (Folland et al., 2017). Training with proper running technique is essential to ensure positive adaptation to training stimulus and reduction in the risk of injury (van Mechelen et al., 1993; Vanrenterghem et al., 2017). In this context, it would be valuable to assess the proportion of a run performed with optimal technique or the proportion of training for which optimal technique could be maintained despite fatigue. Fatigue has been shown to introduce changes in running technique, like shifting the landing mechanics from front foot to midfoot running (Jewell et al., 2017) in fore foot runner, increase in the impact forces, decrease in knee flexion at landing (Mizrahi, Verbitsky, & Isakov, 2000), change in contact and aerial times (J. B. Morin, Samozino, et al., 2011), etc. These changes in technique seem to be the result of both peripheral and central fatigue (Millet, 2011; E. Ross et al., 2007), which describe the reduction in motor output or muscle force and lead to a general feeling of 'exertion' or 'tiredness' respectively. Current research shows that stability (Schütte et al., 2018) and smoothness (Kiely et al., 2019) of the trunk motion, i.e., the ability to maintain a coordinate motion pattern of the lumbar-pelvic-femoral complex, tend to decrease with increased duration of running, likely due to acute fatigue. Neither internal nor external training load metrics can provide information about the influence of fatigue on technique, thus making biomechanical assessment a unique independent descriptor of training sessions. Furthermore, this assessment is crucial for personalization of training, since there is no single perfect running technique, but different techniques are optimal based on the height, weight, strength, injury history, experience, etc. of the athlete (Gindre et al., 2015; Lussiana & Gindre, 2015). Running power, which is amount of mechanical work achieved/performed by the runner per unit time, can provide an insight into the relative force being produced by the athlete for a give pace (van der Kruk et al., 2018). Since increasing the applied force needs additional metabolic energy, outputting more power at a lower heart rate can be an indicator of increased running efficiency, when performed on the same ground/surface/level. Thus, running power can complement the description of running technique for assessing the performance during races or training sessions. Therefore, the goals within the first part of this thesis are the identification of reliable trends associated with fatigue state/onset on running motion, their measurement using wearable sensors, and the estimation of running power using the same or simpler sensor setup.

Maximal capacity measured by functional testing is typically used to personalize the training program for athletes (Figure 1.4) to ensure appropriate training stimuli and optimal positive adaptation. To improve the accuracy of these tests and provide deeper analyses of the athlete strengths/weaknesses, the second part of this thesis aims to instrument a series of three functional tests using wearable sensors; the selection is based on common tests used in a variety of sport contexts. *Sprint test*: The method described

in equation 1.5 to estimate the sprint velocity provides ease of use, it is only valid when the athletes can approach or attain v_{max} , which might not be the case over short distances such as 30 m or they may not be able to maintain v_{max} over longer distances such as 60 to 100 m, especially during training sessions. In addition, maximal sprinting may not always be desirable, especially when resuming training after an injury. Thus, the sprint velocity profile for all athletes does may not always show a first-order exponential behavior. Since GNSS sensor alone cannot track the velocity during push-off (Nagahara et al., 2017), one goal in the thesis was the instrumentation of the sprint test.

T-test: One disadvantage of the COD T-test is that it does not allow precise isolation of the athlete's weaknesses. The cause of limited performance could be a lack of stability, power, technique, strength, speed, etc. Therefore, the COD test can be used to show a drop in the athlete's performance, but it is very difficult to understand the underlying cause. One reason for this is that traditional performance evaluation is based only on the total time of the COD test. As a result, quantitative analysis of the duration of each phase would be a valuable tool for coaches to identify athletes' weaknesses in a particular movement sequence or COD type. For example, an athlete might be particularly poor at running backward or slower at one of the 180° cuts due to a knee injury. Therefore, instrumenting the T-test to automatically detect the five different phases test would be valuable. *12-minute run test*: Running mechanics govern the mechanical power and propulsion generated for a given energy cost and thus influence the RE (Beattie et al., 2014; Moore, 2016; Saunders et al., 2004). Measurement of RE during field running requires the use of portable gas analyzer, which is expensive and inconvenient, while in-field running biomechanics can be assessed accurately and conveniently using wearable inertial measurement units (IMUs) (Camomilla et al., 2018). Running mechanics are modifiable with training and adopting an economical running technique can improve RE and hence performance (Moore, 2016; Saunders et al., 2004). Furthermore, visual classification of running technique according to RE has not proven reliable (Cochrum et al., 2021). Therefore, assessment of running biomechanics during a field capacity test could greatly improve the information obtained regarding endurance capacity and help identify the biomechanical factors that contribute to endurance performance.

Throughout the following chapters, the pronoun 'we' is preferred when referring to a study with multiple authors. From these chapters, the algorithm development for the T-test was carried out during the supervision of a master thesis at EPFL. Work on the sprint test and running power estimation was conducted in collaboration with industrial partner GaitUp S.A. (now Mindmaze S.A.), as a part of the industrial secondment for the EPFLInnovators Fellowship. Except for chapter 4, all other protocols and studies were conducted in real-world conditions. To clarify my contributions to these studies (Chapter 2 - 7), a note is added at the beginning of each chapter. The figure below presents an outline of the thesis, with the two main parts highlighted.

Chapter 1 introduces the concept of training quantification for running, highlighting the role of biomechanical assessment in improving the current paradigm of training. It provides an overview of the biomechanics of running movement and their assessment using a variety of instrumentation. The potential of wearable sensors in improving the

assessment of performance during training is introduced. Finally, the concept functional capacity testing in sports is presented using three field tests and a perspective is provided on their augmentation using wearable sensors.

Introduction

Biomechanical assessment for fatigue and power analysis

- C2. Review on fatigue
- C3. Half-marathon analysis
- C4. Power estimation

Augmentation of functional capacity tests

- C5. Sprint test
- C6. COD test
- C7. Endurance test

Conclusion

Figure 1.13 Outline of thesis with the two main parts, biomechanical assessment for fatigue and power analysis (chapters 2, 3, and 4) and augmentation of functional capacity tests (chapters 5, 6, and 7)

Chapter 2 presents a systematic review of literature on the influence of fatigue on lower extremity biomechanics, with the goal of investigating (i) typical protocols used in research on biomechanical response to running-induced fatigue, (ii) the effect of sport-induced acute fatigue on the biomechanics of running and functional tests, and (iii) the consistency of analyzed parameter trends across different protocols. The review presented evidence that running-induced acute fatigue influences almost all the included biomechanical parameters, with crucial influence from the exercise intensity and the testing environment. Results indicated an important gap in literature caused by the lack of field studies with continuous measurement during outdoor running activities. To address this gap, recommendations for the use of wearable inertial sensors were proposed in the chapter.

Chapter 3 introduces a study exploring the evolution of the biomechanical and psychological facets of acute fatigue during a half-marathon. It provides trends for the changes in the spatiotemporal parameters, symmetry, and variability of gait and the stability and smoothness of the trunk motion. Results provided here hint toward a higher sensitivity of perceived fatigue to neuromuscular changes in the running gait.

Chapter 4 proposes and evaluates three different methods to estimate running ‘power’ using foot-worn inertial sensors. Each method uses features based on gait spatiotemporal parameters, accelerometer and gyroscope signals and is customized for level, uphill, and downhill running conditions. The performance of the methods is validated using the reference ‘power’ measured using force plates. The effects of varying signal-to-noise-ratio (SNR) on the estimation error are explored and a short perspective is provided on the usage of these methods in the field.

Chapter 5 suggests a new method to estimate the instantaneous velocity during straight line sprinting using a sensor fusion approach, by combining the signals from wearable Global Navigation Satellite System (GNSS) and inertial measurement unit (IMU) sensors. This method uses a combination of a gradient descent-based orientation filter and a simple Kalman filter to estimate the velocity and the sprint duration, respectively. Validation of the proposed method using a reference system is provided and the nature of the resultant velocity profile is discussed.

Chapter 7 presents the process of instrumenting the change-of-direction T-test using a wearable GNSS-IMU sensor. The methods introduced in this chapter enable the segmentation of the T-test into its individual phases and allow the analysis of the four COD maneuvers. The results of the algorithm are validated using a video camera as a reference, with the data being collected from an elite soccer team during their preseason training camp.

Chapter 8 discusses the relative contribution of running biomechanics to the endurance performance during a 12-minute Cooper test. It explores different methods of estimating the distance covered in the Cooper test using a wearable global navigation satellite system (GNSS) receiver. It compares the high/low performance groups using statistical tools and extracts the most relevant metrics explaining the contrast in their performance.

Chapter 9 provides a general discussion about the contribution of the current thesis, the limitations of the proposed methods, and recommendations for future work. It also presents Finally, it presents a biomechanical profile representing the running technique and its temporal evolution with acute fatigue, identifying different profiles for runners with highest and lowest endurance performance. This profile could potentially be used in standardized functional capacity measurements to improve personalization of training and rehabilitation programs for athletes.

II. BIOMECHANICAL ASSESSMENT FOR PERFORMANCE AND FATIGUE ANALYSIS

2 BIOMECHANICAL RESPONSE OF LOWER EXTREMITIES TO ACUTE FATIGUE

The systematic review presented in this chapter was the first step towards identifying biomechanical parameters that show consistent trends in response to acute fatigue and identifying a wearable sensor setup to measure them. Furthermore, the study reviewed typical protocols used in research on biomechanical response to running-induced fatigue, the effect of sport-induced acute fatigue on the biomechanics of running and functional tests, and the consistency of analyzed parameter trends across different protocols. Scopus, Web of Science, PubMed, and IEEE databases were searched using terms identified with the Population, Interest and Context (PiCo) framework. Studies were screened following the Preferred Reporting Items for Systematic Reviews and Meta-Analyses (PRISMA) guidelines and appraised using the methodological index for non-randomized studies MINORS scale. Only experimental studies with at least 10 participants, which evaluated fatigue during and immediately after the fatiguing run were included. Summary trends were computed for each parameter based on the results found in individual studies. Of the 68 included studies, most were based on in-lab (77.9%) protocols, endpoint measurements (75%), stationary measurement systems (76.5%), and treadmill environment (54.4%) for running. From the 42 identified parameters, flight time, contact time, knee flexion angle at initial contact, trunk flexion angle, peak tibial acceleration, CoP velocity during balance test showed an increasing behavior and cadence, vertical stiffness, knee extension force during MVC, maximum vertical ground reaction forces, and CMJ height showed a decreasing trend across different fatigue protocols. This work presented evidence that running-induced acute fatigue influences almost all the included biomechanical parameters, with crucial influence from the exercise intensity and the testing environment. Results indicate an important gap in literature caused by the lack of field studies with continuous measurement during outdoor running activities. To address this gap, recommendations for the use of wearable inertial sensors were proposed.

The contents of this chapter have been adapted from the article:

Apte, S.¹, Prigent, G.¹, Stöggl, T., Martínez, A., Snyder, C., Gremeaux-Bader, V., & Aminian, K. (2021). Biomechanical response of the lower extremity to running-induced acute fatigue: a systematic review. *Frontiers in physiology*, 1076.

¹Equal first authorship

Contributions: Performed the systematic search, information extraction, evidence synthesis and conducted the article screening, risk of bias assessment, and study selection, for a portion of articles. Contributed to the study design, discussion of the obtained data and results, and mainly authored the final article.

2.1 INTRODUCTION

Appropriate management of acute fatigue resulting from a training stimulus and aimed at triggering positive adaptation is essential to optimize athletes' adaptation to a training program and reduce their risk of injury (Kellmann et al., 2018). Biomechanical parameters are altered by acute fatigue and therefore these parameters are of interest to re-measure during/after training interventions to investigate how they are affected (Paquette et al., 2020). In this context, acute fatigue refers to the onset of fatigue that occurs concurrently with the exercise activity, with its influence measured during and/or within 30 minutes of the activity. Fatigue is a complex, multifactorial phenomenon characterized by a decrease in work capacity and the inability to muscularly exert the required force to perform simple or more complex tasks (Enoka & Duchateau, 2008; J. L. Taylor et al., 2016). Studying the mechanisms of fatigue development is a complex task, and surrogate measures of fatigue exist, such as a self-reported score and changes in neuromuscular function, biomechanical parameters, and physiological processes (K.-L. Taylor et al., 2012; Thorpe et al., 2017). Physiological responses are generally assessed by monitoring heart rate, blood lactate, near-infrared spectroscopy, measurement of gas exchange, etc., while the rating of perceived exertion (RPE) and visual analog scales (VAS) are used to measure the subjective feeling of fatigue (Thorpe et al., 2017). Neuro-muscular function and maximal force production capacity are usually tested with functional tests such as vertical jump tests, balance tests, and maximal voluntary contraction tests, using performance measures such as maximal jump height, center of pressure movement, and maximal knee flexion moment, respectively (Thorpe et al., 2017). Finally, motion capture systems, force plates, and video analysis are generally used to analyze biomechanical changes (Thorpe et al., 2017). Recently, body-worn IMUs, GNSS receivers, and pressure sensor-based insoles have been used to measure biomechanical changes instead of optical motion capture systems in the laboratory because the former allow measurements in the field (Buckley, O'Reilly, Whelan, Farrell, et al., 2017; Eskofier et al., 2012; Strohrmann, Harms, Kappeler-Setz, & Troster, 2012).

In this work, the biomechanical response of the lower extremities was investigated as a surrogate measure of sport-induced acute fatigue. Kinematics, kinetics, and muscle activity of the leg during running and spatiotemporal gait parameters comprise the lower extremity biomechanical response, in addition to the functional tests mentioned above. Lower extremity injuries are the most common injuries in sports (Emery et al., 2005; Nicholl et al., 1995), especially in athletics (Alonso et al., 2010). Because biomechanical changes are activity-specific and context-dependent, the selection of relevant athletic activities is critical. In track and field, running is an important component of competitive activities and training schedules. Training factors such as high accelerations and large absolute training loads leading to repeated acute fatigue states are an important risk factor for overuse injuries, especially in endurance running (Clansey et al., 2012; Francis et al., 2019; Mizrahi, Verbitsky, & Isakov, 2000, p. 200; Warden et al., 2014). Therefore, the focus of this research is limited to running activities, e.g., short- and long-distance runs, and fatigue protocols on the track and treadmill, using running and/or functional tests as assessment tasks. Examples of such running activities include races such as marathons, half marathons, trail running, etc., and protocols such as re-

petitive sprints, incremental speed tests, etc. A better understanding of the influence of fatigue on biomechanical changes during running and functional testing involving lower extremity neuromuscular response may allow for better management of training load and injury risk.

The current literature on the influence of fatigue on running gait parameters shows conflicting results. For example, one study showed a decrease in contact time after fatigue (J. B. Morin, Samozino, et al., 2011), while another study found no change (J. B. Morin, Tomazin, et al., 2011); one study reported a decrease in peak knee flexion angle during stance phase (Chan-Roper et al., 2012), while another reported an increase (Jewell et al., 2017). The tasks used to induce fatigue varied considerably, ranging from medium-intensity high-volume activities such as ultra-marathons (J. B. Morin, Tomazin, et al., 2011) and 24-hr treadmill runs (J. B. Morin, Samozino, et al., 2011) to severe-intensity intermittent activities like repeated sprints (M. Johnston et al., 2015) or soccer matches (Matthews et al., 2017). Previous reviews (Giandolini et al., 2016; S. Winter et al., 2017) have attempted to examine these conflicting findings on the influence of fatigue on running. However, the first of these papers included a small study sample, considered only distance running, and did not categorize the level of fatigue; the second study was not a systematic review and focused more on graded running and its effects on physiological measures. Neither review presented summary trends nor commented on the sensor systems used for measurement. Therefore, this chapter addresses the primary research question, "How does exercise-induced acute fatigue affect the biomechanics of running and functional tests?" Secondary questions aimed to understand the dominant biomechanical metrics used in fatigue research while examining the consistency of their behavior across studies and the influence of fatigue protocols. The scope of this review is limited to research examining lower extremity biomechanical response in healthy adults published between 1990 to 2021. Only studies in which running was used as the fatiguing activity and analyzed using non-invasive methods during the activity and/or immediately after the activity are included.

2.2 METHODS

2.2.1 *Search strategy and sources*

The search strategy was based on the Population, Interest and Context (PiCo) framework, with the goal of locating studies, which explicitly report the experience of fatigue in healthy adults participating in sport activities (da Costa Santos et al., 2007). The search terms for each of these three categories were combined with a Boolean 'AND' (Table 2.1). 54 search items excluding irrelevant publication types were combined with a Boolean "AND NOT". Scopus, Web of Science, Pubmed, and IEEE databases were searched for papers published from 1990 to 2021 in English language.

Table 2.1 Details of the PiCO strategy used to conceptualize search terms. The following terms were used with a 'AND NOT' to exclude them: "supplement" OR "supplementation" OR "nutrition" OR "diet" OR "therapy" OR "doping" OR "pregnancy" OR "patients" OR "junior" OR "adolescent" OR "ingestion" OR "accident" OR "compression garments" OR "age" OR "animals" OR "immersion" OR "food" OR "disease" OR "epidemiology" OR "fracture" OR "stimulation" OR "dogs" OR "horses" OR "rehabilitation" OR "treat-

ment" OR "concussion" OR "kids" OR "teenagers" OR "military" OR "obese" OR "obesity" OR "weight loss" OR "music" OR "swimming" OR "basketball" OR "rowing" OR "handball" OR "softball" OR "volleyball" OR "badminton" OR "tennis" OR "ice hockey" OR "skiing" OR "boxing" OR "cricket" OR "wrestling" OR "golf" OR "weightlifting" OR "martial art" OR "climbing" OR "gymnastics" OR "kayaking" OR "fencing" OR "shooting" OR "diving" OR "diesel" OR "gas" OR "engine" OR "cycling" OR "football" OR "soccer" OR "rugby" OR "ultramarathon"

Population	Interest	Context
Healthy adults doing sports Elite/non-elite	The experience of fatigue	Sports activities: running
"healthy" OR "athletes" OR "players" OR "sportperson" OR "runners"	"fatigue" OR "exertion" OR "exhaustion" OR "prolonged" OR "marathon" OR "ultramarathon" OR "long distance"	"run" OR "running" OR "endurance" OR "prolonged" OR "long distance" AND ("wearable" OR "sensors" OR "measure" OR "measurements" OR "reporting" OR "assess" OR "evaluate" OR "investigate" OR "collect" OR "collected")

2.2.2 Eligibility criteria

Following the PRISMA method (Liberati et al., 2009), studies obtained from the aforementioned databases were screened using the criteria mentioned below. If all the relevant information to exclude an article was available in the abstract, it was excluded at this stage. If not, the full-text of the articles was screened for compliance. Parameter trends from individual studies were summarized based on significant results and thus wanted to include publication having a reasonable statistical power. However, there is no consensus on the exact number of participants, as the sample size should be estimated based on the expected power and the effect size. Furthermore, a higher cut-off for the number of participants would lead to a larger number of studies being excluded. Thus, a cut-off of 10 participants was used as an appropriate compromise between statistical power of the reported trends and publication exclusion criteria. In addition, this study aimed to understand the evolution of fatigue measurement protocols over the recent decades, especially with regarding the use of wearable sensors and conducting in field measurements. Since the use of wearable sensors was limited before 1990, only studies conducted 1990 onwards were included. For detailed screening criteria, please refer to the Appendix A1.

Inclusion criteria:

- Investigation of acute fatigue induced by one of the sporting activities mentioned above (as primary or secondary outcome) using non-invasive methods.

- The studied sporting activity should involve primarily lower extremity exertion in which running is the dominant activity.
- A study population of at least 10 healthy adults (between 18 and 65 years old) engaged in sports activities.
- Original experiment-based research (systematic review/review/meta-analysis excluded).
- Clear description of the nature of activity, measurement conditions, and sensors used for measurements.
- Measurement of the effect of fatigue on biosignals during or before/after sporting activity.
- Measurement of the effect of fatigue on biosignals within 30 minutes after sporting activity and description of the measurement outcomes with respect to the last training or event

Exclusion criteria:

- Studies that investigate neither running biomechanics nor functional test parameters
- Studies that focus only on physiological responses (brain electrical activity (EEG), electrocardiogram (ECG) or respiration) of fatiguing exercises.
- Studies that only consider biochemical parameters such as lactate, creatine kinase, cortisol, etc. or questionnaires to assess the effect of sport-related fatigue, without using any additional sensors
- Focus was on the evaluation of psychological effects of sport on mental health
- Sole investigation of recovery time or training program after fractures, concussion or any other injuries related to sport.
- Analysis of the effects of various therapies to reduce fatigue
- Investigation of the influence of specific environmental conditions or performance-enhancing substances on fatigue or for training
- Fatigue protocols based on the use of specific exercises, such as repetitive movements or strength training, instead of sporting activities.

2.2.3 Study classification and data extraction

The methodological quality of the selected studies was appraised quantitatively using the validated “methodological index for non-randomized studies” (MINORS) scale (Slim et al., 2003a). The items (see Appendix A2) were scored zero (not reported), one (reported but inadequate), or two (reported and adequate). The total score was normalized by the maximum possible score to obtain a final value between zero and one. The score of each study was used as a weight index for computing the general trends for each extracted parameter. Details of this method can be found in section 2.2.5 and Appendix A2.

Each study was summarized by two authors to record information about the participant demographic, the study protocol, and the reference methods to assess fatigue. Following data about the study protocol were extracted:

- A. *Exercise intensity*: While the level of fatigue is difficult to quantify (Enoka & Duchateau, 2008), it is important to state the level of fatigue reached by the athletes. Thus, the intensity of the fatiguing activity, was graded into four catego-

ries based on the critical power model (Morton, 2006): i) *moderate* - can be continued more than 1 hours, below aerobic threshold, typically in a range of 65-75% of the maximal oxygen uptake (VO_2max) ii) *heavy* - can be performed up to 1 hour, lactate increase, between aerobic and anaerobic thresholds, in a range of 80-90% VO_2max iii) *severe* - which is tolerable for up to 30 minutes, no steady state of VO_2 , muscle metabolic and blood acid-base responses, above anaerobic threshold iv) *high-intensity intermittent* - repetitive efforts such as repetitive sprints or interval runs. It is hereafter referred to as *intermittent* for the sake of brevity.

- B. *Reference*: Criteria used for ascertaining the exercise intensity and designing the fatigue protocol. Examples of these include the measurement of VO_2max , blood lactate, heart rate reserve, and questionnaires. In absence of any information about these methods, nature of competitive activities such as marathons or soccer matches was recorded.
- C. *Environment*: The measurement environment (laboratory or field). Regarding running biomechanics, treadmill and overground evaluations of fatigue were analysed separately, as the biomechanical response to treadmill running may differ from overground running (Van Hooren et al., 2020).
- D. *Timing*: The timing of the data collection to assess fatigue — *continuously* during protocol, *intermittently*, or at the *endpoints* i.e. the beginning/end or before/after the fatigue protocol;
- E. *Measurement system*: Specifications of the measurement systems, in terms of usability, whether they are wearable or stationary;
- F. *Parameters*: The parameters used to assess the effects of the fatigue activity and their category (see 2.2.4 and 2.2.5). Trend for every parameter in response to acute fatigue or an insignificant change was noted.

2.2.4 Parameter definition

Parameters used to assess fatigue were extracted, followed by their respective qualitative trends, whether they increase, decrease or do not change. These parameters were classified into five categories spatiotemporal, kinetic, kinematic, functional test, and muscle activity. The first three categories i.e. the spatiotemporal, kinetic and kinematic parameters are directly relevant to running biomechanics and thus, are extracted only from studies which investigated the influence of fatigue on running. The spatiotemporal (ST) parameters are derived from basic variables reflecting the spatiality and temporality of foot-based placements; they contain cadence, contact time, flight time, stride length, and step width. The kinematic (KM) category refers to the positions, angles, velocities and accelerations of body segments and joints during run. The kinetic (KT) category describes the joint torques, forces, stiffness, and ground impact aspects of running mechanics. The muscle activity (MA) parameters included in this review comprise the electrical activity measured using electromyography (EMG). Finally, functional test (FT) refer to the set of metrics used to analyze jump tests, voluntary maximum contraction (MVC), balance and walking tests. These functional tests are generally used to understand the influence of sport-induced fatigue on neuromuscular function. Unlike the previous three categories, extraction of parameters linked to MA and FT categories was not limited to studies investigating running biomechanics. Since

most of the included parameters are well-known in the fields of sport science; definitions of those parameters are not explained in this work. Description of EMG metrics and complex parameters, such as local dynamic stability (LDS) coefficients are available in the Appendix A3.

2.2.5 *Data synthesis*

Four subgroups were created to consider the intensity of the fatiguing task (moderate, heavy, severe, or intermittent). For the running biomechanics, two subgroups were created to separate treadmill and overground environments. This led to eight subgroups for ST, KM and KT categories, and four subgroups for FT and MA. A parameter was included in data synthesis only if, at least, one of the subgroups had a total number of participants greater than 30, all studies merged. A threshold of 30 participants might correspond to three studies with at least 10 participants or one study including more than 30 participants. This allowed computation of a meaningful median value even if two of those three studies had opposing trends and thus the obtained summary trends would also be meaningful.

The first part of the data synthesis was to collate the number of studies pertaining to the general information from the protocol referring to information A to E in section 2.2.3. The second part was the computation of summary trends for the list of parameters extracted to assess fatigue. Median (MED) and median absolute deviation (MAD) were utilized for this purpose (see Appendix A4), since these are a non-parametric and robust metrics. Parameters with MAD value greater than 0.5 were considered to have no trend, i.e. no consistency across studies. MAD lower than 0.1 indicated agreement across studies and was characterized as “clear decrease” if MED was negative, “non-significant change” if MED equal to zero, and “clear increase” if MED was positive. For $0.1 < \text{MAD} < 0.5$ the trends were characterized as “partial decrease”, “non-significant change” or “partial increase” respectively.

2.3 RESULTS

2.3.1 *Study selection*

The literature search produced 1640 records, which were screened using the process suggested in the PRISMA statement (Liberati et al., 2009) (Figure 2.1A). After removing 20 duplicates, abstracts of the remaining 1620 papers were screened using the criteria described in section 2.2, resulting in 1237 records being excluded. The full-text of the remaining 383 records was assessed for eligibility and 68 studies were included for the final evidence synthesis. The relevant parameters were extracted and classified using the categories defined in section 2.4 (references for each are shown in Figure 2.1B). Detailed summary of the selected studies can be found in supplementary materials⁵.

⁵ https://figshare.com/articles/dataset/Data_Sheet_1_Biomechanical_Response_of_the_Lower_Extremity_to_Running-Induced_Acute_Fatigue_A_Systematic_Review_xlsx/16457868

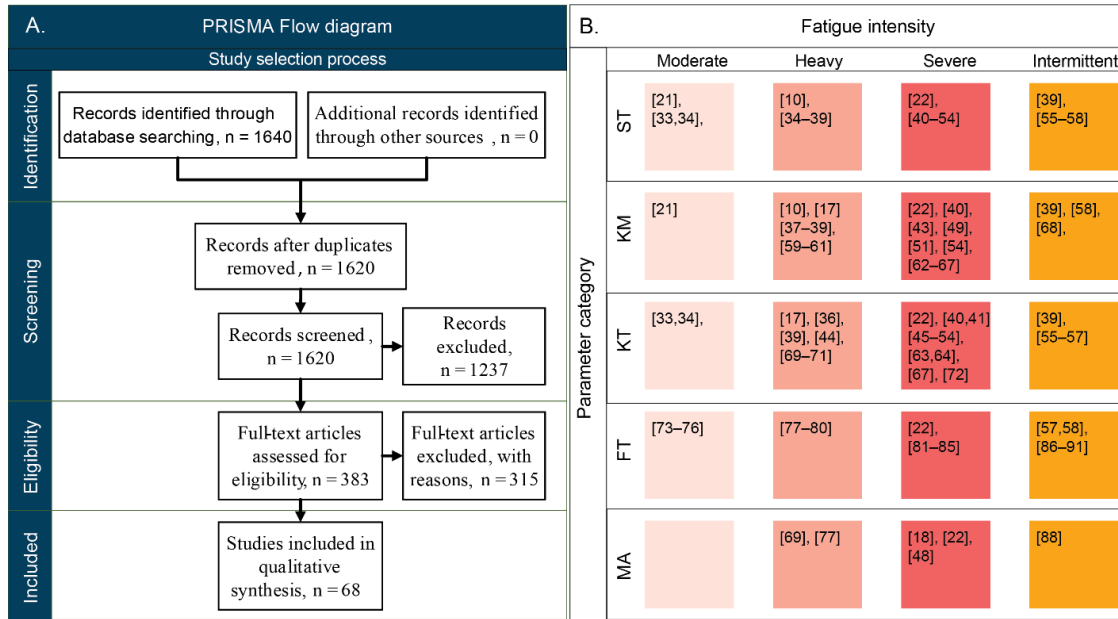


Figure 2.1 Study selection and categorization process. A. PRISMA flow chart for study selection. B. References for the included 101 studies (Abt et al., 2011; Alfuth & Rosenbaum, 2011; Ammann & Wyss, 2015; Anbarian & Esmaili, 2016; Anna et al., 2017; Avogadro et al., 2003; J. P. Bailey, Dufek, et al., 2018; Bisiaux & Moretto, 2008; Borrani et al., 2003; Bovalino et al., 2020; Chan-Roper et al., 2012; Clansey et al., 2012, 2016; Derrick et al., 2002; Dierks et al., 2010; Dittrich et al., 2013; Dutto & Smith, 2002; Easthope et al., 2014; Garcia-Perez et al., 2014; García-Pinillos et al., 2016; Gerlach et al., 2005; Girard et al., 2016, 2017a, 2017b; Gómez et al., 2002; Goodall et al., 2015; Hamacher et al., 2018; Hanley & Mohan, 2014; Hayes & Caplan, 2012; Hoenig et al., 2018; Jewell et al., 2017; M. Johnston et al., 2015; Kolbauer et al., 2014; Maas et al., 2018; Mercer et al., 2003; Mizrahi, Verbitsky, & Isakov, 2000; Mizrahi, Verbitsky, Isakov, et al., 2000; Mo & Chow, 2018b; Möhler et al., 2021; Nagel et al., 2008; Perrey et al., 2010; Rabita et al., 2013; Racinais et al., 2007; Radzak et al., 2017; Riazati et al., 2020; Ribeiro et al., 2018; Rosenbaum et al., 2016; Rosso et al., 2016; Rousanoglou et al., 2016; Sánchez-Sánchez et al., 2018; SILER & MARTIN, 1991; Steib et al., 2013; Stirling et al., 2012; Strang et al., 2008; Strohrmann, Harms, Kappeler-Setz, & Tröster, 2012; Timmins et al., 2014; Verkerke et al., 1998; Voloshin et al., 1998; Weist et al., 2004; Willems et al., 2012; Willson & Kernozek, 1999; Wu et al., 2008; P. Yu et al., 2020, 2021), presented according to the fatigue intensity and the parameter category, where ST: spatiotemporal, KM: Kinematic, KT: Kinetic, FT: Functional test, and MA: Muscle activity parameters. Studies that utilized machine-learning approaches (Buckley, O'Reilly, Whelan, Vallely Farrell, et al., 2017; Eskofier et al., 2012; Op De Beeck et al., 2018) and considered only statistical features are not included in the table as they do not fit into any of the five parameter categories

2.3.2 Characteristics of selected literature

2.3.2.1 Nature of activities

Most of the selected studies involved between 11 and 20 participants (69.2%), with only 11 studies testing more than 30 subjects (10.6%) and a median MINORS index of 0.75. Detailed score for all 68 studies is presented in supplementary material S1. The number of participants ranged from 10 to 459, with a median (MAD) of 20 (± 8) participants. Participants were a mixture of professional, semi-professional, and amateur athletes. While the exact definition of fatigue is not typically stated, six different methods

(Figure 2.2A) were commonly used to investigate the level of fatigue. Questionnaires like the RPE and VAS were the most used reference (31 studies), followed by custom-designed protocols (VO₂max attainment, exhaustion protocols) to justify fatigue (21 studies), and blood lactate measurements (14 studies). The least used methods were based on heart rate and competitive racing events.

The exercise intensity was predominantly severe (52 studies), with protocols such as running until exhaustion (Figure 2.2). Heavy protocols represented 27 studies, while endurance-running activities, classified as moderate, were less commonly included (10 studies). Intermittent protocols such as repeated sprints and high-intensity interval running constituted 27 studies. Majority of the protocols studied spatiotemporal and kinetic parameters, with muscle activity being the least studied parameter group. Detailed information of the selected studies can be found in supplementary materials⁶.

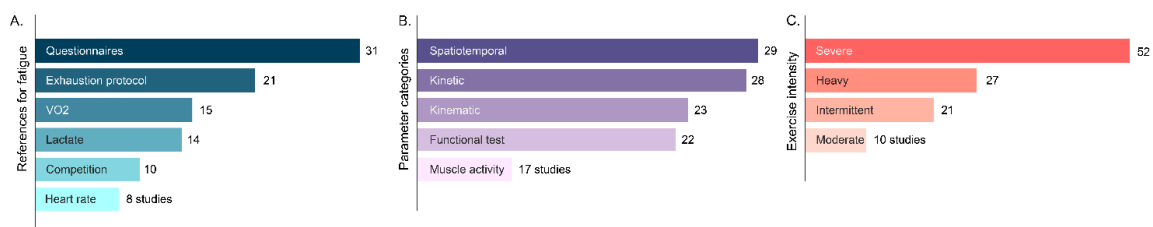


Figure 2.2 Number of studies according to the different aspects of a fatigue protocol. A. Reference methods used to 'ascertain the fatigue intensity; B. Parameter categories studied by the included protocols; C. Exercise intensity investigated

2.3.2.2 Nature of measurement environment

Studies in each of the five parameter categories were classified based on both their measurement system (stationary vs. wearable), and measurement environment (lab vs. field). As shown in Figure 2.3, measurements in the studied literature were mainly performed in-laboratory (77.9%) and typically with stationary measurement systems (76.5%) such as optical motion capture, instrumented treadmill, or force plates. Few studies used wearable sensors such as IMU, GNSS, pressure sensor-based insoles, heart rate telemetry, wireless EMG, or portable gas exchange systems allowing field measurements, which agrees with the low percentage of in field protocols (22.1%). The number of studies analyzing sports-induced fatigue increased from 24 to 51 after 2010 (Figure 2.4), with a similar increase (9 to 14) for studies using wearable sensors. However, the ratio between the number of studies with stationary and wearable systems hardly changed over time. An important aspect of the protocol is the timing employed to perform the measurements. A majority (54%) of the papers included used endpoint assessments by collecting data before and after the fatiguing exercise, followed by intermittent (30.4%) and continuous (15.6%) assessments.

⁶ https://figshare.com/articles/dataset/Data_Sheet_1_Biomechanical_Response_of_the_Lower_Extremity_to_Running-Induced_Acute_Fatigue_A_Systematic_Review_xlsx/16457868

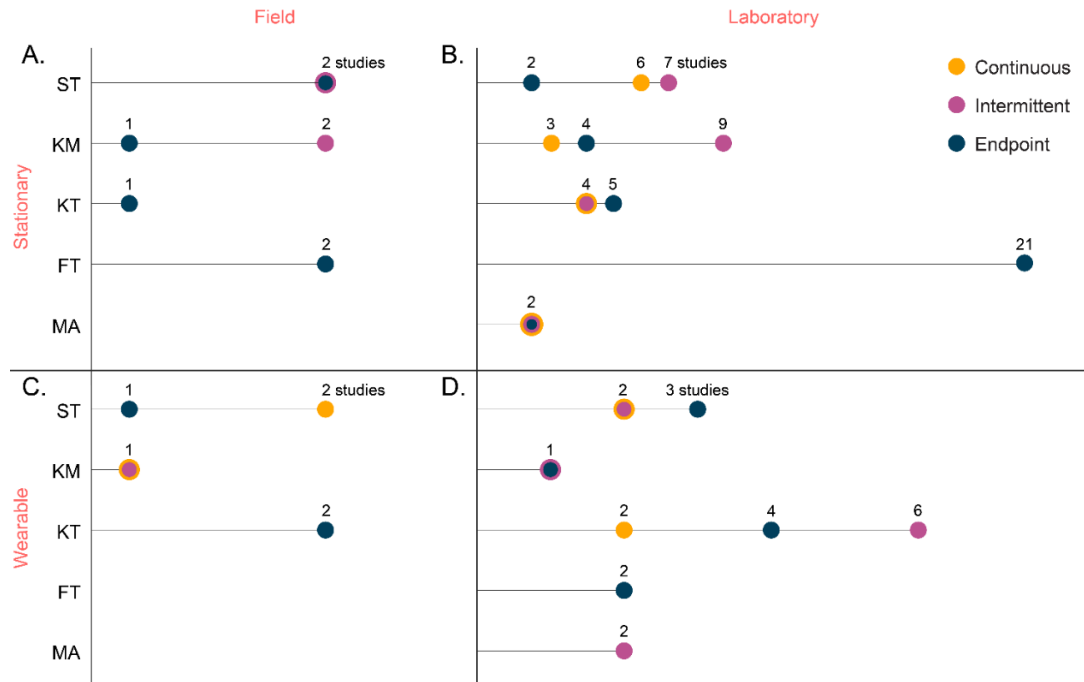


Figure 2.3 Number of studies per parameters category grouped in terms of the timing of the measurement (continuous, intermittent, endpoint) sensors (wearable vs stationary) and location (field vs laboratory). A) Field & stationary B) Laboratory & stationary C) Field & wearable D) Laboratory & wearable. The four sub-figures do not have the same scale on the x-axis. ST: gait spatiotemporal, KM: kinematics, KT: kinetics, FT: functional test, and MA: muscle activity

Most of the studies (71.3%) performed fatigue assessment in laboratory settings using stationary systems (Figure 2.3B). Furthermore, functional tests were usually conducted before/after the fatigue protocol (endpoint) in both laboratory and field environments (Figure 2.3A-B), typically with stationary measurement systems.

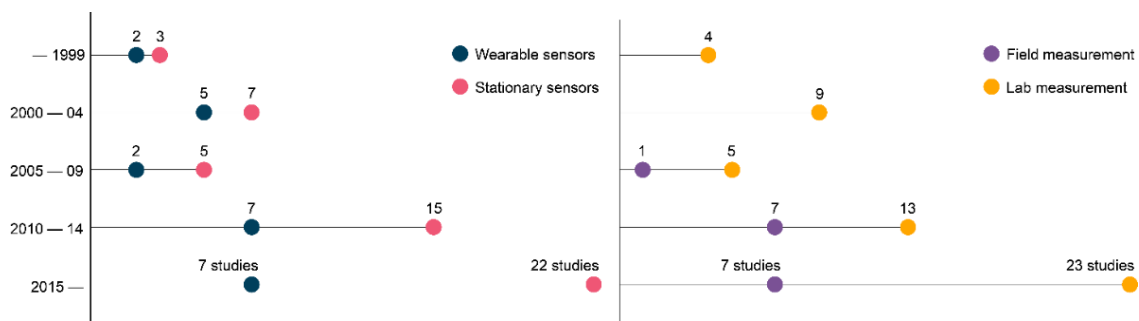


Figure 2.4 Number of studies utilizing wearable and stationary measurement systems and conducting research in lab and in field. The number of studies has increased drastically after 2010, yet the number of field studies and those using wearable sensors has remained low

Wearable sensors, despite their potential for field use, were mainly used in laboratory (Figure 2.3D) for assessing ST, KT or MA parameters continuously and intermittently. Out of the 68 studies, not more than three studies assessed ST, KM or KT parameters continuously or intermittently in field, using wearable sensors (Figure 2.3C).

2.3.3 Parameters for analysis

The systematic extraction of parameters used by the studies to assess fatigue produced a list of 101 metrics. After removing parameters extracted on less than 30 participants (all studies merged), final list of 42 parameters was obtained, as shown in Table 2.3. Supplementary material⁷ contains the complete list of metrics.

2.3.1 Parameter trends

Of the five gait ST parameters considered, cadence was measured most often and step length the least. Apart from cadence, contact time and flight time, which presented reliable and consistent trends (increase) across all different conditions, the trends obtained for stride length (Table 2.2) were dependent on the fatigue protocols and the running environments. Of the 12 parameters in the KT category, only maximum ground reaction force (Max GRF), vertical stiffness, and leg stiffness presented a consistent trend (decrease) across the different exercise intensities and running environments. Max GRF was also the most used metric (12 studies), followed by vertical and leg stiffness (10 studies each). Peak tibial and head acceleration (PTA & PHA) are two parameters extracted from body-worn accelerometers; PHA showed different trends between overground and treadmill running environments. Within the 11 KM parameters investigated, LDS was the least studied (1 study) and the peak knee flexion angle the most studied (7 studies). Peak knee flexion angle at initial contact (IC) and peak trunk flexion showed a clear increase for severe intensity during treadmill running, while ankle plantarflexion angle IC presented a clear decrease. Pelvic and thoracic LDS parameters are documented only for overground running with severe intensity and pelvis rotation range of motion (ROM) and anterior tilt for treadmill running with severe intensity; all present a clear increase due to fatigue.

Table 2.2 Parameter trends in response to acute fatigue, with M: moderate, H: heavy, S: severe, and I: intermittent exercise intensities. For a parameter, S: number of studies with significant results, T: Total number of studies measuring it. Arrows represent following trends, $\downarrow\downarrow$: clear decrease, \downarrow : partial decrease, $\uparrow\uparrow$: clear increase, \uparrow : partial increase, \leftrightarrow : non-significant change, $\uparrow\downarrow$: no trend, and \downarrow : insufficient participants (<30). GRF: ground reaction force, FTI: force-time integral, IC: initial contact, ROM: range of motion, f/e: flexion/extension, LDS: local dynamic stability, CMJ: countermovement jump, SJ: squat jump, DJ: drop jump, CoP: centre of pressure, MVC: maximum voluntary contraction, iEMG: integration over the EMG signal, and MF: median frequency

Parameters	Treadmill				Overground				S/T
	M	H	S	I	M	H	S	I	
ST	Cadence (steps/min)	—	$\downarrow\downarrow$	\downarrow	$\downarrow\downarrow$	\downarrow	\downarrow	\downarrow	14/22
	Contact time (ms)	—	$\uparrow\uparrow$	\uparrow	$\uparrow\uparrow$	$\uparrow\uparrow$	\uparrow	$\uparrow\uparrow$	17/20
	Flight time (ms)	—	\downarrow	$\uparrow\uparrow$	\uparrow	—	—	\downarrow	7/9
	Stride length (m)	—	\uparrow	$\uparrow\downarrow$	\leftrightarrow	$\downarrow\downarrow$	\downarrow	\downarrow	8/16

⁷ https://figshare.com/articles/dataset/Data_Sheet_2_Biomechanical_Response_of_the_Lower_Extremity_to_Running-Induced_Acute_Fatigue_A_Systematic_Review_xlsx/16457868

KT	Max GRF (N)	—	↓	↓↓	↓	↓	↓	↓↓	—	7/10
	Loading rate (N/s)	—	—	↑↓	↓	—	↓	—	—	4/5
	Peak pressure – metatarsal (Pa)	—	↓	↑	—	↑↑	↓	↑↓	—	6/10
	FTI – heel (N)	—	—	↓	—	↔↔	↓	↔↔	—	4/8
	FTI – midfoot (N)	—	—	↑↑	—	↑↓	—	↑	—	4/6
	FTI – metatarsal (N)	—	—	↔↔	—	↑	—	↑	—	5/11
	FTI – toes (N)	—	—	↑	—	↓	—	↑↓	—	4/7
	Peak tibial acceleration (PTA)	—	↑	↑	—	—	↑	—	—	2/8
	Peak head acceleration (PHA)	—	↓	↔↔	—	—	↑	—	—	3/6
	Vertical stiffness (N/m)	—	↓↓	—	↓↓	—	↓	↓	—	8/9
	Leg stiffness (N/m)	—	—	—	↓	—	—	↓↓	—	6/8
	Mechanical work (J)	—	—	↔↔	—	—	—	—	—	1/3
KM	Knee – max. flexion angle (swing)	—	↑↑	↔↔	—	↓↓	↓	—	—	5/7
	Knee – flexion angle at IC	—	—	↑↑	—	—	—	—	↓	2/3
	Knee – ROM f/e angle (stance)	—	↔↔	↑↑	↓	—	—	—	—	2/6
	Hip – ROM f/e angle (stance)	—	↓	↑	↓	—	—	—	—	3/4
	Hip – max adduction angle	—	↑	↑	↓	—	↓	—	—	3/6
	Ankle – PF angle at IC	—	—	↓	—	—	↓↓	—	↓	3/5
	Trunk – max flexion angle	—	↑↑	↑↑	—	—	↓	—	—	5/6
	Pelvis – anterior tilt	—	—	↑↑	—	—	—	—	—	2/2
	Pelvis – rotation ROM	—	—	↑↑	—	—	—	—	—	2/2
	Pelvis and thorax – LDS	—	—	—	—	—	—	↑↑	—	1/1
		M		H		S		I	N	
FT	CMJ height	↓↓		—		↓		↓		5/7
	SJ height	—		—		—		↓		1/2
	DJ stabilization time	—		—		↑↑		—		1/1
	Balance - CoP velocity	—		—		↑↑		↑		2/3
	MVC force (knee extension)	—		↓		↓		↓↓		6/7
	Sprint completion time	—		—		—		↑↑		3/3
	Walking - contact time	↓↓		—		—		—		1/1
	Walking - peak pressure toes	↓↓		—		—		—		1/1
	Walking - total foot contact area	↓↓		—		—		—		1/1
	Walking - forefoot loading imp.	↓↓		—		—		—		1/1
	Gait LDS - dual task walking	—		—		↑↑		—		1/1
MA	iEMG quadricep	—		↓		↑↓		↓		4/5
	iEMG hamstring	—		↓		↓		—		1/3
	iEMG calf	—		↓		↓		—		3/5
	iEMG shin	—		↓		↔↔		—		2/4
	MF Calf	—		—		↔↔		—		1/3

Functional tests were always performed before and after the fatiguing activity, to assess the change in the neuromuscular function. Evaluation based on functional tests does not directly involve a running task and thus, distinction between evaluation on treadmill and overground is irrelevant for this parameter group. Countermovement jump (CMJ) height and isometric MVC knee force were the most frequently studied parameters, both being analyzed in 7 studies and showing a clear decrease due to acute fatigue. Moreover, CMJ height showed the same behavior for moderate and intermittent fatigue, thus showing a consistent behavior across different fatigue protocols. DJ stabilization time was only studied for severe fatigue, and it presented a clear increase. The balance related parameter, center of pressure (CoP) velocity, presented a clear increase due to intermittent and severe intensity protocols.

Metrics from walking as a functional test were obtained from one study with 200 participants and only for moderate fatigue. Contact time, peak pressure, total foot contact area and forefoot loading impulse, showed a clear decrease. Sprint completion time was measured by three studies and showed a clear increase, i.e. worse sprint performance, after intermittent fatigue. The MA parameters were found to be assessed only in studies with severe and heavy intensity protocols. Of these, only iEMG (intergrated EMG signal) calf and iEMG hamstring presented a clear decrease. The other parameters (iEMG and RMS) presented non-significant changes or non-consistent trends (Table 2.2).

2.4 DISCUSSION

2.4.1 *Response to fatigue*

2.4.1.1 *Influence of exercise intensity*

The exercise intensity can modulate the response of the neuromuscular system and running biomechanics to acute fatigue. Indeed, stride length, impact force-time integral, peak tibial acceleration, max knee flexion angle during swing, and knee flexion/extension ROM during stance present different trends for different fatigue protocols, when controlled for the running environment. Aerobic metabolism mainly fulfills the energy requirement in the moderate and heavy protocols and a combination of aerobic and anaerobic metabolism in severe and intermittent protocols (Morton, 2006). It has been suggested that short-term high intensity activities mainly lead to peripheral fatigue (Perrey et al., 2010), whereas high volume activities, especially prolonged running, can lead to central fatigue (Millet & Lepers, 2004), in addition to structural and metabolic modifications. These mechanisms can potentially explain the differences in the neuromuscular response between different fatigue protocols (Brownstein et al., 2020). While there is a wealth of research (Gibala et al., 2012; Laursen, 2010) on long-term adaptation to various exercise intensities, further research to understand the mechanisms leading to the differences in the short-term responses is necessary.

Some parameters, despite the differences between the running environment and the fatigue intensity, presented a consistent response to acute fatigue. Cadence, contact time, flight time, peak tibial acceleration, trunk flexion angle and knee flexion angle at IC increased due to fatigue, not necessarily by the same relative magnitude. Similarly,

max GRF, vertical and leg stiffness responded to acute fatigue by showing a decrease in magnitude. The trends for GRF, knee, and trunk kinematics are in line with a previous review (S. Winter et al., 2017) on the effect of fatigue due to prolonged running, albeit for a study sample of 12. Current work computed the trends not only for prolonged running (S. Winter et al., 2017), but also for shorter, more intense running and interval running. Therefore, it allows for the comparison of parameter trends across different protocols and exercise intensities, highlighting the differences and similarities between the responses to different conditions.

2.4.1.2 *Acute fatigue affects the impact load attenuation and leads to a sub-optimal running technique*

Calf muscles play a crucial role in regulating the stiffness of the muscle–tendon units to tolerate and absorb high impact loads at the beginning of the ground contact and the braking phase (Kyröläinen et al., 2005; Rabita et al., 2013). Acute fatigue leads to a lowered pre-activation in calf muscles, as evidenced by the decreasing trend for iEMG (Table 2.2). This hampers the ability of musculoskeletal system to absorb the energy from impact, sustain the impact loads, and return the stored elastic energy in a coordinated manner during push-off (Avela & Komi, 1998). Reduced absorption of the impact forces is likely to explain (Sheerin et al., 2019) the observed clear increase in peak tibial acceleration during the initial phase of ground contact (Voloshin et al., 1998). The increase of knee flexion angle during initial contact, linked to a lowered vertical stiffness (Table 2.2), might be an alternative attenuation strategy, an adaptation to overcome neuromuscular deficits. Another possible adaptation might be the increase in the relative proportion of ground contact time, thus distributing the impact impulse over a longer duration and reducing peak impact forces (Strohrmann, Harms, Kappeler-Setz, & Tröster, 2012). Peak impact forces can be a risk factor for bone stress injury (I. S. Davis et al., 2016; Hreljac, 2004; Warden et al., 2014), thus highlighting the importance of this result for injury prevention.

Forward leaning, as well as the variability of trunk movements, increase with the fatigue of the lower back muscles (Table 2.2). This might increase injury risk by increasing the strain on the hamstrings and the back during running (Koblbauer et al., 2014; Maas et al., 2018). However, certain studies have also suggested that increased trunk flexion during running might be a compensatory strategy for shock attenuation (Saha et al., 2008). Further investigations should consider the relationship between running kinematics and core stability, their causality, and to what extent these relations affect performance and injury risk.

The observation that acute fatigue leads to a decrease in vertical max GRF (Table 2.2), can be linked to a series of kinematics, kinetics, and muscular adaptations throughout fatiguing activities. The observed rise in contact time, in accordance with muscle fatigue, indicates that runners are not able to lift their feet off the ground as fast as before. Consequently, the push-off force is distributed over a longer duration, with a decrease in the max GRF (S. Winter et al., 2017). This decrease in the maximal force production capacity of the lower limb muscles during the push-off phase is confirmed by the decrease in the generated force during knee extension movements within the MVC tests.

Increased knee and trunk flexion/extension angles, along with a reduction in vertical stiffness, point to an increased vertical motion of the center of mass (COM) due to acute fatigue. According to the spring-mass model, a decrease in vertical stiffness is consistent with the decrease in max GRF and an increase in the vertical displacement of the COM caused by the rise in maximum knee and hip flexion/extension angles and range of motion. These trends are confirmed by our results (Table 2.2) and they support the rationale for increased vertical motion of the COM due to acute fatigue.

Energy efficiency during running is maintained partly by the elastic structures (tendons and muscles) in lower limbs, through the storage and return of elastic potential energy generated from the impact with ground (Novacheck, 1998). The lowered calf muscle activity, increased peak tibial acceleration (PTA) and the vertical displacement of COM, indicate an increased transfer of the impact energy to the COM of the body and a reduction in the elastic potential energy absorbed from impact. Furthermore, a major source of energy loss (Bertram & Hasaneini, 2013) in running is the transition of the body motion from downward to upward direction in each gait cycle. An increase in this vertical motion of the COM, thus points towards a lowered energy efficiency in running gait and a suboptimal running technique. However, it is difficult to ascertain whether the changes in running biomechanics originate from a strategy to protect against injuries or represent a fatigue-induced loss of optimal performance capabilities, or a combination of both.

2.4.2 *Role of functional tests*

CMJ tests typically measure the capacity of the leg extensor muscles to generate mechanical power (Schmitz et al., 2014), whereas MVC tests (Peñailillo et al., 2013) measure the capacity of leg muscles to exert their maximum force against resistive apparatus. Results (Table 2.2) show a decreased hamstring and calf muscles activation, also indicated by the decreased MVC force and increased sprint completion times. This can be explained by neuromuscular alterations, which provoke a slower rate of muscle force production possibly via slower recruitment of motor units.

To date, most research on sport-induced fatigue has been focused on the acute physiological and neuromuscular responses. As indicated in (Degache et al., 2014), postural control is a permanent re-establishment process of balance, which depends on the orientation information derived from the somatosensory, vestibular, and visual inputs sensory sources. Based on relevant postural muscles, the central nervous system actively controls balance. Our results (Table 2.2) show that acute fatigue affects balance, underlined by the consistent increase in the balance parameters such as CoP velocity, LDS, and stabilization time in DJ. These results are consistent with the observation (Nardone et al., 1997) that participating in exhaustive physical activities can lead to a deterioration of the proprioceptive sensory information or its integration, thereby adversely affect the efficiency of the neuromuscular system.

2.4.3 *Influence of protocols*

Treadmill running biomechanics may differ from overground running (Sinclair et al., 2013; Van Hooren et al., 2020) during the foot strike, in terms of peak propulsive force

and sagittal plane joint kinematics like hip flexion/extension angles and range of motion (ROM), knee flexion angle and ROM, foot strike angle and COM vertical displacement. While debated (Van Hooren et al., 2020), some studies also indicate differences in muscle activity, impact peak GRF, and tibial forces (Baur et al., 2018; Kluitenberg et al., 2012; Milgrom et al., 2003). To investigate if these differences modulate the influence of fatigue on running, summary trends for the treadmill and overground running studies were computed separately. For the same exercise intensity, the two running environments led to different trends (Table 2.2) for stride length, peak impact pressure, and impact force-time integral. Thus, there is a considerable interaction between fatigue and type of running ambulation (i.e. treadmill or overground) for parameters directly related to foot strike, in agreement with the results from (Garcia-Perez et al., 2014; Strohrmann, Harms, Kappeler-Setz, & Tröster, 2012).

Fatigue typically leads to a reduction in speed while running overground (Bertram & Hasaneini, 2013), indicated by increased sprint completion time in a fatigued state and a simultaneous decrease in cadence and stride length for moderate intensity acute fatigue. While professional athletes tend to modulate their pace tactically while running overground in competitions (Dierks et al., 2010), studies in this review typically used constant speed exercises on treadmills to analyze the effects of fatigue. Running speed has a direct influence on spatiotemporal parameters (J. P. Bailey, Silvernail, et al., 2018) and forcing a specific treadmill speed prevents fatigued athletes from modulating their running mechanics naturally. Non-motorized treadmills can allow the athletes to run at self-selected speeds, however they can lead to an increased metabolic demand as compared to overground running at the same speed (Edwards et al., 2017); higher metabolic demands can accelerate the development of fatigue. Furthermore, compliance of the running surfaces can affect the ground contact time, step length, plantar loading, and metabolic cost of running (McMahon & Greene, 1979; Smith et al., 2016), thus highlighting the critical nature of the running surface while testing.

2.4.4 *Recommendations for an IMU-based wearable sensor setup*

As seen in earlier section, there is a difference between the results for treadmill and overground running in a fatigued state, especially due to the alternations in speed caused by fatigue while running overground. To improve the translatability of results, in field monitoring of the response of running mechanics to fatigue is essential. Furthermore, continuous measurement of biomechanics during the run can enable an understanding of the temporal evolution of the running technique in response to acute fatigue. If the alterations in running technique are too drastic and occur during several consecutive sessions, it can be an indication of poor adaptation to training. Wearable sensors allow for a continuous measurement during overground and treadmill running and across different real-world contexts such as outdoor training and competitive races. Wearable sensors can also allow the rehabilitation of runners suffering from running-related injuries, based on real-time feedback of running biomechanics and by combining the movement data with the applied training load (Methods et al., 2015). Early detection of such alterations using wearable sensors can be helpful to prevent adverse training adaptations.

Considering the importance of field measurement, some recommendation about the usage of wearable sensors may be helpful. The first step towards the design of an IMU-based wearable sensor setup is the selection of the parameters for measurement. Here, the parameters that showed consistent trends for the influence of acute fatigue (Table 2.2) could be a starting point. Among these parameters, sagittal plane knee angles and vertical GRF can be estimated with one sensor on the shank and one on the sacrum (Lee, Mellifont, et al., 2010; Wouda et al., 2018); contact time, flight time, and vertical stiffness can be computed from either a sensor on the shank or the sacrum. However, foot-based IMUs and pressure insoles provide higher accuracy for the estimation of contact time and GRF (Falbriard et al., 2018) respectively. It is possible to estimate stride length as a combination of the running speed measured from a shank or an upper back sensor (Apte, Meyer, et al., 2020; Yang et al., 2011), and the cadence from a sacrum or foot sensor (Falbriard et al., 2018; Lee, Mellifont, et al., 2010). While previous research has shown the measurement of sagittal hip angles to be possible for fast movements (Fasel et al., 2018), the accuracy of this measurement is susceptible to soft tissue artefacts.

Apart from these biomechanical parameters in running, a single IMU located on the lumbar spine (L1) has been used for the assessment of vertical jump height (Setuain et al., 2016) and postural control ability (Neville et al., 2015). Thus, a minimal sensor configuration (Figure 2.5) based on only three or four sensors: one unit on the shank, one on the sacrum, one on lumbar spine (L1), and optionally one IMU on the foot or pressure insoles could enable the measurement of the evolution of biomechanical parameters in response to acute fatigue. The sensors on shank and foot can be placed on both legs if the goal is also to investigate symmetry. Previous studies on this topic either focused on the biomechanics of the whole body (Op De Beeck et al., 2018; Strohrmann, Harms, Kappeler-Setz, & Tröster, 2012) or a specific body segment (Clansey et al., 2012; Derrick et al., 2002; Garcia-Perez et al., 2014; Mizrahi, Verbitsky, & Isakov, 2000; Voloshin et al., 1998), thereby limiting the outcomes or being cumbersome to replicate. The suggested configuration offers a good balance between the number of sensors and the possibility to study a broad range of parameters that present a reliable response to acute fatigue. Algorithm development in the future might reduce the number of requisite sensors to only one IMU on the trunk (sacrum or L1).

For the measurement using wearable sensors, a static period of few seconds at the start of the run is recommended to facilitate the calibration of the sensors. The sampling rate (SR) of the used sensors should be set according to the movement of interest. For example, a SR of at least 500Hz is recommended for measuring impact acceleration at the heel and other kinetic parameters at the foot, while minimum SR of 333Hz is suggested for estimating step length and 200Hz for kinematic parameters, stride duration, and tibial acceleration (Mitschke et al., 2017). A SR of 1000Hz should suffice for almost all scenarios except sprinting, where a higher SR might be necessary for accurately estimating the impact forces at the foot (Mitschke et al., 2017). A lower-than-appropriate SR leads to inaccuracy in estimation while an excessive sampling rate places a high demand on the battery and the storage. For improved accuracy of measurements, it is essential to ensure correct fixation of the sensors to reduce undesired vibrations due to the impact of the foot on the ground. In case of repeated measurements, it is important

to recheck the sensor fixation to detect any loosening and avoid undesirable movement of the sensors. As the algorithms (Falbriard et al., 2018; Wouda et al., 2018) typically work as desired at different speeds, the protocol can involve either fixed speeds or self-selected speeds. However, around 10 gait cycles at relatively stable speed will provide a more reliable estimate of the gait parameters for a given time (Falbriard et al., 2020).

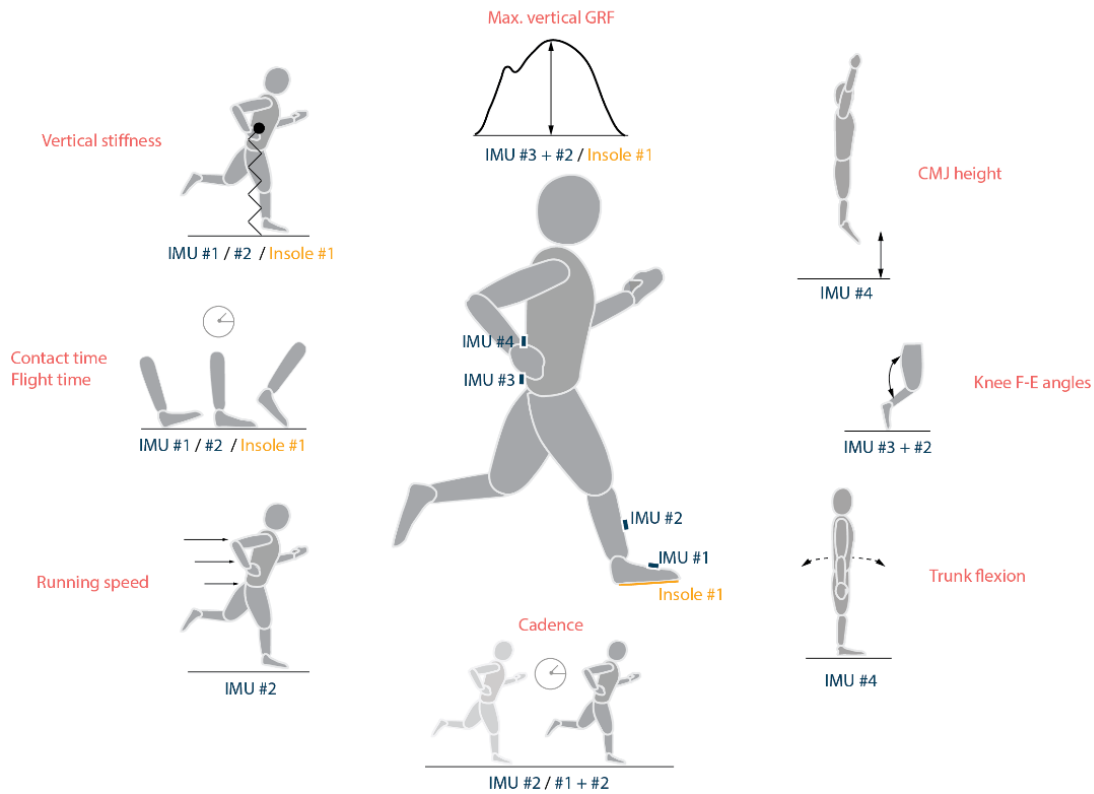


Figure 2.5 Parameters that show a consistent trend in response to acute fatigue and a potential wearable sensor setup to measure them in field. Stride length can be estimated by multiplying running speed and gait cycle time for each stride, while tibial acceleration can be measured directly from IMU#2. IMU refers to inertial measurement unit

2.4.5 On study protocols

The quality of the studies was scored based on the MINORS scale designed for non-randomized studies. The two criteria with usually the lowest scores are the inclusion of consecutive participants and the prospective calculation of study size. Only 11 studies tested more than 30 subjects (10.6%), with males as the large majority (80%). Considering the high inter-subject variabilities in terms of morphology and running techniques, a higher sample size could help improve interpretations of obtained parameter trends by making subgroups. Moreover, less than 30 studies compared amateur and professional athletes: male and female, or exercise intensities (intermittent versus continuous). A higher number of comparative studies would improve the specificity of the results.

As seen in the results section, the most used protocol to induce fatigue was treadmill running until exhaustion, classified as severe. Even in this very specific fatiguing activity, there is no agreement in literature about which reference metric should be used for

measuring fatigue. Several studies used questionnaires (RPE), while others used speed thresholds, VO_2max tests, heart rate zones or a combination of those metrics. This lack of agreement makes it difficult to compare different protocols and explains certain inconsistencies across studies within the four subgroups for fatigue. Finally, this systematic review allows us to highlight the current gaps in literature regarding sport-induced fatigue. One of the main findings is the lack of field studies with continuous measurements, conducted during the actual run. As seen in the results (section 2.3.2.2), stationary measurement systems represent 76.5% of sensors used, significantly more than wearables; and the ratio between stationary versus wearable motion sensor has not changed over time (Figure 2.4). The main reason is that studies performed in-laboratory allow for highly controlled environmental conditions and are generally easier to perform. However, the recent burgeoning market of wearables, the miniaturization of sensors, and development of advanced algorithms (Camomilla et al., 2018) have given researchers the capability to collect and analyze continuous data during sporting activities with good accuracy and precision.

2.4.6 Limitations

The first limitation of this work is that studies involving different athlete groups with varying skill levels (elite athletes versus amateur) and physical capacity were analyzed together to create summary trends. Mixing different study populations might lead to confounding effects in the computation of trends. However, this was done to overcome the limited number of studies within each sub-group and ensure large enough sample size for computing meaningful summary trends. As a result, the trends produced from the analysis can be generalizable across a wide population.

The parameters for analysis were selected based on the threshold of at least 30 participants within a fatigue category and/or running surface. This threshold was chosen with the aim of balancing the strength of evidence and the number of analyzed parameters. While a higher threshold would increase the strength of evidence per parameter, the number of analyzed parameters would have been drastically reduced since most studies had less than 20 participants. A small change in one of the parameters might be more pertinent to the biomechanical response than a large change in another parameter, which makes it difficult to decide the importance of parameters *a priori*. To account for this, and for the lack of a single metric to characterize biomechanical response, a large number of parameters were included, despite the relative lack of research for some of these parameters.

2.5 CONCLUSION

The current review presents evidence that acute fatigue influences almost all the included biomechanical parameters in running, with crucial influence from the exercise intensity and the testing environment. In response to acute fatigue, cadence, flight time, contact time, vertical stiffness, knee flexion angle at initial contact, trunk flexion angle, peak tibial acceleration, CoP velocity during balance test showed an increasing trend with fatigue and knee extension force during MVC, maximum vertical ground reaction forces, and CMJ height showed a decreasing trend across different fatigue protocols. Results reaffirm the observations that acute fatigue causes a reduction in the maximal force production of the muscles and adversely affects the postural control

ability, leading to a more compliant leg and a decreased attenuation of the impact force during each ground contact. The dominant metrics used for fatigue analysis were gait spatiotemporal parameters while stationary sensor systems, treadmill activities, and endpoint measurements were the dominant modalities. The metrics identified here could be used for athlete monitoring in field and the design of optimal training regimens, leading to an enhanced performance improvement/injury risk prevention ratio. Results indicate an important research gap with the lack of field studies with continuous measurement, conducted during actual sporting activities. Emerging technologies like wearable sensors could enable design of such protocols, thus leading to a deeper understanding of the influence of fatigue on the biomechanics of the lower extremities. One outcome of this review is set of recommendations for a wearable sensor configuration based on three or four sensors, which will enable continuous in-field measurement of metrics that show a reliable response to acute fatigue. These recommendations were subsequently used in a wearable sensor-based protocol to simultaneously study the biomechanics of running and perceived fatigue during a half marathon. This study and its results will be discussed in detail in the following chapter.

2.6 APPENDIX

2.6.1 *Eligibility criteria*

Below are some additional exclusion criteria that are not mentioned in section 2.2.2 for the sake of brevity.

Exclusion criteria:

- The study that focused only on biochemical parameters such as lactate, creatine kinase, cortisol, etc. to assess the effect of sport-related fatigue.
- The study which focused only on questionnaires (Borg, fatigue...) to assess fatigue, without additional sensors used.
- The study which evaluated the effect of sport on mental health based on self-reported questionnaires (motivation, mood, depression, self-reported, burnout).
- The study that focused on recovery time or training program after fractures or injuries related to sport. We also excluded the studies investigating sport-related concussion.
- The study that analyzed the effects of certain therapy to reduce fatigue such as phototherapy, cold water immersion therapy, diet, acupuncture, compression garments, moxibustion, etc.
- The study that focused on the effects of specific environmental conditions on fatigue or for training such as extreme conditions, altitude training, hypobaric chamber, acclimatization, hypoxic condition, etc.

- The study that analyzed the effects of performance-enhancing substances such as ergogenic aids, Beta-alanine effects, doping, heat acclimation, metformin, ischemic preconditioning, β 2-agonists, etc.
- Studies that focus only on feedbacks to athletes
- Studies that focus on chemical/brain stimulation and other invasive methods effects on fatigue.
- Studies that focus on recovery time after fracture/injuries related to sport, including but limited to concussion.
- Studies that involve a biopsy procedure
- Studies aimed at validation of functional tests and not the evaluation of the influence of fatigue
- Research that utilizes specific exercises to induce, but which are not sport activity. For example, repetitive shoulder movement or resistance training.
- Studies that focus only on the biomechanics of sports other than running
- Pregnancy-related guidelines on physical activity
- Studies on animals
- Research investigating the effects of age on fatigue, or based on adolescents (<18 years) or old (>65 years) participants
- Studies that focus on biochemical parameters only

2.6.2 *Study appraisal*

The items mentioned below, based on the MINOR scale, were used to appraise the selected studies. Example for one study is provided in Table 2.3; supplementary material S1 presents the same for all studies.

Table 2.3 Adapted MINOR scale (Slim et al., 2003b) used for scoring the studies, with score from 0 to 2 for each metric. Scores for one study (Rousanoglou et al., 2016) are shown here

	A clearly stated aim	Inclusion of consecutive participants	Clear descrip- tion of meas- urement system	Endpoints appropriate to the aim of the study	Unbiased assessment of the study endpoint	Follow-up period appropriate to the aim of the study	Loss to follow up less than 5%	Prospective calculation of the study size:	Total
Rousanogl u2016Jspo rtSciMed	2/2	1/2	2/2	2/2	0/2	2/2	2/2	1/2	12/16

2.6.3 Parameter definition

(1) *local dynamic stability (LDS)*: LDS can be quantified by the determination of the largest Lyapunov exponent λ and is interpreted as the ability to compensate small perturbations to maintain functional locomotion [71]. A higher exponent indicates a lowered ability to maintain stability. (2) *Peak force*: it is the maximum force measured in different regions of the foot (Alfuth & Rosenbaum, 2011; Anbarian & Esmaeili, 2016; Voloshin et al., 1998; Weist et al., 2004; Willson & Kernozek, 1999) using pressure insoles and as such, cannot be directly compared to the ground reaction forces as they represent the summation of forces in all foot regions. (4) *iEMG*: Area under the curve of the rectified EMG signal i.e. the mathematical integral of the absolute value of the raw EMG signal (Avogadro et al., 2003; Dittrich et al., 2013; Weist et al., 2004) (5) *MF*: Median frequency of the EMG power spectrum (Avogadro et al., 2003; Dittrich et al., 2013; Dutto & Smith, 2002; Sánchez-Sánchez et al., 2018; Weist et al., 2004)

2.6.4 Data synthesis

The flowchart for the computation of summary trends for the parameters is shown in Figure 2.6; a process followed for every parameter within each subgroup. For each study (S_i), we extracted quality score (Q_i) and a list of parameters used to assess fatigue with their respective trend ($T_{\{j,i\}}$, j : #parameter, i : #study). The parameter trends ($T_{\{j,i\}}$) were multiplied by the respective study quality score (Q_i) and combined into a vector (A_i). Then, the median (MED) and the median absolute deviation (MAD) of A_i , which correspond to the median and M.A.D of the different trends obtained for this parameter (T_j), were computed. If $MAD(A_i)$ was greater than 0.5, we consider that there is no trend, i.e., no consistencies across studies. $MAD(A_i)$ lower than 0.1, indicated agreement across studies and was characterized as “clear decrease” if $MED(A_i)$ was negative, “non-significant change” if $MED(A_i)$ equal to zero, and “clear increase” if $MED(A_i)$ was positive. For $0.1 < MAD(A_i) < 0.5$ the trends were characterized as “partial decrease”, “non-significant change” or “partial increase” respectively.

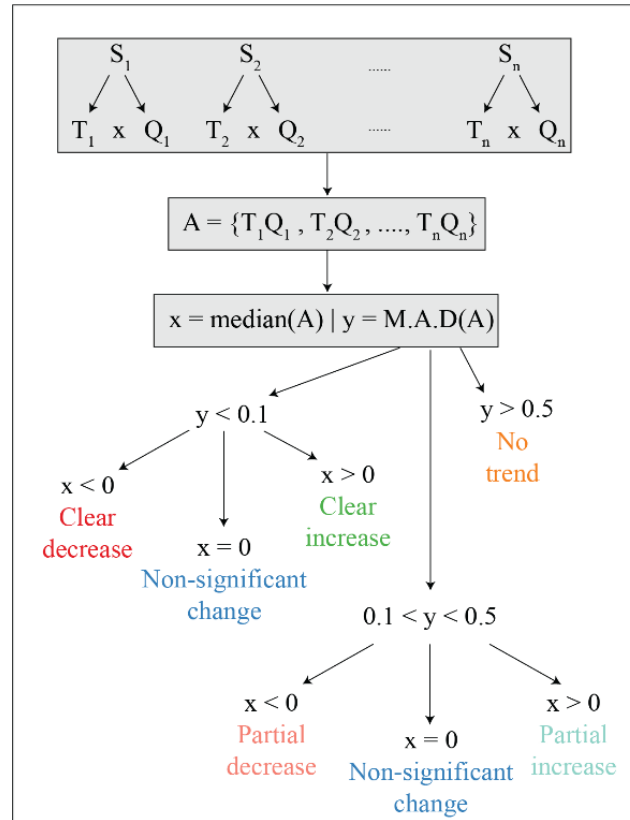


Figure 2.6 Flowchart for the extraction of the summary trends for different parameters, where S: study, T: trend, Q: study quality, and MAD: median absolute deviation. This process is followed for every parameter within each fatigue category

3 CONCURRENT EVOLUTION OF BIOMECHANICAL PARAMETERS WITH PERCEIVED FATIGUE

This chapter presents the second part of the investigation into the biomechanical response to running-induced acute fatigue. It aimed to assess the evolution of the gait spatiotemporal parameters, symmetry and variability of gait, trunk motion, and perceived fatigue during a half-marathon. 13 recreational runners were equipped with one inertial measurement unit (IMU) on each foot, one combined global navigation satellite system-IMU-electrocardiogram sensor on the chest, and an Android smartphone equipped with an audio recording application. Spatiotemporal parameters for the running gait, along with the symmetry of temporal parameters, variability, and complexity of gait cycle time, were computed using validated algorithms. Additionally, smoothness and stability of trunk were assessed. Acute fatigue was assessed as the rating-of-fatigue (ROF) scale at every 10 min of the race. The data was split into eight equal segments, corresponding to at least one ROF value per segment, and only level running parts were retained. During the race, contact time, duty factor, asymmetry of temporal parameters, and trunk anteroposterior acceleration increased, and the foot strike angle, vertical stiffness, and trunk stability and smoothness decreased significantly. The biomechanical parameters showed a significant alteration even with a small change in perceived fatigue. This study highlights measurable influences of acute fatigue, which can be studied only through concurrent measurement of biomechanical and psychological facets of running in real-world conditions.

The contents of this chapter have been adapted from these articles:

Prigent, G.[†], Apte, S.[†], Paraschiv-Ionescu, A., Besson, C., Gremeaux, V., & Aminian, K. (2022). Concurrent Evolution of Biomechanical and Physiological Parameters with Running-Induced Acute Fatigue. *Frontiers in Physiology*, 74.

Apte, S., Evian, V., Gremeaux, V., & Aminian, K. (2022). Concurrent Assessment Of Symmetry, Variability, And Complexity Of Stride During Prolonged Outdoor Running. *ISBS Proceedings Archive*, 40(1), 33.

Apte, S., Laroche, N., Gremeaux, V., & Aminian, K. (2022). Trunk Motion During A Half-Marathon: The Impact Of Perceived Fatigue On Motion Stability And Smoothness. *ISBS Proceedings Archive*, 40(1), 29.

[†]Equal first authorship

Contributions: conceptualized the study design; conducted the data collection; contributed to the analysis and interpretation of the data; drafted the manuscript; supervised semester projects that partly led to the results of the two ISBS papers.

3.1 INTRODUCTION

The tremendous increase in the popularity of running (Rothschild, 2012) as a sport has hastened the need to understand the risk factors for running related injuries (RRI) arising out of maladaptation to training. While the direct relation of biomechanical risk factors and training load to the instances of lower extremity RRIs is debated (Ceyssens et al., 2019; Fredette et al., 2021), these factors are understood to be influenced by acute fatigue, especially resulting from endurance running (Verschueren et al., 2020). Acute fatigue in this context can be understood as the decline in performance caused by physical exertion during sports (Knicker et al., 2011), measured during or immediately after the sporting activity. Fatigue can be characterized as the inability to maintain the intensity of a sub-maximal exercise, caused by the change in the underlying interdependence between the central drive from the motor cortex and the contractile function of the muscles (Enoka & Duchateau, 2016; Vargas & Marino, 2014). Since fatigue depends on the interactions between performance and perceived fatigability, direct measurement of fatigue is difficult (Enoka & Duchateau, 2016). It is often investigated by measuring its concomitant effects on cardiovascular, neuromuscular, and psychological states via sensor-based approaches and self-reported scores on questionnaires (Thorpe et al., 2017). Other approaches include blood tests for lactate, cortisol, etc. and performance monitoring on functional tests like countermovement jump and maximum voluntary contraction (Bourdon et al., 2017). However, these two modalities are constrained to endpoint measurements and thus only useful for testing pre-to-post responses.

Because biomechanical parameters of running such as contact time, flight time, trunk flexion angle, vertical stiffness, GRF, etc., change in response to acute fatigue (Apte et al., 2021), continuous monitoring of these parameters can help understand the effects of fatigue on neuromuscular function (Paquette et al., 2020). Acute fatigue leads to an increase in the asymmetry of kinetic and kinematic variables during running (Radzak et al., 2017; Tabor et al., 2021), but these results were limited to treadmill running and 50-m sprints. A 10% increase in the asymmetry of contact time can lead to increase in metabolic costs of running of up to 7.8% (Beck et al., 2018). Along with the gait parameters, cycle time variability and its long-range correlates (complexity) are an indicator of running technique and a potential predictor of RRIs (Gruber et al., 2021; Meardon et al., 2011), with trained runners exhibiting lower variability and higher complexity (Nakayama et al., 2010). The variability and complexity of stride time varied non-linearly in amateurs and experienced runners during a prolonged run on track (Meardon et al., 2011) and treadmill (Mo & Chow, 2018a), due to acute fatigue. In addition to the motion of the lower extremities (Moore et al., 2019), trunk motion has important implications for the energy cost of running, with a decrease in the stability and smoothness of the trunk motion in the mediolateral axis leading to an increase in energy cost (Kiely et al., 2019; Schütte et al., 2018). In this context, smoothness and stability characterize the proficiency of coordinated movements during running. Current research indicates that stability (Schütte et al., 2018) and smoothness (Kiely et al., 2019) tend to decrease with increased duration of running, likely due to acute fatigue. Acute fatigue also affects trunk flexion during prolonged running (Apte et al., 2021), resulting in increased stress on the knee (Teng & Powers, 2015), which may lead to a higher risk of injury.

The number of studies on continuous and field monitoring of running-induced acute fatigue remains scarce, despite the recent proliferation of wearable measurement systems and movement analysis algorithms in sports science (Apte et al., 2021; Camomilla et al., 2018). Within these, some studies focused on the classification of fatigued and non-fatigued states using machine learning techniques based on statistical features or composite indices (Buckley, O'Reilly, Whelan, Vallyly Farrell, et al., 2017; Clermont, Benson, Edwards, et al., 2019; Eskofier et al., 2012; Tim Op De Beéck, Wannes Meert, 2018), which precludes the investigation of interpretable biomechanical parameters. Studies examining the response of individual biomechanical parameters during long-distance running ($\geq 10\text{km}$) have predominantly analyzed the parameter values at different distances (Alfuth & Rosenbaum, 2011; Meyer et al., 2021b; Ruder et al., 2019; Strohrmann, Harms, Kappeler-Setz, & Troster, 2012). Similarly, results from investigation of symmetry, variability, complexity, stability, and smoothness during running were considered in relation to the progression of the running activity.

This approach has an implicit assumption that different participants develop similar levels of fatigue at similar distances during the run, which may not be true for a heterogeneous participant group employing a variety of pacing strategies. Combined, these studies investigate the neuromuscular response to acute fatigue, but not the perceived fatigability and thus the psychological states during the run. Due to the complex nature of fatigue, perceived fatigability can provide a global overview from a complex system perspective rather than a single biomechanical or physiological parameter (Balagué et al., 2020; Venhorst et al., 2018). Thus, rating of perceived exertion (RPE) (Borg, 1982) or rating of fatigue (ROF) (Micklewright et al., 2017) can provide a more holistic idea of central regulation, especially during the context of an actual running race that involves pacing strategies, making their investigation pertinent (Millet, 2011; Pageaux & Lepers, 2016). This chapter presents an investigation of the evolution of running biomechanics in response to perceived fatigability in recreational runners, using body-worn smartphones, IMU, GNSS and ECG sensors. It aims to complement existing research by providing a synchronous analysis of the stability and smoothness of trunk motion, as well as the symmetry, variability, and complexity of gait cycles and the evolution of perceived fatigue. Hereafter, perceived fatigability will be alternately referred to as ROF and/or fatigue, as it is a reference for acute fatigue.

3.2 Materials and equipment

Measurements were conducted with 13 healthy participants, six (4 males, 2 females, age: 35.5 ± 9.3 y.o. during the Lausanne half-marathon (Switzerland, 27th Oct. 2019) and seven (7 males age: 35.6 ± 5.8 y.o.) during a 21.5 km race-simulation run in Rif (Salzburg, Austria, 25-29th Nov. 2020). The race-simulation in Rif was organized because of race cancellations in 2020 due to the pandemic situation. The half-marathon was chosen to avoid the walking periods that inexperienced participants can have during a full marathon, as we observed during pilot studies. EPFL human research ethics committee (HREC 039-2018) approved the study and all participants provided written consent before the data collection. As shown in Figure 3.1, participants were equipped with a GNSS-IMU-ECG sensor (*Fieldwiz*, *ASI*, *Switzerland*) on the chest using a belt with electrodes (*Polar Pro Strap*, *Polar Electro Oy*, *Finland*), an IMU sensor (*Physilog 5*, *Gaitup SA*,

Switzerland) on each foot, and an Android smartphone on the upper arm. Apart from the sensor setup, the participants dressed as they would for an endurance running race. Following their personal warm-up, the participants were equipped with the sensor setup and were instructed to give their best during the run.

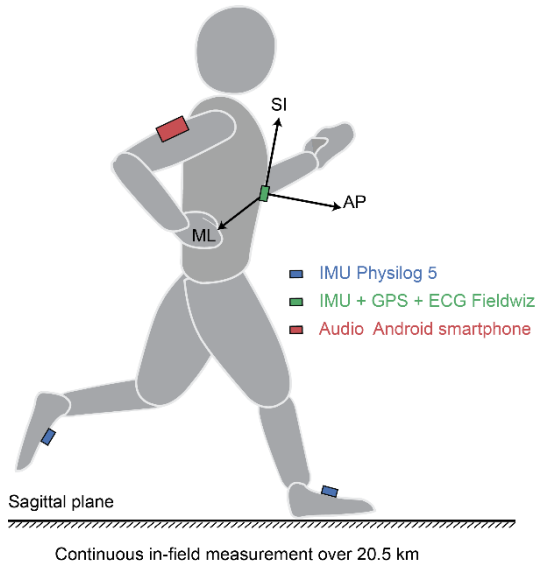


Figure 3.1 Sensor configuration used for the measurement, where AP, SI and ML denote the anterior-posterior, the superior-inferior, and the medio-lateral axis

The *Fieldwiz* and *Physilog 5* wearable sensors were chosen because they have already been used successfully for analysis of outdoor running (Apte, Meyer, et al., 2020; Meyer et al., 2021b). *Fieldwiz* was used with a sampling frequency of 200Hz for the IMU, 250Hz for the ECG, and 10Hz for the GNSS receiver. The *Physilog 5* IMU was sampled at 512Hz, with a range of $\pm 16g$ m/s² for the accelerometer and ± 2000 deg/s for the gyroscope. We installed a custom-built application on the smartphone, which reminded the wearer to speak out their rating of fatigue (ROF) on a scale of 1 to 10 (Micklewright et al., 2017) and recorded this audio with a timestamp. We configured the application to create a reminder every 10 minutes and subsequently record for a period of 30 seconds. The audio files were manually transcribed to store the recorded ROF value.

3.3 METHODS

3.3.1 Preprocessing

The pre-processing steps include synchronization of the sensors and slope detection (Figure 3.2). A shock movement, which consists of a fast up and down movement on the vertical axis while holding all sensors together, was performed before and after the race for synchronizing the *Fieldwiz* and *Physilog 5* wearable sensors (Caruso et al., 2019). As the same motion was recorded on the accelerometer of both sensors, we could compute the lag between the acceleration signal of both sensors using cross-correlation; this lag was then used to adjust their timestamps. The analysis was restrained to bouts of level running to avoid any biomechanical changes biased by inclined running. Official mapping platform of the Swiss Confederation (map.geo.admin.ch) was used to detect slopes on the Lausanne marathon route and the distance was computed using the Haversine formula (Robusto, 1957), with the latitude and longitude information from the GNSS sensor. Slopes were defined as race segments having a gradient greater than 5% over 100 meters and corresponding race sections were excluded from the data. To avoid this procedure, a relatively flat course was selected for the run in Rif, with all gradients below the 5% level.

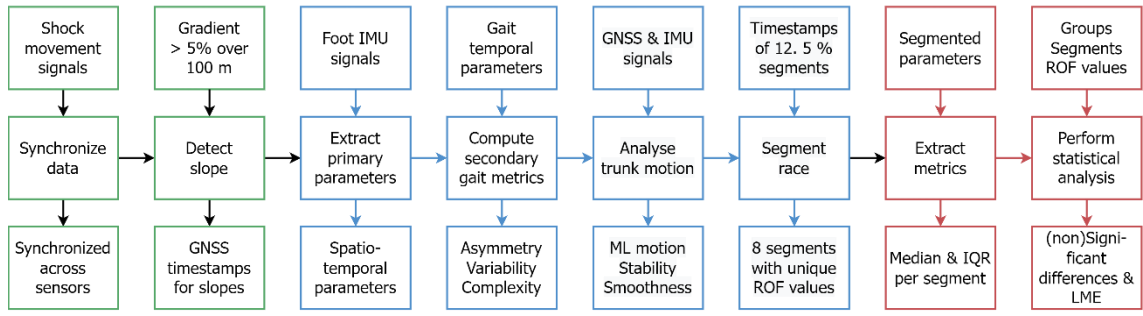


Figure 3.2 Flowchart for the overall procedure, showing three blocks for the pre-processing, feature extraction, and statistical analysis; ML motion: motion of trunk along mediolateral axis, LME: Linear mixed model

3.3.2 Feature extraction

3.3.2.1 Gait spatiotemporal parameters

The accelerometer, gyroscope, and speed signals from the *Fieldwiz* sensor were processed to remove outliers that were more than two standard deviations away from the mean value over a race segment window and replaced with linearly interpolated values. Using validated algorithms (Falbriard et al., 2018, 2020), the raw signals from the foot IMUs were initially used to divide the race into gait cycles based on mid-swings. Following this, we estimated the temporal parameters such as contact time (t_c), flight time (t_f), swing time (t_s), and cycle time (t_g), and kinematics parameters like peak swing velocity of the foot (ω_s), peak swing velocity (p_s) foot strike angle in sagittal plane (FSA), and foot eversion angle (FEA) at initial contact. One value of each spatiotemporal parameter per gait cycle was obtained for the right and the left foot, but only the information from the right foot was used for the subsequent analysis, with the first and last 10 steps of the race being removed to avoid any transient effects. To understand the storage and return of elastic energy, vertical stiffness (k_{vert}) was computed using the spring mass model to characterize running (J.-B. Morin et al., 2005). To consider the positive and negative work during running, the duty factor (d_f) of the gait (Alexander, 1991) was investigated, defined as the ratio between contact and stride time. The computation of the above-mentioned parameters are explained in the publication from Meyer et al., 2021 (Meyer et al., 2021b).

3.3.2.2 Secondary gait metrics

The overall process for the extraction of secondary gait metrics is presented in Figure 3.3. The dataset was based on single values of gait parameters per gait cycle, and thus discrete symmetry coefficients were used, though they are less sensitive than the continuous coefficients (Błażkiewicz et al., 2014; Tabor et al., 2021). To quantify symmetry for spatiotemporal parameters, four metrics (Błażkiewicz et al., 2014) have been previously used: Ratio Index (RI), Symmetry Index (SI), Symmetry Angle (SA), and Gait Asymmetry Index (GAI). However, for RI, SA and GAI, the calculation considers the ratio between the right and left limb values, and thus remains susceptible to influence of the dominant leg. Furthermore, results from (Błażkiewicz et al., 2014) suggested a high similarity between RI and SI, and their advantage over SA. Based on these conclusions, SI (5) was selected as the metric for assessing symmetry.

$$SI = 2 \frac{|X_L - X_R|}{(X_L + X_R)} \times 100\% \quad (3.1)$$

where X_R and X_L are parameters for the right and left limbs. We thus used SI for four gait parameters— contact time (SI_{t_c}), swing time (SI_{t_s}), duty factor (SI_{df}) and peak swing velocity (SI_{p_s}), based on their evolution with acute fatigue during running (Apte et al., 2021; Prigent et al., 2022). SI was also computed for the gait cycle time to check its validity, as the cycle time should present a SI close to zero.

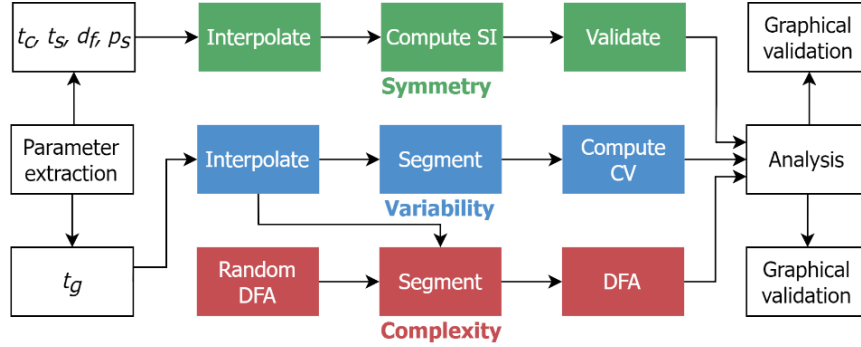


Figure 3.3 Flowchart for the estimation of secondary gait metrics, with the steps for calculating the symmetry, variability, and complexity of the extracted gait parameters shown in green, blue, and red, respectively

To characterize the variability and complexity of stride, gait cycle time was used as a parameter of interest. This choice allowed comparison with results from previous studies (Meardon et al., 2011; Mo & Chow, 2018a) on prolonged running. To assess the stride-to-stride variability and quality of strides over a given time, coefficient of variation (CV) is an efficient metric (Meardon et al., 2011). The race was therefore divided into 25 segments of equal duration and CV of gait cycle time was computed for each of these segments. However, two distinct signals can show the same variance in the form of CV and thus we need to study them further. In order to fully capture the nature of the evolution of the cycle time over the race, the complexity of the stride (Mo & Chow, 2018a) was analyzed. Complexity can be defined as the amount of nonlinear information that a time series conveys over time. A reliable metric to assess the complexity of gait is the α -DFA coefficient (Damouras et al., 2010), that can be computed with Detrended Fluctuation Analysis (DFA). The DFA analysis was performed over a sliding window of size 500 strides, with an increment of 100 strides. A random DFA analysis was also performed to validate the procedure by shuffling the input values and check that obtained vector showed no memory (α -DFA coefficient around 0.5).

3.3.2.3 Characterization of trunk motion

To investigate the orientation of the trunk and its evolution throughout the race, two metrics were computed $-av_{AP}$: the ratio of the acceleration along the anterior-posterior direction and the running speed (v) and av_{ML} : the ratio of the acceleration along the medio-lateral direction and the running speed. Normalization with speed was carried out to investigate the response to fatigue and not the secondary effects of the change in speed. The race was split into windows of 30 seconds and all the stability and smoothness metrics were computed on each window. The acceleration along the mediolateral

axis (a_{ML}) was selected for the computation of stability and smoothness metrics (Figure 3.4), since the acceleration along this axis presents a clear and substantial change with fatigue (Apte et al., 2021; Provot et al., 2021). Furthermore, gait velocity (v) was extracted from the GNNS for the estimation of smoothness.

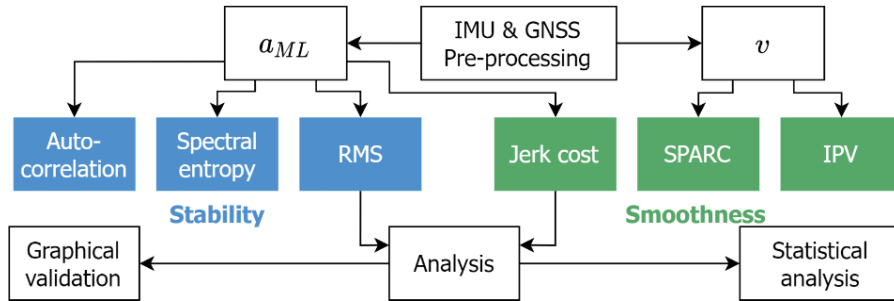


Figure 3.4 Flowchart of the trunk movement characterization process, with the steps for stability and smoothness computation indicated in blue and green respectively

Out of the variety of metrics used to quantify stability present in literature (Bruijn et al., 2013), three different methods (Figure 3.4) were selected to quantify stability. First method was the computation of the root mean squared of the acceleration ($RMSA$) on a window of 1 stride (Schütte et al., 2015). Next, spectral entropy (SE) was used to quantify the regularity of fluctuations within the acceleration profile (Schütte et al., 2015). Finally, the autocorrelation coefficient of the acceleration signal with a lag of one step (R_P) and one stride (R_D) was estimated. Autocorrelation quantifies the similarity of each step (or stride) compared to the others (Cushman, 2010). Loss of stability is indicated by an increase in $RMSA$ and SE , and a decrease in that of R_P and R_D . Smoothness was also evaluated with three different metrics (Figure 1). First, jerk cost (JC), which quantifies the change in the jerk profile and thus loss of smoothness due to rapid changes in acceleration (Kiely et al., 2019). Additionally, the spectral arc length ($SPARC$) (Balasubramanian et al., 2015) on the velocity profile was computed, which is arc length of the Fourier magnitude spectrum within an adaptive frequency range. Smoother movements tend to have less intermittencies and thus a higher $SPARC$ measure. Lastly, smoothness was quantified using the inversed number of peaks (IPV) (Brooks et al., 1973) on the velocity profile, where smooth motion tends to have less peaks.

3.3.3 Statistical analysis

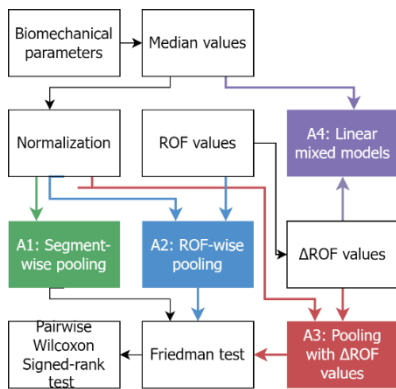


Figure 3.5 Statistical analysis procedure where the biomechanical parameters and the ROF values are used as inputs

Four statistical analyses (Figure 3.5) were conducted to address the following questions:

1. How do parameters evolve over the race?
2. How do parameters evolve over progression of perceived fatigue based on ROF values?
3. At which level of perceived fatigue (ΔROF), are the parameters significantly affected?
4. Are there noticeable differences between fast and slow runners in terms of fatigue progression and the evolution of parameters?

Details of each analysis are provided below, with the statistical significance set at $p \leq 0.05$. All analyses

were performed with MATLAB R2020a (The MathWorks, USA).

3.3.3.1 Feature computation

Following the extraction of parameters, the entire race was segmented into eight periods, each period corresponding to 12.5% of the race. The eight segments were selected to ensure the presence of (at least) one ROF value per segment. For every segment, the median and interquartile range (IQR) were computed for each biomechanical and physiological parameter. As the metrics are highly subject-dependent, the values were normalized by dividing the median value of each segment by the median value of a reference segment. The race segment with the highest running speed was used as reference to normalize.

3.3.3.2 Evolution with race and ROF values

In order to investigate the effects of race progression on parameters, the Friedman test, a non-parametric test to compare three or more repeated measurements, was used to compare segments S1 (begin), S5 (middle), and S8 (end) (Eisinga et al., 2017). The effect size was computed as:

$$es_F = \frac{\chi^2}{n(k-1)} \quad (3.2)$$

Where es_F is the Kendall's W test value, χ^2 is the Friedman test statistic value, n is the sample size, and k is the number of measurements per subject (Tomczak & Tomczak, 2014). Kendall uses Cohen's interpretation guidelines of 0.1 (small effect), 0.3 (moderate effect), and above 0.5 as a strong effect (Abdi, 2007). In addition, pairwise comparisons (S1 vs. S5; S5 vs. S8 and S1 vs. S8) using the non-parametric Wilcoxon signed-rank test were computed. The effect size was defined as:

$$es_w = \frac{Z}{\sqrt{N}} \quad (3.3)$$

where Z is the standardized Z -score and N is the total number of observations on which Z is based. To estimate the effects of fatigue based on the perceived fatigability, segments with the lowest (L), medium (M), and highest (H) recorded ROF values were compared. These fatigue levels were considered individually for each participant and pooled into three different groups (L, M, H) to overcome inter-subject variability in fatigue perception. When the same ROF value was observed on several segments, median parameter value was used for those segments. The Friedman and the Wilcoxon signed-rank test (L vs. M; M vs. H and L vs. H) were utilized as previously explained. Bonferroni correction was not applied for any comparison, since a small number of tests were performed (Armstrong, 2014).

3.3.3.3 Onset of change with Δ ROF level

The goal of this analysis was to investigate the onset of the biomechanical and physiological changes in response to perceived fatigability, measured as ROF. To overcome inter-subject variability in ROF baseline values, the ROF differences between segments (Δ ROF) was computed, by subtracting each ROF value by that at the first segment (baseline). Since participants did not typically report a linear increase of fatigue, a resolution of Δ ROF = 1 is inappropriate and would lead to multiple missing values. Consequently, three states were assumed, by combining Δ ROF 1 and 2, 3 and 4, and all val-

ues ≥ 5 . When the same ΔROF values were obtained for several segments, the median parameter value over those segments was used. Finally, the Friedman and Wilcoxon signed-rank tests were used for comparison, where each $\Delta ROF > 0$ was compared with $\Delta ROF = 0$ (i.e., 0 vs. [1-2]; 0 vs. [3-4]; and 0 vs. ≥ 5).

3.3.3.4 Differences in runners according to performance

A linear mixed-effects (LME) model was applied to investigate the influence of performances (i.e., fast vs. slow runners) on biomechanical and physiological metrics. The participants were divided into two groups based on their performance, ‘fast’ for five fastest runners (race time < 90 min) and ‘slow’ for the five slowest runners (race time > 105 min). A 3-levels LME model was designed with the ΔROF , the performance, and the interaction between ΔROF and performance as the fixed effects (“ $\Delta ROF * performance$ ” in eq. 5). Then, a random effect (intercept and slope) on the subjects was defined (“ $(\Delta ROF|subject)$ ” in eq. 5). As the LME model is robust to missing values, the ΔROF was not grouped into three categories as done in previous section. The three levels correspond to the following models: 1: within-subject model; 2: within-group model (fast vs. slow); and 3: between-group model. We used the equation below as input to the ‘fitlme’ Matlab function, with the ‘responder’ corresponding to a parameter, and the ‘performance’ corresponding to the fast and slow groups:

$$responder \sim \Delta ROF * performance + (\Delta ROF|subject) \quad (3.4)$$

Estimates of the model, p-value, and 95% confidence interval (CI) values of the fixed effects (intercept and slope) for both fast and slow groups were used to understand significant effects. Statistical significance was accepted for $p \leq 0.05$ and if the range of the 95% CI did not include 0. In addition, the coefficient of determination (conditional R_c^2), was used to assess the total variance explained by both fixed and random effects.

3.4 RESULTS

All the thirteen participants (11 males, 2 females) were able to run until the end of the race (race time: 98.4 ± 12.3 min) without substantial walking bouts, and provided information about their ROF before race/after warm-up (3 ± 2) and after race (9 ± 1).

3.4.1 Evolution with race and ROF values

The influence of fatigue on parameters, based on both race progression and ROF values, is summarized in Figure 3.6, Figure 3.7, Figure 3.8 and Table 3.1. Actual values (median and IQR) of the parameters are reported in the supplementary material⁸. Running a half-marathon affected spatiotemporal metrics early in the race, mainly between segments 1 and 5. The t_c , D_f , and the a_{AP} values significantly increase during the race ($p < 0.001$, $es_F > 0.5$). The FSA ($p < 0.001$, $es_F > 0.5$) and the k_{vert} ($p < 0.05$, $es_F \in (0.1, 0.3]$) significantly decrease with high and low effect sizes respectively. Though the statistical tests reveal that the swing time and the peak swing vel. did not change signifi-

⁸ https://figshare.com/articles/dataset/Table_1_Concurrent_Evolution_of_Biomechanical_and_Physiological_Parameters_With_Running-Induced_Acute_Fatigue_XLSX/19160477

cantly when comparing all three segments, significant differences are visible on the pairwise tests.

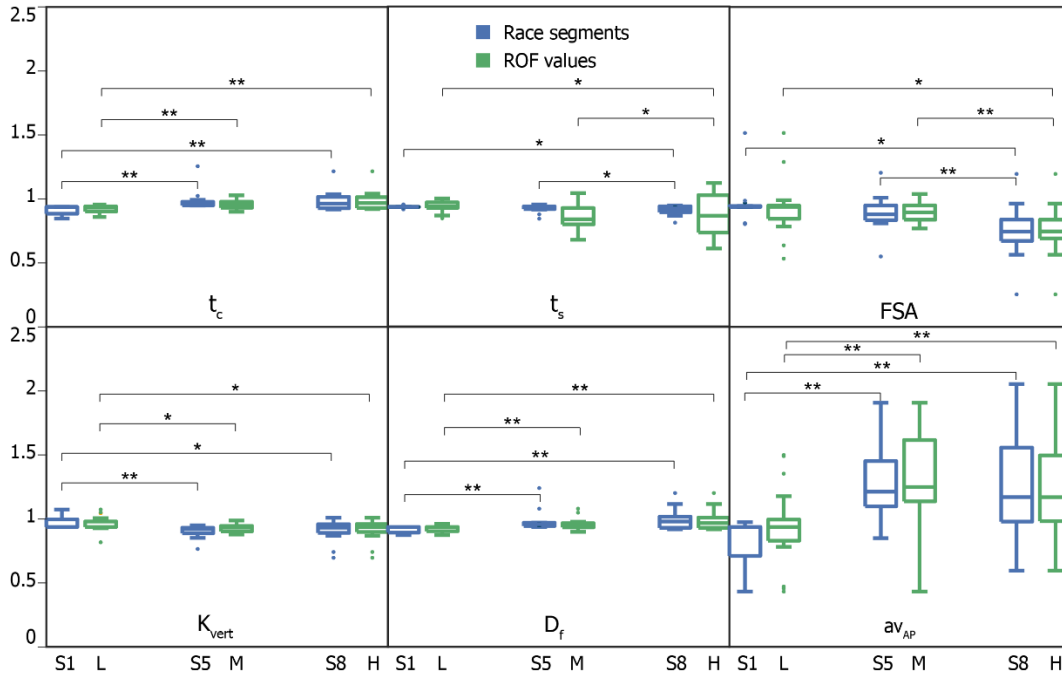


Figure 3.6 Parameters with a significant change with the race segments (in blue) and/or rating of fatigue (in green) with * $p \in [0.01, 0.05)$, ** $p \in [0.001, 0.01)$, and *** $p < 0.001$. S1, S5, and S8 represent the race segments 1, 5, and 8, and L, M, and H the low, medium, and high ROF values

The t_c , ω_s , the k_{vert} , the D_f , and the a_{AP} were altered at the beginning of the race as indicated by the S1|5 significant results ($p \in [0.001, 0.01)$). Only the FSA was altered during the second half of the race ($p \in [0.001, 0.01)$). Comparisons across ROF values showed similar trends for the spatiotemporal parameters as those based on race progression. Remarkably, we observed slightly higher effect sizes across race segments than across ROF values for all the parameters with significant changes.

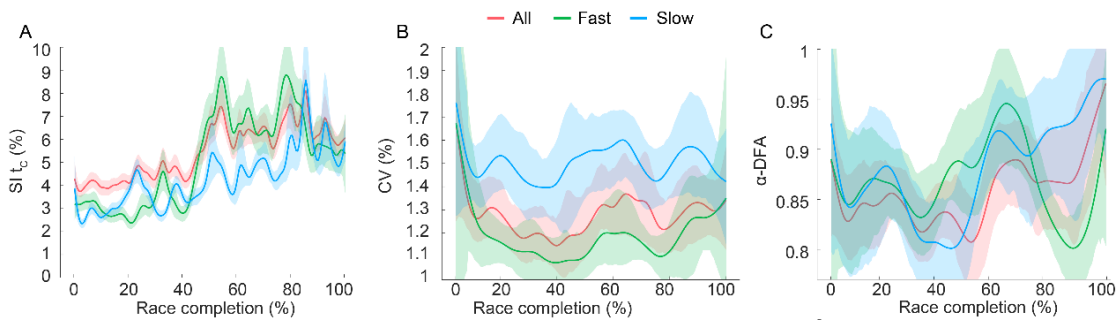


Figure 3.7 Evolution of the secondary gait parameters with race progression. A, B, and C show the actual change with race for $SI t_c$, CV, and α -DFA for cycle time

The overall asymmetry increased for all participants along the race; Figure 3.7A shows the trend for $SI t_c$ and similar trends were observed for $SI t_s$, $SI d_f$, and $SI p_s$. Except for $SI p_s$, all SI metrics showed a significant increase at the end of the race and at high perceived fatigue levels (Table 3.1). Unlike symmetry, the variability and complexity of

the gait changed non-linearly throughout the race after an initial reduction in CV and α -DFA (Figure 3.7B and C). However, the complexity did not show any significant change during the statistical analysis.

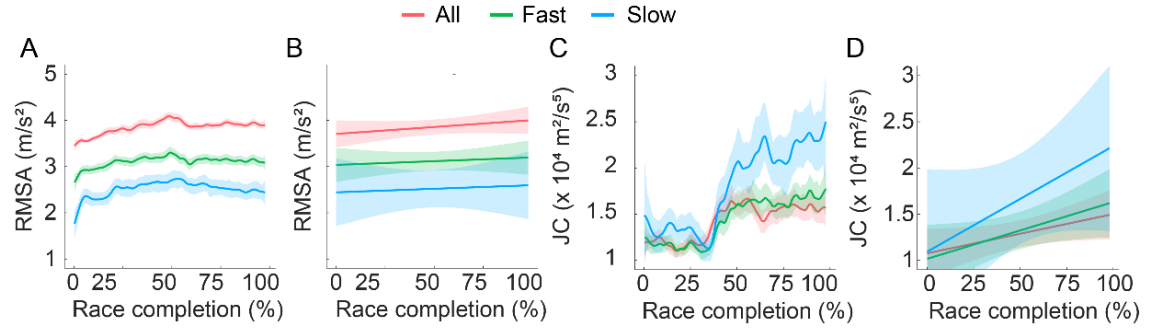


Figure 3.8 Evolution of stability and smoothness with race progression. A and B show the actual change and linear change with race progression for *RMSA*, and C and D for *JC* (jerk cost)

RMSA showed an increasing trend (Figure 3.8A and B) and a significant change (Table 3.1) at the start of the race but did not change significantly as the race continued. Similar results were seen for R_p , R_D , and SE , with significant reduction in stability from low to medium ROF values. However, this reduction was not sustained further. Same trends were seen for the *JC*, with its magnitude increasing with the race progression and perceived fatigue (Figure 3.8C and D). This is also reflected in the statistical analysis (Table 3.1), with significant differences between S1:S5 and S1:S8.

3.4.2 Onset of change

Table 3.1 also provides the evolution of the biomechanical and physiological parameters across fatigue scores, where Δ ROF values are pooled in four states (i.e., 0, [1,2], [3,4], and ≥ 5). Unsurprisingly, parameters showing significant alterations with race progression and ROF values, also present significant changes in Δ ROF. However, these results provide a deeper understanding of the onset of change based on the perceived fatigability. The spatiotemporal biomechanical parameters, t_c , D_f , k_{vert} , and av_{AP} show significant changes at all fatigue states including Δ ROF 1 and 2. Then, a significant decrease of p_s appears at moderate fatigue states (Δ ROF = [3-4]). Finally, FSA and t_s values became significantly lower only at high fatigue scores (Δ ROF > 5). The increasing trend for asymmetry was also observable for other parameters, with Sl_t_s increasing significantly (Table 3.1) for all three Δ ROF levels. Though CV did not show any significant changes with the race, it showed a significant change at low perceived fatigue, despite no significant change in speed. The α -DFA did not present any significant differences with increasing Δ ROF levels. *RMSA* increased significantly at low Δ ROF values but not for Δ ROF ≥ 5 (Table 3.1). R_p , R_D , and SE did show exhibit significant changes at different Δ ROF levels. All participants showed a positive slope for the relation between *JC* and Δ ROF (Figure 3.12B) and significant differences at higher levels of fatigue (Table 3.1). The increase in ROF and Δ ROF scores throughout the race for all participants is presented in Figure 3.9 and shows an important inter-subject variability for the median \pm IQR values at baseline ($ROF(S1) = 4 \pm 2$).

Table 3.1 Effect size results for the statistical analysis A1, A2, and A3 using Friedman (F) test and pairwise Wilcoxon signed-rank (WSR) test. S1, S5, and S8 indicate race segments 1, 5, and 8, whereas L, M, and H denote the low, median, and high ROF values. For significant results, effect size of (0.1,0.3] was considered low, (0.3,0.5] as medium, and >0.5 as high for both W for F test and r for WSR test. The significance was set at $p < 0.05$, with * for $p \in [0.01, 0.05)$, ** for $p \in [0.001, 0.01)$, and *** for $p < 0.001$. Bold indicates the effect size (ES) for significant differences.

Parameter	Across race segments				Across ROF				Across Δ ROF			
	F test	WSR test (es_W)			F test	WSR test (es_W)			F test	WSR test (es_W)		
	(es_F)	S1 5	S5 8	S1 8	(es_F)	L M	M H	L H	(es_F)	0 [1,2]	0 [3,4]	0 ≥ 5
t_c	0.55***	0.62**	0.02	0.58**	0.41**	0.56**	0.34	0.57**	0.61***	0.58**	0.61**	0.61**
t_f	0.17	0.34	0.16	0.28	0.06	0.20	0.17	0.28	0.10	0.31	0.32	0.32
t_s	0.18	0.31	0.45*	0.39*	0.17	0.10	0.45*	0.43*	0.10	0.31	0.28	0.43*
t_g	0.11	0.20	0.36	0.01	0.08	0.21	0.34	0.02	0.06	0.24	0.15	0.03
$Cad.$	0.11	0.20	0.36	0.02	0.08	0.21	0.34	0.02	0.04	0.22	0.14	0.03
FSA	0.57***	0.27	0.62**	0.43*	0.42**	0.20	0.53**	0.49*	0.39**	0.29	0.51	0.47*
FEA	0.02	0.28	0.12	0.21	0.00	0.06	0.17	0.20	0.03	0.17	0.25	0.19
p_s	0.17	0.43*	0.27	0.40*	0.25*	0.31	0.29	0.36	0.35**	0.35	0.57**	0.40*
k_{vert}	0.26*	0.57**	0.08	0.43*	0.19	0.54*	0.09	0.43*	0.29*	0.58**	0.56**	0.47*
D_f	0.54***	0.62**	0.13	0.58**	0.37**	0.55**	0.38	0.58**	0.69***	0.60**	0.61**	0.60**
v	0.08	0.25	0.32	0.21	0.03	0.08	0.05	0.10	0.06	0.10	0.16	0.10
$SI t_c$	0.11	0.28	0.11	0.42*	0.32*	0.08	0.49*	0.46*	0.17	0.21	0.25	0.38*
$SI t_s$	0.31*		0.17	0.46*	0.28*	0.23	0.40	0.49*	0.31*	0.51*	0.42*	0.47*
$SI d_f$	0.11	0.34	0.15	0.46*	0.17	0.12	0.45*	0.44*	0.11	0.30	0.25	0.38*
$SI p_s$	0.03	0.36	0.13	0.30	0.08	0.46*	0.01	0.32	0.23	0.47*	0.47*	0.34
CV	0.06	0.40	0.25	0.17	0.29*	0.45*	0.38	0.06	0.14	0.49*	0.28	0.04
α -DFA	0.07	0.10	0.11	0.11	0.04	0.16	0.11	0.13	0.02	0.17	0.12	0.12
aV_{ML}	0.09	0.32	0.23	0.24	0.01	0.20	0.06	0.13	0.05	0.15	0.19	0.24
aV_{AP}	0.79***	0.62**	0.09	0.62**	0.50**	0.58**	0.01	0.61**	0.44***	0.58**	0.61**	0.61**
R_P	0.11	0.42*	0.01	0.36	0.18	0.51*	0.08	0.35	0.05	0.34	0.39*	0.35
R_D	0.11	0.35	0.02	0.35	0.10	0.46*	0.06	0.34	0.05	0.35	0.32	0.36
SE	0.08	0.37	0.12	0.24	0.10	0.38*	0.05	0.17	0.05	0.31	0.25	0.18
$RMSA$	0.45**	0.56**	0.27	0.53**	0.20	0.46*	0.23	0.4*	0.32**	0.56**	0.56**	0.27
JC	0.29*	0.42*	0.25	0.54**	0.36*	0.32	0.4*	0.54**	0.24*	0.25	0.44*	0.53**
$SPARC$	0.01	0.01	0.12	0.03	0.01	0.11	0.09	0.03	0.01	0.02	0.10	0.02
IPV	0.13	0.30	0.39	0.29	0.24	0.36	0.40	0.24	0.06	0.23	0.00	0.07

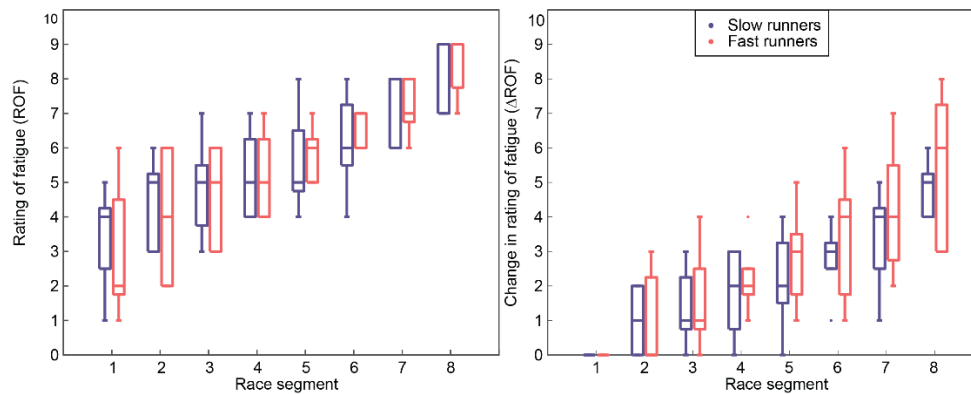


Figure 3.9 Change in perceived fatigability (ROF) with race progression

3.4.3 Differences according to performance

The results of the influence of performances (i.e., fast vs. slow runners) on biomechanical and physiological metrics, based on the LME model, are presented in Figure 3.10.

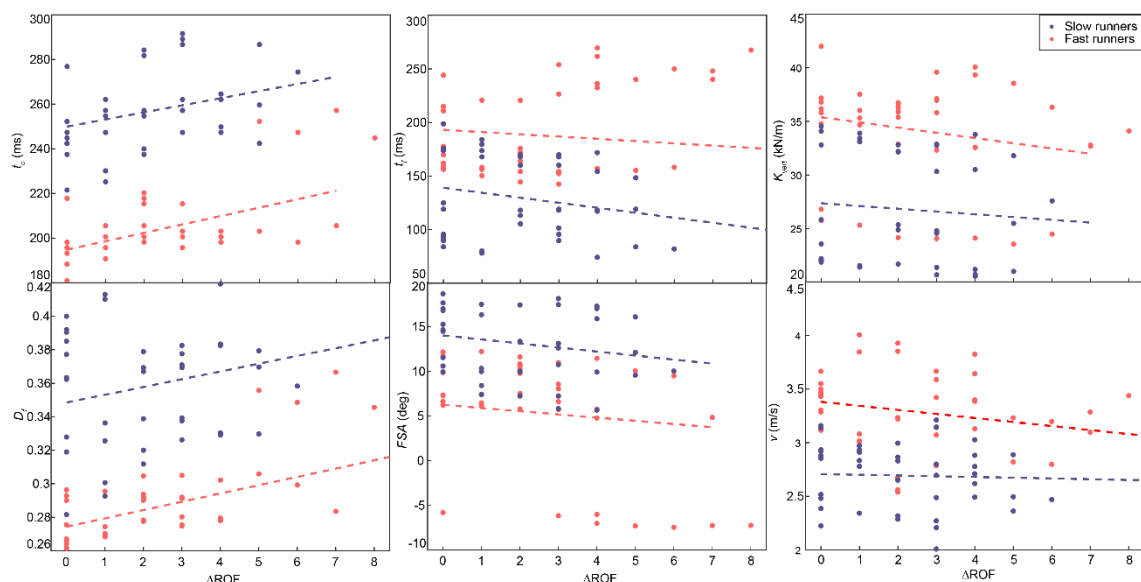


Figure 3.10 Results of the LME models for the response of the gait parameters, based on the fast and slow groups

Only a subset of metrics showing significant differences between groups on fixed-effects, intercept, or slope, are presented. Interestingly, the spatiotemporal biomechanical parameters showed significant differences in the intercept values between fast and slow runners, while the slopes were similar. Compared to fast runners, the slower group presented a higher t_c , D_f , and FSA , and lower k_{vert} (Figure 3.10) throughout the race. The estimate, p-values, 95% confidence interval (CI), and conditional R_c^2 of the fixed effects (intercept and slope) for both fast and slow groups are reported in the supplementary materials⁹.

⁹ https://figshare.com/articles/dataset/Table_1_Concurrent_Evolution_of_Biomechanical_and_Physiological_Parameters_With_Running-Induced_Acute_Fatigue_XLSX/19160477

The increase of asymmetry is higher for the fast runners halfway through the race and only they showed an increase in Sl_t for change in perceived fatigue (Figure 3.11A). Fast group showed a consistently lower CV than slow group (up to 20%) throughout the race and with ΔROF (Figure 3.7B and Figure 3.11B) but presented an increase in CV at the end of the race. α -DFA decreased for fast and slow groups till around 40% of the race (Figure 3.7C), followed by a sudden increase for slow group and a cyclic change for fast group. This is also reflected in the linear trend for ΔROF (Figure 3.11C), where α -DFA is increasing for slow runners, and decreasing for fast runners. However, the complexity did not show any significant change (Table 3.1) in the statistical analysis.

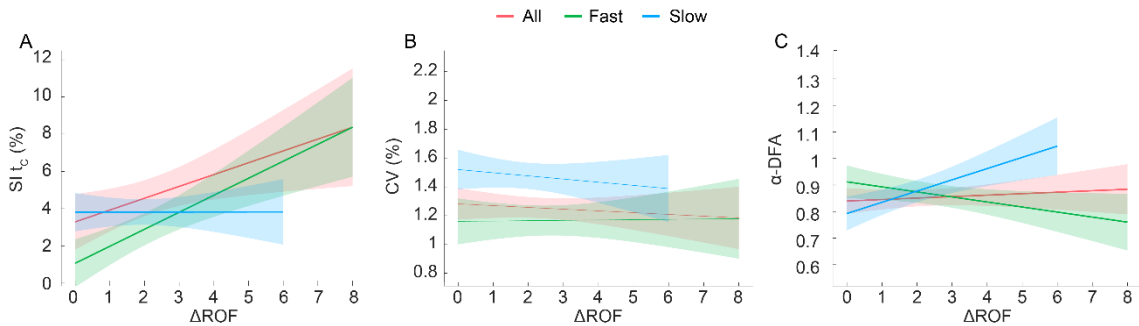


Figure 3.11 Evolution of the secondary gait parameters with perceived fatigability. A, B, and C show the linear trends for Sl_t , CV, and α -DFA for cycle time

RMSA presented a good ability to differentiate between experience and amateur runners. For ΔROF (Figure 3.12A), it showed difference in slopes for the slow and fast groups, with fast runners showing a moderate increase and slow runners showing a decline. R_P , R_D , and SE did not differentiate well between fast and slow runners. JC presented a sudden increase around 40% of the race and continued to increase throughout race for the slow group (Figure 3.8C). However, for the fast group, it barely increased after halfway point of the race. The continued increase for slow runners is reflected in the ROF comparison (Table 3.1), with significant different for M:H and L:H groups. Slow group presented a considerably larger slope with ΔROF (Figure 3.12B) but a similar intercept as fast group for JC for the LME analysis.

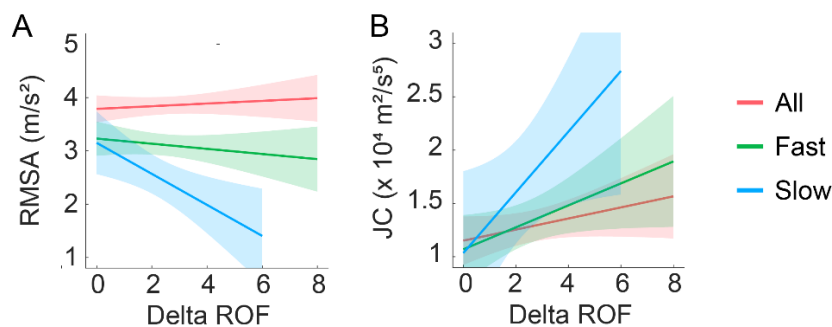


Figure 3.12 Evolution of stability and smoothness with perceived fatigability. A and B show the linear change for RMSA and JC, respectively

3.5 DISCUSSION

The goal of the present study was to measure concurrently and continuously the response of the biomechanical and psychological parameters to acute fatigue during a half-marathon run. The influence of fatigue on gait spatiotemporal parameters and secondary gait parameters and the differences between the fast and slow runners is discussed in section 3.5.1 and 3.5.2, respectively. The evolution of trunk motion with ROF and race progression, and the comparison between the fast and slow group is discussed in section 3.5.3.

3.5.1 *Gait spatiotemporal parameters and perceived fatigue*

Concerning the biomechanical parameters, our analysis confirms previous results (Apte et al., 2021; Meyer et al., 2021b), showing a stable gait cycle time, an increase in contact time and duty factor, as well as decreases in pitch angle, swing time and vertical stiffness. The alteration in running biomechanics observed in the present study results from strategies to compensate for neuromuscular fatigue (Apte et al., 2021). Vertical stiffness represents the global response of spring-mass model to acute fatigue, thus rendering it crucial to the understanding of biomechanical changes (J.-B. Morin et al., 2005). Decreased vertical stiffness indicates an increase in the vertical motion of the COM and/or a decrease in the peak vertical GRF. The decrease in vertical stiffness is consistent with the observations in shorter time trials (800 m) but not for a longer mountainous ultramarathon race (330 km) distance (Degache et al., 2016). However, these comparisons must remain anecdotal due to the difference in running conditions, intensities and in methods for stiffness estimation. Except the *FSA*, the above-mentioned biomechanical alterations appeared during the first half of the race and maintained throughout the race (Table 3.1).

Furthermore, our results demonstrate that the gait parameters are affected by a lower increase in fatigue (Table 3.1). Moreover, once the biomechanical parameters start changing, the participants find it difficult to recover the deteriorating running technique. Interestingly, some biomechanical parameters are affected from the first sensation of fatigue (Δ ROF [1,2]), suggesting a correlation between perceived fatigue and neuromuscular impairments; these impairments are known as the underlying mechanism responsible for running technique alteration. This observation is in line with other studies suggesting that peripheral muscle fatigue would be the constantly regulated variable (Calbet, 2006), with a continuous sensory feedback coming from working muscles to the central nervous system (Esteve-Lanao et al., 2008). Neuromuscular fatigue seems to be the dominant mechanism influencing perceived fatigue during the initial portion of the run.

These findings are consistent with previous studies demonstrating that a large amount of muscle activation impairments is obtained early on a self-paced exercise (Azevedo et al., 2019). The widely recognized critical point associated to fatigue in marathon race, known as “hitting the wall”, and characterized by a late-race slowdown (Buman et al., 2008), was not observed when performing group statistics in our study. The fact that most of our participants were not ‘hitting the wall’, shown by a reasonably stable running speed, might explain why we do not observe additional significant alterations

(Table 3.1) of the biomechanical parameters during the second part (between S5 and S8). We notice only few differences for parameter trends based on ROF (low, medium, high), compared to race progression. The main difference resides in smaller effect sizes for A2 statistical analysis, which might be explained by high inter-subject variability in perceived fatigue. This was caused by the pooling in A2 statistics, which led to the parameters at highest ROF of highly fatigued runners being pooled with the parameters at highest ROF of moderately fatigued runners. Thus, it seems relevant to compute ΔROF as a fatigue score for assessing acute fatigue. Furthermore, we did not necessarily find a linear increase of ROF, in contrast to earlier findings during in-laboratory incremental tests (Gronwald et al., 2018). This underlines the importance of measuring perceived fatigue during a running event that involves pacing strategies, as the difference in pacing strategies was clearly visible in fast and slow groups.

3.5.2 Secondary gait parameters

The overall asymmetry increased for all participants along the race. While the range of increase in overall asymmetry (~10%) is in accordance with the results from literature (Radzak et al., 2017), a full race profile for asymmetry has been presented here, which complements the existing pre-post results. The increase of asymmetry is higher for the fast runners halfway through the race; they typically have a lower t_c and d_f , which can accentuate the dominant leg effect. Since velocity (v) (Table 3.1) did not show any significant changes, we can conclude that acute fatigue led to the observed increase in asymmetry. The values and trends for variability (CV) were consistent with literature (Meardon et al., 2011), albeit in the context of a real outdoor competition. Faster runners exhibited lower CV, which coincides with the observations from laboratory studies (Mo & Chow, 2018a). This is likely because fast runners are more experienced with managing the regularity of the gait and adjusting their pacing strategy accordingly. The obtained values for $\alpha\text{-DFA}$ are in the similar range as those previously observed in a lab protocol (Mo & Chow, 2018a), with the differences in profiles for fast and slow runners possibly arising out of the differences in respective pacing strategies adopted by them (Mo & Chow, 2018a). This is also reflected in the linear trend for ΔROF (Figure 3.11C), where $\alpha\text{-DFA}$ is increasing for slow runners, and decreasing for fast runners. The decrease in CV and $\alpha\text{-DFA}$ at low ΔROF levels (beginning of the race) is consistent with the significant changes for spatiotemporal parameters at low ΔROF levels (Table 3.1). The difference in results for secondary gait parameters with race progression and ΔROF highlights the relevance of the measurement of perceived fatigue during outdoor running protocols.

3.5.3 Progression of the trunk motion

In addition to lower body biomechanical changes, we observed a significant increase in the trunk anteroposterior acceleration, most likely linked with a fatigue of the lower back postural muscles. *RMSA* showed an increasing trend with race progression for both fast and slow groups (Figure 2A, B), which is consistent with the findings from Schütte et al. (Schütte et al., 2015). For ΔROF , it showed difference in slopes for the slow and fast groups, with fast runners showing a moderate increase and slow runners showing a decline. Participants in slow group likely have a lower experience in managing the level of fatigue compared to those in the fast group. Thus, they might adopt a

strategy of lowering their overall acceleration at higher ΔROF to manage their dynamic stability (Provot et al., 2021), leading to a decline in the *RMSA*. It also increased significantly at low ΔROF values but not for $\Delta ROF \geq 5$, which can also be attributed to the reduction in *RMSA* for the slow group. This change at the beginning of the race coincides with results for primary gait parameters, where significant biomechanical changes were observed soon after the beginning of the race. Differing trends were observed for stability based on the choice of metric, with *RMSA* presenting the most consistent trends. *RMSA* depends on the running velocity, with fast runners showing a higher *RMSA* than slow runners at the beginning of the race. However, any intra-participant significant changes in velocity (v) (Table 3.1) were not observed. Thus, *RMSA* provides a clear indication that stability of the trunk decreases with perceived fatigue, more so for amateur runners.

All groups showed a positive slope for the relation between *JC* and ΔROF (Figure 2F), with slow group presenting a considerably larger slope but a similar intercept as fast group. The increase in *JC* points to a reduction in smoothness of movement and consequently a higher energy cost of running (Kiely et al., 2019; Provot et al., 2021; Schütte et al., 2018). These results suggest that faster runners tend to better manage the energy costs of running and do not experience the cascading effect (Figure 3.8C) of increased energy costs on running smoothness and decreased running smoothness on increased energy costs. Moreover, unlike stability, slow runners seem unable to recover the smoothness of movement with reduced overall acceleration. Compared to *JC*, *SPARC* measures and *IPV* did not show any significant change and could not differentiate well between FG and SG. Whereas *JC* was computed on a_{ML} , these metrics were calculated using v , where the velocity profile did not change significantly throughout the race. Furthermore, *SPARC* value depends on the choice of cut-off frequency (Balasubramanian et al., 2015), which might have affected the results. Thus, we observed that *JC* quantified well the quality of the continuity of movements and remained independent of amplitude of speed (Kiely et al., 2019). Apart from those specific observations, it can be observed, generally, that the variance (on all results) for slow runners is higher than for fast runners.

3.5.4 Limitations

The estimation of *FSA* can be rendered less accurate for participants with a forefoot strike (Falbriard et al., 2020), which was the case with one participant in the fast group. The sample size in the study is limited to 13 subjects and is too low to conclude any statistical results for between-group comparison of fast and slow runners. However, the clear trends for each group could be relevant for a future between-group study design. In addition to a bigger sample size, background data about the participants, such their VO_{2max} values, sleep quality, stress, and emotional health can improve the interpretation of the results. Furthermore, improving the resolution of the collection of *ROF* samples can enable a finer analysis of the evolution of perceived fatigability and its influence on the biomechanical and physiological parameters. Finally, the perceived fatigability can be assessed more holistically by also including the measurement of the valence, arousal, flow state, and action crisis (Venhorst et al., 2018). While this addi-

tional measurement was not feasible during the race, a pre/post assessment could provide a more complete understanding of the affective, sensory, and cognitive processes.

3.6 CONCLUSION

This work is one of the first to measure the evolution of running biomechanics concurrently and continuously in response to perceived acute fatigue during a half-marathon run. The biomechanical parameters presented a significant alteration even with a small change in perceived fatigue for all levels of runners. This study showed that fatigue leads to an increase in asymmetry of gait and influences variability and complexity of gait cycle time. Faster runners showed a lower variability than slower runners, but a higher increase in asymmetry with fatigue. A significant decrease for stability and smoothness of trunk movement was observed with progression in the race and perceived fatigue. The metrics led to different trends, with jerk cost and RMS acceleration presenting reliable results for smoothness and stability, respectively. Assessment with respect to perceived fatigue provided different results than that with race progression for some metrics. Less experienced runners were able to slightly recover the stability of their trunk movement but not the smoothness. These results indicate the ability of faster runners to better perceive their physiological limits and hint towards a higher sensitivity of perceived fatigue to changes in the running gait. Assessment with respect to perceived fatigue provided different results than that with race progression for gait variability. This study highlights measurable influences of acute fatigue, which can be studied only through concurrent measurement of biomechanical and psychological facets of running in real-world conditions. It may serve as a springboard for the design of studies that measure the association of biomechanical and physiological parameters and its evolution with acute fatigue. Use of such wearable sensor setups may further allow a more personalized approach to fatigue analysis and help runners to optimize their pacing strategies by understanding their running technique better.

4 ESTIMATION OF RUNNING POWER WITH FOOT-WORN IMUS

In addition to the evolution of running technique with acute fatigue, training assessment can be augmented by the evaluation of running power, which indicates the intensity of the run. Feedback of ‘power’ during running is a promising tool for training and determining pacing strategies. However, current power estimation methods show low validity and are not customized for running on different slopes. Towards this, three machine-learning models were developed to estimate peak mechanical power for flat, uphill, and downhill running using gait spatio-temporal parameters, accelerometer and gyroscope signals extracted from foot-worn IMU. The prediction was compared to reference power obtained during running on treadmill with an embedded force plate. For each model, an elastic net and a neural network was trained and validated with a dataset comprising of 34 active adults, over a range of speeds and gradients. For the uphill and level running, the concentric phase of gait cycle was considered, and the neural network model led to the lowest error (median \pm interquartile range) of 1.7 ± 12.5 % and 3.2 ± 13.4 %, respectively. The eccentric phase was considered relevant for downhill running, wherein, the elastic net model provided the lowest error of 1.8 ± 14.1 %. Results demonstrated a similar performance across a range of various speed/slope running conditions. The findings highlighted the potential of using interpretable biomechanical features in machine learning models for estimation of power. The simplicity of the models makes them suitable for implementation on embedded systems with limited processing and energy storage capacity. The proposed method meets requirements for applications needing accurate near real-time feedback and complements existing gait analysis algorithms based on foot worn IMUs.

The contents of this chapter are under review as an original research article in the IEEE Journal of Biomedical and Health Informatics.

Contributions: designed and implemented the estimation method; contributed to the analysis and interpretation of the data; drafted the manuscript.

4.1 INTRODUCTION

Mechanical power generated during running is a measure of the intensity of the run. As an indicator of intensity, power can be used to augment external load monitoring for training programs and to develop pacing strategies for competitions (Aubry et al., 2018). A reduction in running power for a constant running speed indicates a decrease in aerobic power and thus an improvement in running economy (Cerezuela-Espejo et al., 2018; Taboga et al., 2021). Internal factors such as fatigue, stress, hydration, etc., or environmental factors such as humidity, temperature, presence of competitors, etc., can influence the perception of internal load and heart rate response (Halsen, 2014). Since these factors do not directly affect the running power, it can serve as a useful additional metric for monitoring training load during exercise (Paquette et al., 2020). Unlike heart rate, which is affected by cardiac drift and has a higher response latency (Billat et al., 2020; Coyle & González-Alonso, 2001), power provides an immediate measure of running intensity and can thus potentially help optimize pacing strategies. Additionally, measurement of power can help in detecting early decrease in running economy, indicating fatigue onset. In cycling, the widespread use of mechanical power as a tool for optimizing performance and training adaptation has been facilitated by the availability of reliable power meters (Erp et al., 2019; Foster et al., 2017). Since crankshaft force can be measured with a strain gage and speed with a wheel sensor, mechanical power can be measured directly with sensors integrated into the bicycle design (Passfield et al., 2017). However, such a direct measurement of force and speed during real-world running is challenging.

Mechanical power is defined as the time derivative of mechanical work or the rate at which work is performed. Thus, quantification of mechanical work during running provides a way for estimating the power. Different in-lab approaches have been proposed to measure the total mechanical work produced by the body and derive the power for level running over a range of speeds (Cavagna et al., 1964; Cavagna & Kaneko, 1977; Rabita et al., 2015; van der Kruk et al., 2018; Williams & Cavanagh, 1987). Mechanical work is classified into two types: internal work, that is, the work done in moving the limbs with respect to the center of mass (CoM) of the body and external work, which results from the movement of CoM of the body with respect to the environment (Cavagna & Kaneko, 1977). Limb motion is usually measured with marker-based motion tracking systems, whereas CoM kinetics and ground reaction forces (GRF) additionally require the use of force plates. When comparing estimated mechanical power at similar speeds, existing approaches based on these instrumentation resulted in different findings and an universally accepted approach has not been established (Arampatzis et al., 2000; van der Kruk et al., 2018; E. M. Winter et al., 2016). The inclusion of GRF and running speed in the estimation of work and power, though, improved accuracy and matched the expected increase in power due to an increase in running speed (Arampatzis et al., 2000). The incline of the running surface may influence the speed and the GRF, and possibly the running power (Wickler et al., 2000). Therefore, the GRF, running speed, and incline of the running surface can be considered together as a reference system for the estimation. However, accurate measurement of GRF with force plates is impractical in real-world running conditions.

Wearable inertial measurement units (IMU) have been used to estimate vertical GRF and peak anteroposterior GRF (Neugebauer et al., 2014; Thiel et al., 2018; Wouda et al., 2018). However, the complete anteroposterior GRF profile is essential for estimation of mechanical work (and power) involved in push-off and braking phases (Arellano & Kram, 2014). Furthermore, these estimations of GRF have been validated for level running and may not show similar performance for uphill and downhill conditions. Of the commercially available body-worn devices, studies recommend the foot-worn Stryd device due to its high repeatability of measurements and its concurrent validity ($r \geq 0.911$, $SEE \leq 7.3\%$) with respect to the VO_2 values (Cerezuela-Espejo et al., 2018). One study reports the power estimated by the Stryd device for different treadmill speeds during level running to reflect (mean difference: -1.04 Wkg^{-1} , Limits of agreement: -2.3 to 0.18 Wkg^{-1}) the reference power measured as a dot product of horizontal (in the direction of running) and vertical forces and velocity respectively, obtained from a force plate (Taboga et al., 2021). Another study, however, reports an underestimation of power from the Stryd device (Imbach et al., 2020). Further, this system has not been validated for running on slopes, which is an important requirement for trail running or long-distance races. Finally, the estimated power output has shown inadequate changes in response to intentional changes in running technique and temporal parameters (Baumgartner et al., 2021), such as step frequency ($\pm 10\%$ change), contact time (~ -20 ms), and arm swing (presence/absence). Other analytical models focus either on the characterization of the overall race performance (Mulligan et al., 2018) or only on the power requirement while running on flat terrain (Jenny & Jenny, 2020). An approach based on simulated wearable IMUs has shown promise (RMS error range $4.2 - 20.1\%$), but requires data from 15 body segments (Fohrmann et al., 2019). In this study, IMU data was simulated with the virtual acceleration and angular velocity values obtained from a full-body marker-based motion capture system. Neither of these power estimation approaches are particularly suitable for accurate near real-time feedback.

Given the potential of body-worn IMU and global navigation satellite system (GNSS) to estimate running speed (Apte, Meyer, et al., 2020; Falbriard et al., 2021), the relationship between mechanical power and running speed (García-Pinillos et al., 2019) could be used to predict power. However, this relationship is affected by terrain slope and running technique. Terrain slope can be estimated using accelerometer signals (Herren et al., 1999) or barometer (Moncada-Torres et al., 2014) while running technique can be identified by spatiotemporal gait parameters. One parameter is the vertical stiffness of the spring-mass model used to simulate running, which explains the higher efficiency of running movement that exceeds analytic muscle efficiency. Although vertical stiffness cannot be measured directly under real running conditions, it can be estimated indirectly using spatiotemporal parameters such as contact time, flight time, and running speed. Previous research has presented an accurate assessment of these parameters (Falbriard et al., 2018, 2020) and their application in real-world conditions (Apte, Troxler, et al., 2022; Meyer et al., 2021b; Prigent et al., 2022), using foot-worn IMUs.

Current study aims to extend this work by estimating running power during level and graded running at different running speeds. Here, power is defined as including only the components of force and velocity in the running direction (horizontal). This definition is suitable for the purpose of a feedback tool for training, which is our main appli-

cation, even though it violates the definition of power as a scalar mechanical quantity, which is the dot product of force and velocity in a 3-D space (Vigotsky et al., 2019). With a single IMU on each foot, the aim is achieve a performance that is similar, if not better, to the one (RMS error range 4.2 – 20.1%) achieved using a simulated full-body IMU setup (Fohrmann et al., 2019). Achieving an acceptable accuracy that does not depend on the conditions will be an important technical hurdle that should be overcome, thanks to a complete data acquisition protocol that covers the different situations and provides enough "ground truth" data to learn our models. The different situations include a range of running speeds and inclines, the knowledge of which will serve as complementary information to the one obtained from IMU signals. Moreover, the models proposed here are aimed to be computationally inexpensive, to enable their application to near real-time performance estimation with traditional embedded electronic devices.

4.2 MATERIALS AND PROTOCOL

Measurements were conducted with 34 healthy subjects (age: 35 ± 11 years; height: 174 ± 10 cm; weight: 69 ± 12 kg; max. aerobic speed: 16.89 ± 2.81 km/h) on motorized treadmill (T-170-FMT, Arsalis, Belgium). The treadmill was customized to enable an adjustable inclination. The treadmill incorporated a force plate with 3-D force recording at a sampling frequency of 1000 Hz. The participants were equipped with IMUs (Physilog 5, GaitUp, Switzerland, 512 Hz, 16g, 2000 °/s) attached to the shoelaces using rubber clips, a heart rate monitoring belt on the chest (V800 watch with H10 belt, Polar, Finland, RR intervals), and wore a gas exchange mask connected to a O₂/CO₂ gas analyzer system (Quark CPET, Cosmed, Italy, breath-by-breath). Figure 4.1A illustrates this sensor setup.

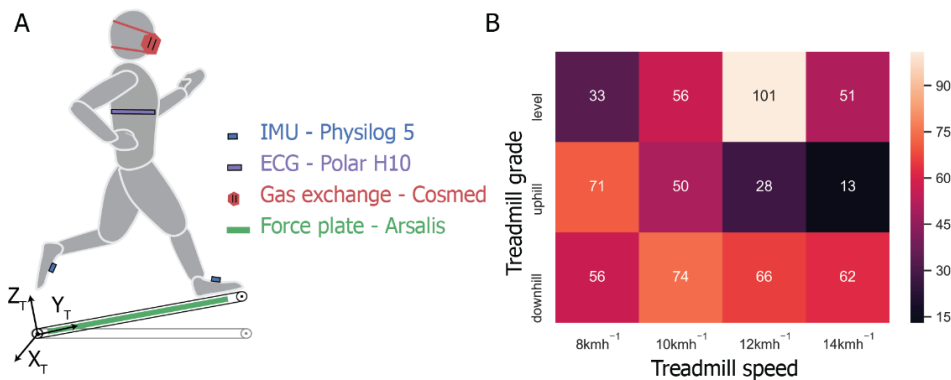


Figure 4.1 Measurement systems and data collection protocol. A) An IMU was attached to each foot, and force plate data were used as a reference. X_T - Y_T - Z_T represent the frame of reference attached to the treadmill. Gas exchange was used during the incremental speed test to determine endurance capacity, and the ECG monitor indicated the exertion, B) Number of recorded running trials for each treadmill speed for all three treadmill grades. This information was used for balancing the dataset

The treadmill running protocol comprised of 4 sessions, separated enough to allow recovery in between, with multiple combinations of treadmill speed and gradient. The first session aimed to evaluate participants' fitness, based ventilatory threshold and VO_{2max} assessments, using an incremental speed test. These thresholds were used to

personalize the energy consumption of the different running conditions and avoid excessive fatigue of the participants in the subsequent sessions (McGawley, 2017; Morgan & Daniels, 1994). This helped the participants to avoid entering a state of advanced fatigue that could bias the measurements. In sessions 2, 3, and 4 the participants went through a series of 4 minutes running bouts at different running speed (i.e., 8, 10, 12, and 14 km/h) and slope gradient (i.e., 0%, $\pm 5\%$, $\pm 10\%$, $+15\%$, and $\pm 20\%$). Among all the participants, 100% (34) completed the first session, 88% (30) the second session, 79% (27) the third, and 71% (24) the fourth session. The resulting dataset was imbalanced (Figure 4.1B) due to the sequential reduction in the participation because of increasing physical intensity of the protocol. The increasing intensity corresponded to an increasing treadmill speed and grade. As an incentive, each participant received an evaluation of their running performance (ventilatory thresholds and $\text{VO}_{2\text{max}}$) and running technique. Ethical approval for the study was obtained from the human research ethics committee (CER-VD 2015-00006) and prior written consent was obtained from all the participants. Monitoring of gas exchange and heart rate was included in this study for purpose of assessing the endurance capacity of the participants and their state of exertion during the protocol, and their data were not used for the estimation of power.

4.3 METHODS

4.3.1 Reference power estimation

The process for reference power estimation is presented in Figure 4.2A. Force plate signals along the sagittal plane, in the direction of running (F_y) and perpendicular to it (F_z) were checked for outliers and linear interpolation was used to replace them.

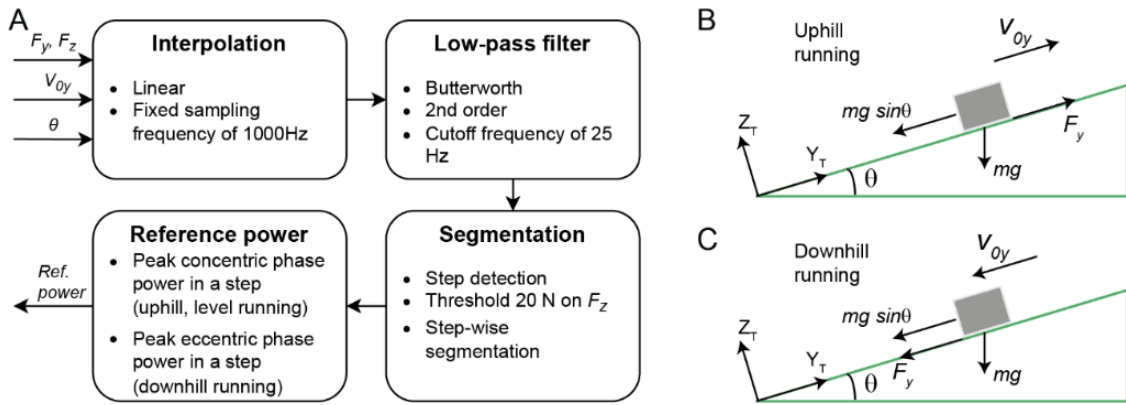


Figure 4.2 Estimation of reference power (A) Processing force plate data. (B) Free body diagram for stance phase during uphill running on treadmill, with the runner represented as a rigid body. (C) Similar free body diagram for downhill running

The signals were subsequently filtered using a zero-phase lowpass Butterworth filter, of order 3 and cutoff frequency 25 Hz, based on the recommendation of using around 20 Hz for matched lowpass filtering of kinematic and force plate data (Mai & Willwacher, 2019). A threshold of 20N on the F_z signal was used to detect the stance phase (Zeni et al., 2008). First frames with F_z higher and lower than 20 N for a length of at least 40 samples were ascertained as initial and terminal contact. A threshold of 300N was considered for the mid-stance to segment the signal into gait cycles.

Two main approaches have been considered in literature for the estimation of power (Arampatzis et al., 2000), first based on the GRF and the CoM motion, and second based on the estimation of the product of force-velocity or moment-angular velocity of all the individual limb segments (Cavagna et al., 1964; Cavagna & Kaneko, 1977). The latter method requires precise 3D motion tracking of each segment and is prone to more outliers. Furthermore, the first method shows a better correspondence with oxygen uptake (Arampatzis et al., 2000). In this method (Rabita et al., 2015), the antero-posterior (in the direction of the run) AP GRF is used to estimate the AP acceleration, velocity, and directional power of the CoM during the stance phase. This method was adapted for uphill running, as illustrated in Figure 4.2B, using the following equations:

$$a_y = \frac{F_y - mg \sin \theta}{m} \quad (4.1)$$

$$v_y = v_{0y} + \int_0^t a_y dt \quad (4.2)$$

$$P_y = v_y \times F_y \quad (4.3)$$

$$W_y = W_{0y} + \int_0^t P_y dt \quad (4.4)$$

where y is the direction of running and F_y is the force recorded by force plate along y , a_y is the instantaneous acceleration of the CoM, v_y is the instantaneous velocity of the CoM, P_y is the 'power', W_y is the 'work', m is the body mass, t is the time elapsed since the beginning of the stance phase. v_{0y} is the average velocity of the CoM during running, i.e., speed of the treadmill and the slope θ is assumed to be positive. For downhill running (Figure 4.2C), the direction of running (direction of F_y , a_y , v_y , v_{0y}) is reversed, leading to a different equation for a_y :

$$a_y = \frac{F_y + mg \sin \theta}{m} \quad (4.5)$$

During the implementation of these equations, all the quantities are considered as scalars since the direction (y) is already considered. Therefore, P_y is not a real power in a strict mechanical sense, as it represents only one component of a three-dimensional movement. In case of level and uphill running, the maximum power in the concentric phase was assumed as the reference power (P) value for one step (Roberts & Belliveau, 2005). For downhill running, the minimum power (negative peak) during the eccentric phase was considered as the reference value (P) for one step. Peak values in both phases are less susceptible to estimation errors as compared to average values, since the latter also depend on the accurate estimation of the duration of the individual phases. Assuming only the power produced during concentric phase and averaging it over the entire stance phase (Taboga et al., 2021) does not provide useful information during downhill running, since it mainly involves eccentric activation of the thigh muscles (Eston et al., 1995).

4.3.2 IMU data processing

The main steps for IMU data processing are presented in Figure 4.3. A 4th-order low-pass Butterworth filter ($F_c = 50$ Hz) was first applied onto the raw acceleration ($a_s(t)$)

and angular velocity ($\omega_s(t)$) signals to reduce the noise of the sensors. The filtered IMU signals were aligned with the functional frame ($a_f(t)$, $\omega_f(t)$) of the foot using functional calibration. The calibration process included data from a 5-seconds static period before the run, followed by the initial steps of the run (Falbriard et al., 2018). Following this, each signal ($a_f(t)$, $\omega_f(t)$) was segmented into mid-swing to mid-swing cycles and temporal events of the gait were detected within each cycle (Falbriard et al., 2018).

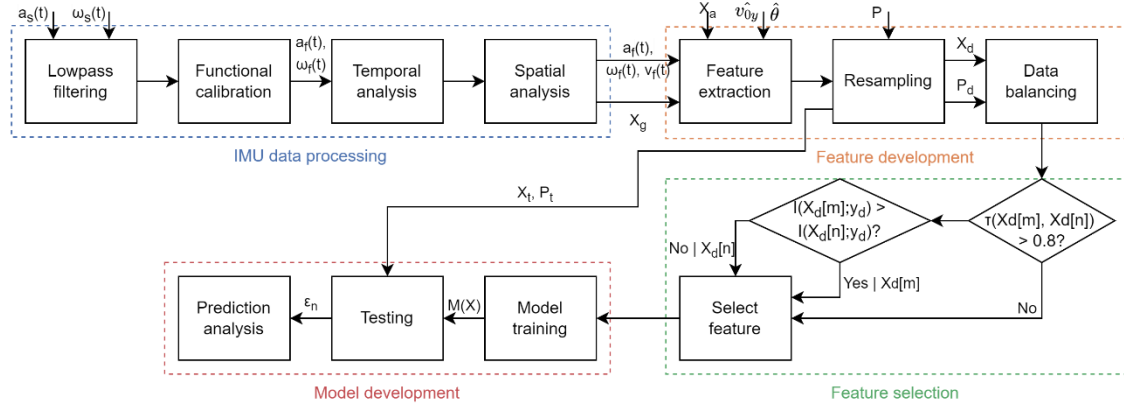


Figure 4.3 Flowchart for the proposed power estimation method. The process is divided into four main parts – i) processing of the IMU signals, ii) extraction of features based on IMU signals, biomechanical and anthropomorphic parameters, treadmill speed, and slope, iii) selection of features based on reducing redundance and maximizing the relevance, and iv) Development and validation of the three models for level, uphill, and downhill running, respectively. P : reference power, X_d : development feature set, P_d : development set for response variable (power), X_t : test feature set, P_t : test set for response variable, $M(x)$: developed model, ϵ_n : error

As literature suggested association between the changes in the duration of the gait phases and the running speed (Apte et al., 2021), hence also the mechanical power, the ground contact time, the flight time, the swing time, and the step duration for each step were computed. These temporal parameters were used as inputs to the model proposed by Morin et al. (J.-B. Morin et al., 2005) to estimate leg and vertical stiffness. Subsequently, we computed the orientation of the foot in the global frame (X_T - Y_T - Z_T) and transformed the foot acceleration from the foot frame (FF) to the GF, after removing the gravitational acceleration. The resulting acceleration (in GF) was integrated using a trapezoidal rule to get a first estimate of the speed of the foot. Speed of the foot was considered to be zero during the stance phase and, therefore, estimated and removed the integration drift by linearly resetting the speed at each stance phase (Falbriard et al., 2021). Finally, we applied the inverse transformation to get the drift-corrected stride velocity of the foot segments ($v_f(t)$) in the FF, that is subsequently to develop features for the models. It is important to note that $v_f(t)$ is different from v_{0y} , which is the treadmill speed.

4.3.3 Feature development

4.3.3.1 Feature extraction

The overall feature development process is presented in Figure 4.3. The gait spatio-temporal and stiffness parameters extracted from the IMUs form the first feature set

(X_g). To supplement this feature set, several statistical features were extracted from the $a_f(t)$, $\omega_f(t)$, and $v_f(t)$ signals. Since each of signals contains 3 channels (x, y, and z), the statistics for each channel were calculated separately. Also, the Euclidean norm was calculated for each signal, followed by the statistics for that norm. Note that the statistical features (X_s) were captured on the signals of a single stride. Compared to a step-based segmentation, a stride-based segmentation is more likely to capture the complete period of a gait cycle. The features X_s aimed to encapsulate information about the intensity of the signal (e.g., mean, STD, RMS), the shape of its distribution (e.g., skewness, kurtosis), and its shape in a compressed format (e.g., coefficient of the auto-regressive model (Table 4.1). Since the temporal parameters already contain relevant periodic information, features in the frequency domain were not considered.

Table 4.1 Statistical features (X_s) extracted for each stride on the continuous acceleration $a_f(t)$, angular velocity $\omega_f(t)$, speed $v_f(t)$. Variables T and C correspond to the signal (a, ω , v_f) and the channel (x, y, z, or n i.e., norm), respectively. AR: Auto-regressive model

Type	Feature	Description
Intensity	μTC	Mean value
	σTC	Standard deviation
	medTC	Median
	iqrTC	Interquartile range
	maxTC	Maximum
	rmsTC	Root-mean-square
Shape	kurtTC	Kurtosis
	skewTC	Skewness
Compression	arm1TC	1 st coeff. of 3 rd order AR model
	arm2TC	2 nd coeff. of 3 rd order AR model
	arm3TC	3 rd coeff. of 3 rd order AR model

In addition to the sensor-based features, the anthropomorphic information of the participants was considered. The height, age, mass, and the leg length (measured from hip to the foot) of the participants were included as features (X_a). Since the mass is used in the calculation of P_y (equations 4.1 – 4.3), it was expected to be an important feature. Finally, information of the running conditions was used to complete the feature set. Running conditions were defined in terms of the slope (θ) and the treadmill speed (v_{0y}). However, to simulate real-world conditions where θ and v_{0y} will be estimated from IMU and barometer signals, noise was added to the known θ and v_{0y} values. For v_{0y} , the maximum standard deviation and bias of error for IMU-based estimation are 0.16 m/s and 0.0 respectively (Falbriard et al., 2021). So, a white noise of range $[-0.16, 0.16]$ was added to the treadmill v_{0y} data before using it as a feature. Apart from this maximum noise condition (100%), two other conditions were also considered, a smaller noise (50%) of $[-0.8, 0.8]$ and no noise i.e., perfect estimation of v_{0y} . These three conditions allowed us to explore the performance of our methods under different performances of speed estimation algorithm. The same process was repeated for θ . Assuming a 10 s window, the minimum distance estimated at the lowest treadmill speed (2.22 m/s or 8 km/h) would be $(2.22 - 0.16) \times 10 = 20.6$ m. Assuming a relative height estimation error of ± 1 m using a barometer (Ye et al., 2018), the error in grade was com-

puted to be $\pm 4.86\%$. So, a white noise of range $[-4.86, 4.86]$ was added to the grade data before using it as a feature. The final feature set (X_c) thus consisted of the noisy speed ($\widehat{v_{0y}}$) and grade ($\widehat{\theta}$) data. The overall feature set (X), with each feature as a vector of values with a resolution of one step, is shown below:

$$X = [X_g, X_s, X_a, X_c] \quad (4.6)$$

4.3.3.2 Resampling and data balancing

Because the feature set was based on segmentation of gait cycles, some inevitably misidentified gait cycles resulted in missing values. To address this problem, the data was resampled at a resolution of one value per second. Similarly, the reference power data were resampled at the same resolution and considered as the response variable (P). The resulting dataset was imbalanced (Figure 4.1B) due to the sequential reduction in the participation because of increasing physical intensity of the protocol. The increasing intensity mainly corresponded to an increasing treadmill speed and grade. By considering the speed as a class and dividing the grade into three conditions (level, uphill, downhill), the classes were balanced using random over sampling (ROS) of underrepresented classes (Pes, 2020). Compared to random under sampling (RUS), ROS duplicates information rather than randomly removing samples of potentially rare conditions (e.g., high speed during uphill running). For i^{th} class with n_i samples, ROS was implemented as:

$$\hat{n}_i = n_i \times \left(\frac{n_{\max}}{n_i}\right)^\alpha \quad (4.7)$$

Where \hat{n}_i is modified sample size, n_{\max} is size of the largest class, and α is a hyperparameter. After trying values from 0.5 to 0.95 in steps of 0.05, the α was set to 0.8. Finally, data from one-third of the participants ($n = 11$) were reserved as the test set (X_t, P_t), while the remaining data were used as the development and validation set (X_d, P_d) for the feature selection and model training phases. All data of a single participant were attributed to only one of the subsets; this removed the performance bias associated with the models trained and tested on measurements originating from the same subjects (Halilaj et al., 2018). To form the development and test sets, the participants were selected randomly.

4.3.4 Feature selection

The feature set obtained as a result of feature extraction included a total of 171 features. To develop a simpler and more efficient model, we performed a feature selection process (Figure 4.3) using filter methods to remove the redundant and irrelevant features (Li et al., 2017). To identify the redundant feature pairs, we calculated the correlation between all possible feature pairs. Kendall's τ was used to quantify the correlation between features; it is more robust than Spearman's correlation coefficient and less sensitive to errors and discrepancies in the data (Newson, 2002). Whereas Pearson's correlation only considers the linear relationship between variables, Kendall's τ relies on the number of concordant and discordant pairs in the variables and does not require a specific functional relationship between variables (de Siqueira Santos et al., 2014). For feature pairs $X_d[m]$ and $X_d[n]$ with N samples, τ is quantified as:

$$\tau = \frac{2}{N(N-1)} \sum_{i < j} \text{sgn}(X_d[m, i] - X_d[m, j]) \times \text{sgn}(X_d[n, i] - X_d[n, j]) \quad (4.8)$$

$$\text{sgn}(x) = \begin{cases} 1 & \forall x > 0 \\ 0 & \forall x = 0 \\ -1 & \forall x < 0 \end{cases} \quad (4.9)$$

Feature pairs with $\tau < 0.8$ (selected based on trials with a range from 0.5 to 0.95) were selected for model development (see Figure 4.3), while others were further examined for their relevance to the response variable (y_d) using the mutual information (I) metric, which quantifies the amount of information obtained about one variable, through the availability of another variable (Kraskov et al., 2004). If $X_d[m]$ is considered as X and P_d as Y , I can be expressed as:

$$I(X; Y) = \sum_{y \in Y} \sum_{x \in X} p_{(X,Y)}(x, y) \log \left(\frac{p_{(X,Y)}(x, y)}{p_X(x)p_Y(y)} \right) \quad (4.10)$$

where p_X and p_Y are the marginal probability density function for X and Y , and $p_{(X,Y)}$ is the joint probability mass function of X and Y . For feature pairs with $\tau(X_d[m], X_d[n]) > 0.8$, feature $X_d[m]$ was selected if $I(X_d[m]; y_d) > I(X_d[n]; y_d)$ and vice-versa (Vergara & Estévez, 2014). The selected feature set contained 117, 125, and 120 features for level, uphill, and downhill running, with around 30% features being removed through the selected feature selection technique.

4.3.5 Model development

4.3.5.1 Model training

The goal was to develop one model for each of the three running conditions. To ensure that features contributed equally to the model training and that coefficients were properly scaled, the features were rescaled using a z-score normalization method (Jain et al., 2005); hence, after normalization, the features mean was zero, and standard deviation was one. Two approaches were pursued for model development – a linear model using Elastic net regularization (EN) and a nonlinear model using a neural network.

Linear models enable computationally efficient implementation for near real-time analyses on commercial embedded devices. Furthermore, in case of similarly performing linear and nonlinear models, EN allows us to understand the feature importance. EN is a generalization of the lasso regression method, which that linearly combines the L1 penalty of the lasso regression method and the L2 penalty of the ridge regression method (Zou & Hastie, 2005). EN tends to maintain a similar feature sparsity as the lasso method while providing improved accuracy. Similarly, it overcomes the lasso limitation of retaining only one of a group of linearly correlated predictors and tends to include the entire group (Hastie et al., 2008a; Zou & Hastie, 2005). The EN is implemented as shown in (9), with $P_{d,i}$ being the response at observation i , N the total number of observations, $X_{d,i}$ the feature vector with k features at observation i , λ the positive regularization parameter corresponding to one value of Lambda, β the coefficient, and β_0 the intercept.

$$\min_{\beta_0, \beta} \left(\sum_{i=1}^N (y_{d,i} - \beta_0 - x_{d,i}^T \beta)^2 + \lambda K_Y(\beta) \right) \quad (4.11)$$

$$K_Y(\beta) = \sum_{j=1}^k \left(\frac{(1-\gamma)}{2} \beta_j^2 + \gamma |\beta_j| \right) \quad (4.12)$$

Where γ is the hyperparameter that sets the balance between the lasso and ridge regression methods. It was set at 0.5 for the model development. To account for interactions between biomechanical features and nonlinear relationships between biomechanical parameters and ‘power’, a Neural network (NN) was also implemented with output layer of 1 neuron and a hidden layer of 10 neurons (Hastie et al., 2008b). The default Matlab feedforward network was trained using the Levenburg-Marquadt back-propagation algorithm (H. Yu & Wilamowski, 2011), with a tan-sigmoid and linear transfer functions for the hidden and output layers, respectively. Two configurations of the NN were trained, with differing distributions of the training dataset (X_d, y_d) :

- NN15: 80% development, 15% validation, and 5% test
- NN35: 60% development, 35% validation, and 5% test

4.3.5.2 Model validation and testing

The EN, NN15, and NN35 models were tested with the test set (X_t, P_t) to estimate ‘power’ \hat{P}_t . Following this, the P_t and \hat{P}_t were smoothed by averaging over a 10 s sliding window with an overlap of 5 s. This provided a power estimation every 5 s, which is satisfactory for application as a feedback tool during running, while enabling the estimation of running speed (\widehat{v}_{0y}) and terrain grade ($\hat{\theta}$) using the foot IMU and barometer signals. The estimated power \hat{P}_t was compared to the reference power P_t using the percentage error (ε_n):

$$\varepsilon_n = \frac{P_t - \hat{P}_t}{P_t} \times 100 (\%) \quad (4.13)$$

Median and interquartile range (IQR) of ε_n were calculated to determine the bias and precision of the power estimate. Median and IQR were also computed for each grade and treadmill speed to understand the performance of the algorithm under different running conditions. The mean absolute error (MAE) was also computed using ε_n to understand the overall error. In addition, the Bland-Altman approach (Bland & Altman, 2003) was used with P_t and \hat{P}_t to investigate the agreement between our algorithm and the force plate-based power estimation. Finally, cumulative distribution plots of ε_n were constructed for the three noise assumptions ($\epsilon_{100}, \epsilon_{50}, \epsilon_0$) on speed and slope, for all running conditions. These plots can provide insight into the effects of the noise in the features on the error distribution.

4.4 RESULTS

Data was analyzed from 34 participants who ran on a treadmill at various speeds and inclines, including a total of 210.7 minutes of level, 74.6 minutes of uphill, and 112.4 minutes of downhill running, used for training and testing the algorithm. The reference power estimated from the force plate data followed a nearly linearly increasing relationship with treadmill speed, with uphill running exhibiting a higher peak power during the concentric phase of stance than level running, at the same speed. Figure 4.4 presents the magnitude of reference power (P_t) for all treadmill speeds; reference power increased with speed and was higher when running uphill than when running on level treadmill.

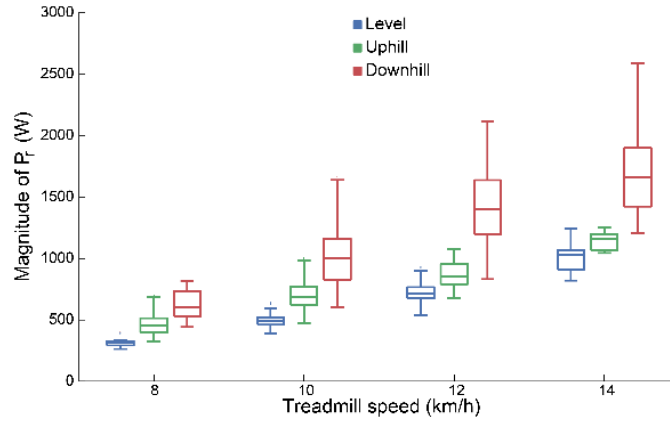


Figure 4.4 Relationship between the reference power and the treadmill speed

The cumulative distribution of the error for all running conditions and noise levels, is shown in Figure 4.5. At all conditions the error remains below 20% for 90% of the participants, including any outliers. In contrast to level running, there is a larger influence of noisy running conditions (X_c) on the error distribution for running on inclines.

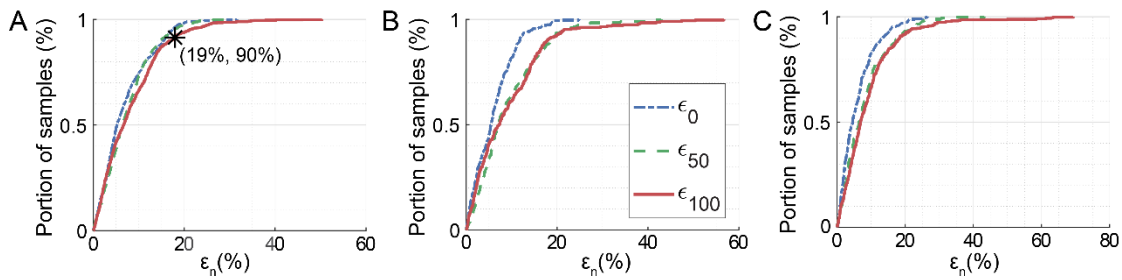


Figure 4.5 Cumulative distribution of ϵ_{100} , ϵ_{50} , ϵ_0 (%) of the proposed method for level (A), uphill (B), and downhill (C) running, across all three noisy conditions. For example, in plot A, the * shows the error for level running is less than 19% for 90% of the population, when using 100% of noisy running condition (X_c).

Figure 4.6A and B show the best case and worst-case scenarios for the prediction of power for level running respectively. The increasing power (stair pattern) corresponds to different running trials, each with higher speed than earlier one. The former does not exhibit a substantial difference between the prediction for the zero-noise level (ϵ_0).

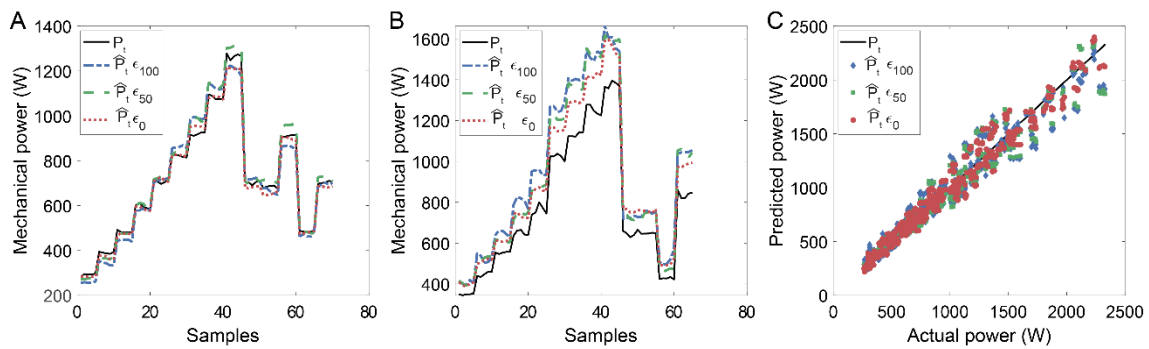


Figure 4.6 Illustration of reference and predicted power for level running for all three noise levels on features. A) participant with the best estimation of power, B) participant with the worst estimation C) Linear agreement between predicted and estimated values.

All three noise levels of running conditions resulted in excellent agreement ($R^2 > 0.9$) between the predicted and reference values based on linear correlation (Figure 4.6C). An increase in noise levels resulted in a higher deviation between predicted and reference power at high magnitudes of power. The Bland-Altman analysis plot for power estimation with maximum noise (ϵ_{100}) is presented in Figure 4.7, with samples from different participants represented by unique colors. It confirms low correlation between the error and estimated speed values ($\tau = 0.08$ for level, $\tau = -0.01$ for uphill, and $\tau = 0.09$ for downhill running) and an increase in error values with an increase in mean ($\frac{P_t + \hat{P}_t}{2}$) values. However, only 2 participants out of 11 show a high error at higher mean values for three running conditions. Downhill running (Figure 4.7C) indicates a possible non-linear relationship between the mean and difference of reference (P_t) and estimated power (\hat{P}_t) for power estimation.

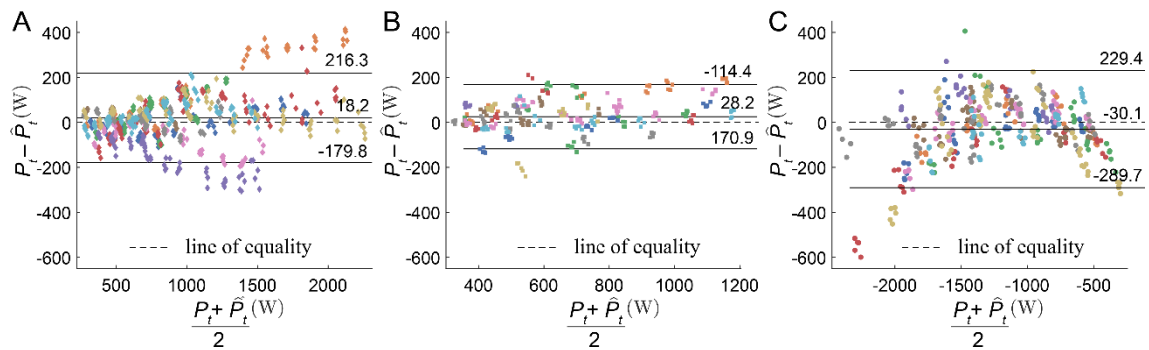


Figure 4.7 Bland–Altman analysis for power estimation with maximum noise (ϵ_{100}), samples from each participant in the test set are shown in different colors. P_t and \hat{P}_t are measured in terms of Watts (W), L.O.A. are the limits of agreement and M.D. is the mean difference. (A) Level running, (B) Uphill running, (C) Downhill running

Figure 4.8A and B present the bias and precision for the power estimation error across all treadmill speeds and slopes. For each positive slope and the -10% and -20% slopes, the bias was largest at the highest speed reached (10.4% at 20% slope, 18.4% at -20% slope). In contrast to the bias and the precision at the lowest treadmill speed (8 kmh^{-1}) was generally high (21 ± 5.9 %) at all slopes, including level running. At the 10 kmh^{-1} and 12 kmh^{-1} conditions, the estimation error showed a better precision (10.7 ± 2.0 %).

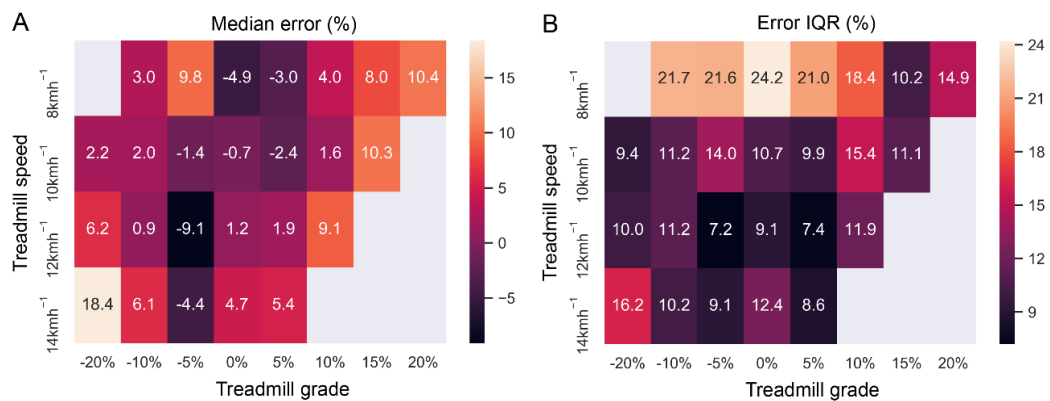


Figure 4.8 Estimation error (%) for all speeds and slopes. A) Median error, B) Error IQR

Linear correlation (R^2) between P_t and \hat{P}_t and the bias (median), precision (IQR), and the MAE for the error (%) are presented in Table 4.2. Even with the assumption of max. noise (ϵ_{100}), the median \pm IQR for error were low (1.7 ± 12.5 % for level, 7.1 ± 13.4 % for uphill, and 2.0 ± 13.3 % for downhill) for all three conditions. Reduction in noise typically led to a reduction in the IQR of the error. Kendall's test showed a high correlation ($R^2 = 0.95$ for level, $R^2 = 0.91$ for uphill, and $R^2 = 0.93$ for downhill) between P_t and \hat{P}_t .

Table 4.2 Bias (median), precision (IQR) and mean absolute error (MAE) of the power estimation algorithm for the three running conditions, with different levels of noise on the features of speed and grade

Condition	Noise	Best model	MAE (%)	Bias (%)	Precision (%)	R^2
Level running	ϵ_{100}	NN35	6.5	1.7	12.5	0.95
	ϵ_{50}	NN35	6.4	3.3	10.9	0.96
	ϵ_0	NN35	5.2	2.1	9.6	0.97
Uphill running	ϵ_{100}	NN15	7.1	3.2	13.4	0.91
	ϵ_{50}	NN15	6.3	-0.2	13.1	0.91
	ϵ_0	NN35	5.4	2.4	8.9	0.95
Downhill running	ϵ_{100}	EN	6.8	2.0	13.3	0.93
	ϵ_{50}	NN35	6.9	2.1	11.9	0.95
	ϵ_0	NN35	4.6	-1.9	8.4	0.97

For all three running conditions, the coefficients, and labels for the 15 most important features of the EN models are presented in Table 4.3. The most important features were usually the mass (m) and the treadmill speed (\hat{v}_{0y}), followed by the slope ($\hat{\theta}$).

Table 4.3 Labels and coefficients for the 15 most important features of the EN models. Statistical features are defined according to Table 4.1 and are indicated in bold, with the signal direction (or norm) indicated using a subscript. Other features are defined as kvert: vertical stiffness, fzmax: maximum vertical force, Δz : maximum vertical displacement of the CoM, strd: stride duration, and fsa: foot strike angle before initial contact. For downhill running, negative sign indicates a positive contribution to the power estimation model since the predicted power is negative.

Level		Uphill		Downhill	
Label	Coef.	Label	Coef.	Label	Coef.
\hat{v}_{0y}	73.8	m	48.9	\hat{v}_{0y}	-139
m	60.0	iqr _{ay}	34.0	m	-97.9
kvert	51.5	\hat{v}_{0y}	32.6	$\hat{\theta}$	93.8
fzmax	42.8	$\sigma\omega_y$	-32.4	arm1 ω_y	67.4
skew _{vfn}	-39.2	μv_{fy}	28.7	kurt ω_x	-65.1
μa_z	37.4	iqr _{vfx}	27.4	fzmax	-59.8
skew _{ay}	-36.5	kurt _{az}	-26.2	med _{ay}	59.1
max _{vfn}	34.7	μa_y	-25.6	σa_n	-57.2
μa_y	-33.5	strd	19.9	fsa	-54.8
Δz	29.2	skew ω_x	-19.9	max _{az}	52.0
rms _{ay}	27.7	Δz	19.7	rms _{an}	-51.9
iqr _{ay}	26.3	max ω_x	-19.3	μa_y	-50.9
arm1 _{vfx}	22.4	$\hat{\theta}$	18.5	iqr ω_y	50.5
skew _{vfy}	-22.4	lenleg	-18.1	arm3 ω_y	48.9
σv_{fz}	21.6	max _{az}	-17.0	skew _{ay}	-47.6

4.5 DISCUSSION AND CONCLUSION

This work presented a method for accurate estimation of power running with a foot-worn IMUs under various simulated real-world conditions. Different inclines and running speeds were considered to test the method. Force plate data was used to estimate peak reference power by adapting the method proposed by Rabita et al. (Rabita et al., 2015). P_r showed a positive linear relationship with the treadmill velocity (v_{0y}). At the same speed, uphill running exhibited a higher peak power during the concentric phase of stance than level running (Figure 4.4). These results are in agreement with the findings of Arampatzis et al. (Arampatzis et al., 2000), who compared different methods of estimating power from kinematic and ground reaction force (GRF) data, and recommended the use of GRF data-based methods.

The proposed method was able to follow the reference peak power estimated from the force plates in a speed range from 8kmh^{-1} to 14kmh^{-1} and at slopes from -20% to 20% . It achieved a MAE 6.5% to 7.1%, an IQR (precision) of 12.5% to 13.4%, and a $R^2 \geq 0.91$ across all running conditions (Table 4.2). Though obtained using a single IMU on each foot, these error magnitudes lie within the range of RMSE values (4% to 20%) obtained using a simulated full-body IMU setup (Fohrmann et al., 2019). The bias (median error) was highest in the conditions with the highest speed and slope (Figure 4.8). Running at these intense conditions is highly demanding, which limited the availability of data for model training and likely biased the models toward lower or moderate intensity running conditions. The precision (IQR for the error) at the lowest treadmill speed (8kmh^{-1}) was generally high ($21 \pm 5.9\%$). The high IQR may also be the result of from the running biomechanics associated with the low speed, as 8kmh^{-1} is within the average range of the transition speeds ($4.68 - 9.18\text{kmh}^{-1}$) from walking to running for healthy participants (Thorstensson & Roberthson, 1987). In addition to biomechanics, the higher IQR may also be the result of noise added to the speed value. Because the amount of noise was fixed, the signal-to-noise ratio (SNR) was lowest at the lowest speed (8kmh^{-1}). Combined with the fact that speed is one of the most important features (Table 4.3) for the EN model, a low SNR can lead to a higher error. Compared to the 8kmh^{-1} condition, the 10kmh^{-1} and 12kmh^{-1} speed conditions resulted in a lower IQR of error ($10.7 \pm 2.0\%$). These two conditions are within the range of average preferred running speeds in the field: 9.86kmh^{-1} (95% CI: $9.54-10.15\text{kmh}^{-1}$) for females and 11.7kmh^{-1} (95% CI: $11.45-12\text{kmh}^{-1}$) for males. Furthermore, these conditions also correspond to the optimal treadmill speeds in the laboratory, which result in minimal net cost of transport for running. Thus, in the context of usage in real-life scenarios, we can expect the algorithm to perform adequately. Furthermore, it is important to note that these results are for the condition with the highest noise ($\epsilon 100$, Table 4.2). With a more accurate estimation of speed and slope, we can only expect the error IQR to reduce, as is evident in the error distribution plot (Figure 4.5) and Table 4.2.

The best models for level, uphill, and downhill running (Table 4.2) were the neural network with 35% validation set (NN35), the neural network with 15% validation set (NN15), and elastic net regularization (EN), respectively. Based on the magnitude of their coefficients, the EN model allows us to rank the features according to their importance (Zou & Hastie, 2005). The list of the 15 most important features shows the

mass (m) and the treadmill speed ($\widehat{v_{0y}}$), followed by the slope ($\hat{\theta}$). This is expected due to the use of θ , v_{0y} , and θ in equations 4.1 – 4.4 for the estimating the reference power from force plate. The SNR for $\hat{\theta}$ is much lower for lower values of the gradient (e.g. ± 4.86 % noise for a gradient value of 5%). Compared to downhill running, uphill running has less than half the data samples at higher gradients (15 or 20%) and thus likely shows relatively much lower feature importance (Table 4.3) for gradient. Biomechanical parameters such as vertical stiffness (k_{vert}), maximum vertical force ($f_{z\text{max}}$), maximum vertical displacement of the CoM (Δz), stride duration (strd), and foot strike angle immediately before initial contact (f_{sa}) were also among the important features. With an increase in speed, Δz decreases, $f_{z\text{max}}$ increases, and so does the total contribution of a_y and F_y , leading to an increase in power (Cavagna et al., 2005; Farley & Ferris, 1998). While this implies that features are correlated, their strength of correlation (τ) was likely below the selected threshold of 0.8. k_{vert} , $f_{z\text{max}}$, and Δz are directly related to the storage and return of elastic energy in the spring-mass model of running, and a decrease in k_{vert} due to fatigue has been associated with a decrease in performance (J.-B. Morin et al., 2005, 2006; Prigent et al., 2022). Some of the important statistical features are associated with signals in the X direction, i.e., the axis perpendicular to the sagittal plane. This suggests that the 2-D model (Figure 4.2B and C) used to estimate reference power can be extended to account for motion in all three dimensions. In addition, this model assumes that the athlete is a point mass driven by the GRF. Although the model is mechanically in equilibrium (van der Kruk et al., 2018), it can be augmented to include the 3-D kinetics of the body segments to improve its accuracy. Body weight normalization of the estimated power could help to compensate for variations across individuals, although weight normalized errors would translate different to heavier and light individuals.

Taboga et al. compared commercially available power meters with force-plate measurements for level running only (Taboga et al., 2021) and found a good agreement (L.O.A -154.8 to 12.6 W, M.D. -70.8 W, assuming a reported average mass of 68.1 kg). While upper limit of the L.O.A is lower than our findings (L.O.A -179.8 to 216.3 W, M.D. 18.2 W), the M.D. is higher. However, L.O.A in our case have been extended mainly due to the samples from two participants, as shown in Figure 4.7A. We could not find existing validation studies for graded running for comparison. In case of commercially available devices vertical force and velocity is considered for estimation of power (Arampatzis et al., 2000; Taboga et al., 2021), hopping on the spot or increased vertical movement of the CoM during running may result in a higher power measurement. If the goal of using power as a feedback tool is to understand the intensity of the run, ‘power’ in the direction of running is a more interesting metric as it relates to the propulsion produced by the athlete (Jaskólski et al., 1996). This is despite the fact that power is a scalar quantity and ‘directional power’ does not mechanically represent power (van der Kruk et al., 2018; Vigotsky et al., 2019). During the terminal stance phase, maximum mechanical power correlates with the push-off force generated by the concentric contraction of the thigh muscles, while maximum mechanical power absorbed during the initial contact indicates the energy absorbed by the eccentric contraction of the calf muscles (R. A. Mann & Hagy, 1980). The ability to run downhill at the same speed and gradient, but with a lower negative mechanical work i.e., lower magnitude of ‘power’ in the eccentric contraction phase is beneficial, as exercise-induced

muscle damage during eccentric loading has a significant adverse effect on endurance performance (Marcora & Bosio, 2007). The reduction in impact forces can decrease the muscle fatigue accumulated during downhill running and possibly reduce injury risk over an entire training program for trail running. Commercial devices only consider the power produced during the concentric phase and average this power over the entire stance phase duration, thus providing no insight over the ‘power’ during the motion cycle. If both phases are considered together, it can lead to the averaging of positive and negative power, leading to their negation.

In this work, we accurately estimated peak eccentric and peak concentric power, which can potentially be used to define the volume of training for level and trail running. Athletes susceptible to or recovering from muscle injuries can use the eccentric power peak as a threshold for designing training programs with adequate mechanical load and assessing their readiness to return to running in various conditions. Furthermore, the ratio between the absolute power from concentric work and eccentric work could potentially be utilized as a metric of mechanical efficiency (Vernillo et al., 2017). To enable the application of our method in practice, algorithms like the one using accelerometer signals (Herren et al., 1999) or barometer (Moncada-Torres et al., 2014) can be devised to identify uphill, downhill, and level running. While our model has been tested on young healthy adults running on treadmills, it can be extended further and personalized to account for different populations (Hoenig et al., 2020). Moreover, it could be validated on other populations such as older adults and Paralympic athletes, the latter using instrumented prosthetic feet (Lee et al., 2012). In addition to sensors worn on the foot, IMUs on other body segments, particularly the wrist and trunk, must be examined to estimate power. Wrist location offers ease of use and has been used for gait analysis (Kammoun et al., 2022), while the trunk provides a position close to the CoM of the body. Finally, power estimation can be complemented by estimating the vertical and anteroposterior GRF peaks. This can provide athletes and coaches with a more comprehensive understanding and feedback and support the personalization of training programs.

III. AUGMENTATION OF IN-FIELD FUNCTIONAL CAPACITY TESTING

5 SPRINT VELOCITY ESTIMATION USING GNSS-IMU SENSOR FUSION

This chapter presents the method used to instrument the sprint functional test with a wearable sensor and its validation in the field. Power-Force-Velocity profile obtained during a sprint test is crucial for designing personalized training and evaluating injury risks. Estimation of instantaneous velocity is requisite for developing these profiles and the predominant method for this estimation assumes it to have a first order exponential behavior. While this method remains appropriate for maximal sprints, the sprint velocity profile may not always show a first-order exponential behavior. Alternately, velocity profile has been estimated using inertial sensors, with a speed radar, or a smartphone application. These methods either relied on the exponential behavior or timing gates for drift removal or estimated only the mean velocity. The proposed method aims to estimate the instantaneous velocity during sprinting using a sensor fusion approach, by combining the signals from a wearable GNSS-IMU system. For the data collection, nine elite sprinters, equipped with a wearable GNSS-IMU sensor, ran two trials each of 60m and 30m/40m sprints. An algorithm was developed using a gradient descent-based orientation filter, which simplified the problem to a linear one-dimensional model, thus allowing the use of a simple Kalman filter (KF) for velocity estimation. Two cascaded KFs were used to segment the sprint data and to estimate the velocity and the sprint duration, respectively. The median RMS error for the estimated velocity ranged from 6% to 8%, while that for the estimated sprint duration lied between 0.1% to -6.0%, when compared to speed radar and photocell data, respectively. The Bland-Altman plot showed close agreement between the estimated and the reference values of maximum velocity. Examination of fitting errors indicated a second order exponential behaviour for the sprint velocity profile, unlike the first order behaviour previously suggested in literature. The proposed sensor-fusion algorithm compensates for and improves upon the accuracy of the individual IMU and GNSS velocities and enables the use of wearable sensors in the analysis of the sprint test.

The contents of this chapter have been adapted from this article:

Apte, S., Meyer, F., Gremeaux, V., Dadashi, F., & Aminian, K. (2020). A sensor fusion approach to the estimation of instantaneous velocity using single wearable sensor during sprint. *Frontiers in Bioengineering and Biotechnology*, 8, 838.

Contributions: conceptualized the study design; conducted the data collection; designed and implemented the algorithm; contributed to the analysis and interpretation of the data; drafted the manuscript.

5.1 INTRODUCTION

Sprinting not only represents the peak of human speed but also forms the basis of performance in a variety of sports. The capacity to generate maximal force and power in the direction of running is a decisive factor behind an athlete's performance in sports such as athletics, soccer, hockey, rugby, etc. (J. Cronin & Hansen, 2005). To ascertain this capacity, sprint tests with a distance varying from 20m to 60m are typically utilized. Prior research into sprint mechanics (Buchheit et al., 2014; M. R. Cross et al., 2015; Haugen & Buchheit, 2016; J.-B. Morin et al., 2012; Rabita et al., 2015) has shown that parameters such as maximum power produced by the sprinter, maximum horizontal force, horizontal velocity at zero acceleration, maximum theoretical horizontal force (f_0), maximum theoretical horizontal power (p_{max}), maximum theoretical horizontal velocity (v_0) etc., along with the horizontal force-velocity (F-V) and horizontal power-velocity (P-V) profiles can be crucial for designing personalized training programs, evaluating injury risks, and athlete readiness to resume high intensity training and return to competition after injury (J.-B. Morin 2016). These parameters and the force-power-velocity profiles can be ascertained using the velocity profile during sprint. An accurate estimation of the in-field sprinting velocity can thus be immensely helpful to improve the performance of athletes in a multitude of sports. The prominent model of estimating instantaneous sprint velocity ($v_{mdl}(t)$) is based on the use of a Doppler radar to measure the maximum velocity in combination with the (7) (Furusawa et al., 1927; Samozino et al., 2016):

$$v_{mdl}(t) = v_{max} \left(1 - e^{\left\{ -\frac{t}{\tau} \right\}} \right) \quad (5.1)$$

where v_{max} is the maximum horizontal velocity during the sprint and τ is a constant, estimated using ensemble experimental data. The obtained velocity profile ($v_{mdl}(t)$) is differentiated to obtain horizontal acceleration, and subsequently the F-V and P-V profiles. While this method provides ease of use, it is only valid when the athletes can approach or attain v_{max} . However, the sprinters may not achieve v_{max} over short distances such as 30 m or they may not be able to maintain v_{max} over longer distances such as 60 to 100 m, especially during training sessions, and thus the sprint velocity profile for all athletes may not necessarily show a first-order exponential behavior. Sprint velocity has also been estimated with a recently developed application (Stanton et al., 2016) for a smartphone; wherein the in-built camera tracks and records the motion. Based on the distance entered manually, the application calculates the total sprint time and subsequently the mean velocity. Thus, this application cannot estimate instantaneous velocity and the measurable sprint distance might be limited by the field-of-view of the camera.

While wearable inertial sensors have shown promising results in the assessment of temporal gait parameters in running and sprinting (Bergamini et al., 2012; Falbriard et al., 2018; Leitch et al., 2011; Norris et al., 2014) their use for analysis of instantaneous sprint velocity and other sprint mechanics has been rather rare. Recently, a magnetic and inertial measurement unit (MIMU) based algorithm (Setuain et al., 2018) has been developed to assess sprint mechanics with various parameters such as maximal velocity, maximal horizontal force and power, velocity at zero horizontal force, etc., for 20m sprints. Though this work allows the measurement of sprint mechanics using a single MIMU mounted on the trunk, the algorithm relies on the use of split times from photo-

cells at specific distances to remove the accumulated drift in the velocity. Other works on velocity estimation using a trunk-based MIMU (Gurchiek et al., 2018, 2019), utilized equation 5.1 for drift removal and used machine learning to estimate the parameters v_{max} and τ respectively. Nevertheless, as explained earlier, equation 5.1 may not hold true over different sprint distances and sub-maximal efforts. Finally, Global Navigation Satellite System (GNSS) with wearable receiver provides another avenue of running velocity measurement in field and has been used to assess training and match performance in sports like soccer and rugby (Cummins et al., 2013). However, the ground velocity signal from GNSS is not responsive enough to measure the velocity during sprint (Nagahara et al., 2017) and can lead to an underestimation of the sprint velocity. This issue is even more exacerbated among elite athletes, who produce a high magnitude of horizontal acceleration and for whom, the timing difference can be critical (J.-B. Morin & Samozino, 2016).

A Kalman filter-based sensor fusion approach to combine GNSS and MIMU signals can overcome their respective limitations of responsiveness and drift-induced errors, as demonstrated successfully in sports applications such as skiing (Brodie et al., 2008; Meyer et al., 2007; Zihajehzadeh et al., 2015) and running (Tan et al., 2008). However, the works on skiing utilized magnetometers and focused on estimating and validating the skier's trajectory and not the velocity, whereas the running movement did not present the challenge of high starting acceleration encountered in sprinting. Use of sprinting as a functional capacity test also imposes an important constraint in terms of usability for in-field implementation, thus limiting the number of wearables that can be utilized. To address the problem of estimating instantaneous velocity in sprinting over a range of distances, this chapter introduces a new approach based on using a gradient descent algorithm as an orientation filter (Madgwick et al., 2011), in combination with cascaded simple Kalman filters used for precise data segmentation and velocity estimation, respectively. The orientation filter utilizes the IMU data to convert the acceleration signals from the sensor frame to the global frame, which is then given as input to the first Kalman filter for estimating the precise sprint duration. This duration is used to segment the sensor data, which is then provided to the second Kalman filter, which fuses the GNSS signal and IMU acceleration to estimate the instantaneous velocity. To test this approach, the instantaneous velocity obtained from a Doppler effect-based radar was used for validating the estimated velocity and sprint timings acquired from a photocell for comparing the sprint duration.

5.2 MATERIALS AND EQUIPMENT

Measurements were conducted with nine healthy elite-level sprinters, four (3 male, 1 female, 60m sprint time 7.49 ± 0.35 s) at the Aix-les-Bains Athletics club and five (4 male, 1 female, 60m sprint time 7.65 ± 0.67 s) from the Lausanne Athletics club respectively. Ethical approval for the study was obtained from the university human research ethics committee (HREC 039-2018) and prior written consent was obtained from all the participants. The Aix-les-Bains cohort performed 2x40m and 2x60m sprints, while the Lausanne one performed 2x30m and 2x60m sprints. These distances are typically used in sprint tests and for training sprinters. For both measurements, participants were wearing a vest equipped with the GNSS-IMU sensor (*Fieldwiz*, *ASI*, *CH*,) on the upper

back (Figure 5.1). Apart from the vest, the sprinters dressed as they would for a regular training session.

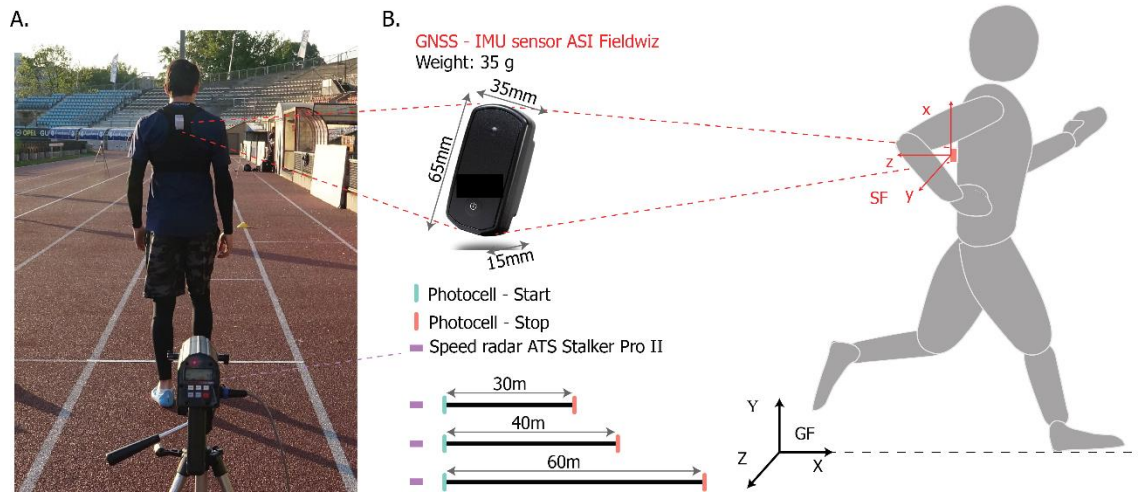


Figure 5.1 Sensor setup and measurement protocol, A) Snapshot of a sprinter wearing the Fieldwiz sensor with the speed radar in the foreground B) Specifications of the Fieldwiz sensor and the measurement protocol, wherein the sprinters ran two trials each of 60m and 30m or 40m distances with the speed radar as the velocity reference. Photocells were positioned at the start/end to record the sprint duration. GF and SF represent the global and sensor frames

This GNSS-IMU wearable sensor was chosen because it is already used in soccer training for performance and training monitoring (Clemente et al., 2018). This sensor, with a sampling frequency of 200Hz for the IMU and 10Hz for the GNSS unit, was used in the 'airborne < 4g' configuration of the in-built *u-blox* GNSS module. A speed radar (*ATS Pro II, Stalker Sport, USA*) with a sampling frequency of 50Hz, selected based on recommendations from Haugen et al. (Haugen & Buchheit, 2016), was positioned directly behind the starting point (Figure 5.1A) of the sprinter. Data from the radar was used in the measurements as a reference value for velocity. Photocells (*Witty, Microgate corp, Italy*) from the respective athletics clubs were used at the start and the end to provide the reference value for the sprint duration.

5.3 METHODS

5.3.1 Velocity and duration estimation algorithm

The flowchart for the algorithm is shown in Figure 5.2; the algorithm includes three phases: i) sprint segmentation ii) velocity estimation and iii) sprint duration estimation. Sprint segmentation aims to detect the period for each specific sprint. First, the data recorded on the GNSS-IMU sensor is segmented by manually selecting an approximate starting sample for the relevant sprint. Following this, the algorithm is designed to choose a precise starting time (t_s) by selecting an appropriate threshold (0.3 m/s) on the velocity obtained from the GNSS sensor. A sensitivity analysis (Appendix) was conducted to see the impact of this threshold on the velocity estimation error. Using gravity and the IMU data during the static period at the start of sprint, the initial orientation is estimated along X and Y direction, wherein the direction of sprinter progression is

assumed to be the global X-axis and Y is the vertical axis. The changes from this initial orientation are estimated using the gyroscope data and corrected with the accelerometer data using a gradient-descent based optimization method (Madgwick et al., 2011). Thus, the X-axis here is not truly a global axis and it is defined anew for every sprint. The changes in orientation are represented by quaternions q , which are used to convert the acceleration signals from the segmented data from the sensor frame (SF) to the global frame (GF) X-Y-Z using equation below:

$$a_{GF} = q \otimes [0 \ a_{SF}] \otimes q^* \quad (5.2)$$

where q represents the quaternions transforming the sensor frame (SF) to the global frame (GF) and q^* their transpose. These quaternions are estimated by fusing accelerometer and gyroscope data using a gradient descent algorithm (Madgwick et al., 2011); a_{SF} is the acceleration in the sensor frame, and a_{GF} is the acceleration in the global frame X-Y-Z with positive X-axis representing the direction of sprinting.

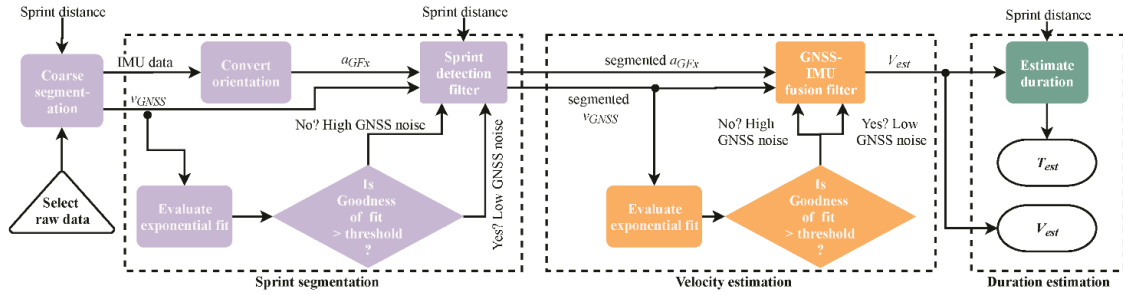


Figure 5.2 Flowchart for the sprint velocity estimation algorithm. The ‘coarse segmentation’ block is manual and creates a window to select the approximate starting point of the relevant sprint, while remaining algorithm is automated. The ‘Sprint detection’ and ‘GNSS-IMU fusion’ filters are simple Kalman filters. a_{GFx} denotes the horizontal acceleration in the global frame, v_{GNSS} the ground velocity from the GNSS sensor, while v_{est} and T_{est} represent the estimated velocity and sprint duration respectively.

The acceleration along the positive X-axis of the global frame (a_{GFx}) is provided as an input to the Sprint detection filter (linear Kalman filter) in combination with the ground velocity (v_{GNSS}) from the GNSS sensor. The main assumption here is that the sprinters run along a straight line (within sagittal plane), thus the acceleration a_{GFx} can be assumed to represent acceleration along the direction of running and the dynamical model of the system can be assumed to be constant. This assumption is also used for the measurements with a speed radar; in our case, it simplified the system to a linear model and allowed the use of a simple Kalman filter, which is the optimal estimator for a linear system (Burl, 1998). This filter has the following prediction and update steps:

Prediction:

$$v_{est}(n|n-1) = [1] \ v_{est}(n-1) + [\Delta t] \ a_{GFx}(n-1) + \mu \quad (5.3)$$

Update:

$$v_{est}(n|n) = v_{est}(n|n-1) + K(n)(v_{GNSS}(n) - v_{est}(n|n-1)) \quad (5.4)$$

Kalman gain:

$$K(n) = p(n|n-1)(p(n|n-1) + \eta)^{-1} \quad (5.5)$$

Where v_{est} is the estimated horizontal velocity, $a_{GFx}(n)$ is the horizontal acceleration in global frame, Δt is the sampling time, μ is the process (accelerometer) noise, $v_{GNSS}(n)$ is the velocity measured by the GNSS sensor, $K(n)$ is the Kalman gain, $p(n)$ is the estimation uncertainty, and η is the measurement (GNSS) noise. Since a_{GFx} has a sampling frequency of 200 Hz, v_{GNSS} is sampled up from 10 Hz to 200 Hz by ‘zero padding’. If the velocity from v_{GNSS} is non-zero, the update sequence is initiated, otherwise the prediction model continues to run without update. The magnitudes of η and μ were set to 0.01 and 0.4 respectively, obtained via manual tuning of the filter. To refine the magnitude of η further, the rationale of the exponential behavior of sprint velocity (Samozino 2016) is utilized. By subtracting both sides of eqn. 5.1 from v_{max} , we get:

$$v_{max} - v_H(t) = v_{max} \left(e^{\left\{ \frac{-t}{\tau} \right\}} \right) \quad (5.6)$$

Based on this equation, v_{GNSS} is subtracted from the maximum velocity and an exponential curve was fitted to it and if fit is good ($R^2 > 0.91$), the value of η_k is unchanged from 0.01. In case of a bad fit, this value is increased by an order of magnitude to 0.1. The velocity (v_{est}) obtained from this Kalman filter is integrated from the starting time (t_s) to obtain the distance profile, which is subsequently compared to the actual sprint distance and used to estimate the ending time (t_e) and segment sprint period ($t_d = t_e - t_s$) precisely. In the second phase, a more accurate exponential fitting is made using a more refined sprint period (t_d) obtained in the first phase. Precisely segmented v_{GNSS} and a_{GFx} are provided as inputs to the GNSS-IMU fusion filter, which is also a simple Kalman filter, with the same process and measurement models as the first filter. This filter is used to update the final sprint velocity (v_{est}) precisely by considering the sprint period and the fine-tuning of GNSS noise. In the final step, v_{est} is integrated to obtain the displacement-time profile and the timestamp at the relevant sprint distance is computed. The starting time (t_s) of the sprint is then subtracted from the value of this timestamp to obtain the sprint duration (T_{est}).

5.3.2 Estimation of profiles – velocity, force, and power

To estimate force-velocity and power-velocity profiles, the first step is to estimate the approximate velocity profile from v_{est} using the exponential fit (Samozino et al., 2016) presented in (9). While the maximum velocity during the sprint (v_{max}) and the velocity at the end (v_{end}) are the same in case of an ideal exponential velocity profile, this may not be the case with real-world velocity profiles. As a result, v_{max} and v_{end} tend to deviate from each other. To investigate which velocity profile leads to a better fit, the two first-order velocity profiles, based on v_{max} ($v_{mdl_max,1}(t)$) and v_{end} ($v_{mdl_end,1}(t)$) respectively, were compared to a second-order velocity profile, defined as:

$$v_{mdl,2}(t) = a e^{\tau_1 t} - a e^{\tau_2 t} \quad (5.7)$$

Where τ_1 , τ_2 and a were computed with the ‘trust-region reflective’ algorithm, using the ‘lsqcurvefit’ function native to Matlab application. Approximate velocity profile obtained from the best performing fitting method is differentiated to obtain the approximate horizontal acceleration $a_{mdl}(t)$, which in combination with the sprinter’s mass (M), led to the force profile:

$$F_{mdl}(t) = M \times a_{mdl}(t) \quad (5.8)$$

Finally, the power profile was calculated as a product this force profile and the velocity profile, where only the magnitudes of the force and velocity are considered:

$$P_{mdl}(t) = F_{mdl}(t) \times a_{mdl}(t) \quad (5.9)$$

5.3.3 Validation process

The velocity measured at 50 Hz by the radar ($v_R(t)$) was used as reference for velocity validation. To match the sampling frequency of the reference signal, v_{est} was sampled down from 200 Hz to 50 Hz by keeping the first sample and every fifth sample after the first, and v_{GNSS} was sampled up from 10 Hz to 50 Hz using linear interpolation. An error vector (equation 5.10) between v_{est} and v_R was then computed for each trial. Following this, the RMS, mean, and standard deviation (SD) for each error vector were calculated. Finally, pooled mean and standard deviation were computed for each sprint distance to investigate the bias and precision respectively. Similar procedure was applied to estimate error for v_{GNSS} .

$$\varepsilon_v(t) = \frac{v_R(t) - v_{est}(t)}{\max(v_R(t))} \times 100\% \quad (5.10)$$

In order to investigate the different fitting methods explained earlier, the error vectors were calculated (19) of the fitted curves $v_{mdl}(t)$ (i.e., $v_{mdl_max,1}(t)$, $v_{mdl_end,1}(t)$ and $v_{mdl,2}(t)$) with respect to v_R , followed by calculating RMS and pooled mean and pooled SD. Further, the fitting performance was qualitatively investigated by observing the different fitted velocity profile curves. Similarly, the error for fitted curves with respect to v_{est} was calculated.

$$\varepsilon_{fit}(t) = v_R(t) - v_{fit}(t) \quad (5.11)$$

The time recorded in the photocells (T_{Ref}) was used as reference for validation of the estimated sprint duration (T_{est}). Percentage error for the sprint duration was calculated as:

$$\varepsilon_t = \frac{T_{Ref} - T_{est}}{T_{Ref}} \times 100\% \quad (5.12)$$

Similar process was carried out for the duration obtained from the radar (T_{rad}) to compare the performance of the algorithm with that of the radar. Subsequently, the RMS, mean, and standard deviation for these error values were calculated. Lastly, the maximum velocity is an important metric according to earlier research on sprint mechanics (J.-B. Morin et al., 2012) and thus, the value obtained from our method was compared with that from the radar. Another reason to focus on the maximal speed was that the RMS error did not capture this parameter properly. The Bland-Altman plot (Bland & Altman, 2003) was used for this purpose, along with the calculation of the Lin's concordance correlation coefficient (ccc) at 95% confidence interval (Lin, 1989) as a measure of agreement between the proposed method and the radar. A correlation coefficient value greater than 0.7 was considered 'strong', according to the ranges suggested for sports science research (Hopkins et al., 2009). Bland-Altman plots were also utilized to compare the theoretical maximum theoretical velocity v_0 (m/s), maximum

theoretical horizontal force per unit mass f_0 (N/kg), and maximum theoretical horizontal power p_{max} per unit mass (W/kg) values obtained from the $v_{est}(t)$ using the second-order exponential fit to those computed from the $v_R(t)$. The p_{max} values were obtained from the apex values of the P-V profile.

5.4 RESULTS

Data for nine athletes (7 male, 2 female, 60m sprint time 7.39 ± 0.37 s) was utilized in this research. Four athletes performed 2x40m sprints and 2x60m sprints, while remaining five athletes performed 2x30m sprint and 2x60m sprints. For one 60m sprint and three 30m sprints, a delay in triggering the reference radar system was noticed during data processing. Since the sprint start was not recorded for these sprints, their data was discarded from the final analysis. Thus, a total seven sprints were considered for 30m distance, eight for 40m, and 17 for 60m. Out of these, data for two 40m sprints was used for tuning the algorithm, while the data for all sprints was used for validation.

5.4.1 Velocity estimation

Figure 5.3 illustrates one example each of situations where v_{GNSS} severely underestimated the actual v_R (Figure 5.3A) and when the v_{GNSS} approximately matches v_R (Figure 5.3B). In both cases, v_{est} matched v_R closely. Figure 5.3C, in turn, represents the intermediate ‘Evaluate exponential fit’ block of the algorithm (Figure 5.2), for adjusting the measurement noise parameter of the Kalman filter. For the case presented here, $v_{GNSS}(t)$ did not show an exponential behaviour ($R^2=0.66$) and so the measurement noise, ($\eta=0.1$) was set higher than scenario when $v_{GNSS}(t)$ would have been exponential ($R^2 > 0.91$) in nature. Apart from this one case of 30m, $v_{GNSS}(t)$ did not show an exponential behaviour in one of 40m sprints.

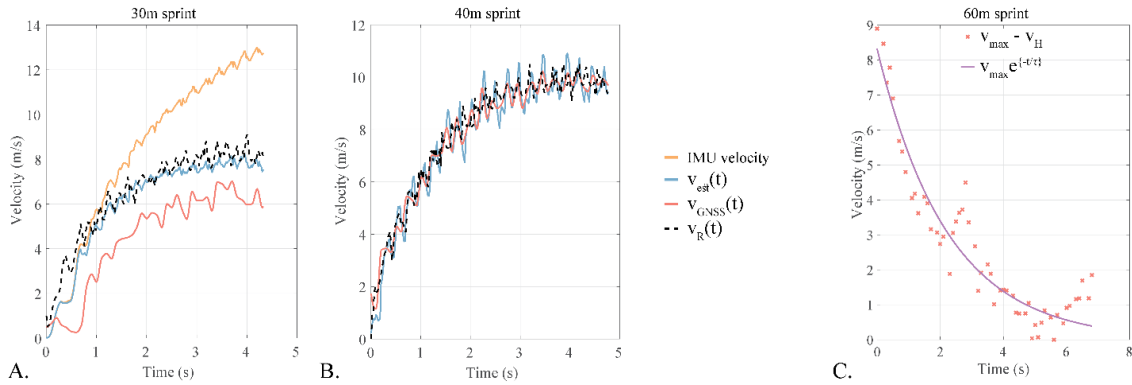


Figure 5.3 Scenario illustrating the estimated velocity profile. A) Example of a specific case of 30m sprint when $v_{GNSS}(t)$ was inaccurate while $v_{est}(t)$ is accurate B) Example of a specific case of 40m sprint when $v_{GNSS}(t)$ and $v_{est}(t)$ were accurate C) Example of exponential fit (equation 5.6) used to adjust measurement (GNSS) noise for the Kalman filter. IMU velocity: velocity obtained by strapdown integration of IMU signals, $v_{GNSS}(t)$: GNSS velocity, $v_R(t)$: radar velocity, $v_{est}(t)$: estimated velocity by GNSS-IMU fusion

5.4.2 Validity of estimated velocity

The error results for v_{est} and v_{GNSS} are shown in Table 5.1 and Figure 5.4; v_{est} presents a similar error magnitude as v_{GNSS} for 40m and 60m, while showing a lower error for

the 30m sprint. The median of RMS errors of the v_{est} ranged from 6.2% to 8.1% (Figure 5.4, Table 5.1) for the three sprint distances and was lower or like that of the v_{GNSS} . Furthermore, the IQR (Table 5.1) for the RMS errors for the v_{est} was lower than that of the v_{GNSS} , especially for the 30 m and 60 m sprint distances.

Table 5.1 Median (IQR) values of the RMS error for v_{GNSS} , v_{est} , T_{rad} and T_{est} for all three sprint distances. RMS error was calculated based on equations 5.10 and 5.12.

Distance (m)	% error for v_{GNSS}	% error for v_{est}	% error for T_{rad}	% error for T_{est}
30	5.6 (4.9 to 12.0)	6.2 (5.2 to 7.2)	3.3 (1.8 to 4.5)	0.1 (-1.7 to 1.9)
40	10.2 (5.1 to 11.4)	8.1 (6.1 to 11.4)	-0.8 (-2.0 to 0.2)	-4.5 (-9.8 to 0.1)
60	6.1 (4.7 to 8.5)	6.5 (5.4 to 7.9)	-2.1 (-3.4 to -0.2)	-6.3 (-12.8 to -2.4)

The median error for T_{est} ranged from 0.1% to -6.3% (Figure 5.4B), while that for T_{est} varied from 3.3% to -2.3%, thus both showed a similar range. The IQR (Table 5.1) for T_{rad} were lower as compared to T_{est} for 40m and 60m sprints. For 30m sprint, T_{est} had a lower median error, but a higher IQR than T_{rad} . For the maximum velocity (v_{max}), the Bland-Altman plot showed close agreement between the estimated and the reference magnitudes, with all the values lying between the two standard deviations and the Lin's concordance correlation coefficient being 0.76 ($p < 0.05$). The estimated values, however, showed a slight negative bias of -0.16 m/s, although this was miniscule as compared to actual maximum velocities, which are around 10 m/s.

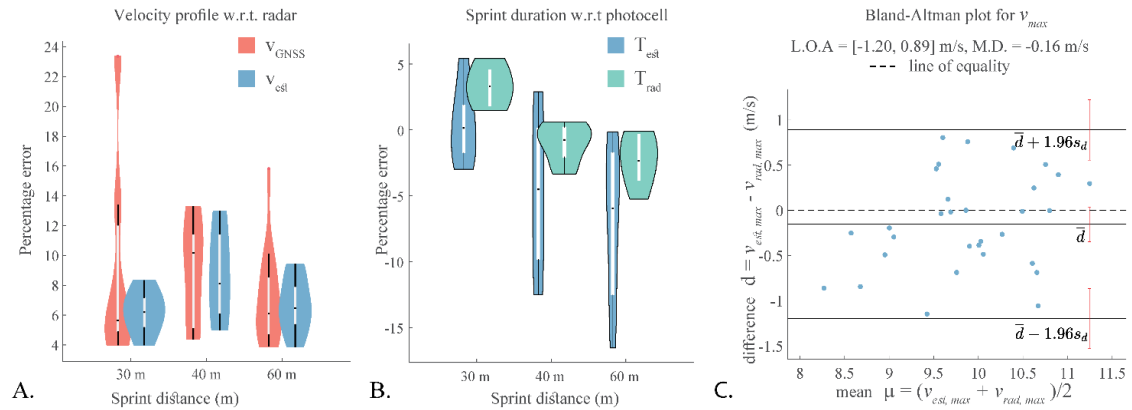


Figure 5.4 Validation of estimated velocity profile, A) RMS error of the estimated velocity and GNSS velocity w.r.t. the radar speed B) RMS error of the predicted sprint duration from the proposed algorithm and the radar speed with the photocell duration as reference C) Bland-Altman plot for the maximum estimated velocity with the maximum radar speed as reference. Here, L.O.A. are the limits of agreement and M.D. is the mean difference

For the v_0 , f_0 , and p_{max} the Bland-Altman plot (Figure 5.5) showed close agreement between the estimated and reference values, with almost all values lying between the two standard deviations. v_0 presented a bias of -0.17 m/s which is like that of v_{max} , f_0 showed almost zero bias, and the bias for p_{max} was -0.31 W/kg, which is substantially smaller than the actual p_{max} values, which range from 16 to 28 W/kg.

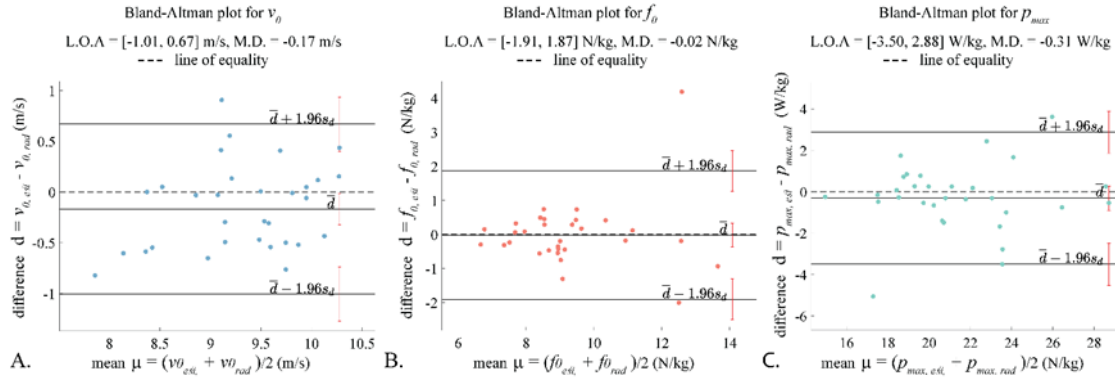


Figure 5.5 Bland-Altman plots for sprint parameters with the values calculated from radar speed as reference, where L.O.A. are the limits of agreement and M.D. is the mean difference. The values here are obtained using the second-order exponential fit, A) Maximum theoretical velocity v_0 (m/s) B) Maximum theoretical horizontal force per unit mass f_0 (N/kg) C) Maximum theoretical horizontal power p_{max} per unit mass (W/kg)

5.4.3 Validity of exponential fitting

A qualitative presentation of the different types of first order ($v_{mdl_max,1}$, $v_{mdl_end,1}$) and second order ($v_{mdl,2}$) exponential fits can be seen Figure 5.6A. For both v_{est} and v_R , the second order fit has the lowest RMS error (Figure 5.6B and C) and lower mean and standard deviation than both first order fits (Table 5.2). $v_{mdl_end,1}$ fit has similar mean error values as $v_{mdl_max,1}$ fit for 30m and 40m sprints, while it has considerably higher mean value and standard deviation for the 60m sprint (Table 5.2).

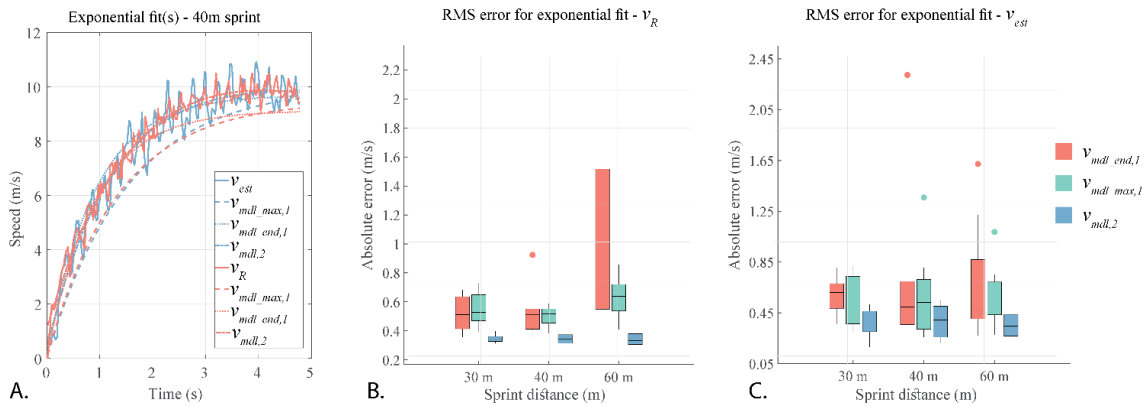


Figure 5.6 Modelling of the sprint velocity profile, A) Three methods for exponential fit B) RMS error for exponential fit(s) on radar speed (v_R) C) RMS error for exponential fit(s) on estimated velocity (v_{est})

Force-velocity (F-V) and power-velocity (P-V) obtained from the second order (order 2) exponential are shown in Figure 5.7 B and C, respectively. These profiles were created from the best trial of the nine selected athletes for the 60m sprint and sorted from the lowest to the highest finish times.

Table 5.2 RMS error for the modelled velocity profile. RMSE was calculated based on equation 5.11. The second order fit ($v_{mdl,2}$) presents the lowest median (IQR) for both v_{est} and v_R

Dist.	$v_{mdl,max,1}$		$v_{mdl,end,1}$		$v_{mdl,2}$	
	Fit on v_R	Fit on v_{est}	Fit on v_R	Fit on v_{est}	Fit on v_R	Fit on v_{est}
30 m	0.53	0.49	0.51	0.61	0.34	0.34
	(0.47 to 0.65)	(0.36 to 0.74)	(0.41 to 0.64)	(0.48 to 0.68)	(0.33 to 0.36)	(0.30 to 0.46)
40 m	0.52	0.53	0.51	0.50	0.34	0.40
	(0.46 to 0.55)	(0.32 to 0.71)	(0.41 to 0.55)	(0.36 to 0.70)	(0.31 to 0.37)	(0.26 to 0.50)
60 m	0.64	0.51	1.16	0.47	0.33	0.35
	(0.54 to 0.72)	(0.43 to 0.69)	(0.55 to 1.52)	(0.40 to 0.87)	(0.31 to 0.38)	(0.27 to 0.44)

5.5 DISCUSSION

5.5.1 Validity of the proposed method

The proposed sensor-fusion algorithm can compute an accurate velocity profile with respect to the radar; it can compensate for and improve upon the accuracy of the individual IMU and GNSS velocities, as seen in Figure 5.3B. When v_{GNSS} is relatively accurate, the algorithm output (v_{est}) closely resembles the v_{GNSS} profile (Figure 5.3C). This is underlined by the percentage error for the velocity (Figure 5.4A); the median RMS error values for the v_{est} are only slightly lower than those for v_{GNSS} , whereas the standard deviation is considerably less. Thus, the velocity estimation algorithm based on GNSS and IMU fusion is robust in terms of accuracy and precision, despite the inaccuracies in the GNSS velocity. None of the previous works on estimation of sprint mechanics (Gurchiek et al., 2018; Samozino et al., 2016; Setuain et al., 2018; Stanton et al., 2016) conducted a validation of the instantaneous velocity or the overall profile with respect to a speed radar. (Stanton et al., 2016) validated the mean velocity over an entire sprint, while (Gurchiek et al., 2018) validated the mean velocity over 10 m intervals. This method is the first one to provide validated instantaneous analysis of the sprint velocity profile over multiple distances using only one wearable sensor, and thus it is not possible to compare our results with the state-of-the-art.

The mean error for sprint duration (T_{est}) increased from 0.5% to -7.1% for 30 m to 60 m distances respectively, clearly showing an overestimation. This is a result of the minor underestimation of velocity caused by the residual drift in the IMU strapdown integration and the inaccuracies of the GNSS velocity. While the work by (Setuain et al., 2018) used photocells for drift estimation, only the research from (Stanton et al., 2016) considered a validation with respect to the photocell data. The mean error reported in the latter case (2.6%) for 10 m sprint was higher than the one presented here i.e., $0.5\% \pm 2.8$ (Table 1) for a 30 m sprint. Furthermore, it was validated solely for 10 m sprints, and the algorithm was focused only on the calculation of the mean velocity. The mean error and its SD for estimated sprint duration (T_{est}) is higher than the one obtained from the speed radar (T_R), except for 30 m sprint where the mean error is lower (Table 5.1). Thus, the algorithm is less robust than the radar. This might be the result of the assumption of purely sagittal plane motion, which can be violated to different degrees by the different magnitude of mediolateral motion resulting from the varied running techniques of the sprinters.

Comparison of the estimated maximum velocity to that from the radar (Figure 5.4C) showed a bias of -0.12 m/s, which is in agreement with the slight underestimation of velocity discussed in the preceding paragraph and lower than the 0.20 m/s value reported in (Gurchiek et al., 2018). Despite this bias, the estimated maximum velocity showed a ‘strong’ agreement with the measured one, indicated by the magnitude of the Lin’s concordance correlation coefficient (ccc) being 0.76 ($p < 0.05$). In comparison, (Setuain et al., 2018) compared the estimated maximum velocity with the measured one, obtaining a ccc value of 0.81 ($p < 0.05$). However, the maximum velocity in this work was estimated indirectly through a linear force-velocity relationship based on the first order exponential fit model (equation 5.1) for both, the IMU and the reference force plate data. For the v_{max} , the limits of agreement (L.O.A.) for the Bland-Altman plot range from -1.20 to 0.89 m/s, this range being smaller than one (-1.25, 1.64 m/s) presented in (Gurchiek et al., 2018). L.O.A for the v_0 parameter varied from -1.01 to 0.67 m/s, which is similar in extent to one (-0.7 to 1.3 m/s) showed in (Samozino et al., 2016). The f_0 and p_{max} magnitudes were computed in terms of per unit mass and hence the L.O.A cannot be directly compared to the ones from (Samozino et al., 2016).

5.5.2 Exponential fitting and athlete profiles

Use of a first order exponential fit (Samozino et al., 2016; Setuain et al., 2018) is the dominant method of estimating the sprint velocity profile and subsequently the force (F)-power (P)-velocity (V) relationships. In this work, we compared the accuracy of this first order exponential and a second order exponential in approximating the velocity profile produced by our algorithms and by the reference radar system. Figure 5.6A showed the second order fit to better approximate the velocity profile, while the first order fits led to an underestimation of the velocity. For all sprint distances, the median RMS error for second order exponential was consistently less than that for the first order exponentials; this was true for both fits based on v_R or v_{est} . The error values are different across athletes and different sprint distances, emphasizing the idea that the velocity profile does not necessarily present first order exponential behavior. While the first order fit is suitable to represent a maximal effort during sprint competitions (Samozino et al., 2016), the athletes may not necessarily undertake a maximal effort during training sessions. Thus, a second order exponential can offer a truer representation of the sprinter’s velocity profile across different contexts. However, estimating the three variables (a , τ_1 , τ_2) is an optimization problem, leading to a higher computational cost than solving the equation 5.1 for a single variable τ . This added complexity could be detrimental in case of real-time processing.

Use of a first order exponential leads to linear F-V and parabolic P-V profiles, which have been investigated previously (J.-B. Morin & Samozino, 2016) for their potential to predict risk of injury and to plan training goals. The second-order exponential leads to more accurate albeit non-linear F-V and non-parabolic P-V profiles, as seen in Figure 5.7. As expected, the area under the curve for both profiles are higher for athletes with lower finish times and vice-versa. For the top two athletes (6.93 s and 7.05 s), the F-V profile (Figure 5.7B) shows an interesting contrast, one (6.93 s) of them starts with a higher acceleration, has a stronger reduction in the same, and yet the athlete continues

to accelerate throughout the 60 m. Whereas the second (7.05 s) athlete starts with a lower acceleration but has a slower reduction in its magnitude. Such differences, when observed over multiple trials, can help in identifying the strengths and the areas of improvement for athletes. Whether the increased accuracy resulting from the second order exponential improves the analysis of athletes is a potentially important practical research question for sports scientists.

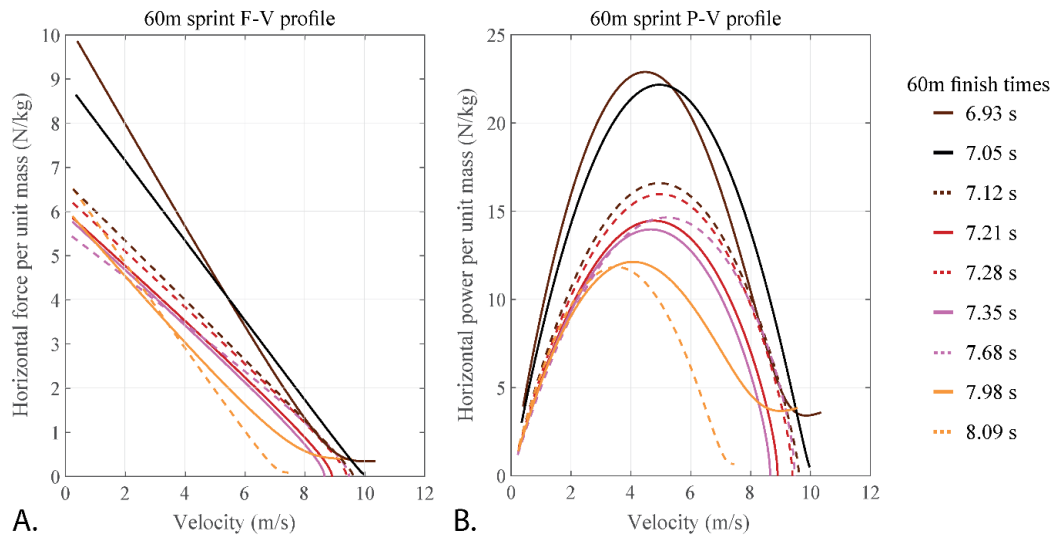


Figure 5.7 Force-velocity and power-velocity profiles, A) Horizontal force (per unit mass) - Velocity profile for the respective best 60m performance of nine athletes C) Power (per unit mass) - Velocity profile, based on second order exponential fit, for the respective best 60m performance of nine athletes

5.5.3 Limitations and future work

The two main limitation of the proposed algorithm arise primarily out of the gradient descent (Madgwick et al., 2011) procedure used for converting the IMU acceleration from the sensor frame to the global frame. First, this procedure necessitates the use of magnetometer for reliable estimation of the acceleration in the lateral direction. We assume that the motion occurs purely in the sagittal plane, thus negating the necessity of using lateral acceleration and simplifying the process model in the Kalman filter to a one-dimensional linear model. This assumption holds because of the approximate straight-line motion of the sprinter; it also forms the basis of radar-based velocity measurement. Thus, the proposed algorithm is valid for straight-line sprints and not for curve sprinting or sprints with direction changes.

Second, the gradient descent uses a static period to determine the orientation with respect to gravity and thus the algorithm is sensitive to the selected starting point of the sprint. Thus, absence of a static period before the start of the sprint can lead to unreliable conversion of the acceleration to the global frame. To ensure the availability of this static period, we visualize the raw GNSS velocity plot and manually select the starting point for the segmentation of the sprint data. However, an automated segmentation procedure, possibly based on the GNSS velocity, can allow for a more robust and repeatable segmentation, and subsequently enable a more accurate estimation of sprint

velocity. Automated segmentation can also simplify the analysis when a battery of tests, such as the agility T-test (Pauole et al., 2000), the sprint test, and the bleep test (Iaia & Bangsbo, 2010), are performed together. This is typically the case for pre-season testing in team sports such as soccer, rugby, hockey, etc. The limited sample size of this study constitutes the last limitation. However, this study is aimed strictly towards the technical validation of the proposed algorithm, and we attempted to overcome this limitation by conducting multiple trials per participant. While this study was mainly focused on the algorithm development and validation, there is a potential for a follow-up study with different groups of sprinters of varied skills to test the discriminatory power of the results from the algorithm.

5.6 CONCLUSION

The goal of this study was accurate estimation of the sprint velocity profile using a back-worn GNSS-IMU sensor and its validation with the reference system i.e. a Doppler speed radar. To overcome the individual limitations of the GNSS and IMU sensors, we utilized a sensor-fusion approach based on Kalman filter to fuse the GNSS velocity and the IMU acceleration signals. Velocity profile estimation was achieved with a median error ranging from 6.14% to 8.11% respect to the radar speed profile, for sprint distances varying from 30 m to 60 m. Additionally, an improved approximation of the velocity profile was presented using a second order exponential model, thus raising doubts over the dominant approach of using a first order exponential model. Further studies should investigate the advantage of utilizing second order exponential model in athlete training and monitoring. To extend this work in future, we may automate the segmentation procedure and use the IMU signals to analyse the gait temporal parameters. By pursuing this path, we hope to augment the potential of sprint test used in training to assess injury risk of athlete and improve their performance.

5.7 APPENDIX

A sensitivity analysis was conducted to examine the change in the percentage RMS error with a corresponding change in the threshold (section 5.3.1) used to detect the start of the sprint. The algorithm was tested for a range of thresholds around the chosen value of 0.3 m/s (Figure 5.8), increasing in steps of 0.05 m/s, from 0.2 m/s to 0.4 m/s. For the 30 m sprint, the algorithm showed around 1% change in RMS error at thresholds lower than the chosen one but almost no change for threshold higher than 0.3 m/s. For 40 m and 60 m sprints, the RMS error resulting from the algorithm presented almost negligible sensitivity to the threshold.

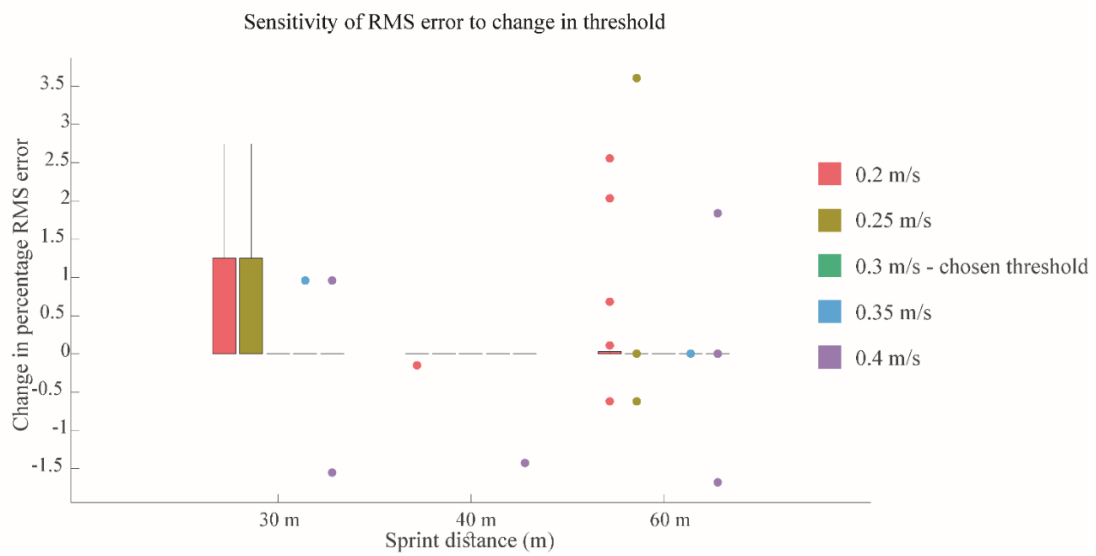


Figure 5.8 Change in the percentage of RMS error from its value at the chosen threshold of 0.3 m/s. The RMS error is slightly sensitive to the threshold for the 30m sprint, especially when the threshold is below 0.3 m/s. For other distances, the error is almost insensitive to the threshold.

6 DEVELOPMENT OF AN INSTRUMENTED CHANGE-OF-DIRECTION FIELD TEST

This chapter presents the algorithms used to augment the Agility T-test, which is a functional test for measuring change of direction (COD) ability of athletes. It involves five sequential movements and the transition between these movements is characterized as COD. The test is traditionally scored based on the total completion time, with a lower timing indicates better performance. However, the test in its current form does not provide information about the performance based on the five individual movements and the respective CODs. Instrumenting the T-test with wearable sensors provides an avenue to measure detailed metrics in the field, which extend beyond the total time. During their pre-season testing, data from 25 professional soccer players was recorded using a GNSS-IMU sensor on upper back. Video data recorded with a GoPro camera was used for validation. The proposed method detects the start and end of the five sequential movements, based on the acceleration impulse estimated between peak values of the antero-posterior acceleration signal enhanced through wavelet analysis. The detected start and end of each movement provide a mean error and standard deviation of -0.03 ± 66 (ms) for COD detection. The relative mean error and standard deviation for each COD duration and each sequential movement duration is less than 3.5 ± 16 (%) and less than 7 ± 7 [%], respectively. By reliably estimating the duration of the five motion sequences and the transitions between them, the proposed method can serve to be a valuable performance evaluation tool for coaches. For the five fastest/slowest athletes according total time, the obtained results differences between the duration of the total cutting time and the displacement phases. These results can be studied further to understand the sensitivity of the new metrics can be extracted using the proposed methods. Furthermore, asymmetrical performance between displacement in the right and in the left direction and/or the COD between them can be highlighted using the presented algorithm. Athletes returning to sport after a knee anterior cruciate ligament (ACL) injury can be assessed using this asymmetry. By enabling a richer analysis in the field, this work can enable coaches to develop more personalized training and rehabilitation programs.

The contents of this chapter are under review as an original research article in the Sports Medicine – Open journal.

Contributions: conceptualized the study design; conducted the data collection; recommended the methodology for data labelling and algorithm development, contributed to the analysis and interpretation of the data; drafted the manuscript; supervised the master project that led to the results of this chapter.

6.1 INTRODUCTION

Agility is an important ability for practitioners of sports like soccer, rugby, hockey, tennis, badminton, etc., as they are required to respond quickly to events on the field. In this context, the capacity to perform a "rapid whole-body movement with change of velocity or direction in response to a stimulus" (Sheppard & Young, 2006) is defined as agility. Agility is broadly based on two components: a reactive component involving cognitive factors as perception, reaction time, anticipation, etc., followed by an athletic component involving speed, acceleration, strength, coordination, technique etc., to execute the planned movement. Agility, being multifactorial, is difficult to evaluate quantitatively during in-field training and testing. However, the second component of agility, i.e., the ability to rapidly execute a pre-planned movement, can be evaluated using change-of-direction (COD) tests in the field. Each COD speed test consists of various COD maneuvers, preceded, and followed by various displacement phases. The most important factors affecting the technical execution of direction changes are the approach speed and the COD angle, where the latter is defined as the angle between the approach direction before the COD and the exit direction after. While there is no "gold-standard" COD test assessing the general performance of the athletes, a "T" shape of ten yards (Pauole et al., 2000) is commonly used in sports such as soccer (Sporis et al., 2010), basketball (Chaouachi et al., 2009), football (Gleason et al., 2015), tennis (Sekulic et al., 2017), etc. It involves five sequential movements (Figure 6.1) while facing in the same direction:

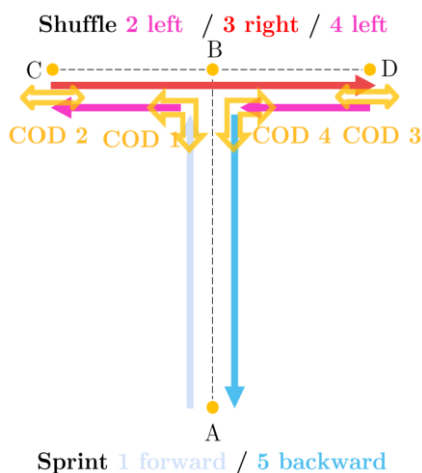


Figure 6.1 Conventional T-test for COD performance assessment

It involves five sequential movements (Figure 6.1) while facing in the same direction: i) Sprint forward (A to B) ii) Shuffle left (B to C) iii) Shuffle right (C to D) iv) iv) Shuffle left (D to B) v) Sprint backwards (B to A). A is the starting point and B-C-D are the points where the cutting maneuver (or cut) takes place and are marked by cones. Cutting maneuver is undertaken to change the direction of movement. This test has been shown to be reliable, and effectively measure a COD ability (Pauole et al., 2000; Stewart et al., 2014). Furthermore, it is popular among coaches and athletes because of the ease of use – one trial is usually less than 15 s, only cones are needed to mark the path and a pair of photocells are required for timing, and the test needs limited space. Thus, the T-test is the focus of this of the work presented in this chapter.

Performance on COD speed test is not biased by cognitive factors, as the trajectory is known and the athletes can plan their movement in advance. This makes the measurements more homogeneous in an elite athlete population and eliminates the necessity to measure variable such as reaction time, cognitive load, etc., which are difficult to evaluate on the field. The big advantage of COD speed test is that they assess a mix of physical abilities in a single movement. The required qualities to perform at cutting maneuver are supposed to be a mix of: speed, balance, technique (anticipatory and proprioception skills), strength, power, plyometric capacity etc. (Sheppard & Young, 2006). Therefore, COD speed tests are an effective way to assess multiple physical abili-

ties at once in an environment closer to the field. Rapid performance of COD requires an extended knee position, greater knee abduction angles, and large ground reaction forces. As these factors are associated with knee joint strength and stability (Dos' Santos et al., 2019), COD testing is also used as a tool for assessment of return to sport for athletes with anterior cruciate ligament (ACL) injuries. ACL injury presents a frequent prognosis in sports with an emphasis on COD skills, with the incidence of ACL injuries rises to 0.23 per thousand skier days, and up to 0.2 per thousand exposures in female soccer (0.09 for male) (Davey et al., 2019). Deterioration in the ability of athletes to rapidly decelerate before COD has been linked to neuro-muscular coordination loss, strength loss, unconscious speed reduction before COD due to fear of re-injury, reduced range of motion etc. and thus can be detected through detailed analysis of COD tests (Kim et al., 2020).

The main metric for assessment during the COD test is the total competition time for the test. With the use of force plates or video analysis, advanced metrics such as ground contact time (total duration of ground contact of the feet) during COD can also be assessed (Sasaki et al., 2011). A lower magnitude for both metrics implies a better performance. Force plates may also be used to evaluate the magnitude of GRF, with a high reaction force, especially during the braking phase before COD, being correlated to a better performance (Shimokochi & Shultz, 2008). Complementing the force plates with a motion capture system can provide additional metrics such as speed before/after the cutting maneuver, movement of the center of mass (COM), range of motion (ROM) of trunk rotation along mediolateral axis, knee adduction moment (KAM), etc. (Welch et al., 2021). Furthermore, asymmetries of the range of motion of the shank between right and left side can be a way to measure knee stability (Kim et al., 2020) and the movement of COM and the magnitude of GRF can be used to ascertain vertical stiffness (Maloney et al., 2017) during COD. A high vertical stiffness, low COM vertical displacement, low trunk angle ROM, and a high KAM are typically related to a high performance on the test (Maloney et al., 2017; Sasaki et al., 2011; Welch et al., 2021). While this measurement setup can enable the analysis of a large variety of metrics (McBurnie et al., 2021), it is cumbersome and highly expensive to use during regular training and testing sessions on the field. In contrast, wearable sensor-based methods can provide an easier avenue for analysis in the field and have been previously used to augment functional capacity tests (Ahmadian et al., 2020; Apte, Troxler, et al., 2022; Picerno et al., 2011; Willy, 2018).

Trunk-worn IMU has been used to detect different types of CODs (Meghji et al., 2019), based on the changes in the body rotation around the vertical axis. In the T-test, knowledge of COD type can help in the segmentation of different phases and assessment of individual durations. However, this method assumes the athlete to look in the direction of running after COD, which is not applicable for the T-test. An IMU on sacrum was shown to approximate the GRF well, based on the use of the magnetometer for estimating heading angle and the assumption of the sacrum representing the location of the COM (Gurchiek et al., 2017). However, magnetometer is highly sensitive to environmental magnetic field and the COM assumption may be violated because of the trunk rotation during COD. Another study used sacrum-worn IMU to distinguish between two different techniques used in a slalom run (McGinnis et al., 2017) using a K-

means clustering analysis. However, the drift-reduction technique employed to assess the trunk orientation was not validated quantitatively. Machine learning approaches have also been employed to estimate running speed before/after turns using pelvis-mounted IMU (Zago et al., 2019) and knee joint loading using an IMU each on the thigh and the shank (Stetter et al., 2019). However, the former work provided a association of $R^2 < 0.7$ and only considered 180 deg cuts, while the latter study utilized a sleeve to attach the IMUs to the leg, thus making the estimating susceptible to soft tissue artefacts, especially during highly dynamics movements of a COD test. None of these works considered the T-test in particular and only one study (Meghji et al., 2019) utilized a wearable sensor that is commonly used by high level athletes in their daily training routine.

A fast COD test implies not only strength in the legs or speed, but also coordination, technique, balance, or other physical capabilities that have yet to be defined (Young et al., 2015). A disadvantage of the non-specificity of the COD test is that it does not allow precise isolation of the athlete's weaknesses. While the COD test can be used to show a drop in the athlete's performance, but it is difficult to understand the cause. One reason for this is that traditional performance evaluation is based only on the total time of the COD test. Therefore, a quantitative analysis of the duration of each phase would be a valuable tool for coaches to identify athletes' weaknesses in a particular movement sequence or COD type. For example, an athlete might be particularly poor at running backward or slower at one of the 180° cuts due to a knee injury. Therefore, a method that allows automatic detection of the different phases of a T-test for COD can be a valuable tool. This chapter details the development and validation of such a method using a wearable GNSS-IMU sensor, which is commonly used for training and match analysis in soccer (Clemente et al., 2018). Furthermore, it presents the validation of the duration of the detected phases and an initial exploration of the different performance metrics that can be estimated using this method.

6.2 MATERIALS AND EQUIPMENT

Twenty-two male professional soccer players (height: 181.4 ± 5.4 cm, weight: 75 ± 5.6 kg, age: 25.1 ± 4.3 years) from Swiss league football were enrolled in this study. Each athlete was asked to perform two trials of the standard T-test with an IMU-GNSS sensor (AdMos from ASI sensors) placed on the upper back (Figure 6.2). This sensor setup was chosen as it is commonly used in soccer (Clemente et al., 2018) and it was previously used to instrument the sprint test (Apte, Meyer, et al., 2020). Since the sprint test is typically carried out together with the T-test during pre-season testing in soccer, instrumentation of both testing using the same sensor setup can be valuable. The AdMos sensor was configured to measure 3D acceleration and angular velocity with the sampling frequency of 200 Hz as well as GNSS ground speed with the sampling frequency of 10 Hz. Video data of all tests was recorded with a camera (GoPro Hero 5, frame rate = 60 fps), placed facing the athlete. This data was used as reference for labelling the different phases of the test. The total completion time of the test is measured using a photocell (Witty, Microgate corp, Italy) placed at the start line. The photocell makes a sound when the athlete cross the start line at the start and the end of the test. During

the test, the athlete faced forward, touched each cone, and was not allowed to cross the feet when shuffling sideways.

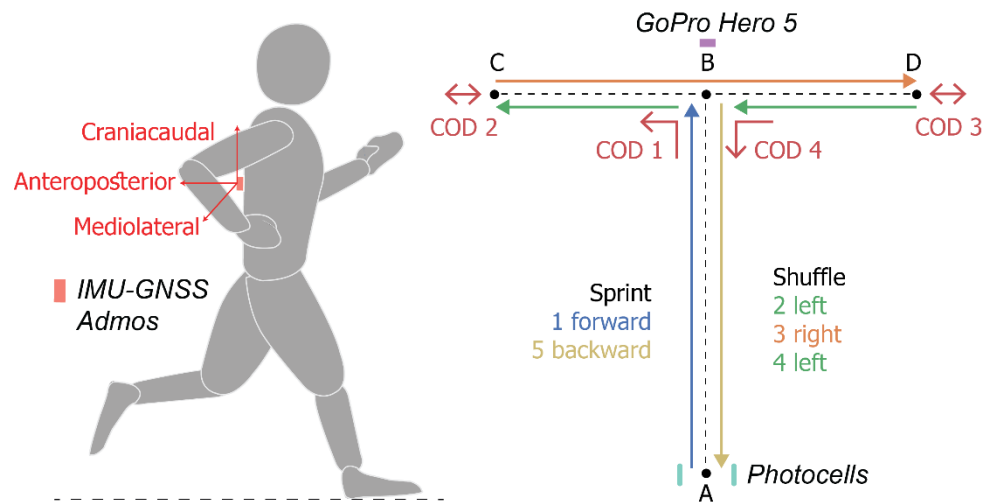


Figure 6.2 Sensor setup and the nine phases of the Agility T-test. Instrumentation used for the protocol is presented in *Italics*

Each T-test is divided in 9 segments which consists of 4 change of directions (CODs) and 5 displacement phases (DPs). For each cutting maneuver, the athletes must touch the cones, indicated by points B, C, and D:

- DP1: Forward sprint from A to B which begins with the photocell sound
- COD1: 90° angle change of direction using side step, from forward sprint to sideways displacement in the left direction
- DP2: First left shuffle which is sideway displacement from B to C
- COD2: 180° angle change of direction using split-step, from left shuffle to sideways displacement in the right direction
- DP3: Right shuffle which is sideway displacement from C to D
- COD3: 180° angle change of direction using split-step, from right shuffle to sideways displacement in the left direction
- DP4: Second left shuffle which is sideway displacement from D to B
- COD4: 90° angle change of direction using side step, from left shuffle to backward sprint
- DP5: Backward sprint from B to A that ends with the second photocell sound

6.3 METHODS

6.3.1 Labelling of video data

For validation of segmentation algorithms, it is important to label each of defined segments from the recorded videos. For each COD segments, we can define five distinctive events: two heel strikes (right foot + left foot), two toe-offs (right foot + left foot) and one for touching the cone. The COD motion can be divided into two main phases: the eccentric phase (braking) and the concentric phase (pushing). The transition between the two phases occurs approximately when the athlete touches the cone. Just before the eccentric phase and just after the concentric phase (of both legs), the athlete

is no longer in contact with the ground. COD duration is the time the athlete is in contact with ground, after the first heel strike of the last flight phase of the approach displacement phase and the last toe-off of the first flight phase after the COD. Assigned events for each COD segment are depicted in Figure 6.3.

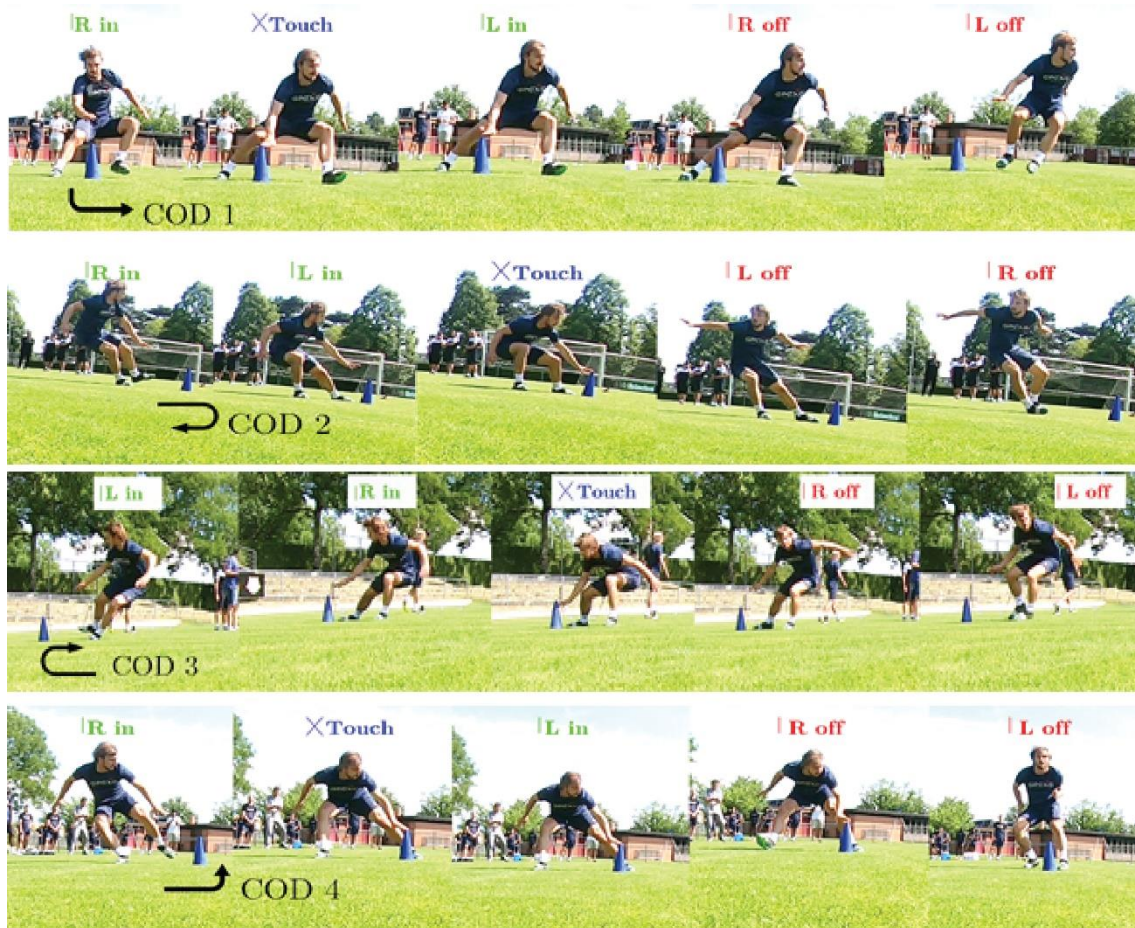


Figure 6.3 Event labels for each COD segment to be used as reference data; COD 1 and COD 4 involve 90 deg turn with a side step, COD 2 and COD 3 involve 180 deg turn with a split step, R in: right foot heel strike, L in: left foot heel strike, Touch: cone touch, R off: right foot toe-off, L off: left foot toe off

Time frames of each test were recorded using Kinovea™ and then imported into MATLAB. Each test data was manually cut in a 15-second window (the duration of the T- test is ~ 10s) for subsequent algorithm development and validation.

6.3.2 Algorithm development

A macro-micro approach was followed to detect COD segments, following its successful prior application in biomechanical assessment using wearable IMUs (Hamidi Rad et al., 2021). First, a macro-analysis of the signal is performed to identify the beginning and end of the test as well as the transient phases corresponding to each of COD segments. Then, micro-analysis methods are developed for a more accurate detection of step patterns in each COD segments. All algorithms were developed using the data from 6 out of the 23 athletes.

6.3.2.1 Macro-analysis

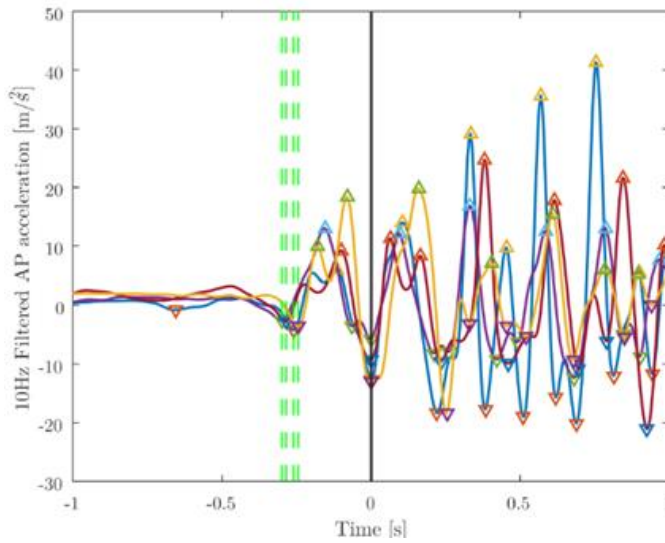


Figure 6.4 Start of motion (dashed green lines) and first step (black line) detection. Data shown for 4 participants.

The reference for the beginning of the test when the athlete crosses the start line and the corresponding sound the photocell. Due to lack of synchronization between photocell and IMU system, it is not possible to locate the exact timestamp of the beginning of the test on the IMU signal. Therefore, it was decided to synchronize the video and the signal based on the event of the first step. The sound of photocell from the video is assumed to be reference starting point, while this first step is detected from the IMU signals as follows.

Acceleration in the anterior-posterior (AP) direction is used to determine the beginning of the test. While the axes are defined in the sensor frame (Figure 6.2), they are assumed to align with the body frame due to the location of the sensor within the vest and the tight fit of the vest. Thus, we can assume negligible movement of the sensor with respect to the trunk. This signal is filtered using a zero-phase 2nd order Butterworth low-pass filter with a cut-off frequency of 10 Hz. The first two local maxima above 4 ms^{-2} are detected from this signal using the *peakfinder* function in MATLAB 2020b. The first peak likely originates from the straightening of the upper body as the athlete begins to push on the ground whereas the second peak likely comes from the impact during the first step of the test. Therefore, the local minimum before these two peaks is defined as the start of the movement and the first heel strike (first step). This procedure is shown in Figure 6.4 for 4 randomly selected subjects. The end of the test cannot be identified using only IMU signal, since the athlete doesn't stop when they cross the finish line. Therefore, we consider the end of the test by adding total completion time (from photocell) to the detected timestamp for beginning of the test. The 10 Hz sampling rate of the GNSS receiver is too low to capture the end of the test accurately, even though the total distance each phase is known.

Four transient phases corresponding to each of COD segments were visible with a simple visualization of the AP acceleration signal (Figure 6.5). It is well known that for transient signals, wavelet analysis allows reconstruction of the signal with little to no phase shift and with little loss of information. It is also known that wavelet decomposition preserves features such as a discontinuity better than spectral analysis [46]. Some studies have also shown that the magnitude of variables (such as vertical acceleration while running) strongly depends on the filter cut-off frequency [47]. Therefore, in this work, wavelet decomposition within a range of 0.5 – 15 Hz was used to approximate the shape of AP acceleration signal. The mean value of the AP acceleration (zero fre-

quency) was then added back to the wavelet-approximated signal to synchronize it with the original signal. Local minima below a specific threshold (T_{MA} in equation 6.1), with prominence greater than 15 ms^{-2} , were detected using the MATLAB peakfinder algorithm. T_{MA} was chosen as a function of the average peak value (resulting from the ground contact):

$$T_{MA} = \frac{1}{4} \times \frac{\sum (\text{local max. peak value})}{\text{number of local max. peaks}} \quad (6.1)$$

The AP acceleration between each detected local minima was then numerically integrated using the *cumtrapz* function to approximate the change of velocity during a foot stance. This change in velocity during the COD motion is referred to as the acceleration impulse (AI). As we see in Figure 6.5, the acceleration impulses (in blue) are around 5 to 7 ms^{-1} during COD and between 1 to 3 ms^{-1} during displacement phases. Four pairs of the detected minima with the maximum AI values were selected as the COD segments. Since the order the 90 deg and 180 deg COD segments and the timestamps of the four pairs of minima are known, the COD type was also classified.

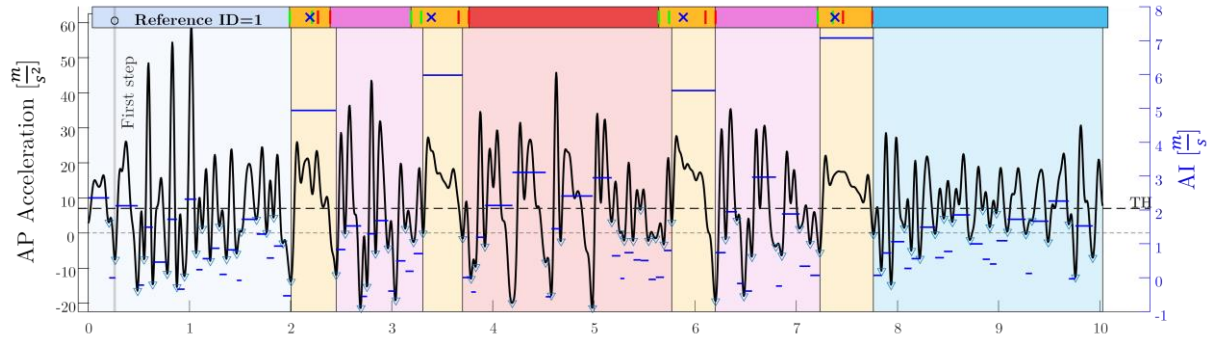


Figure 6.5 Segmentation of one test sample using reconstructed AP acceleration signal. T_{MA} is indicated by dotted horizontal line. Blue horizontal line shows the acceleration impulse between each local minimum; blue triangles show all the local minimum; time line at the top comes from video reference with the blue crosses showing the instance of cone touch, the green and red vertical lines indicating heel strike and toe off, respectively. This timeline is shaded darker than the segments below, to highlight its role as reference from video

6.3.2.1 Micro-analysis

The COD detection algorithm presented in the macro-analysis section is used as a first approximation for the beginning and end of the COD events. The micro analysis algorithm was subsequently used to allow more precise patterns to be detected from the signal and improve the detection of the start/end of the COD segments. The typical key event during each COD is defined using the last step before shifting to the new direction, called ‘final foot contact’ (FFC) (Dos’Santos et al., 2018), which is indicated as second heel-strike (for example, L_{in} in COD 2) in Figure 6.3. However, research has also shown the importance of the step preceding the FFC, especially for sharp turns. This step is called ‘penultimate foot contact’ (PFC), indicated as the first heel strike (for example, R_{in} in COD 2) in Figure 6.3, and is used to brake prior to the COD (Dos’Santos et al., 2018; Nedergaard et al., 2014). For COD greater than 60° , it is recommended to brake strongly during the PFC, thus making it important (Dos’Santos et al., 2019). For the micro-analysis, five candidate methods were developed based on the observation of the signals and the obtained error over 6 participants was used to

test these methods. M3 utilized the 2-norm of the acceleration signal, while others were based on the AP acceleration.

- M0: The COD detection from macro analysis (Figure 6.5) was used. Start and end of the COD were the local minima between the largest AP AI.
- M1: Within the selected local minima, a smaller wavelet range (0.5 to 5 Hz) was applied, and the resultant local minima were selected as start and end events.
- M2 (only for 180 deg COD): If there was large peak just before the start detected from macro-analysis, this method brought forward the start of COD by a local minimum. The goal was to move the detected start from the second heel strike to the first one (Figure 6.3) i.e., the PFC. The end of COD detected from macro-analysis was shifted forward by a local minimum if the detected minima (end) was less than 0. This was done to shift the endpoint to the second toe-off.
- M3: First points on the acceleration *norm* signal with magnitude $< g$ were found, which occur immediately near the approximate COD start/end found with the macro analysis. Acceleration $norm < g$ indicates the flight phases, which occurs immediately before the first heel strike and after the second toe-off (Figure 6.3).
- M4: For the first 90° COD (COD 1), the COD end detected from the macro-analysis was pushed forward by one local minimum if the detected end was immediately followed by a peak. This peak indicates the second toe-off, which occurs at the end of the COD 1 (Figure 6.3).

6.3.2.2 Validation

For each of five proposed methods in micro-analysis, the error (ε_s for start and ε_e for end) in ms between detected COD start (T_{ests}) and end (T_{este}) timestamps with respect to the corresponding reference timestamps (T_{refs} and T_{refe}) obtained from the video labels:

$$\varepsilon_s = T_{refs} - T_{ests} \quad (6.2)$$

$$\varepsilon_e = T_{refe} - T_{este} \quad (6.3)$$

Based on the start and end points, duration of each segments (4 CODs and 5 DPs) was also computed, as it is an important metric for analysis of the performance during the T-test (Welch et al., 2021). For the durations, the absolute error (ε_{da}) in ms and relative error (ε_{dr}) in % were also computed from estimated (D_e) and reference (D_r) durations. The error on total completion time (ε_t) was also computed, based on the difference between the duration labelled with the video (D_{vt}) and that recorded by the photocell (D_{pt}). Finally, The Bland-Altman plot (Bland & Altman, 2003) was utilized to check whether errors are correlated with the detected events or not.

$$\varepsilon_{da} = D_r - D_e \quad (6.4)$$

$$\varepsilon_{dr} = \frac{D_r - D_e}{D_r} \times 100 \% \quad (6.5)$$

$$\varepsilon_t = D_{vt} - D_{pt} \quad (6.6)$$

6.3.3 Metrics for performance in COD test

While the proposed method for instrumenting the agility test can provide additional data during the COD, the performance metrics were defined using the literature (Dos' Santos et al., 2019; McBurnie et al., 2021; Welch et al., 2021; Young et al., 2015). While a larger set of metrics can be estimated using a combination of force plate and motion capture systems, the metrics that can be estimated using the current sensor setup were selected for analysis and comparison of the athlete's performance during the test. To investigate whether the metrics can differentiate between athletes with different performances, five participants with lowest and highest total completion time on the test were selected as the 'best' and 'worst' groups. The 'best' and 'worst' performance was assessed with the total completion time, as this is the standard metric used to evaluate the T-test. These metrics can be divided into three categories:

- **Duration-based metrics:** The total completion time of the test is the standard performance metric. This value came from the photocells and was used as the standard performance metric. The duration of each COD and displacement phases was used to gain insight into the potential weakness/strength for different movements. Finally, the total cutting time, which is the sum of the approach phase (DP before COD) duration, the COD duration, and the exit phase (DP after COD) duration, was computed to assess the performance of a single COD. Pearson correlation (Benesty et al., 2009) between total cutting time for each COD and the total completion time was evaluated to investigate the relevance of total cutting time as a performance metrics. Additionally, the individual durations of all nine segments, the total cutting time for each COD were visually compared for the five athletes with highest and lowest total completion times. This provides an insight into potential key factors in performance.
- **Velocity-based metrics:** The approach and exit velocity for each COD indicate the ability to maintain and transfer momentum during the COD. Consequently, using the GNSS, the minimum velocity during the COD and the entry/exit velocities were selected as performance metrics, with higher values implying a better transfer of momentum and possibly, a faster COD. GNSS velocity was processed to remove any outliers and replace them with linear interpolation.
- **Acceleration-based metrics:** Acceleration evaluates the forces experienced and generated by athletes during the test. Acceleration impulse (AI) reflects the change in momentum of the athlete during the COD, generated from the deceleration and acceleration required to change direction. This metric was calculated by numerically integrating (using the trapezoidal method) the acceleration during the COD phases. The peak absolute acceleration is an indicator of the impact magnitude detected on the athlete's upper back during the COD. These peak values are influenced by the intensity of the braking phase before the cut and by the COD preparatory movement performed to reduce the load on the lower limbs. All these acceleration metrics were computed on all three acceleration axes (AP: anteroposterior, ML: mediolateral, and CC: craniocaudal) and their norm.

6.4 RESULTS

6.4.1 Labelling of video data

For each T-test, the results of video labelling consist of 27 frames corresponding to one event, with the most important events (test start, COD start/stop, etc.) are shown below.

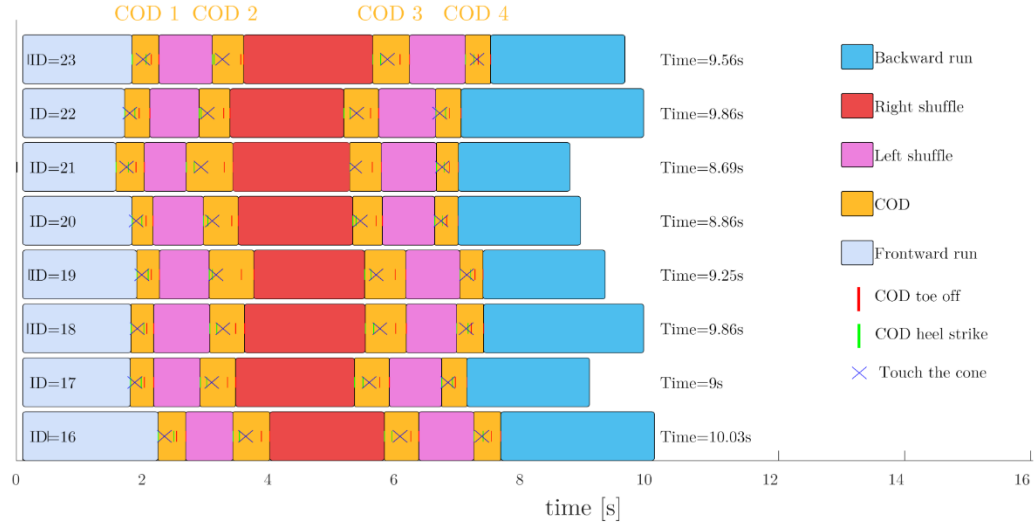


Figure 6.6 Segmentation of the T-test based on video labelling for 8 of the 23 athletes. The total completion time of the T-test (based on video) are given on the right of split T-test

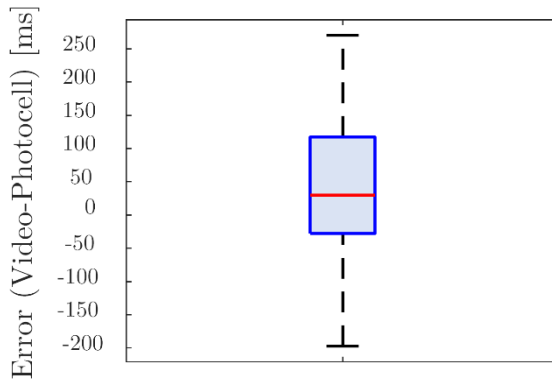


Figure 6.7 Error between video-based duration and photocell duration

The error for total completion time based on the video labelling is shown in Figure 6.7. This error is the difference between the total test duration based on the videos and the duration based on the photocell sensors (equation 6.6). Despite video is used as ground truth, photocell was expected to be more precise. That's why photocell time is used to define the end of the test in the algorithm. Median \pm IQR for this error is 38 ± 121 ms, but the maximum value can reach 250 ms.

6.4.2 Detection and duration of COD

The proposed method was able to identify detect all the COD phases and differentiate between the 90 deg and 180 deg CODs. The mean total test completion time was 9.32 ± 0.35 s. With the detected first step assumed as the start ($t = 0$ s), T-test timelines for four participants are illustrated in the Figure 6.8 below.

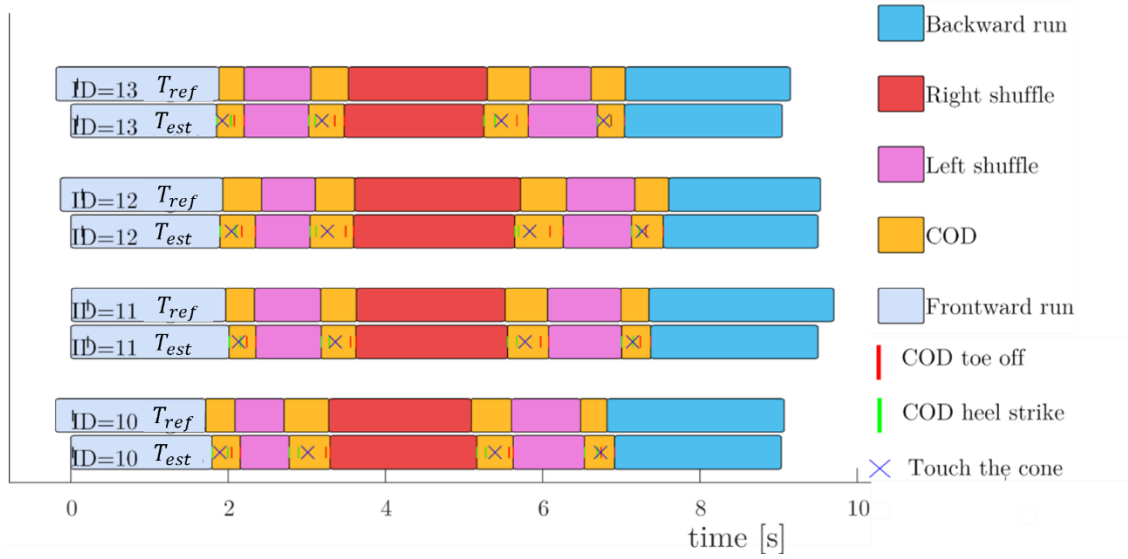


Figure 6.8 Time of event from video and from algorithm for four T-tests. Both timelines are aligned using the first step and the end of the signal time line is the duration from the first step to the photocell end time. Results from the method M0 are shown here

ε_s and ε_e for each COD from the four micro-analysis methods are presented in Figure 6.9. Based on the lowest error, M0 was the best method for detecting the start of COD 1 and the start and stop for COD 4. For COD 2 and COD 3 (180 deg COD) M2 produced the lowest error for both, start and stop. Finally, for detecting the end of COD 1, M4 led to the best result. The errors resulting from the combination of the above-mentioned best methods are presented in Table 6.1. The maximum mean and standard deviation (S.D.) for relative errors were less than 7% and 15% for the estimation of phase and COD duration, respectively.

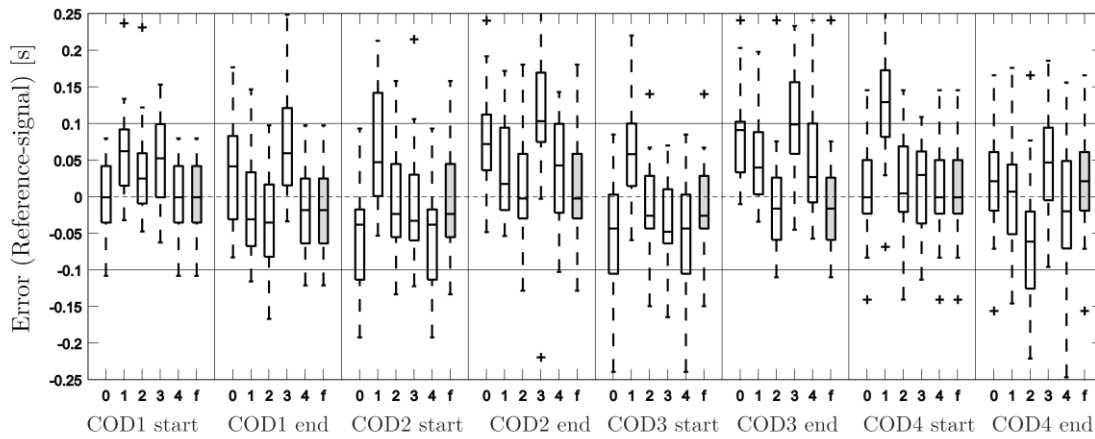


Figure 6.9 Box plot of ε_s and ε_e for COD detection for each micro analysis method. The "f" boxplot shows the best method for each event detection, among the five methods.

Table 6.1 Mean \pm S.D. of estimation error and (%) for each displacement phase and COD

DP duration	DP 1	DP 2	DP 3	DP 4	DP 5
ε_{da} (ms)	-3 ± 53	-2 ± 42.2	-20 ± 68.2	19 ± 50.4	-135 ± 142.7
ε_{dr} (%)	-0.2 ± 3.13	-0.3 ± 5.16	-1.1 ± 3.65	2 ± 6.01	-6.7 ± 6.93

COD duration	COD 1	COD 2	COD 3	COD 4
ε_{da} (ms)	-10 ± 51.4	25 ± 72.3	2 ± 69.8	5 ± 59.6
ε_{dr} (%)	-2.7 ± 14.08	3.5 ± 13.21	-0.2 ± 12.32	1.3 ± 14.47
COD event	COD 1	COD 2	COD 3	COD 4
ε_s (ms)	-2.5 ± 53	-12.9 ± 55.3	-8.7 ± 73.7	11.4 ± 63.9
ε_e (ms)	-12.7 ± 59.3	16.5 ± 77.9	-7.4 ± 75.4	16.5 ± 69.6

Figure 6.10 shows the Bland-Altman plot for the estimation of the COD start/end events using the combination of best methods presented above. Signal time represents the timestamp of the detected event using the proposed method, while reference time represents the timestamp for the same event obtained using the video data. The 95% limit of agreement (LOA) of the proposed method is between -130 and 130 ms and the mean difference (\pm S.D) is 0.03 ± 0.66 ms. The Bland-Altman plot does not present a systematic bias for the estimation errors.

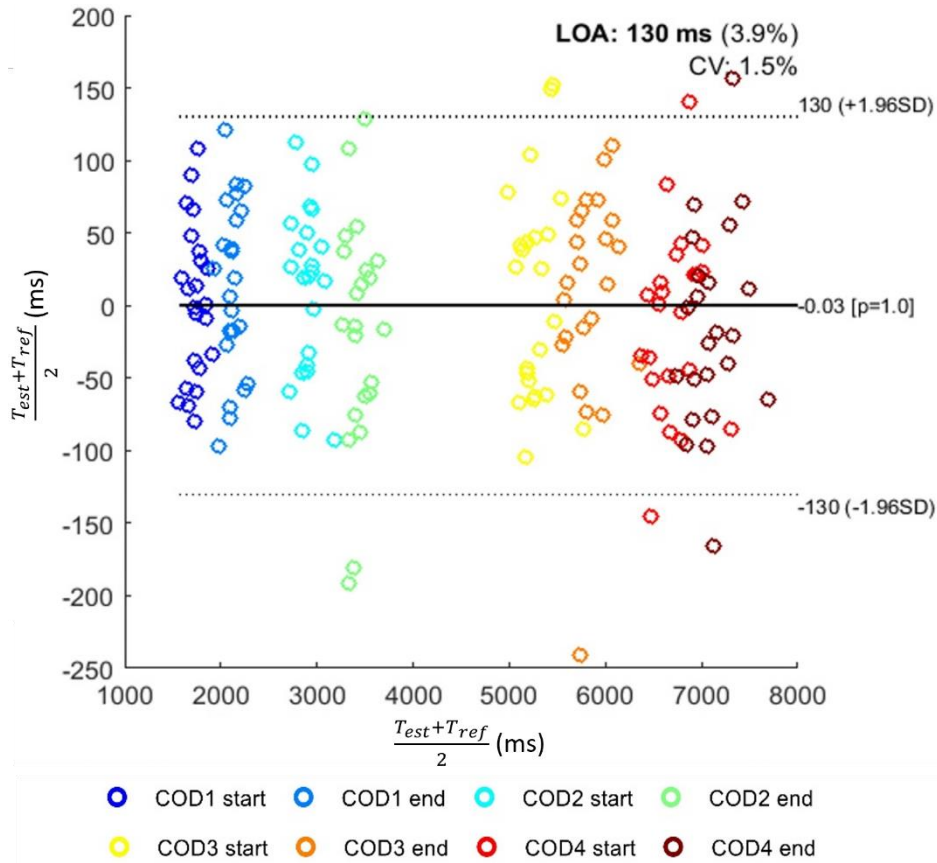


Figure 6.10 Bland-Altman plot for detected COD start/end events. Results of the combination of best methods are presented here, LOA (ms): Limits of Agreement and CV (%): constant Coefficient of Variation

6.4.3 Performance metrics

The mean \pm S.D. across all participants for the total cutting time (s), velocity in (ms^{-1}), velocity out (ms^{-1}), and minimum velocity (ms^{-1}) are presented in Table 6.2. Similarly,

the minimum velocity (ms^{-1}) during the 180 deg COD is substantially lower than for the 90 deg COD, as expected.

Table 6.2 mean \pm S.D. for performance metrics across all four COD segments

Performance metric	COD 1	COD 2	COD 3	COD 4
Total cutting time (s)	3.18 ± 0.14	3.16 ± 0.18	3.28 ± 0.17	3.47 ± 0.25
Approach velocity (ms^{-1})	4.4 ± 0.7	3.2 ± 0.4	3.9 ± 0.5	3.2 ± 0.4
Exit velocity (ms^{-1})	3.0 ± 0.5	1.4 ± 0.7	1.6 ± 0.6	2.9 ± 0.4
Minimum velocity (ms^{-1})	2.8 ± 0.6	0.9 ± 0.7	1.0 ± 0.5	2.8 ± 0.3
Acceleration impulse (AI)				
AP (ms^{-1})	5.18 ± 1.22	7.68 ± 1.23	7.89 ± 0.88	6.47 ± 0.84
ML (ms^{-1})	-3.76 ± 1.14	3.93 ± 1.82	-4.12 ± 1.22	1.84 ± 1.57
CC (ms^{-1})	-0.5 ± 1.2	-0.44 ± 1.46	-0.34 ± 1.49	0.59 ± 1.83
Norm (ms^{-2})	8.35 ± 1.41	10.95 ± 1.41	11.33 ± 1.09	8.34 ± 1.06
Peak absolute value				
AP (ms^{-2})	25.01 ± 4.83	27.68 ± 3.21	29.14 ± 4.46	31.38 ± 6.21
ML (ms^{-2})	27.4 ± 5.65	19.84 ± 6.88	22.61 ± 5.65	19.69 ± 5.51
CC (ms^{-2})	17.91 ± 4.57	19.12 ± 9.32	19.43 ± 7.02	16.43 ± 5.49
Norm (ms^{-2})	39.88 ± 6.30	39.6 ± 5.91	41.19 ± 5.89	40.59 ± 6.67

The profile for mean \pm S.D. for the velocity (obtained using the GNSS receiver) is presented in the Figure 6.11. It can be observed that the magnitude of the velocity indeed reaches its lowest values during the 180 deg COD segments, while the velocity reaches its peak magnitude closer to the end of the first displacement phase that involves running forward. Furthermore, we can observe that participants did not accelerate as strongly in the last displacement phase as during the first one.

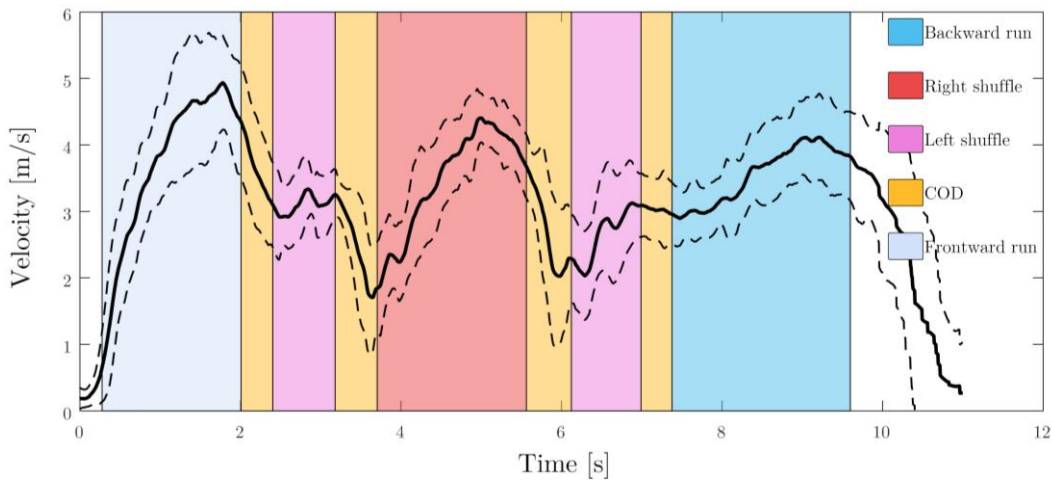


Figure 6.11 Mean (solid line) and S.D. (dashed lines) for the velocity during the T-test. Colored rectangles show phases based on mean event time found with the segmentation algorithm, with standard deviation of these events omitted for the sake of clarity.

It was observed that total cutting time of each COD was correlated to total completion time (Figure 6.12), thus indicating that this performance metric indeed reflects the general T-test performance for elite athletes. The duration of COD did not correlate in any way with the duration of the test, with fastest five and slowest five athletes spending similar amount of time during COD (Figure 6.13).

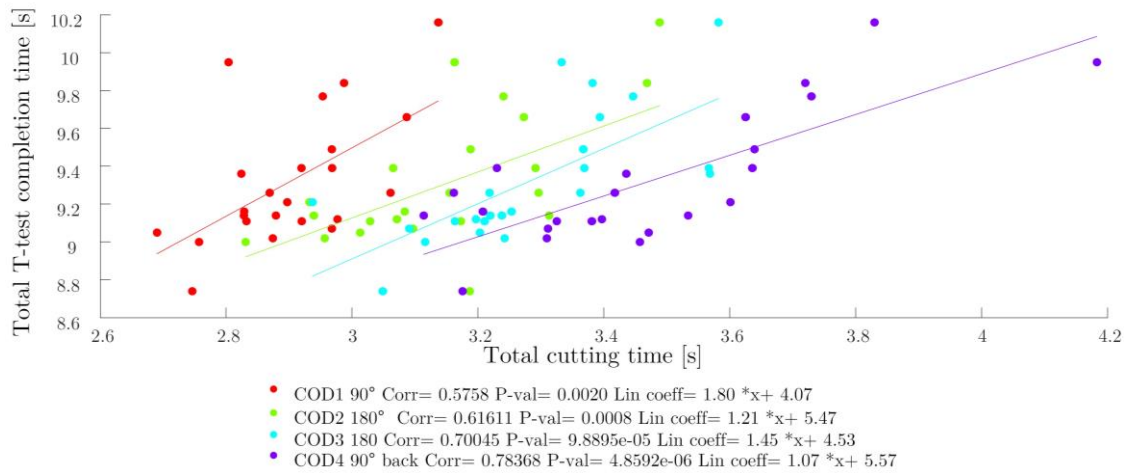


Figure 6.12 Correlation between total cutting time for each COD and the total completion time of the T-test, correlation, p-value (calculated using Student T-test) and linear fit.

The best and worst groups spent similar time in CODs (Figure 6.13), but that fast athletes are generally faster during the displacement phases. The difference in performance seems to arise more from the long shuffle to the right and the backward sprint than from other displacement phases. Furthermore, all four total cutting times, as seen with the correlation, can also differentiate well between the two performance groups.

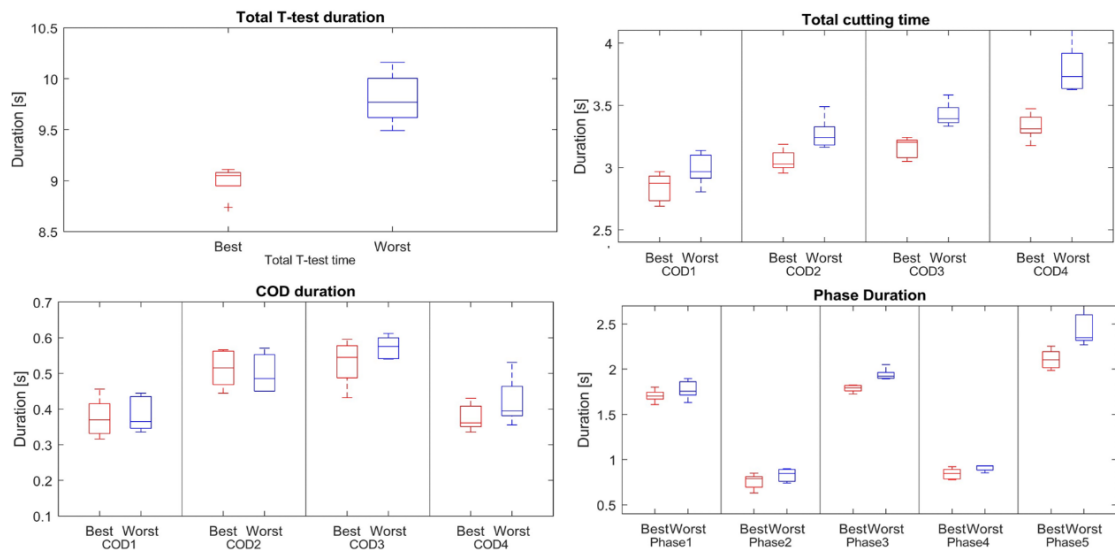


Figure 6.13 Comparison between the five best (red) and worst (blue) participants. Best and worst groups comprised of five participants each with lowest and highest total completion times on the test, respectively.

6.5 DISCUSSION

6.5.1 Validity of the proposed method

The labelling accuracy of each event is around 3 frames, which corresponds to an error of approximately 50 ms for a camera with 60 Hz frame rate. Compared to this, the total completion time error was relatively high (38 ± 121 ms), mainly due to the human fac-

tors of labeling. There was a delay in hearing the photocell (when the athlete crosses it) in the videos, the delay between the sound in the video and the moment the pause button was pressed at the beginning and the end of the test. The synchronization with the first step allows to have a median error close to zero for the many events of the test, which highlights the accuracy of using this method. However, the end of the test was not detectable reliably using either the GNSS or the IMU signals. Therefore, the error on the duration of the test will have the same order of magnitude as the error from labelling process (error on duration between photocell and video labelling). Furthermore, few athletes started from a position slightly away from the photocell, resulting in the first step happening before the photocell beep, further adding to the error.

The S.D. of the error for detection of all COD events (Figure 6.10) was 66 ms, which is close to the expected range of 50 ms discussed previously. It is also in the similar range as other studies, which utilized IMU and video reference to segment motion phases during highly dynamic activities (Hamidi Rad et al., 2021). In Figure 6.9, we can see a minimal bias in the COD1 and COD4 (90° angle) events detection, whereas the 180° COD are relatively more biased. This is because the method M0, directly based on the macro-analysis, detects sometimes the second step in and the first step off the 180 deg COD. This doesn't happen in 90° COD because almost all the braking motion happens during the first step in (only one step before cone touch). The 90° angle change is characterized by one step before touch and 180° COD by two steps before touch. In method M2, if a large peak is detected just prior to the COD start reference from macro detection, the COD start point is moved before this peak. For the COD end, if the AP acceleration is bigger than 0, the end is pushed to the next local minimum smaller than 0. This method thus allows to get the first step in if the second heel strike is detected by the macro analysis and the second toe off if the first was previously detected by the macro analysis. Therefore, this method provides gives the best results (Figure 6.10) for the COD 2 and COD 3, with the 180° rotation. Method M4 improves the detection of the end of the first 90° COD (COD 1), by using the same principle as method M2 of shifting the detected end by one local minimum.

While one cause behind the S.D. of COD event detection to range from 53 to 77.9 ms (Table 6.1) was the low frame rate of reference video, another important cause was the COD technique employed by the athletes. The athletes who "cheated" by crossing the legs during COD or the side shuffle were identified from video but not directly eliminated, since this phenomenon is difficult to address during routine testing in the field (Marshall et al., 2014). Regarding technique, almost all athletes used the same step pattern. The only exception is when the athlete places their first step too far from the cone. This forces the athlete to take a small extra step during the COD to be able to touch the cone. These extra steps are not considered in the labelled step pattern because they are not important, neither to brake nor to accelerate during the COD.

As explained in (Dayakidis & Boudolos, 2006; Glaister et al., 2008; Nedergaard et al., 2014; Welch et al., 2021), the COD motion implies an important antero-posterior (AP) and medio-lateral (ML) acceleration impulse on the ground and on the trunk to decelerate and then accelerate the body in the new direction. These impulses measure the change in momentum (or more precisely a change of velocity) during a COD, and that

this motion at high velocities will require a larger change of momentum than straight displacement. These AP and ML impulses were clearly observable in the IMU signal and were enclosed by the labeled step events defining the change of direction. The detected AP acceleration impulse (Figure 6.5) was positive for each COD, even though COD angle and technique exhibit large differences on the video recordings. This is likely because of the positive reaction force in AP direction created by the braking force on the foot of the athlete. For the same reason, local minimum before high peaks on the AP acceleration align with the impact of each step during every motion phase (Figure 6.5), despite the different motion techniques (shuffle, sprint forward, sprint backward). Before each COD, the first contact with the ground is synchronized with the first foot (local minima) of AP acceleration impulse. The toe-off instants following the COD are exhibiting a negative AP acceleration following the AP impulse. The likely explanation of this behavior is the straightening up of the trunk during the pushing phase at the end of the COD.

The error on phase duration has an absolute mean error smaller than 25 ms for all displacement phases, except for the backward run phase, which has a mean error of -135 ms. This larger error comes from both the error on the total duration of the test (between photocells time and video) and the choice to synchronize the signal and the video with the first step. This synchronization brings a bias because the athletes don't cross the starting line exactly at the same time. Some athlete crossed the starting line before their first step and others after. As the first step was considered as the beginning of the test in the IMU signal analysis, this creates an error on the end time of the test only. As seen in (Table 6.1), the mean relative error for motion phases is around 5%, but the standard deviation of the relative error for the COD duration is around 15%. This shows that the confidence in the computed COD duration using the algorithm can be improved. This likely because the COD duration is short (~ 500 ms), compared to the precision of the general method (~ 50 ms). To have a better confidence interval on COD duration, a more precise way to measure the ground contact time could be used, such as a force plates, IMU on the feet, pressure insoles, etc.

6.5.2 *Performance metrics*

Throughout the T-test, the duration of CODs did not correlate in any way with the duration of the test, with fast and slow athletes spending similar amount of time during COD (Figure 6.13), despite the time spent to change direction represents roughly 20% of the total T-test duration. Conversely, the duration of each displacement phase reflects better the performance of the T-test (total completion time). Therefore, it seems less useful to "rush" the COD movement to save time on the T-test, but better to focus on the speed during the displacement phases. However, this claim needs to be validated over a larger sample of athletes with varied skill levels. The COD duration can also be used as a measure of performance alone. For example, dribbling in football is a skill that requires rapid changes of direction, but where initial and run-up speeds need not be particularly high. While this skill cannot be accounted for in the traditional scoring method of the T-test, it can be assessed using the proposed algorithm. Another important outcome is the correlation between the total test completion and the total cutting time for each COD (Table 6.2). In other word, each of the four cutting performance

reflects the general T-test performance for elite athletes. This observation confirms the fact that T-test assess a mix of functional capacity in each displacement phase and that the difference in performance in elite athletes comes from each part of the test (Dos'Santos et al., 2019; Pauole et al., 2000; Young et al., 2015).

Approach velocity is an important factor affecting COD biomechanical requirements (Dos'Santos et al., 2018), with higher velocities increases lower limb stress and risk of ACL injury. A study (P. A. Jones et al., 2017) showed that a better performance (in terms of total cut time) had a higher velocity reduction during PFC. In (Hader et al., 2015), the researchers highlighted the fact that the ability to maintain a high velocity during COD may be critical to COD performance for 90° motion. Using the IMU data and the splitting algorithm described before, similar results were found for 180° COD. Fast approach velocity correlates with total cutting time for 180° cut ($R=-0.45$, $p=0.01$ for COD2 and $R=0.57$, $p=0.002$ for COD3). Interestingly, there is no correlation between approach speed and total cutting time for 90° tasks (COD1 and COD4). This shows that COD performance depends on the COD task. The main difference between 90° and 180° COD tasks is that athletes are forced to stop during a 180° COD while they can keep momentum during the 90° task. This is clearly observable by looking at minimum velocities during COD in Table 6.2 where athlete's velocities reach $\sim 3 \text{ ms}^{-1}$ during 90° and less than $\sim 1 \text{ ms}^{-1}$ during 180° COD. These observations show that angle and velocity influence the biomechanical demands of CODs and are critical factors for efficient execution of COD (Dos'Santos et al., 2018). A practical consequence of this is that using minimum velocity is a way to classify COD and to distinguish their angle (Slaughter & Adamczyk, 2020).

A typical pattern was observed for fast and slow athletes (Figure 6.14); faster athletes show a higher velocity drop just before or during the COD's. Also, a stronger acceleration after 180° cuts can be observed. This suggests that the ability to accelerate during shuffle phases is a key parameter of T-test performance. Interestingly, the minimum speed during the first 90° cut on COD is lower in fast athletes. This suggests that the ability to decelerate quickly is more important than absolute speed during the COD. These observations highlight the fact that the ability to perform a COD speed test depends not only on the COD itself, but also on the ability to accelerate and decelerate during the displacement phases. Consequently, data collection during these displacement phases could help to better understand cutting performance. In the future, this data collection could be easily implemented using the dataset from IMU and the proposed algorithm, and the findings about the velocity can be investigated further in a larger and more varied population.

Acceleration impulse (AI) is a characteristic variable reflecting the change in momentum during the COD. In this work, IMU is placed on the upper back. Therefore, acceleration impulse is linked to motion of the trunk too, which is known to be an important factor in the change-of-direction performance (Sasaki et al., 2011). The results (Table 6.2) show a larger AP acceleration impulse for the 180° cut than for the 90° cut. This result could be explained by the observation that athletes must perform a larger vertical displacement to touch the cones in COD2 and 3 than in COD1 and 4. ML acceleration impulse is negative for COD 1 and 3 and positive for COD 2 and 4, which makes

this metric reliable to assess the direction of COD for both 90° and 180° COD. The fact that the AI norm for the 180° cut is higher than for the 90° cut is probably related to the fact that the 180° cut forces the athlete to stop completely and thus experience a greater total change of momentum. The peak acceleration is an indicator of the impact on the athlete's back. The large impact and distance between the foot and the center of the body during COD result in a large adduction (and abduction) moment in the knee, which is known to be a critical factor in knee injuries (Mornieux et al., 2014). Therefore, limiting impact during COD is an important goal in a clinician's point of view.

Though peak acceleration is similar (Table 6.2) for each COD ($\sim 40[m/s^2]$), peak acceleration direction changes in depending on the COD type. The three COD (2,3,4) preceded by a shuffle displacement phase show greater impact in the AP direction than in the ML direction. Inversely, COD preceded by a straight sprint (COD 1) shows a bigger impact in the ML than in the AP direction. The athlete has the possibility to distribute the impact mainly in the approaching displacement phase direction, by distributing the deceleration phase between steps (Dos' Santos et al., 2019). The approach direction for COD 1 is AP, while that of COD (2,3,4) is ML, which explains the observations for peak acceleration. Similarly, anticipatory movement of the trunk can improve the COD performance by generating additional changes desired changes in momentum (Mornieux et al., 2014; Sasaki et al., 2011; Welch et al., 2021). For 90° motion (COD 1 and 4), the impact on the upper back is higher in the exit direction than in the approach direction. This shows that the athlete changes the direction of its momentum already during the first COD step. It could be interesting to see how this result varies if the COD direction is not pre-planned (less anticipation possible). Trunk-worn IMU data could thus bring enable a deeper quantitative analysis of anticipatory postural adjustments (APAs) during COD tasks.

6.5.3 *Limitations and future work*

The synchronization between video and IMU was done using first step of T-test, which can be improved by, asking the athlete to do an easily detectable movement (eg. standing jump) before the test. A better way to synchronize the photocells and the IMU signals would be to use a simultaneously detectable electronic pulse or obtain the precise UNIX or GMT timestamp for both systems. Similarly, knowing the precise GMT time of the photocell when it is triggered would be valuable, specifically to get a precise timing for the end of the T-test. Adding IMU on the feet would allow to differentiate right and left leg ground contact time (or PFC from FFC) and thus have data which is comparable to existing research from force plates. This would also allow investigation into how the impact on the ground is transferred to the trunk. Adding an IMU on the sacrum could help to get data which are more related to the lower limb and independent of the compensatory movement of the trunk. This addition of COD would be interesting if one want to precisely study the effect body position/loads on performance. However, to detect COD precisely, the single IMU on the back is sufficient. The single IMU on trunk worn in a vest, is commonly used in existing testing protocols and during competitive games by soccer players. Therefore, using the same sensor may allow easier application of the proposed methods in practice.

The micro analysis algorithm uses many external inputs such as relative thresholds, frequency range of reconstruction, or time window around COD. Therefore, a sensitivity analysis to external input can be carried out to improve the robustness of the algorithm. The maximum acceleration is taken on the 15Hz wavelet reconstructed to avoid nonrealistic peak acceleration values. The range of frequency of this reconstructed signal affects the maximum acceleration value (Wundersitz et al., 2013). Therefore, the exact correlation between maximum GRF and maximum IMU (in the upper back) reconstructed acceleration should be clarified in the future. The ML angular speed changes sign during COD because of the straightening of the chest after the athlete touches the cone. Because trunk motion correlates with COD cutting performance, ML angular velocity profile could provide a complementary method to detect COD. It may also provide a way to distinguish between the eccentric and concentric COD phases.

For velocity measurements, the validity of the GNSS ground speed during COD should be checked using traditional methods because its sampling frequency (10Hz) is low compared to the COD duration ($\sim 0.5s$). This also makes it difficult to detecting the end of the T-test by integrating GNSS signal and measuring the time taken to cover the known distance of the backward run. However, this limitation can be addressed by fusing the IMU and GNSS information, wherein the IMU can provide the necessary sampling rate and the GNSS speed can be used to correct the drift in the IMU-based speed (Apte, Meyer, et al., 2020) important source of variability in movement mechanics is the athlete population, with females demonstrating significantly less peak hip abduction than did males during COD maneuvers (Pollard et al., 2004). Thus, the proposed methods should be at least validated separately for female soccer players.

6.6 CONCLUSION

The proposed method can be used to determine the duration of the five displacement and detection of the COD events using a trunk-worn GNSS-IMU unit during a T-test. It uses the large anteroposterior change in momentum caused by the braking and acceleration phases of the COD to detect them. The Bland-Altman analysis for all COD events detected in the T-test shows a mean error of -0.03 ± 66 ms and a 95% confidence interval of ± 130 ms (3.9%), compared to reference data from video camera. Thus, the T-test were successfully divided into 9 phases, allowing coaches to better understand the athletes' technique and physical qualities during each displacement phase and COD types, and may prove to be a valuable performance evaluation tool for coaches. For example, the observation that total cutting time is correlated to the total completion or that the displacement phase duration could differentiate between the best/worst five performers, could be useful for identifying athletes' strengths and weaknesses. Furthermore, asymmetrical performance between displacement in the right and in the left detection can be highlighted, which can potentially provide information on the position on the field where the player will perform the best. Right and left asymmetries during COD duration could be sign of fatigue in one of the knees and/or an asymmetry in the strength of the muscles used for braking (Maloney et al., 2017). This information about can help the coach and the strength and conditioning staff to develop a more personalized training and rehabilitation program.

6.7 APPENDIX

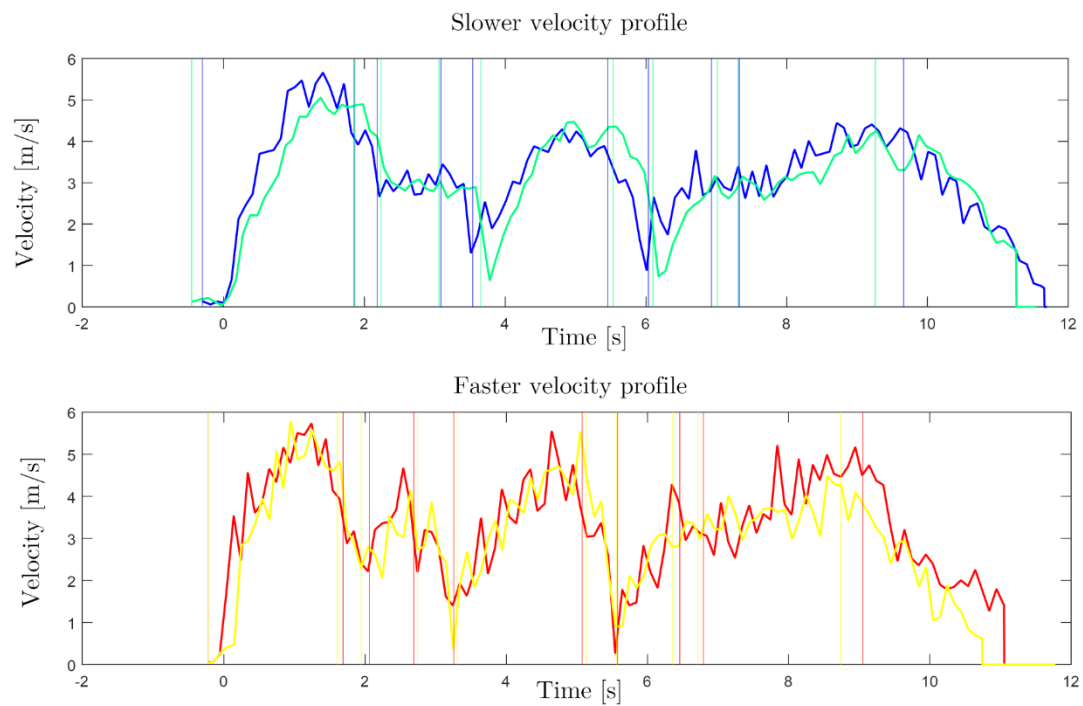


Figure 6.14 Velocity profile during the T-test for two fastest and slowest athletes. Vertical lines show the key events during the T-test (start and end of the COD, end of the T-test). The velocity profiles are aligned using the first step

7 BIOMECHANICAL CONTRIBUTIONS TO PERFORMANCE IN A COOPER TEST

Running mechanics are modifiable with training and adopting an economical running technique can improve running economy and hence performance. Running mechanics can be assessed accurately and conveniently using wearable IMUs. The proposed work extended this wearables-based approach to the Cooper test, by assessing the relative contribution of running biomechanics to the endurance performance. Furthermore, different methods of estimating the distance covered in the Cooper test using a wearable global navigation satellite system (GNSS) receiver were explored. Thirty-three runners (18 highly trained and 15 recreational) performed an incremental laboratory treadmill test to measure their maximum aerobic speed (MAS) and speed at the 2nd ventilatory threshold (sVT2). They completed a 12-minute Cooper running test with foot-worn IMUs and a chest-worn GNSS-IMU on a running track 1-2 weeks later. Using the GNSS receiver, an accurate estimation of the 12-min distance was obtained (accuracy of 16.5m and precision of 1.1%). Using this distance, MAS and sVT2 ($R^2 > 0.9$, RMSE $\in [0.07, 0.25]$ km/h) were estimated reliably. Biomechanical metrics were extracted using validated algorithm and their association with endurance performance was estimated. Additionally, the high/low performance runners were compared using pairwise statistical testing. All performance variables, MAS, sVT2 and average speed during Cooper test, were predicted with an acceptable error ($R^2 \geq 0.65$, RMSE ≤ 1.80 kmh⁻¹) using only the biomechanical metrics. The most relevant metrics were used to develop a biomechanical profile representing the running technique and its temporal evolution with acute fatigue, identifying different profiles for runners with highest and lowest endurance performance. This profile could potentially be used in standardized functional capacity measurements to improve personalization of training programs.

The contents of this chapter have been adapted from this article:

Apte, S., Troxler, S., Besson, C., Gremeaux, V., & Aminian, K. (2022). Augmented Cooper test: biomechanical contributions to endurance performance. *Frontiers in Sports and Active Living*, 337.

The appendix briefly summarizes this article:

Kammoun N., Apte, S., Karami, H., & Aminian, K. (2022). Estimation of temporal parameters during running with a wrist-worn inertial sensor: an in-field validation. *Proceedings of 2022 44th Annual International Conference of the IEEE Engineering in Medicine Biology Society (EMBC)*

Contributions: conceptualized the study design; conducted the in-field data collection; designed and implemented the algorithms; contributed to the analysis and interpretation of the data; drafted the manuscript; supervised the semester project that led to the results of the EMBC paper.

7.1 INTRODUCTION

Training prescription for runners is typically based on personal physiological capacity (Reilly et al., 2009), with training intensity determined by a certain fraction of variables such as maximal oxygen uptake ($\text{VO}_{2\text{max}}$), maximal heart rate (HR_{max}), or others, usually assessed during exercise with increasing intensity (Nes et al., 2013). Both physiological variables are indicators of cardiorespiratory capacity (S. Seiler, 2011). However, given the difficulty in measuring these variables in field training sessions, other metrics may be more convenient to use. For example, the maximal aerobic speed (MAS), i.e., running speed when $\text{VO}_{2\text{max}}$ is reached, is commonly used to prescribe training intensity (Berthoin et al., 1994). Another approach for prescription of training intensity is to use zones near the ventilatory threshold (VT) and/or lactate threshold (LT) because they represent the submaximal response of the individual athletes and indicate their ability to sustain a high fraction of $\text{VO}_{2\text{max}}$ for an extended period of time (Bassett, 2000). Athletes exhibit different levels of lactate accumulation for the same fraction of $\text{VO}_{2\text{max}}$, so using thresholds instead of $\text{VO}_{2\text{max}}$ may produce less interindividual variation in metabolic response and create a more homogeneous training stimulus (T. Mann et al., 2013). An important reason for using VT is polarized endurance training (PET), which is based on a training that is mostly below the first VT (VT1) and 10–20% being at/and above the second VT (VT2) (Muñoz et al., 2014). PET may increase positive adaptation to training stimuli and reduce the risk of overtraining, chronic fatigue, and injury (Muñoz et al., 2014; Wolpern et al., 2015). Evidence shows that elite endurance athletes perform their training mainly below VT1/LT1 and/or clearly above the VT2/LT2, thus highlighting the importance of these thresholds in training (Haugen et al., 2022).

The gold standard for measuring $\text{VO}_{2\text{max}}$ and VT2, and consequently the MAS and speed at VT2 (sVT2) is a treadmill test in the laboratory with gas exchange analysis (Bellenger et al., 2015). However, such a test requires highly trained personnel, is expensive, and only one person can be tested at a time. To overcome these constraints, it seems attractive to develop and conduct simple field tests that do not require extensive equipment, are inexpensive and can be integrated into athletes' routines. In these tests, measurement accuracy is partially sacrificed in favor of ease of use and potential for repeatability throughout the season for multiple athletes simultaneously. An example is the Cooper field test (Cooper, 1968), which is used to estimate $\text{VO}_{2\text{max}}$ based on the total distance run. It is a simple test that involves 12 minutes of track running with self-paced maximal effort, and provides a good assessment of $\text{VO}_{2\text{max}}$, MAS, and a reasonable prediction of half marathon time (Alvero-Cruz et al., 2019). Although incremental treadmill testing has been used to predict VT using portable near-infrared spectroscopy (NIRS) (Rodrigo-Carranza et al., 2021) or portable heart rate monitor (Gronwald et al., 2020), to our knowledge there is currently no simple field test for predicting sVT2.

The performance of long-distance runners depends not only on the $\text{VO}_{2\text{max}}$ and the ability to maintain a high fraction of $\text{VO}_{2\text{max}}$ during running, but also on running economy (RE) (Folland et al., 2017; Moore, 2016; Preece et al., 2019). RE is the metabolic energy expenditure for a given speed during submaximal running and can vary by up to 30% among runners with a similar $\text{VO}_{2\text{max}}$ (J. T. Daniels, 1985; Morgan et al., 1989). Running mechanics determine the mechanical power and propulsion produced for a given en-

ergy expenditure, thus influencing RE. Running biomechanics during ground contact, particularly during the propulsive phase, show a strong correlation with RE during treadmill running (Beattie et al., 2014; Moore, 2016; Saunders et al., 2004). Measuring RE during field running requires the use of a portable gas analyzer, which is expensive and impractical, whereas field running biomechanics can be accurately and conveniently assessed using wearable inertial measurement units (IMUs) (Benson et al., 2018; Buckley, O'Reilly, Whelan, Farrell, et al., 2017; Strohrmann, Harms, Kappeler-Setz, & Troster, 2012). The use of an economical running technique can improve RE and thus performance (Moore, 2016; Saunders et al., 2004). Therefore, evaluating running biomechanics during a field capacity test could greatly improve endurance performance information and help identify the biomechanical factors that contribute to endurance performance.

Research in this direction has mainly focused on differentiating between highly experienced and inexperienced runners based on their running technique. Clermont et al. and Carter et al. used data from IMU, collected using fixed-speed treadmill protocols (Carter et al., 2022; Clermont, Phinyomark, et al., 2019). Preece et al. extended this approach to running overground over a distance of 32 m at four different fixed speeds and analyzed the running kinetics and kinematics at three different steps during the run (Preece et al., 2019). While these studies showed promising results and highlighted important biomechanical characteristics of high-performance runners, they did not account for the natural variability (Meardon et al., 2011; Mo & Chow, 2018a) and asymmetry (Beck et al., 2018; Radzak et al., 2017) that occur at self-selected speeds, nor did they consider the effects of fatigue when running longer distances (Prigent et al., 2022), which are common in field tests of endurance capacity. The use of wearable IMU and global navigation satellite systems (GNSS) has shown promise in the improvement and augmentation of field testing for countermovement jump (Picerno et al., 2011), single-leg hop (Ahmadian et al., 2020), sprint (Apte, Meyer, et al., 2020), balance (W. Johnston et al., 2016), and so on. This chapter aimed to extend this wearables-based approach to the Cooper test by evaluating the relative contribution of running biomechanics to the endurance performance. In addition, it investigated whether the use of biomechanical parameters improves the prediction of MAS and sVT2 during the field test and explores different methods for estimating the distance covered in the Cooper test using a wearable GNSS.

7.2 MATERIALS AND EQUIPMENT

7.2.1 *Participants and study design*

Measurements were conducted with 18 highly trained (18 males, age 27.7 ± 5.4 years; height 178.8 ± 4.8 cm; weight 69.6 ± 10.1 kg; personal best below 90 minutes for a half-marathon) and 15 recreational runners (5 females, 10 males, age 31.5 ± 5.9 years; height 173.7 ± 9.9 cm; weight 67.8 ± 14.7 kg), all runners having an age between 18 – 50 years. To recruit highly trained runners, if there was no time reference in this distance, we classified the participants based on their personal best on 10km or 5km with the Riegel Formula's half marathon time estimation (23). The university human research ethics committee (HREC 039-2018) approved the study and all participants provided written

consent before the data collection. Participants performed an incremental laboratory treadmill test to measure MAS and sVT2. 1-2 weeks later, they completed a Cooper running test with wearable sensors on a running track.

7.2.2 Laboratory test

Prior to the lab test, participants were instructed to have no meals 2 hours before the test, and not have performed intense training 48 hours prior to the test. Height and weight of the participants were measured before they performed a maximal incremental running test on a treadmill (Pulsar, HP Cosmos, Nussdorf-Traunstein, Germany), while wearing a mask for Cortex Metalyzer 3B gas exchange analyzer (Cortex Biophysik GmbH, Leipzig, Germany) and a heart rate belt (H10, Polar Electro OY, Kempele, Finland) on the chest. For the highly trained group (Figure 7.1A), the testing protocol involved 3 minutes of rest, a 5-minute warm-up at 9 kmh^{-1} , followed by an increase in the speed of 1 kmh^{-1} every minute until 14 kmh^{-1} , and finally an increment of 0.5 kmh^{-1} every minute until volitional exhaustion. For the second group (Figure 7.1B), the protocol involved a 7 kmh^{-1} start, followed by increments of 0.5 kmh^{-1} . Oxygen consumption (VO_2), carbon dioxide production (VCO_2), ventilation (VE), and heart rate (HR) were measured continuously throughout the test. Participants were provided encouragement throughout the test to ensure attainment of maximal effort.

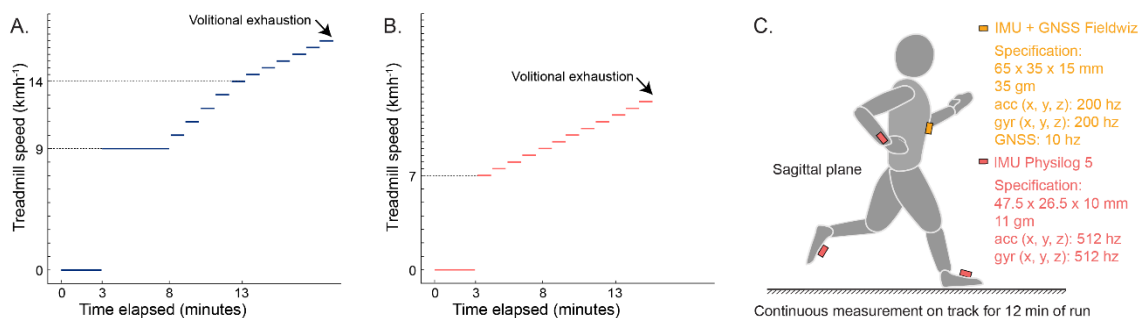


Figure 7.1 Protocol and sensor setup for the 12-minute field test, (A) Incremental speed protocol till volitional exhaustion for highly experienced runners (B) Incremental speed protocol till volitional exhaustion for amateur runners (C) sensor configuration for field measurement; IMU, inertial measurement unit; GNSS, global navigation satellite system; acc: accelerometer; gyr: gyroscope

Maximal effort was controlled according to the following criteria: plateauing of the VO_2 -speed relationship with VO_2 increasing by $<2\text{ ml}\cdot\text{kg}^{-1}\cdot\text{min}^{-1}$ despite speed increase, a peak respiratory exchange ratio (RER) >1.10 , or peak HR within 10 beats min^{-1} of the age-predicted maximum. Gas exchange variables were averaged on 20 sec. The speed value at which the VO_2 plateau began was considered as MAS. Second ventilatory threshold (VT2) was determined according to 3 criteria (Beaver et al., 1986; Cerezuela-Espejo et al., 2018) by an experienced exercise physiologist: 1) increase in both respiratory equivalent (VE/VO_2 and VE/VCO_2), 2) a decrease in PETCO_2 , 3) a loss of linearity from VE/VCO_2 plots. The speed attained at VT2 was considered as sVT2.

7.2.3 Field test

After 10 minutes of warm-up, participants were equipped with an IMU (Physilog 5, Gaitup SA, Switzerland) on each foot, right wrist, and a GNSS-IMU sensor (Fieldwiz, ASI, Switzerland) on the chest using a belt with electrodes (Polar Pro Strap, Polar Electro Oy, Finland). The wrist-worn IMU is not relevant here, but was used to investigate the possibility of estimating the temporal gait parameters using only wrist-worn IMU signals. A short overview of this study (Kammoun et al., 2022) is provided in the appendix of this chapter. Apart from the sensor setup (Figure 7.1C), the participants dressed as they would for an endurance running race. The Fieldwiz and Physilog 5 wearable sensors were chosen because they have already been used successfully for continuous analysis of running in the field and do not hinder the running movement (Prigent et al., 2022). Fieldwiz was used with a sampling frequency of 200 Hz for the IMU, 250 Hz for the ECG, and 10 Hz for the GNSS receiver. The ECG was not utilized as the focus of this study was on biomechanical contributions to endurance performance. The Physilog 5 IMU was sampled at 512 Hz, with a range of ± 16 g for the accelerometer and $\pm 2,000$ deg/s for the gyroscope. The participants ran on a 400m tartan track for 12 minutes and were instructed to cover highest distance possible. They were asked to rate their perceived fatigue from 1 to 10 before/after the run using the rating of fatigue (ROF) scale (Micklewright et al., 2017), which considers 1 as no fatigue and 10 as maximal. The participants performed the test in groups of 2-4 to increase their motivation. Two instructors provided verbal encouragement, supervised the test, and calculated the total distance covered in 12 minutes by counting the number of 400m laps and the meters covered in the final lap. The distance (D_{ref}) was measured by considering the closest scale on the track, which provides a resolution of 10m and are usually used to measure distance during training.

7.3 METHODS

7.3.1 Preprocessing and parameter estimation

The pre-processing steps include synchronization of the sensors and segmentation of the Cooper test run (Figure 7.2) for each participant. To synchronize the Fieldwiz and Physilog 5 sensors, a shock movement was performed before and after the 12-minute run. This movement consists of a quick up and down movement on the vertical axis while holding all sensors together (Caruso et al., 2019). Since the same acceleration data was recorded on both sensors, we computed the lag between their acceleration signals with cross-correlation and used this lag to adjust their timestamps. Segmentation of data for each participant was done based on the magnitude of acceleration norm from the IMU on the right foot, the ground speed data from GNSS and the known duration of 12 minutes. Outliers that were more than two standard deviations away from the mean value over a 1-minute sliding window, were removed from the GNSS ground speed signal and replaced them with linearly interpolated values. The 12-minute run was segmented into individual gait cycles using the angular velocity values of the right foot at mid-swings, following a validated algorithm (Falbriard et al., 2018). For each gait cycle, the gait temporal parameters like contact time (CT), flight time (FT), swing time (ST), and gait cycle time (GT), and kinematics parameters such as peak swing ve-

locity of the foot (PSV), foot strike angle in sagittal plane (FSA), and foot eversion angle (FEA) at initial contact (Falbriard et al., 2018, 2020), were estimated.

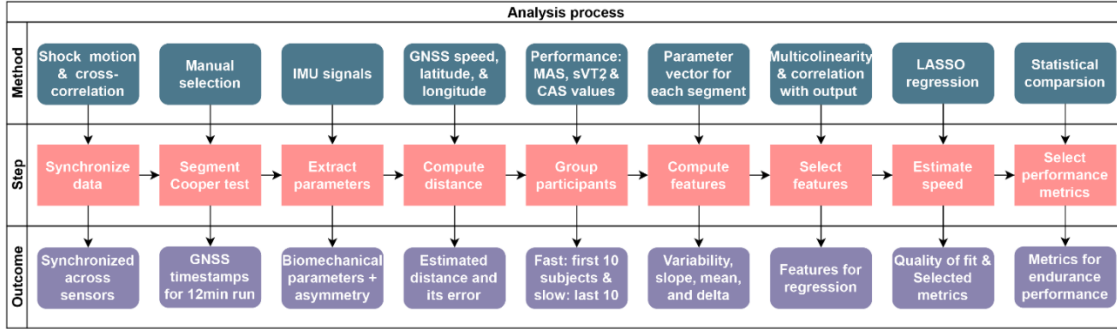


Figure 7.2 Flowchart of the overall procedure for selection of metrics; LASSO: Least least absolute shrinkage and selection operator; CAS: Average speed during the test

Duty factor (DF) is one of the main descriptors of running style, which we estimated as the percentage ratio of CT to GT (Alexander, 1991) for every gait cycle. Due its importance for efficient storage and return of elastic energy (da Rosa et al., 2019), the vertical stiffness (VS) was computed using the spring-mass model gait model (J.-B. Morin et al., 2005). Meyer et al. have presented the computation of the above-mentioned parameters in detail (Meyer et al., 2021b). Fatigue influences asymmetry of gait spatio-temporal parameters (Apte, Evian, et al., 2022) and thus, to understand its influence on endurance performance, the asymmetry was quantified using the symmetry index (SI):

$$SI = 2 \times \frac{|X_L - X_R|}{(X_L + X_R)} \times 100\% \quad (7.1)$$

where X_R and X_L are parameters for the right and left limbs. The SI was first computed for the gait cycle time to check the validity of the SI, as the cycle time should present a SI close to zero. Following that, SI was used with four gait parameters – contact time (CT_{SI}), flight time (FT_{SI}), swing time (ST_{SI}), and peak swing velocity (PSV_{SI}), based on their evolution with acute fatigue during endurance running (Apte et al., 2021; Prigent et al., 2022). All the computations were done using MATLAB R2020b and the plots showing the evolution of biomechanical parameters and running speed during the Cooper test were created using the Gramm package (Morel, 2018) and smoothing (Eilers, 2003) for averaging the trajectories.

7.3.2 Extraction of metrics

To address the influence of accelerating at the beginning of the test and strategy of exerting higher near the end of the test, the first and last minute of the data was removed from subsequent analysis. Within those 10 minutes, for each biomechanical parameter, five different *time segments* (Table 7.1, Figure 7.1) were considered for extraction of metrics:

- Total (t): all 10 minutes
- Steady (sy): running at the middle (Minute 5th to 8th) of the test
- Start (s): first minute of the remaining 10 minutes
- End (e): last minute for the same
- Delta (d): difference between the values for the start and end segments.

For all time segments, three features were extracted – mean (μ): arithmetic mean of parameter values over one time segment, variability (σ): standard deviation of parameter values over a window of 10 gait cycles and the arithmetic mean of these windows over a time segment, and slope (m): ratio of the difference between the last and the first parameter values of a time segment and the length of the time segment. Mean (μ) and slope (m) features were computed for all biomechanical parameters, whereas, variability (σ) only for the first nine parameters and not asymmetry parameters. Following this method, we obtained a total of 175 metrics using 13 biomechanical parameters, five segments of time, and three features. For example, μVSt denotes “Mean feature (μ) of vertical stiffness (VS) for Total time segment (t)”. For each parameter (except asymmetry), one value per gait cycle for the left and right foot was computed, but only the information from the right foot was used for the extraction of metrics.

Table 7.1 List of biomechanical parameters (units) extracted using the data from foot IMU sensors, the features computed on these parameters, and the time segments over which they are computed. An example notation for one metric is provided in the last row.

Biomechanical parameters	1. Contact time (CT) (ms), 2. Flight time (FT) (ms), 3. Swing time (ST) (ms), 4. Gait cycle time (GT) (ms), 5. Vertical stiffness (VS) (kNm^{-1}), 6. Foot strike angle (FSA) ($^{\circ}$), 7. Foot eversion angle (FEA) ($^{\circ}$), 8. Peak swing velocity (PSV) ($^{\circ}\text{s}^{-1}$), 9. Duty factor (DF) (%) 10. CT asymmetry (CT_{SI}) (%) 11. FT asymmetry (FT_{SI}) (%) 12. ST asymmetry (ST_{SI}) (%) 13. PSV asymmetry (PSV_{SI}) (%)
Features	1. Mean (μ), 2. Variability (σ) – not for asymmetry parameters, 3. Slope (m)
Time segments	1. Total (t): Minute 2 nd to 11 th , 2. Steady (sy): Minute 5 th to 8 th , 3. Start (s): 2 nd minute, 4. End (e): 11 th minute, 5. Delta (d): 11 th minute – 2 nd minute
Metric example	Mean feature of vertical stiffness for Total time segment: μVSt

7.3.2.1 Categorization

In addition to physiological aspects, performance during endurance running depends on the RE, the ability of runners to efficiently translate metabolic energy into mechanical work, and the capacity to sustain an efficient running technique over a relatively long duration (Folland et al., 2017; Moore et al., 2019; Preece et al., 2019). Based on these findings, the above-mentioned 175 metrics were divided into five different categories, with the goal of understanding the relative contribution of each category to the endurance performance:

- *Technique*: It is set of metrics that describe the running technique. Low vertical oscillation and thus, VS, has been linked to a better RE (Moore, 2016; Zhang et al., 2021), relative durations of CT and FT have been used to classify runners into terrestrial/aerial (Gindre et al., 2015), FSA and FEA directly influence the direction and magnitude of impact force on initial contact (Hoenig et al., 2020; Lieberman et al., 2010; Muniz-Pardos et al., 2018), and the DF is considered as an important independent descriptor of running style (van Oeveren et al., 2021). Thus, only the mean feature (μ) for CT, FT, VS, FSA, FEA, DF for all time segments except Delta was considered in this category.
- *Regularity*: It is category of metrics that quantify the variability of gait and includes only the variability feature (σ) for all parameters except asymmetry, across all time segments except Delta. Variability of stride has a functional pur-

pose, considered to offer flexibility of adaption to task and environmental constraints (Hausdorff, 2007). Stride time variability has been previously studied to investigate differences in trained and non-trained runners (Nakayama et al., 2010), and also to investigate the influence of acute fatigue (Gindre et al., 2015; Mo & Chow, 2018a).

- *Asymmetry*: As the name implies, this set of metrics quantify the asymmetry of gait cycles, using only the mean feature (μ) for CT_{SI} , FT_{SI} , St_{SI} , and PSV_{SI} , across all time segments except Delta. A 10% increase in CT_{SI} can lead to a 7.8% increase in the metabolic cost of running (Beck et al., 2018) and increasing asymmetry has been linked to overuse injuries due to increase kinetic demands (Radzak et al., 2017).
- *Fatigue*: Acute fatigue has an adverse effect on technique during prolonged running, by increasing the CT, DF, reducing FSA, VS, and so on (Apte et al., 2021; Meyer et al., 2021b; Prigent et al., 2022). The ability to maintain an efficient running technique for a longer duration can thus improve the endurance performance. To quantify this ability, for all parameters, the μ , σ , and m features for Delta time segment and the slope feature (m) for other segments, were used.
- *Pace*: The last category is comprised of metrics that quantify the rate of movement and did not fit into the previous four categories. Though the gait cycle time (cadence) is not necessarily linked to efficiency of technique or fatigue resistance, it is often used for performance evaluation and manipulation of running speed via different pacing strategies (Hauswirth & Brisswalter, 2008; Musgjerd et al., n.d.). In addition to μ feature for GT, the μ feature for ST, and PSV for all time segments except Delta, were included in this group.

7.3.3 Selection of metrics

To select the metrics that contribute to endurance performance, three performance variables were considered, the MAS and sVT2 obtained in the lab measurements, and the average speed during the Cooper test (CAS). Unlike the VO_{2max} , it is convenient to prescribe and measure training intensity in terms of MAS and sVT2 due to the ease of measuring speed in the field. Use of CAS instead of total distance allows the use of same units (kmh^{-1}) and similar magnitude across the performance variables, thus enabling a reasonable comparison for the errors in their prediction. To streamline the number of metrics, each metric was normalized using z-score normalization across 33 participants and the normalized metrics were tested for their Pearson correlation with each other. Within metric pairs showing a correlation coefficient above 0.95, the metric computed over a larger time segment was retained. Using this multicollinearity property (Mansfield & Helms, 1982), the number of metrics was reduced. To further reduce the metrics, their Pearson correlation coefficient (r) was computed in relation to MAS, sVT2, and CAS, and only the metrics with $r \geq 0.3$ were retained for the final modelling step.

To investigate the combined predictive power of the biomechanical metrics and D_{ref} , the MAS and sVT2 were estimated using linear regression, once using D_{ref} and once with the D_{ref} and the biomechanical metrics selected in the previous steps. To understand the relative contribution of biomechanical metrics to endurance performance, the

same process was repeated for MAS, sVT2, and D_{ref} with only the biomechanical metrics, using the Least absolute shrinkage and selection operator (LASSO) method for metric selection (Hastie et al., 2001). This is a forward-looking selection for linear regression, which enables interpretability of the model and can also enhance the prediction accuracy. Using leave-one-out-cross-validation with the LASSO method (Shao, 1993), the coefficients for each metric for prediction of the three performance variables were estimated. Within the results of the LASSO method, the coefficient vector with the least number of non-zero coefficients that led to an error of one standard deviation higher than that of the minimum mean square error (Hastie et al., 2001), was selected. This led to a minimal model with a reasonable level of accuracy in prediction and reduced the chance of overfitting (Loh, 2011). Among the metrics with non-zero coefficients, those with a relative weight of less than 5% of the total sum of weights were removed due to their minimal importance. Furthermore, the absolute weights of variables within the same category were summed to quantify the relative contribution of each category to the regression model. The prediction results of all the regression processes are presented in terms of the cross-validated determination coefficient (R^2) and the root mean square error (RMSE) in kmh^{-1} . R^2 determines the degree of association between predicted and actual performance variables, and the RMSE quantifies the difference between them. The overall process is illustrated in Figure 7.3.

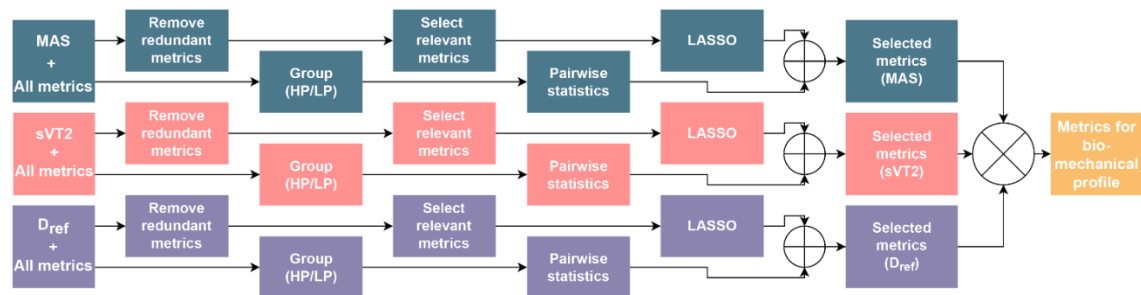


Figure 7.3 Procedure for selection of performance metrics for the biomechanical profile

Non-linear shifts in gait parameters have been observed with the increase in speed, possibly related to a transition to a sprinting-like technique (Burns et al., 2021) at high speeds. To consider these non-linear transitions and complement the selection of metrics through linear methods, statistical analysis was conducted to investigate the differences between the 10 highest (HP) and 10 lowest (LP) performing participants according to MAS, sVT2, and D_{ref} . The reason for considering all three factors separately is that the participants comprising HP and LP may differ depending on the considered performance variable. The metrics selected using multicollinearity were compared using a pairwise Welch's t-test with the statistical significance set at $p < 0.05$. It was preferred over the Student's t-test due to unequal variances for the fast and slow groups (Ruxton, 2006). The effect size was calculated using the same formulation as Cohen's d (Gignac & Szodorai, 2016). For every performance variable, the metrics that were selected through LASSO and those with statistically significant differences were combined (union of sets). Following this, an intersection of these three (MAS, sVT2, and D_{ref}) sets was used to select metrics that contribute mainly to the endurance performance and a visual profile representing these metrics and their respective categories

was developed. To illustrate its utility, the five highest and five lowest performing participants according to their MAS and sVT2 were represented on this profile.

7.3.4 Distance estimation

Cooper test uses the total distance D_{ref} (in km) covered in 12 minutes to estimate the $\dot{V}O_{2\text{max}}$ ($\text{ml.kg}^{-1}.\text{min}^{-1}$) and MAS as follows (Bandyopadhyay, 2015; L. Léger & Mercier, 1984):

$$\dot{V}O_{2\text{max}} = 22.351 \times D_{\text{ref}} - 11.288 \quad (7.2)$$

$$\text{MAS} = \frac{\dot{V}O_{2\text{max}}}{3.5} \quad (7.3)$$

Since the MAS estimation is directly dependent on the distance, it is important to estimate the distance accurately. The reference value for this distance (D_{ref}) corresponds to the distance measured at the 10m markers on the track. Five different methods were used for estimating the distance (Figure 7.4) and compared them to the reference (D_{ref}) using Bland-Altman analysis, Mean Absolute error (MAE), and percentage (Median \pm IQR) error. We computed the percentage error for every method across all participants. Below is a brief description of each method:

- Strapdown integration of the ground speed obtained from the GNSS receiver with outliers removed, and total distance at the end of 12 minutes was considered as total distance (D_s).
- Using the Haversine formula (Robusto, 1957) with the latitude and longitude coordinates from the GNSS sensor, and distance at the end of test was considered as total distance (D_c).
- The average distance (d_a) between the peaks on the latitude signal was assumed to be the time required to complete one lap. This was followed by estimating the number of laps by counting the number of peaks (n_p) and length of signal (l_s) outside the peaks was computed. Since the length of one lap is 400m, the total distance was computed as:

$$D_L = (n_p - 1) \times 400 + \frac{l_s}{d_a} \times 400 \quad (7.4)$$

- Combination of the first and third method, by counting the number of laps using peak detection and using strapdown integration of ground speed on the signal outside the peaks. The total distance (D_{LS}) is the sum of number of laps multiplied by 400 and the total distance on the strapdown integration before and after the first and last peaks, respectively.
- Combination of the second and third method, by counting the number of laps using peak detection and using Haversine formula with the coordinates on the signal outside the peaks. The total distance (D_{LC}) is the sum of number of laps multiplied by 400 and the distance obtained with the coordinates before and after the first and last peaks, respectively.

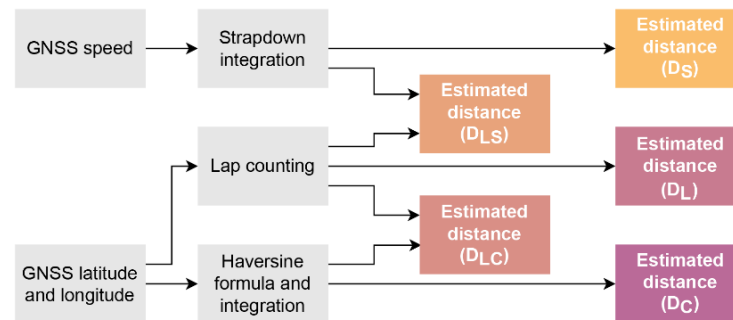


Figure 7.4 Methods for the estimation of distance covered over the 12-minute run

7.4 RESULTS

All 33 participants completed the 12 minutes of Cooper test with a maximal effort, reporting a ROF ≥ 8 at the end. Representative trajectories are shown in Figure 7.5A for participants grouped according to D_{ref} , with the latitude and longitudinal values aligning well with those of the track at the stadium. Participant's running speed (Figure 7.5B) generally decreased over 12 minutes of Cooper test, except for the first and last minute, which showed an increase. As expected, the HP (fast) group showed higher mean speed and a lower reduction in speed with time than the LP (slow) group. Figure 7.5C shows the performance of participants for the MAS, sVT2, and CAS, with the range of speeds being 9 kmh^{-1} to 21.5 kmh^{-1} and an average difference of around 7 kmh^{-1} between the top and bottom 10 participants for all three performance variables. However, the top 10 participants according to each variable different. The details on their performance can be found in supplementary material¹⁰

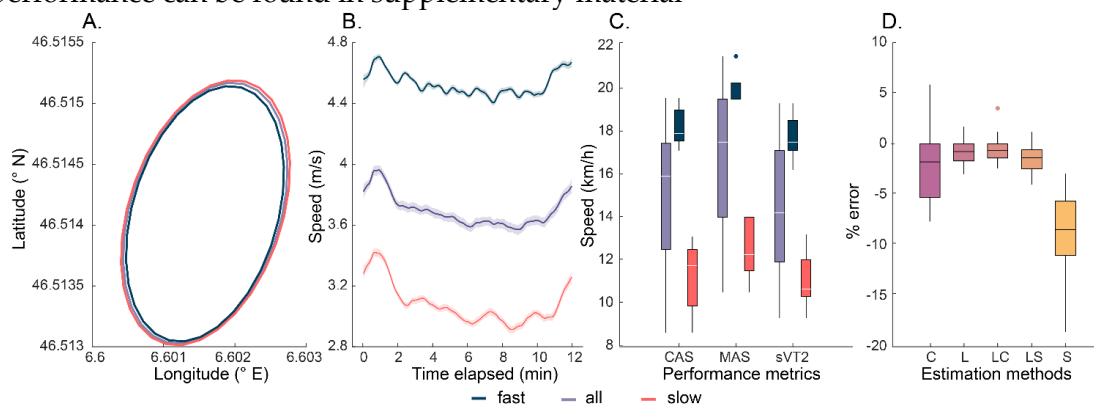


Figure 7.5 Performance of participants grouped according to D_{ref} and GNSS tracking. The smoothed mean of original profiles and the 95% confidence interval is shown for easier comprehension of their overall group trend and and plotted using the Gramm toolbox (Morel, 2018). A) Representative trajectory of the run during the Cooper test B) Representative speed profile of the participants during the Cooper test C) Xoxplot showing the median and interquartile range of performance across three speed variables D) Median and IQR of error in the estimation of distance using five different methods, with C, L, and S corresponding to methods based on Haversine formula with the GNSS coordinates, lap counting, and strapdown integration of ground speed. LC and LS refer to a combination of lap counting with methods based on ground speed and coordinates respectively.

¹⁰ <https://www.frontiersin.org/articles/10.3389/fspor.2022.935272/abstract>

7.4.1 Distance and speed estimation

The distance estimated using all five methods showed a median error of -0.6 to -8.4% (Table 7.2), with the strapdown integration of speed presenting the highest MAE (250 m) and the lap counting plus Haversine formula presenting the lowest (26.5 m) error. All three methods based on lap counting show a considerably lower IQR and CV for error, relative to the other two methods (Figure 7.5D). All the methods led to an under-estimation of the distance compared to the measurement (D_{ref}) with markings on the track. Results of the Bland-Altman analysis are provided in the supplementary material¹¹. Estimation of the MAS and sVT2 using the D_{ref} as predictor metric in linear regression led to R^2 values of 0.93 and 0.93 respectively, and RMSE of 0.91 kmh^{-1} and 0.88 kmh^{-1} respectively. Following linear equations were obtained:

$$\text{MAS} = 5.0629 \times D_{\text{ref}} + 1.5427 \quad (7.5)$$

$$\text{sVT2} = 4.6486 \times D_{\text{ref}} + 0.7878 \quad (7.6)$$

where MAS and sVT2 are in kmh^{-1} and D_{ref} in km. Bland-Altman analysis for the prediction of sVT2 using this equation is presented in the supplementary material¹². Adding the biomechanical metrics to the D_{ref} as additional predictor metrics marginally improved the prediction, with R^2 values of 0.93 and 0.93, and RMSE of 0.88 kmh^{-1} and 0.81 kmh^{-1} respectively for MAS and sVT2.

Table 7.2 Error rates for the five distance estimation methods. The mean absolute error (MAE) was obtained by subtracting each estimated distance from the reference value. The bias, coefficient of variation (CV), and the limits of agreement (LOA) were obtained through Bland-Altman plots.

Method	MAE (m)	MAE (%)	Bias (m)	CV (%)	LOA 1 (m)	LOA 2 (m)
D _s	250	8.9	-250	4.1	-30	-470
D _c	102.7	3.4	-83	3.7	120	-290
D _L	30.4	1.07	-17	1.2	49	-84
D _{LS}	43.5	1.6	-36	1.3	38	-110
D _{LC}	26.5	0.9	-16	1.1	44	-76

7.4.2 Selection of metrics

Using the method explained in 7.3.3 and Table 7.1, a total of 175 biomechanical metrics were obtained for the 13 biomechanical parameters. Apart from SI parameters, the evolution of other parameters during the run is presented in Figure 7.6. The number of metrics reduced from the 175 to 110 using multicollinearity, which were then used for statistical analysis and tested for correlation with the MAS, sVT2, and CAS. The final number of metrics for each performance variable were 33, 35, and 28 respectively. The cross-validated values for the fit of LASSO regression model for each performance variable are presented in Table 7.3. The model fits all variables with a $R^2 \geq 0.65$ and a

¹¹ <https://www.frontiersin.org/articles/10.3389/fspor.2022.935272/abstract>

¹² <https://www.frontiersin.org/articles/10.3389/fspor.2022.935272/abstract>

RMSE of $\leq 1.80 \text{ kmh}^{-1}$. The highest R^2 and lowest RMSE is for the MAS. The biomechanical metrics selected through LASSO method for each performance variable are reported in Table 7.3, with a positive coefficient value indicating a positive contribution to performance and vice-versa for negative values.

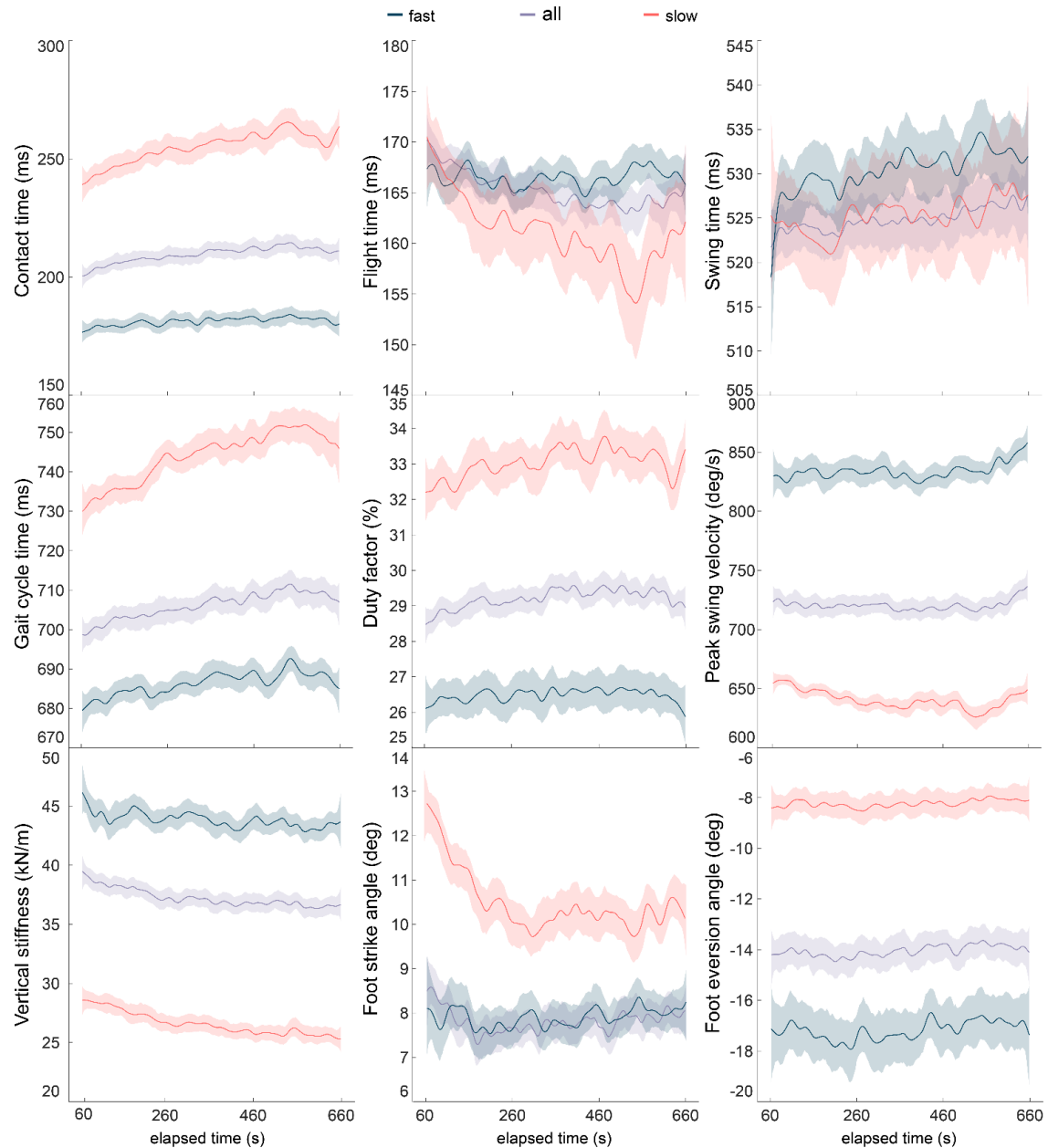


Figure 7.6 Profile for the biomechanical parameters during the Cooper test with participants grouped according to D_{ref} . The smoothed mean of original profiles and the 95% confidence interval is shown for easier comprehension of their overall group trend and plotted using the Gramm toolbox (Morel, 2018). Compared to the high performance group, the low performance group typically showed a larger change in all the parameter values over 10 minutes, except for swing time and foot eversion angle at initial contact.

Table 7.3 Biomechanical metrics selected through LASSO regression and statistical testing. Positive contribution denotes a positive coefficient obtained through the LASSO regression and vice-versa for negative contribution. Significant differences for pairwise statistical testing are indicated with * $p \in (0.01, 0.05)$, ** $p \in (0.001, 0.01)$, and *** $p \leq 0.001$

Performance variables	Fit quality		LASSO metrics	
	RMSE	R ²	Positive contribution	Negative contribution
MAS	1.62 kmh ⁻¹	0.75	μ VSt, μ PSVt, mSTt, mFSAt	σ CTd, μ CTt, σ CTt, σ GTt, σ GTs, μ CTd, mFTE, mFEAe, σ DFt, μ GTs, μ FEAt
sVT2	1.78 kmh ⁻¹	0.65	μ VSt, μ PSVt, σ FEAt, mVSe, mFSAt, mFTsy	σ GTs, σ GTt, μ DFt, μ GTs, σ CTt, μ FEAt
CAS	1.80 kmh ⁻¹	0.66	μ VSt, μ PSVt	μ GTs, σ CTt, μ CTt
Pairwise statistical testing metrics				
MAS	μ CTt**, μ GTt**, μ VSt**, μ FEAt**, μ PSVt**, μ DFt**, σ CTt**, σ FTt**, σ FEAt*, mFSAt*, mFTsy**, μ GTs**, μ FSAs*, σ CTs**, σ FTs*, σ GTs**, σ FEAs*, mPSVs*, σ CTe*, σ FTE**, mFEAe*, μ CTd*			
sVT2	μ CTt**, μ GTt**, μ VSt**, μ FSAt**, μ FEAt**, μ PSVt**, μ DFt**, σ CTt**, σ FTt**, σ FEAt*, mFSAt**, μ GTs**, μ FSAs**, σ CTs**, σ FTs*, σ GTs**, σ FSAs*, σ FEAs*, mFSAs*, μ FSAe*, σ CTe*, σ FTE**, mVSe*, μ FSAd*, μ CTd*			
CAS	μ CTt**, μ GTt**, μ VSt**, μ FEAt*, μ PSVt**, μ DFt**, σ CTt**, σ FTt**, mFSAt**, mFTsy**, μ GTs**, σ CTs**, σ GTt*, mFSAs*, σ CTe*, σ FTE*, μ CTd*			

The sum of coefficients for metrics belonging to the same category and their relative contribution is shown in Figure 7.7. All performance metrics present a different relative contribution for each category. MAS shows a similar contribution for fatigue (29.2%) and technique (31%) categories, but sVT2 (40.4%) and CAS (46.5%) show a dominant contribution of the technique category.

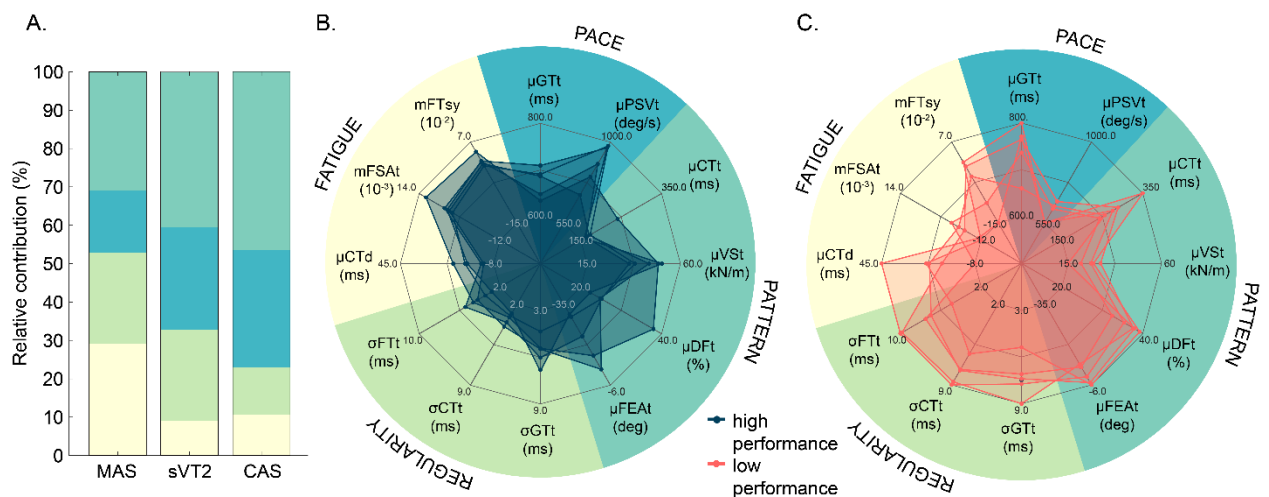


Figure 7.7 Selected metrics and their categories. Relative contribution of metric categories to each endurance performance variable. B. Biomechanical profile for top 5 (high performance) participants according to their MAS. C. Biomechanical profile for bottom 5 (low performance) participants according to their MAS.

Metrics showing a statistically significant ($p < 0.05$) difference between highest and lowest performing participants are also reported Table 7.3. The effect sizes can be found in the supplementary materials¹³. MAS, sVT2, and CAS led to the selection of different biomechanical metrics, with the highest number of metrics selected for MAS through LASSO regression and for sVT2 through statistical testing. The metrics common to each performance variable across both methods were selected and used to create a biomechanical profile for the participants. The metrics included on the profile are – i) Technique: μCTt , μVSt , μDFt , μFEAt ii) Regularity: σCT , σFT , σGT iii) Asymmetry: none iv) Fatigue: μCTd , mFSAt , mFTsy v) Pace: μGTt , μPSVt . Figure 7.7B and C show the profiles for the top and bottom 5 participants ranked according to their MAS respectively.

7.5 DISCUSSION

This work investigated the association between endurance performance quantified by three variables – MAS, sVT2, and CAS, and the biomechanical metrics measured during the performance of a Cooper test protocol. The selected metrics and the rationale behind their selection are discussed in this section. This is preceded by a short deliberation on the estimation accuracy of the distance ran during the test and the subsequent prediction of the three performance variables.

7.5.1 Distance and speed estimation

Estimating the distance using all three lap counting methods led to better precision than the methods using strapdown integration of speed and Haversine formula alone. The lack of precision or the higher IQR of the error is likely due to the bias and the noise in the GNSS ground speed and latitude/longitude signal. The integration of the data from these signals leads to signal drift, which can vary considerably across participants, leading to a higher IQR of error. The GNSS ground speed is typically estimated using the phenomenon of Doppler shift while the Haversine formula relies on the actual co-ordinates recorded by the GNSS (Hofmann-Wellenhof et al., 2012), which could explain the differences between the errors for the two methods. The lap counting methods reduced the impact of drift by restricting the strapdown integration to signals recorded in partial laps.

Compared to the MAE for state-of-the-art GNSS sport watches (Gilgen-Ammann et al., 2020), the MAE for lap counting methods was similar or lower. However, the sport watches were tested for one participant, over a maximum distance of 4296.9 m. While the GNSS sport watches underestimated the distance in urban and forest areas, they overestimated it on a running track. The authors (Gilgen-Ammann et al., 2020) attribute to this overestimation in unobstructed conditions (Ranacher et al., 2016) to a possible correction algorithm used by the manufacturers to compensate the general underestimation in difficult areas. In our situation, a general underestimation of distance by all five algorithms was observed. One reason could be the lack of correction in the sensors, since they were used in the ‘airborne <4g’ configuration of the uBlox GNSS chip.

¹³ <https://www.frontiersin.org/articles/10.3389/fspor.2022.935272/abstract>

Another reason could be the assumption that all laps have a length of 400 m (equation 7.4), which is lower than the actual distance for lane 2 (~407 m) and lane 3 (~415 m), which were used to compute the reference length during the Cooper test. The formula used in the lap counting algorithm can be updated to consider the lap length for a given lane (Aftalion & Martinon, 2019), thus reducing the underestimation of distance.

MAS was estimated accurately (R^2 0.91, RMSE 0.98 kmh⁻¹) with the Cooper test distance (D_{ref}) as a sole predictor (equation 7.5). This value of R^2 is comparable to those in literature for the prediction of VO_{2max} – 0.897 for the original study (Cooper, 1968), 0.87 to 0.93 for young males (Bandyopadhyay, 2015; Grant et al., 1995; McNaughton et al., 1998) and 0.72 to 0.83 in a systematic review (Mayorga-Vega et al., 2016) that determined the criterion validity of 12 min Cooper test to be moderate for predicting VO_{2max} . Though the addition of biomechanical metrics only improved the prediction slightly (R^2 0.93, RMSE 0.88 kmh⁻¹), it could prove to be more influential in case of studies with a larger and diverse set of participants. D_{ref} proved to be an accurate predictor of sVT2 (R^2 0.92, RMSE 0.84 kmh⁻¹) and addition of biomechanical metrics did not improve the prediction substantially (R^2 0.93, RMSE 0.81 kmh⁻¹). To our knowledge, this is the first study to estimate sVT2 using the 12-minute Cooper test. However, testing of this equation for a broader and larger set of participants is recommended. Estimation of sVT2 using a simple field test can enable its wider adoption for the design of threshold-based training programs and as a metric to measure the endurance capacity of athletes. Furthermore, estimation of sVT2 and MAS using field tests can facilitate studies which compare their predictive power for performance in endurance races and contrast their use in improving positive adaptation to training.

7.5.2 Selection of metrics

The biomechanical metrics selected via LASSO for MAS, sVT2, and CAS differ from each other (Table 7.3). Similarly, participants in the high/low performance groups selected according to the highest and lowest MAS, sVT2, and CAS values differed, and consequently, the metrics showed statistically significant differences. These results highlight the dissimilarity of the nature of information obtained from these variables, although they all quantify the endurance performance. For the same fraction of VO_{2max} arising out of training at a certain fraction of MAS, athletes may have different levels of lactate accumulation, and therefore training based on fraction sVT2 can lead to a more homogenous training stimulus (T. Mann et al., 2013). Both, MAS and sVT2 can be reliably and accurately estimated using D_{ref} (or CAS), as shown previously. However, D_{ref} (or CAS) also contains information about the efficient conversion of endurance capacity on the track, which is determined by the running biomechanics and the running economy (RE). One study has shown that the high aerobic capacity of Kenyan runners is not reflected in treadmill running, due to their lack of familiarity with and the resulting negative influence on RE (Saltin et al., 1995). The results highlight the importance of running technique, with the running technique making the highest relative contribution to the estimation of CAS (Figure 7.7 Figure 7.7 A).

The metrics selected within ‘technique’ category are: $\mu FEAt$, μCTt , μVSt , and μDFt . Mean foot eversion angle ($\mu FEAt$) had a negative contribution to MAS and sVT2, as

indicated by the LASSO coefficients (β) ranging from -0.26 to -0.02, with the faster runners having a higher inversion angle at initial contact. This result is consistent with previous studies that reported that an increase in running speed resulted in an increase in the ankle roll angle and thus the amount of external rotation (Muñoz-Jimenez et al., 2015; Orendurff et al., 2018). Foot roll before contact is lower in athletes with heel-strike and increases with midfoot and frontfoot strike (Lieberman et al., 2010), leading to a higher inversion angle at contact. Midfoot strike loads the calf and shin muscles similarly, thereby stabilizing the ankle; forefoot strike causes the outer part of the foot to strike the ground at contact, preloading the calf muscles and allowing for a quick push-off with a minimal contact phase (Almeida et al., 2015). A higher CT and FSA was observed in slower runners, thus indicating a tendency towards heel-strike. This tendency, in combination with the lower speed, may explain the lower inversion angles observed in slower runners.

All three performance variables were negatively related ($\beta \in [-0.39, -0.08]$) (Table 7.3) to mean contact time over 12 minutes (μCTt). The five fastest runners had a lower μCTt than the five slowest (Figure 7.7). μCTt and gait cycle time are negatively affected by the gait speed and thus a lower μCTt might be expected for faster runners, regardless of their technique. However, a lower mean duty factor over 12 minutes (μDFt) was also observed in the faster runners (Figure 7.7), and μDFt had a negative ($\beta \in [-0.37, -0.24]$) contribution (Table 7.3) to the performance variables. These findings highlight the fact that lower μCTt was due to running technique and not just the speed. Similar findings of lower μDFt and μCTt have been reported in treadmill running for the comparison between elite and highly-trained runners (Burns et al., 2021) for a speed range (10 – 24 kmh^{-1}) and a larger cohort of elite and well-trained runners at lower speeds 10 – 12 kmh^{-1} (Folland et al., 2017). It has been reported that 10-km performance while running on an indoor track equipped with a force plate is moderately negatively correlated with CT (Williams & Cavanagh, 1987). Previous research has also linked a lower CT and DF to better performance in terms of RE (Folland et al., 2017; Moore et al., 2019; Mooses et al., 2021; Nummela et al., 2007).

In contrast to CT and DF, mean vertical stiffness (μVSt) contributed positively to all three performance variables ($\beta \in [0.90, 1.2]$), and the fastest runners had a considerably higher μVSt than the slowest runners (Figure 7.7). Similar results have been reported for comparisons between elite runners, well-trained runners, and other (non-runner) athletes during treadmill running (Burns et al., 2021; da Rosa et al., 2019; Moore et al., 2019). For a comparable propulsive force, a higher VS results in a lower vertical excursion of the center of mass (COM) and a lower mechanical energy loss due to vertical oscillations. The relatively lower CT and higher VS indicate the ability of faster runners to better utilize the spring mass dynamics for efficient storage and release of elastic energy during the stance phase (Zhang et al., 2021). With a rise in speed, the contribution of the elastic energy to the running energy cost has been shown to increase (Alexander, 1991), increasing the importance of efficient recycling of elastic energy. Ground reaction forces (GRF) have a strong positive influence on running speed (Weyand et al., 2000), but likely increase the vertical oscillation of COM, which is negatively correlated with RE (Folland et al., 2017; Moore, 2016; Saunders et al., 2004). Higher vertical and

leg stiffness may reduce vertical oscillation while allowing for higher GRF, allowing higher speeds and better RE (Butler et al., 2003).

Within the ‘pace’ category, two metrics were selected: μGTt and μPSVt . Mean gait cycle time (μGTt) had a negative ($\beta \in [-0.45, -0.14]$) contribution to the three performance variables, whereas mean peak swing velocity (μPSVt) had a positive ($\beta \in [0.35, 0.72]$) contribution. Faster runners had much lower μGTt and higher μPSVt compared with slower runners (Figure 7.7). For a given stride length, a lower μGTt results in higher running speed and is associated with higher vertical stiffness, which is consistent with our results (Butler et al., 2003). Even a 10% increase in step rate results in a considerable reduction in loading in the knee and hip joints, improvement in RE, and a reduction in vertical excursion of COM (Heiderscheit et al., 2011; Musgjerd et al., n.d.; Quinn et al., 2021). An increase step rate results in more upright posture during stance, reducing the muscle forces needed during the loading-response phase of the gait cycle (Lenhart et al., 2014). Combining an increased step rate with a forefoot strike resulted in a greater reduction in joint impact loading than a midfoot or heel strike (Huang et al., 2019). The transition to a forefoot strike at a higher step rate was also reported to be easier than midfoot and heel strike in that order, which is consistent with our observation that faster runners report a lower μGTt and a tendency toward a midfoot and forefoot strike pattern. The lower μGTt increases the loading in the hip flexors muscles during the early swing because the trailing leg must be brought forward more quickly (Lenhart et al., 2014), possibly leading to an increased μPSVt . However, to decelerate the leg and position it for ground contact, the hamstrings and hip extensor muscles apply higher forces during the late swing phase. This indicates a higher capacity for positive and negative mechanical work in the thigh muscles for the faster runners.

The pace and technique categories primarily consider the mean values of the various biomechanical metrics. The acute fatigue developed during the Cooper test can affect the magnitude of the biomechanical parameters, so the fatigue category mainly considers the change in the mean values of the parameters. Within this category, three metrics were selected: μCTd , mFSAt , mFTsy . Slower runners showed a higher increase in mean contact time (μCTd) between the 2nd and 11th minute, indicating a limited ability to resist biomechanical changes due to fatigue. This is consistent with previous studies in which runners of different performance levels showed similar trends for the increase in CT with perceived acute fatigue (Prigent et al., 2022), but the magnitude of change in CT was higher in less trained runners. In the fatigue category, the FSA and flight time (FT) are reduced less in the faster runners than the slow runners (Figure 7.7), leading to a higher slope for the FSA (mFSAt) and FT (mFTsy) in faster runners. This is reflected in the positive ($\beta \in [0.07, 0.25]$) contribution of mFSAt and mFTsy ($\beta = 0.13$) to the estimation of sVT2 and MAS. Acute fatigue may decrease calf muscle preactivation, resulting in a decreased ability to absorb and return energy generated during impact and produce a lower push-off force (Apte et al., 2021). Increased CT to distribute the impact impulse over a longer duration, a tendency of footstrike moving away from forefoot (reduced FSA), and the reduced FT indicate fatigue in the calf muscle, with less trained runners unable to adapt to these changes and recover their running technique.

The regularity category of metrics quantifies the variability of running and therefore the following metrics were selected within this category: σ_{CT} , σ_{FT} , and σ_{GT} . The variability of CT (σ_{CT}), FT (σ_{FT}), and GT (σ_{GT}) had a negative contribution ($\beta \in [-0.47, -0.14]$) to the estimation of all three performance variables. The fast runners showed a lower variability (Figure 7.7) of temporal gait parameters over 10-step windows, although they had lower mean values for these parameters. Gait variability has been previously studied with novice, well-trained, and elite runners on a treadmill (Burns et al., 2021; Mo & Chow, 2018a; Nakayama et al., 2010), on a track (Meardon et al., 2011), and during a half-marathon (Apte, Evian, et al., 2022). Except for Meardon et al. who compared recently-injured and healthy runners, all other studies found an inverse relationship between gait variability and training level. An increase in temporal gait variability was associated with an increase in energy cost of running (Candau et al., 1998). In a longitudinal endurance training program, a reduction in stride rate variability and an improvement in RE were reported as outcomes, although participants' oxygen capacity changed only slightly (Slawinski et al., 2001). Thus, the lower values of σ_{CT} , σ_{FT} , and σ_{GT} during the Cooper test indicate a better RE for the faster runners.

7.5.3 Limitations and recommendations

The estimation of sVT2 in this study is based on a relatively small sample consisting predominantly of male subjects. The evaluation of the proposed equations (7.5 and 7.6) can be performed for a larger sample, with a better sex ratio, and possibly with nonlinear methods. Similarly, the well-trained runners were composed exclusively of male subjects, while the less trained group was a mixture of male and female participants. The results of the comparison between the five fastest and the five slowest runners (Figure 7.7) are therefore biased by the low sex ratio. Some differences in the regularity of running mechanics occurred when competitive and recreational runners were compared within male and female subjects (Clermont, Benson, Osis, et al., 2019). However, males and females with similar training levels have been reported to have similar values for RE ($\text{mlO}_2 \cdot \text{km}^{-1} \cdot \text{kg}^{-1}$) (J. Daniels & Daniels, 1992) and the energy cost of running when running at a similar intensity (Bunc & Heller, 1989). In this study, the spring-mass model was used to estimate VS (J.-B. Morin et al., 2005), based on the estimated values of FT and CT. Since VS showed the highest positive contribution for all performance variables, a direct estimation of VS using force plate measurements and motion tracking from COM may be a valuable follow-up study.

Reduction in the stability and smoothness of running movement, resulting from acute fatigue, has been linked to a surge in the energy cost of running (Kiely et al., 2019; Schütte et al., 2018). Using the IMU on the chest, it is possible to estimate the stability and smoothness of the trunk motion in real-world conditions (Apte, Laroche, et al., 2022) and extend the proposed biomechanical profile. Together with the variability of gait temporal parameters, the long-range correlations (LRC) for stride time can be investigated, indicating the adaptability of gait. Highly trained runners and elite runners have shown a higher adaptability, and the LRC have been associated with injury history (Meardon et al., 2011; Mo & Chow, 2018a). However, the interpretation of the LRC, stability, and smoothness is not obvious for the coaches and the athletes, these parameters were not included. Finally, the pre/post measurement of the subjective fatigue

(ROF) was used to ensure the maximal intensity for the Cooper test. Although the ROF scale correlates well with the biomechanical and physiological influences of acute fatigue (Prigent et al., 2022), it can be supplemented with a pre/post assessment of blood lactate.

7.6 CONCLUSION

In this study, we presented an accurate (MAE 16.5 m) and precise (error CV 1.1%) estimate of the 12-min distance with a chest-worn GNSS receiver, despite interindividual variations in track running trajectories. Using this distance, we showed a reliable estimate ($R^2 > 0.9$, RMSE $\in [0.07, 0.25]$ kmh⁻¹) of the MAS and sVT2, with reference values from the laboratory. Using the foot-worn IMU, we estimated several biomechanical metrics and assessed their contribution to the endurance performance. All performance variables were predicted with an acceptable error ($R^2 \geq 0.65$, RMSE ≤ 1.80 kmh⁻¹) when only the biomechanical metrics were used with the LASSO method. The metrics selected using LASSO and the statistical comparison were used to create a biomechanical profile representing the running technique and its temporal evolution. Within this profile, the selected categories can be used to characterize runners and identify their key strengths and weaknesses. Based on this, a training program can be developed to target specific aspects of running technique and provide the resulting profile to runners as post-training feedback. This profile can be tracked over a season to understand the development of running technique and the adaptation of runners to training. Profiles at the beginning and the end of a long-distance training session reflect the impact of fatigue, providing complementary information to internal training load metrics. This profile can provide coaches and athletes a deeper insight into the running mechanics and allow evaluation of intraindividual changes following training programs and rehabilitation after injury. Interindividual differences in the profile can be used to develop a tailored training program and monitor the improvement in the resulting running mechanics. Use of such a wearable system in standardized capacity measurements may open a new perspective for personalization of training and rehabilitation.

7.7 APPENDIX: RESULTS FOR ESTIMATION WITH WRIST-WORN IMU

Wrist-worn location offers more convenience compared to foot-worn IMUs and the additional potential to be integrated into a smartwatch (Erdem et al., 2019). Therefore, this study aimed to extend the estimation of temporal parameters for real-world running using wrist-worn IMU. The data from the highly-trained group for the 12-minute was used for this estimation and compared to the parameter values estimated with the foot-worn IMU, computed using previously validated algorithm (Falbriard et al., 2018). Peak detection on the angular velocity signal was used to first estimate the cycle time, followed by the extracted of features on windows containing 40 gait cycles. These features were used to train models based on convolutional neural networks, Gaussian Process regression, and Lasso regression. Lasso model performed the best, with the root mean square error for cycle time, swing time, flight time, and contact time being $0.27 \% \pm 0.1 \%$, $2.6 \% \pm 1.7 \%$, $7.3 \% \pm 4.9 \%$, and $10.6 \% \pm 5.5 \%$, respectively. Details of the proposed method and its results can be accessed in the published conference proceedings (Kammoun et al., 2022).

IV. CONCLUSION AND RECOMMEN- DATIONS FOR FUTURE WORK

8 CONCLUSION AND DISCUSSION

8.1 CONTRIBUTIONS

As discussed in Chapter 1, running technique is one of the critical factors explaining the differences in performance and economy between runners with comparable physical abilities. Training with proper running technique is essential to ensure positive adaptation to the training stimuli and thus improve performance, and to reduce the risk of injury. Fatigue has been shown to cause changes in running technique, such as shifting landing mechanics, increasing impact forces, decreasing knee flexion during landing, altering contact and flight times, etc. (Verschuere et al., 2020). Neither internal nor external training load metrics can provide information on the influence of fatigue on technique, thus making biomechanical assessment a unique independent descriptor of training sessions (Paquette et al., 2020). Running power, the amount mechanical work performed by the runner per unit time, can provide information into the relative force applied by the athlete at a given pace. Since an increase in applied force requires additional metabolic energy, a higher power output at a lower heart rate may be an indicator of higher running efficiency when performed on the same surface. Thus, running power can complement the description of running technique to describe performance during training sessions or races. Current conventional training framework does not consider all these factors and can therefore benefit from analysis of running biomechanics during training and functional capacity testing. In this context, performance during a training session can represent the proportion of training in which optimal technique and prescribed intensity were maintained despite fatigue.

The biomechanics of running can be altered through specific training, and an economical running technique can reduce the energy cost of running (per unit distance) (Moore, 2016). For example, in a longitudinal endurance training program using feedback on the variability of gait cycle, reductions in stride rate variability and energy cost were reported as outcomes (Slawinski et al., 2001, p. 20), although participants' oxygen capacity changed only slightly. At a similar running speed, loading forces and moments are influenced by body mass index (BMI), stride length, foot angle at ground contact, running shoes, running surface, etc. However, there is not one perfect running technique, but different techniques that are more efficient and less likely to cause injury depending on the length of the race, physical fitness, anthropometric features, etc. Thus, the biomechanical assessment must be customized for each athlete, preferably during field activities to maintain the ecological validity. Therefore, the objectives of the first part of this work were to identify reliable trends related to the fatigue state or onset of fatigue during running, measure them with wearable sensors, and estimate running performance and power with the same or a simpler sensor setup. The second part dealt with the personalized measurement of capacity using functional tests in the

field and the study of biomechanical relationships with functional capacity. Together with the capacity measured during testing, the biomechanics studied can help coaches determine appropriate training loads, with a focus on developing technique during a training and/or return-to-sport program.

8.1.1 *Part I: Biomechanical assessment for performance and fatigue analysis*

To identify reliable trends that represent the influence of fatigue on running movement, and the selection of meaningful metrics that encapsulate running technique, a two-pronged approach was considered in this thesis, i) A systematic review to investigate and coalesce results from fatigue protocols involving running ii) Continuous in-field measurements of the training for marathons and during the race, to reaffirm the trends obtained from the systematic review and to measure the changes in running technique due to fatigue. Chapter 2 documented a systematic review of literature and investigated the typical protocols used in research on biomechanical response to running-induced fatigue, the effect of sport-induced acute fatigue on the biomechanics of running and functional tests, and the consistency of analyzed parameter trends across different protocols. It presented evidence that acute fatigue influences almost all the included biomechanical parameters in running, with crucial influence from the exercise intensity and the testing environment. To the author's knowledge, this was the first systematic review to categorize study protocols according to fatigue intensity and synthesize trends for each category separately. Some parameters (step length, sagittal knee angle range of motion, max. knee flexion angle, etc.) presented different trends for different fatigue intensities, thus highlighting the importance of this categorization.

From the 42 parameters identified in response to acute fatigue, flight time, contact time, knee flexion angle at initial contact, trunk flexion angle, peak tibial acceleration, CoP velocity during balance test showed an increasing behavior. Whereas, cadence, vertical stiffness, knee extension force during MVC, maximum vertical ground reaction forces, and CMJ height showed a decreasing trend across different fatigue protocols. The findings reaffirmed the observations that acute fatigue causes a reduction in the maximal force production of the muscles and adversely affects the postural control ability, leading to a more compliant leg and a decreased attenuation of the impact force during each ground contact. This may partly explain the decrease in running efficiency and the increased likelihood of injuries arising from running while fatigued. The dominant metrics used for fatigue analysis were gait spatiotemporal parameters, while stationary sensor systems, treadmill activities, and endpoint measurements were the dominant modalities. The 68 included studies indicated an important gap in literature caused by the lack of field studies (only 22.1%) with continuous measurement (< 25%) during actual outdoor activities. Emerging technologies like wearable sensors could enable the design of such protocols, thus leading to a deeper understanding of the influence of fatigue on the biomechanics of the lower extremities. An outcome of this review is the proposal of a wearable sensor configuration based on three or four sensors, which will enable continuous in-field measurement of metrics that show a reliable response to acute fatigue. The potential of this sensor setup was successfully demonstrated in Chapter 3, with the concurrent assessment of running biomechanics and perceived fatigue during a half-marathon race.

Chapter 3 presented the assessment of the evolution of the biomechanical and psychological facets of running with acute fatigue during a half-marathon using a minimal wearable sensor setup. Spatiotemporal parameters for the running gait, along with the trunk stability, gait symmetry, variability and complexity were computed using validated algorithms and metrics chosen from literature. During the race, contact time, duty factor, and trunk anteroposterior acceleration increased, and the foot strike angle and vertical stiffness decreased significantly. Both stability and smoothness decreased significantly, shortly after the race onset. For stability and smoothness respectively, RMSA and JC showed a clear change with acute fatigue and differentiated well between the fast and slow groups. For future studies in this area, these metrics can be used to characterize the stability and uniformity of body segment motion during running. Less experienced runners were able to slightly recover the stability of their trunk movement but not the smoothness. Therefore, smoothness of running gait might be important parameter to understand the deterioration of running technique due to fatigue during training. Gait asymmetry increased significantly toward the end of the race and at higher perceived fatigue; faster runners showed a greater increase in asymmetry. Variability increased significantly at the beginning of the race and then remained stable for all participants, but faster runners showed up to 20% less variability, thus indicating a likely importance of variability to running performance. Assessment with respect to perceived fatigue provided different results than that with race progression for some metrics. This difference in results highlights the relevance of the measurement of perceived fatigue during outdoor running protocols. This work is one of the first to simultaneously and continuously measure the response of biomechanical and psychological parameters to acute fatigue during a half-marathon run. It confirmed the findings of the systematic review during a real-world competitive running environment. It may serve as a springboard for the design of studies that measure the association of biomechanical, psychological, and physiological parameters and its evolution with acute fatigue.

In chapter 4, methods were developed to enable the use of running power as a tool for feedback during training. Power is a promising tool for measuring training intensity and determining pacing strategies. However, to realize its potential as feedback tool, validated methods are required to reliably estimate power across different conditions. Furthermore, to enable their use in the field, these methods should be simple enough to be implemented on embedded systems with limited processing and energy storage capacity. This work proposed three minimal machine-learning models to estimate mechanical power (MP) for flat, uphill, and downhill running on treadmill. It was hypothesized that supplementing typically used statistical features on the accelerometer and gyroscope signals with biomechanical features would improve the accuracy of the models. Furthermore, since the power likely depended on the running speed and terrain slope, the accuracy of the models was tested in worst-case scenarios of estimated speed and slope. For uphill and level running, peak concentric phase power was estimated with a median \pm interquartile range error of $1.7 \pm 12.5\%$ and $3.2 \pm 13.4\%$, respectively. While existing devices only consider the concentric phase power, the proposed methods can estimate the peak eccentric phase power absorbed during downhill running with an error of $1.8 \pm 14.1\%$. Downhill running is an eccentric exercise and may

lead to muscle damage or tendon/joint overload at high running intensity. Thus, to reduce the likelihood of injuries, it is pertinent to get used to downhill running progressively. The proposed models can thus enable athletes to monitor their downhill running power and adjust their training to progressively increase this power. Results in this chapter, obtained for the worst-case scenarios, demonstrated a similar performance across a range of running conditions. The proposed algorithm meets requirements for applications needing accurate near real-time feedback and complements existing gait analysis algorithms based on foot-worn IMUs.

8.1.2 *Part II: Augmentation of in-field functional capacity testing*

Chapter 5 proposed a new method for instantaneous measurement of sprinting velocity using a single wearable device. A sensor fusion approach was followed, by combining the signals from wearable GNSS and IMU devices and the estimated velocity and duration were validated with speed radar and photocell data as reference. The median RMS error for the estimated velocity ranged from 6 to 8%, while that for the estimated sprint duration lied between 0.1 and -6.0%. The Bland-Altman plot showed close agreement between the estimated and the reference values of maximum velocity. Examination of fitting errors motivated an improved approximation of the velocity profile using a second order exponential model, thus raising doubts over the dominant approach of using a first order exponential model previously suggested in literature. The proposed sensor-fusion algorithm is valid to compute an accurate velocity profile with respect to the radar; it can compensate for and improve upon the accuracy of the individual IMU and GNSS velocities. The device used here is typically worn by athletes during their testing, training, and competitions. Thus, the proposed methods can be adopted easily by the sporting staff without disturbing their established practices. Using the proposed algorithm with a wearable device instead of radar and photocells also allows testing a cohort of athletes simultaneously, which makes its utility even more evident. It can thus augment the sprint test to assess injury risk of the athletes, identify their strengths/weakness using an accurately estimated force-velocity profile, and enable the coaches to design a personalized training program.

Chapter 6 a showed a method for instrumenting the agility T-test with wearable IMU and GNSS system, thus providing an avenue to measure detailed metrics like individual phases and change-of-direction (COD) durations. The algorithm developed in this work detected the start and end of the five COD using the peaks in the wavelet-processed anteroposterior acceleration signal. The mean error and standard deviation (S.D.) for detecting all COD events was -0.03 ± 66 ms, with the relative mean and S.D. on each COD duration being less than 3.5 ± 16 %. This algorithm can be used to determine the duration of the five motion sequences and provides new metrics for provides new variables for a detailed analysis of performance during the T-test. Within these metrics, the total cutting time for all COD was highly correlated to the total completion time of the test, thus emphasizing its importance to the athletes. While the COD duration was surprisingly similar across the best/worst performing athletes, the duration of individual displacement phases was markedly different. This result highlights the importance of the sprinting and shuffling movements undertaken during the displacement phases. Furthermore, asymmetrical performance between displacement in the

right and in the left direction can be highlighted using the respective phase durations, and help to assess the condition of the dominant and/or healthy leg with respect to the recently injured and/or non-dominant leg. Thus, the proposed method can augment the existing COD to understand the athlete's specific strengths/weaknesses on each COD and displacement phase and thus prove to be a valuable performance evaluation tool. Eventually, it can help the sporting staff to develop more individual training programs and help in the assessment for return to sport.

Chapter 7 extended the wearables-based approach to the 12-minute Cooper test, by assessing the relative contribution of running biomechanics to the endurance performance. Furthermore, different methods of estimating the distance covered using a wearable GNSS receiver were explored, with the estimation achieving an accuracy of 16.5 m and precision of 1.1%. Using this distance, a reliable estimation ($R^2 > 0.9$, RMSE $\in [0.07, 0.25]$ km/h) of the MAS and sVT2 was presented. To the author's knowledge, this is the first work to present a field test of sVT2, which is the lower boundary for the definition of "high intensity" and therefore this work may be of great interest to the coaches for prescribing intensity. All performance variables, MAS, sVT2 and average speed during Cooper test, were predicted with an acceptable error ($R^2 \geq 0.65$, RMSE ≤ 1.80 kmh⁻¹) using only the biomechanical metrics extracted from foot-worn IMU. These metrics were categorized into five groups based on their relevance – fatigue, pace, pattern, regularity, and symmetry. Runners with the best endurance performance showed better maintenance of their running technique despite fatigue and had a higher regularity and pace of running. Furthermore, their running showed a higher vertical stiffness, lower contact time and duty factor than the worst performers. To enable their use in the field, these metrics were used to develop a biomechanical profile representing the running technique and its temporal evolution with acute fatigue, identifying different profiles for runners with highest and lowest endurance performance. The identification of these metrics and their visual representation can help the sporting staff target the weaknesses of runners with customized training. Additionally, data from the test was used to develop machine learning models to estimate the temporal gait parameters using a wrist-worn IMU during an outdoor run. While it is easier to compute running gait parameters using foot IMUs, a wrist IMU is more convenient and less obtrusive when it comes to data acquisition. The models were validated using a foot-worn IMU reference system, with the RMS error for cycle time, swing time, flight time, and contact time being $0.27 \% \pm 0.1 \%$, $2.6 \% \pm 1.7 \%$, $7.3 \% \pm 4.9 \%$, and $10.6 \% \pm 5.5 \%$, respectively. This study can thus be a first step towards a detailed spatio-temporal analysis of the running technique in the field using a simple wrist-worn IMU.

8.1.3 *Potential application to training*

In this thesis, methods were developed to extract and identify biomechanical metrics based on their contribution to endurance performance, characterization of running technique through stability, smoothness, symmetry, response to fatigue, etc., and running power. These methods were based on a minimal body-worn sensor setup with foot-worn IMUs and a single trunk-worn IMU-GNSS unit. These setup and methods have been used and validated in a variety of situations, such as pre-season testing of a professional soccer team, training sessions of elite sprinters, the Lausanne half-

marathon race, etc., highlighting their potential for real-world application. As a first step to enable this application, these metrics can be used to create a biomechanical profile (illustrated example in Figure 8.1) representing the running technique and its temporal evolution. Within this profile, the selected categories can be used to characterize runners and identify their key strengths and weaknesses. Based on this, a training program can be developed to target specific aspects of running technique and provide the resulting profile to runners as post-training feedback. This profile can be tracked over a season to understand the development of running technique and the adaptation of runners to training.

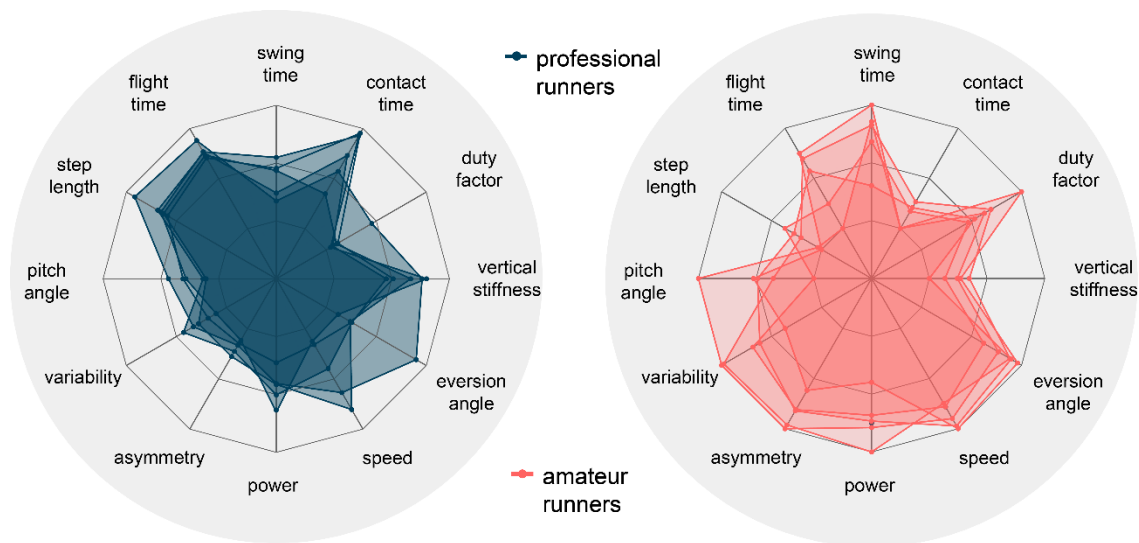


Figure 8.1 Profile for runners based on the biomechanical parameters. This profile can represent the individual running technique and can be used as feedback during training. The example shown here is illustrative, a profile based on measurements is shown in Figure 7.6.

Profiles at the beginning and the end of a long-distance training session reflect the impact of fatigue, providing complementary information to internal training load metrics. This profile can provide coaches and athletes a deeper insight into the running mechanics and allow evaluation of intraindividual changes following training programs and rehabilitation after injury. Additionally, athletes susceptible to or recovering from muscle injuries can use the eccentric power peak as a threshold for designing training programs with adequate mechanical load and assessing their readiness to return to running in various conditions. The ratio between the absolute power from concentric work and eccentric work could potentially be utilized as a metric of mechanical efficiency, reflecting the athlete's ability to store and re-use energy. Interindividual differences in the profile can be used to develop a tailored training program and monitor the improvement in the resulting running mechanics. Use of such a wearable system in standardized capacity measurements and training sessions may open a new perspective for personalization of training and rehabilitation.

8.2 LIMITATIONS

8.2.1 *Protocol*

Within the systematic review, that studies involving different athlete groups with varying skill levels (elite athletes vs. amateur) and physical capacity were analyzed together to create summary trends. Though mixing different study populations might lead to confounding effects, this was done to overcome the limited number of studies within each subgroup and ensure large enough sample size for computing meaningful summary trends. This also allowed the summary trends to be analysis can be generalizable across a wide population. The parameters for analysis were selected based on the threshold of at least 30 participants within a fatigue category and/or running surface. This threshold was chosen with the aim of balancing the strength of evidence and the number of analyzed parameters. While a higher threshold would increase the strength of evidence per parameter, the number of analyzed parameters would have been drastically reduced since most studies had <20 participants. For the concurrent analysis of perceived fatigue and running biomechanics during prolonged running, the overall sample was limited to 13 subjects and the sample size of fast/slow groups was too low for a meaningful statistical comparison. In addition, the resolution of the collection of ROF samples (10 minutes/sample) was limited due to the consideration of the participant's comfort.

Similarly, the limited sample size for the sprint velocity estimation study constitutes an important limitation. However, this study was aimed strictly toward the technical validation of the proposed algorithm, and this limitation was compensated by conducting multiple trials per participant. For the study on the Cooper test and power estimation, the sample size issue was addressed with larger sample of more than 30 participants. However, the sample inadvertently consisted predominantly of male subjects. Similarly, the well-trained runners were composed exclusively of male subjects, while the less trained group was a mixture of male and female participants. The results of the comparison between the five fastest and the five slowest runners for the Cooper test are therefore biased by the low sex ratio. Some differences in the regularity of running mechanics occurred when competitive and recreational runners were compared within male and female subjects (Clermont, Benson, Osis, et al., 2019). However, males and females with similar training levels have been reported to have similar values for RE ($\text{mlO}_2 \cdot \text{km}^{-1} \cdot \text{kg}^{-1}$) (J. Daniels & Daniels, 1992) and the energy cost of running when running at a similar intensity (Bunc & Heller, 1989).

Background data about the participants, such their VO₂max values, sleep quality, stress, and emotional health was not collected and could improve the interpretation of the results. Finally, the perceived fatigability could have been more holistically assessed by also including the measurement of the valence, arousal, flow state, and action crisis (Venhorst et al., 2018). While this additional measurement was not feasible for us during the half-marathon, a pre/post assessment could provide a more complete understanding of the affective, sensory, and cognitive processes. For the t-test, only one reference camera was present in the frontal plane, with a limited sampling rate of 60 Hz. An additional reference video cameras in a sagittal plane, with both video cameras

having a higher sampling rate can improved the overall reliability of the proposed method. The power estimation method was validated only in the lab, with downhill running simulated using an uphill incline and operating the treadmill in the opposite direction of rotation. While this should not affect the biomechanics directly, an indirect psychological effect on the participants may be possible and affect the biomechanics indirectly. Furthermore, due to the intensity of the protocol, only athletic participants were considered in this project.

In addition to the sprint, COD, and endurance tests, the functional test for hopping and the Y-balance test can be instrumented and augmented with wearable sensors in the future. Hop test is a battery of tests typically used to assess athlete readiness after injury rehabilitation (M. D. Ross et al., 2002). It consists of four tests: i) Single hop with the aim of achieving the maximum distance ii) 6m timed trial with the goal to finish as early as possible iii) Triple hop where the participant aims to jump as far as possible within three hops on a single leg iv) Crossover hop with the goal of achieving maximum distance through three crossover hops on a single leg. The goal of these tests is to achieve less than 10% difference in the performance with the healthy and injured leg. In addition to the symmetry, the quality of landing mechanics and knee joint kinematics is assessed qualitatively. This test can be augmented to quantify the landing mechanics and joint kinematics, thus improving the accuracy and personalization of assessment. The Y-Balance test is a simplified version of the Star-Excursion balance test, used to measure postural control and strength (Shaffer et al., 2013). It is generally used to assess athlete readiness after injury rehabilitation. During the test, the athlete stands on one leg and tries to reach as far as possible along the three directions with the other leg. The test is evaluated as one-third of the ratio of the sum of the distances reached in three direction and the leg length. The goal here is to obtain less than 10% difference the relative reach distance for the healthy and injured leg. Additionally, the physiotherapist assesses the stability of the trunk and the standing leg qualitatively. During rehabilitation for restoring locomotion capability, stability of motion has been highlighted as an important aspect (Cajigas et al., 2017; Plooi et al., 2021). The aim of instrumenting this test may be to quantify the dynamic stability of the standing leg and the trunk during each reaching movement. Furthermore, the kinematics of the reaching movement could also be measured quantitatively.

8.2.2 *Algorithm development and analysis*

In the marathon, power estimation, and Cooper test studies, the spring-mass model (J.-B. Morin et al., 2005), was used to estimate the vertical stiffness (VS), based on the estimated values of the flight time and the contact time. Since VS showed the highest positive contribution for all performance variables, a direct estimation of VS using force plate measurements and motion tracking from COM may be a valuable follow-up study. While such a study is not possible during field measurements and competitions such as half-marathons, the model for estimating VS can be investigated further. For example, more complex models gait models (Aoi et al., 2019; Rajagopal et al., 2016) could be used to simulate the COM motion and VRGF and their VS values can be compared. A similar model-based approach has been previously implemented to investigate gait modalities in different environments for walking (Apte, Plooi, et al., 2020).

Furthermore, these studies did not consider the limb kinematics and joint moments, which can provide additional information about the running technique and effect of fatigue (Koblbauer et al., 2014). Though the sagittal foot kinematics was considered, estimation of the footstrike angle can be rendered less accurate for participants with a forefoot strike (Falbriard et al., 2020) which was the case with one participant in the fast group of the marathon. The statistical comparison was conducted by computing the summary values for each of the eight race segments and can be complemented by a non-linear analysis of the continuous race trends. For the power estimation, the reference power method considered the athlete as one rigid body and used a specific threshold and filtering process on the force plate. Sensitivity analysis with regards to the threshold and cut-off frequency, and the consideration of relative movements of the body segments can help in exploring the generalizability of the method.

For the sprint study, the use of gradient descent procedure to convert IMU acceleration from sensor to global frame necessitated the assumption of motion in the sagittal plane. This assumption holds because of the approximate straight-line motion of the sprinter; it also forms the basis of radar-based velocity measurement. Thus, the proposed algorithm is valid for straight-line sprints and not for curve sprinting or sprints with direction changes. Secondly, the gradient descent method uses a static period to determine the orientation with respect to gravity and thus the algorithm is sensitive to the selected starting point of the sprint. Thus, absence of a static period before the start of the sprint can lead to unreliable conversion of the acceleration to the global frame. To ensure the availability of this static period, the raw GNSS velocity plot was visualized and manually select the starting point for the segmentation of the sprint data. Within the algorithm development for the t-test, the synchronization between video and IMU was done using first step of t-test. This step was assumed to synchronize with crossing of the first photocell, but this isn't always the case. To improve synchronization between video and IMU, asking the athlete to do an easily detectable movement (i.e., standing jump) before the test could help. The perfect way to synchronize video and IMU signal would be to have the precise GMT time of the video recording start. Furthermore, the algorithm uses many external inputs such as thresholds, frequency range of reconstruction or time window around COD, making the results sensitive to these inputs. Therefore, a sensitivity analysis to external inputs can help in investigating the generalizability of the method.

8.3 FUTURE DEVELOPMENT

8.3.1 *A more inclusive study population*

All the studies can benefit with inclusion of a larger population, especially with a better balance of the sex ratio. For example, male and female runners with patellofemoral pain show differences in running mechanics, thereby indicating sex-specific therapies (Willy et al., 2012). Furthermore, a systematic review of lower limb running injuries in runners showed the predominate injury in females was to the knee, while males showed a more even distribution of injury between the knee, shank and ankle-foot complex (Francis et al., 2019). Similarly, participants from different ethnic background and age ranges can be included, thereby extending the generalizability of the results

and/or finding differences in the various groups and addressing them in a more customized manner. By including a larger sample size of different sexes, the biomechanical profile (Figure 8.1) can be more personalized according to the sex, ethnicity, and age of the athlete, thereby improving the personalization of training. The studies focused on algorithm development for the sprint test and t-test mainly rely on a relatively smaller group of highly trained athletes. While this study was mainly focused on the algorithm development and validation, there is potential for follow-up studies with different groups of athletes of varied skills to test the discriminatory power of the results from the algorithms. The fatigue analysis during half-marathon can be expanded to include a larger sample size of both, highly trained and novice runners. This would allow a statistically meaningful analysis of the difference in trends for the gait parameters, stability, smoothness, symmetry, complexity etc. between the fast and slow groups. The power estimation our model has been tested on young healthy adults running on treadmills, it can be extended further and personalized to account for different running styles (Hoenig et al., 2020). Moreover, it could be validated on other populations such as older adults and Paralympic athletes, the latter using instrumented prosthetic feet (Lee et al., 2012).

8.3.2 *Methodological development*

The half-marathon analysis did not consider the knee kinematics and the ground reaction forces, despite their response to acute fatigue (Apte et al., 2021), due to the limitation in their estimation using foot-worn and/or chest-worn IMU. However, by using additional IMU on the shank and the sacrum, these parameters may be estimated in the field (Wouda et al., 2018) and can enrich the concurrent analysis of perceived fatigability and running biomechanics. Though it would be difficult to conduct such an analysis during an actual road race, simulated prolonged running protocols can be implemented. This sensor setup can improve our understanding of the biomechanical contributions to endurance performance, since the work in chapter 7 only considered spatiotemporal parameters, indirectly estimated vertical stiffness, and footstrike angles. Use of foot-worn IMUs during the sprint test and the t-test can aid in the detection of the foot contact. This will allow a better understanding of step-to-step variation in speed, cycle time, step length, etc. during sprinting and enable the coaches to further refine the training programs. In case of the t-test, detection of foot contact may enable the segmentation of COD into eccentric and concentric phases. Since these phases are directly impacted by different muscles groups (Eston et al., 1995), time spent during each phase can provide valuable information about the physical condition of the muscles and the readiness of the athlete to maximally exert them after injury rehabilitation. Additionally, foot contact can enable comparison with traditional metrics for COD, derived from the use of force plates.

The assumption of straight line sprinting in case of the velocity estimation algorithm can be addressed by fusing the IMU signals with magnetometer data, and obtaining the heading (yaw) angle of the body motion (Caruso et al., 2019). The magnetometer utilizes earth's magnetic field as a constant reference frame of reference for correction of the orientation error. This can improve the generalizability of the algorithm to longer sprinting distances, which involve the curved sections of the running track. The

magnetometers, however, are sensitive to the ferromagnetic objects in the environment and changes in environment might necessitate recalibration of the magnetometer (Kok & Schön, 2016). To further allow ease of use in the field, an automated segmentation procedure for the sprinting and running, possibly with thresholds on the GNSS ground speed, can allow for a more robust and repeatable segmentation. Automated segmentation can also simplify the analysis when a battery of tests, such as the agility T-test (Pauole et al., 2000), the sprint test, and the bleep test (Bangsbo and Krstrup, 2001), are performed together. This is typically the case for pre-season testing in team sports such as soccer, rugby, hockey, etc. The instantaneous velocity during sprinting can be complemented by other validated gait parameters to further enhance the utility of the sprint test.

In addition to foot-worn sensors, IMUs on other body segments, particularly the wrist and trunk, can also be used to estimate power. Wrist location offers ease of use and has already been used for gait analysis (Kammoun et al., 2022), while the trunk provides a position close to the CoM of the body. A sensor fusion approach could also be utilized to combine the data from all these locations to further improve estimation accuracy. To enable the application of the proposed method in practice, a simple decision tree can be developed using the barometer to identify uphill, downhill, and level running. Furthermore, the foot worn IMUs can be used to estimate the energy expenditure during running, complementing an existing IMU setup on the thigh and the shank that has achieved a relative error of 13.7% (Slade et al., 2021). By estimating the mechanical power and energy expenditure, a notion of running efficiency could be quantified using foot worn IMUs. This efficiency term can then be extracted across different datasets obtained in this thesis and its discriminatory power can be explored. Eventually, a reliably estimated running efficiency term can prove to be an invaluable addition to the biomechanical profile and personalization of training.

8.3.3 *Augmenting training prescription*

Signal processing algorithms and models developed in this work enable the translation of recorded signals into easily interpretable and actionable information. One example of this is the biomechanical profile used for characterizing runners. Based on this information, coaches and physical therapists can develop customized training programs that target the relevant parameters. The proportion of the training session performed with an appropriate running technique, while maintaining the prescribed running power could be used to characterize the quality of a training session. Neither internal training load (iTL) nor external training load (eTL) metrics can provide this information, thus making ‘quality’ the third unique descriptor of training sessions. In this context of an extended framework of training, as described in the introduction (Figure 1.4, section 1.1.4), a model can be developed to predict the iTL and the quality of training resulting from a given eTL stimulus. A prior study quantified the relationship between RPE (iTL) and GPS-based eTL variables for Australian Rules Footballers using generalized estimating equations and artificial neural networks (Bartlett et al., 2017), but did not consider the quality of training. Similar approaches like linear models or machine learning methods can be followed to estimate the relationship between the training input (eTL) and outputs like heart rate and RPE-based iTL and quality. Corre-

lation matrices can be utilized to estimate the relative influence of different eTL metrics on the output and determine their importance to the model. This may be followed by the development of a load estimation model for designing an optimal training program. It could be considered as a constrained optimization problem, with (eTL) metrics as inputs to an objective function designed to maximize the positive adaptation to training stimulus, with the constraints of the internal training load (iTL) not exceeding a critical value of acute-chronic work ratio (ACWR) and the resulting quality of training not dropping below a specific threshold. Outcomes of the functional tests will form the basis for the values used to initialize the optimization; the objective function can be based on existing fitness-fatigue models (Busso et al., 1994; Chiu & Bradford, 2003) and the competition schedule. A previous study approached load estimation as an optimization problem (Carey et al., 2018), however quality of training was not considered. The development and validation of these models could further contribute to the personalization of training and rehabilitation programs, thereby improving adaptation to training and reducing the incidence of injury in athletes.

BIBLIOGRAPHY

- Abdi, H. (2007). The Kendall rank correlation coefficient. In *Encyclopedia of Measurement and Statistics* (pp. 508–510). Sage.
- Abt, J. P., Sell, T. C., Chu, Y., Lovalekar, M., Burdett, R. G., & Lephart, S. M. (2011). Running kinematics and shock absorption do not change after brief exhaustive running. *Journal of Strength and Conditioning Research*, 25(6), 1479–1485. <https://doi.org/10.1519/JSC.0b013e3181ddfcf8>
- Adams, D., Pozzi, F., Carroll, A., Rombach, A., & Zeni, J. (2016). Validity and Reliability of a Commercial Fitness Watch for Measuring Running Dynamics. *Journal of Orthopaedic & Sports Physical Therapy*, 46(6), 471–476. <https://doi.org/10.2519/jospt.2016.6391>
- Aftalion, A., & Martinon, P. (2019). Optimizing running a race on a curved track. *PLOS ONE*, 14(9), e0221572. <https://doi.org/10.1371/journal.pone.0221572>
- Ahmadian, N., Nazarahari, M., Whittaker, J. L., & Rouhani, H. (2020). Quantification of Triple Single-Leg Hop Test Temporospatial Parameters: A Validated Method Using Body-Worn Sensors for Functional Evaluation after Knee Injury. *Sensors*, 20(12), 12. <https://doi.org/10.3390/s20123464>
- Aiello, L. C., & Wheeler, P. (1995). The Expensive-Tissue Hypothesis: The Brain and the Digestive System in Human and Primate Evolution. *Current Anthropology*, 36(2), 199–221. <https://doi.org/10.1086/204350>
- Alexander, R. M. (1991). Energy-saving mechanisms in walking and running. *Journal of Experimental Biology*, 160(1), 55–69. <https://doi.org/10.1242/jeb.160.1.55>
- Alfuth, M., & Rosenbaum, D. (2011). Long distance running and acute effects on plantar foot sensitivity and plantar foot loading. *NEUROSCIENCE LETTERS*, 503(1), 58–62. <https://doi.org/10.1016/j.neulet.2011.08.010>
- Alkjaer, T., Simonsen, E. B., & Dyhre-Poulsen, P. (2001). Comparison of inverse dynamics calculated by two- and three-dimensional models during walking. *Gait & Posture*, 13(2), 73–77. [https://doi.org/10.1016/S0966-6362\(00\)00099-0](https://doi.org/10.1016/S0966-6362(00)00099-0)
- Almeida, M. O., Davis, I. S., & Lopes, A. D. (2015). Biomechanical Differences of Foot-Strike Patterns During Running: A Systematic Review With Meta-analysis. *Journal of Orthopaedic & Sports Physical Therapy*, 45(10), 738–755. <https://doi.org/10.2519/jospt.2015.6019>
- Alonso, J. M., Tscholl, P. M., Engebretsen, L., Mountjoy, M., Dvorak, J., & Junge, A. (2010). Occurrence of injuries and illnesses during the 2009 IAAF World Athletics Championships. *British Journal of Sports Medicine*, 44(15), 1100–1105. <https://doi.org/10.1136/bjsm.2010.078030>
- Alvero-Cruz, J. R., Carnero, E. A., Giráldez García, M. A., Alacid, F., Rosemann, T., Nikolaidis, P. T., & Knechtle, B. (2019). Cooper Test Provides Better Half-Marathon Performance Prediction in Recreational Runners Than Laboratory Tests. *Frontiers in Physiology*, 10. <https://www.frontiersin.org/article/10.3389/fphys.2019.01349>
- Aminian, K., Najafi, B., Büla, C., Leyvraz, P.-F., & Robert, Ph. (2002). Spatio-temporal parameters of gait measured by an ambulatory system using miniature gyroscopes. *Journal of Biomechanics*, 35(5), 689–699. [https://doi.org/10.1016/S0021-9290\(02\)00008-8](https://doi.org/10.1016/S0021-9290(02)00008-8)
- Ammann, R., & Wyss, T. (2015). Running asymmetries during a 5-km time trial and their changes over time. *IcSPORTS 2015 - Proceedings of the 3rd International Congress on Sport Sciences Research and Technology Support*, 161–164.
- Anbarian, M., & Esmaeili, H. (2016). Effects of running-induced fatigue on plantar pressure distribution in novice runners with different foot types. *Gait & Posture*, 48, 52–56. <https://doi.org/10.1016/J.GAITPOST.2016.04.029>
- Anna, R., Malgorzata, N., Anna, R., & Jaroslaw, F. (2017). Changes in plantar pressure distribution after long-distance running. *New Medicine*, 21(2), 58–68. <https://doi.org/10.25121/NewMed.2017.21.2.58>
- Aoi, S., Ohashi, T., Bamba, R., Fujiki, S., Tamura, D., Funato, T., Senda, K., Ivanenko, Y., & Tsuchiya, K. (2019). Neuromusculoskeletal model that walks and runs across a speed range with a few motor control parameter changes based on the muscle synergy hypothesis. *Scientific Reports*, 9(1), 1. <https://doi.org/10.1038/s41598-018-37460-3>
- Appelbaum, L. G., & Erickson, G. (2018). Sports vision training: A review of the state-of-the-art in digital training techniques. *International Review of Sport and Exercise Psychology*, 11(1), 160–189. <https://doi.org/10.1080/1750984X.2016.1266376>
- Apte, S., Evian, V., Gremeaux, V., & Aminian, K. (2022). Concurrent Assessment Of Symmetry, Variability, And Complexity Of Stride During Prolonged Outdoor Running. *ISBS Proceedings Archive*, 40(1), 33.
- Apte, S., Laroche, N., Gremeaux, V., & Aminian, K. (2022). Trunk Motion During A Half-marathon: The Impact Of Perceived Fatigue On Motion Stability And Smoothness. *ISBS Proceedings Archive*, 40(1), 29.

- Apte, S., Meyer, F., Gremeaux, V., Dadashi, F., & Aminian, K. (2020). A Sensor Fusion Approach to the Estimation of Instantaneous Velocity Using Single Wearable Sensor During Sprint. *Frontiers in Bioengineering and Biotechnology*, 8. <https://www.frontiersin.org/article/10.3389/fbioe.2020.00838>
- Apte, S., Plooi, M., & Vallery, H. (2020). Simulation of human gait with body weight support: Benchmarking models and unloading strategies. *Journal of NeuroEngineering and Rehabilitation*, 17(1), 81. <https://doi.org/10.1186/s12984-020-00697-z>
- Apte, S., Prigent, G., Stöggel, T., Martínez, A., Snyder, C., Gremeaux-Bader, V., & Aminian, K. (2021). Biomechanical Response of the Lower Extremity to Running-Induced Acute Fatigue: A Systematic Review. *Frontiers in Physiology*, 12, 1076. <https://doi.org/10.3389/fphys.2021.646042>
- Apte, S., Troxler, S., Besson, C., Gremeaux, V., & Aminian, K. (2022). Augmented Cooper test: Biomechanical contributions to endurance performance. *Frontiers in Sports and Active Living*. <https://doi.org/10.3389/fspor.2022.935272>
- Arampatzis, A., Knicker, A., Metzler, V., & Brüggemann, G.-P. (2000). Mechanical power in running: A comparison of different approaches. *Journal of Biomechanics*, 33(4), 457–463. [https://doi.org/10.1016/S0021-9290\(99\)00187-6](https://doi.org/10.1016/S0021-9290(99)00187-6)
- Arellano, C. J., & Kram, R. (2014). Partitioning the Metabolic Cost of Human Running: A Task-by-Task Approach. *Integrative and Comparative Biology*, 54(6), 1084–1098. <https://doi.org/10.1093/icb/icu033>
- Armstrong, R. A. (2014). When to use the Bonferroni correction. *Ophthalmic and Physiological Optics*, 34(5), 502–508. <https://doi.org/10.1111/oppo.12131> PM - 24697967
- Aubry, R. L., Power, G. A., & Burr, J. F. (2018). An Assessment of Running Power as a Training Metric for Elite and Recreational Runners. *The Journal of Strength & Conditioning Research*, 32(8), 2258–2264. <https://doi.org/10.1519/JSC.0000000000002650>
- Aughey, R. (2011). Applications of GPS Technologies to Field Sports. *International Journal of Sports Physiology and Performance*, 6, 295–310. <https://doi.org/10.1123/ijspp.6.3.295>
- Avela, J., & Komi, P. V. (1998). Reduced stretch reflex sensitivity and muscle stiffness after long-lasting stretch-shortening cycle exercise in humans. *European Journal of Applied Physiology and Occupational Physiology*, 78(5), 403–410. <https://doi.org/10.1007/s004210050438>
- Avogadro, P., Dolenc, A., & Belli, A. (2003). Changes in mechanical work during severe exhausting running. *European Journal of Applied Physiology*, 90(1–2), 165–170. <https://doi.org/10.1007/s00421-003-0846-y>
- Azevedo, R. de A., Cruz, R., Couto, P., Silva-Cavalcante, M. D., Boari, D., Lima-Silva, A. E., Millet, G. Y., & Bertuzzi, R. (2019). Characterization of performance fatigability during a self-paced exercise. *Journal of Applied Physiology*, 127(3), 838–846. <https://doi.org/10.1152/jappphysiol.00090.2019> PM - 31318614
- Baechele, T. R., Earle, R. W., & National Strength & Conditioning Association (U.S.). (2008). *Essentials of strength training and conditioning*. Human Kinetics.
- Bailey, J., Mata, T., & Mercer, J. A. (2017). Is the Relationship Between Stride Length, Frequency, and Velocity Influenced by Running on a Treadmill or Overground? *International Journal of Exercise Science*, 10(7), 1067–1075.
- Bailey, J. P., Dufek, J. S., Freedman Silvernail, J., Navalta, J., & Mercer, J. (2018). Understanding the influence of perceived fatigue on coordination during endurance running. In *Sports Biomechanics*. <https://doi.org/10.1080/14763141.2018.1508489>
- Bailey, J. P., Silvernail, J. F., Dufek, J. S., Navalta, J., & Mercer, J. A. (2018). Effects of treadmill running velocity on lower extremity coordination variability in healthy runners. *HUMAN MOVEMENT SCIENCE*, 61, 144–150. <https://doi.org/10.1016/j.humov.2018.07.013>
- Baker, R. (2007). The history of gait analysis before the advent of modern computers. *Gait & Posture*, 26(3), 331–342. <https://doi.org/10.1016/j.gaitpost.2006.10.014>
- Balagué, N., Hristovski, R., Almaraz, M., Garcia-Retortillo, S., & Ivanov, P. C. (2020). Network Physiology of Exercise: Vision and Perspectives. *Frontiers in Physiology*, 11, 1607. <https://doi.org/10.3389/FPHYS.2020.611550/BIBTEX>
- Balasubramanian, S., Melendez-Calderon, A., Roby-Brami, A., & Burdet, E. (2015). On the analysis of movement smoothness. *Journal of NeuroEngineering and Rehabilitation*, 12(1), 112. <https://doi.org/10.1186/s12984-015-0090-9>
- Bale, J. (2004). *Running Cultures: Racing in Time and Space*. Routledge. <https://doi.org/10.4324/9780203499313>
- Bandyopadhyay, A. (2015). Validity of Cooper's 12-minute run test for estimation of maximum oxygen uptake in male university students. *Biology of Sport*, 32(1), 59–63. <https://doi.org/10.5604/20831862.1127283>
- Barré, A., Jolles, B. M., Theumann, N., & Aminian, K. (2015). Soft tissue artifact distribution on lower limbs during treadmill gait: Influence of skin markers' location on cluster design. *Journal of Biomechanics*, 48(10), 1965–1971. <https://doi.org/10.1016/j.jbiomech.2015.04.007>
- Bartlett, J. D., O'Connor, F., Pitchford, N., Torres-Ronda, L., & Robertson, S. J. (2017). Relationships Between Internal and External Training Load in Team-Sport Athletes: Evidence for an Individualized Approach. *International Journal of Sports Physiology and Performance*, 12(2), 230–234. <https://doi.org/10.1123/ijspp.2015-0791>
- Bassett, D. R. J. E. T. H. (2000). Limiting factors for maximum oxygen uptake and determinants of endurance performance. *Medicine & Science in Sports & Exercise*, 32(1), 70.

- Bauer, J. J., Fuchs, R. K., Smith, G. A., & Snow, C. M. (2001). Quantifying Force Magnitude and Loading Rate from Drop Landings That Induce Osteogenesis. *Journal of Applied Biomechanics*, 17(2), 142–152. <https://doi.org/10.1123/jab.17.2.142>
- Baumgartner, T., Held, S., Klatt, S., & Donath, L. (2021). Limitations of Foot-Worn Sensors for Assessing Running Power. *Sensors*, 21(15), 15. <https://doi.org/10.3390/s21154952>
- Baur, H., Hirschmüller, A., Müller, S., Gollhofer, A., & Mayer, F. (2018). Muscular activity in treadmill and over-ground running. *Isokinetics and Exercise Science*, 15(3), 165–171. <https://doi.org/10.3233/ies-2007-0262>
- Beattie, K., Kenny, I. C., Lyons, M., & Carson, B. P. (2014). The Effect of Strength Training on Performance in Endurance Athletes. *Sports Medicine*, 44(6), 845–865. <https://doi.org/10.1007/s40279-014-0157-y>
- Beaver, W. L., Wasserman, K., & Whipp, B. J. (1986). Bicarbonate buffering of lactic acid generated during exercise. *Journal of Applied Physiology*, 60(2), 472–478. <https://doi.org/10.1152/jappl.1986.60.2.472>
- Beck, O. N., Azua, E. N., & Grabowski, A. M. (2018). Step time asymmetry increases metabolic energy expenditure during running. *European Journal of Applied Physiology*, 118(10), 2147–2154. <https://doi.org/10.1007/s00421-018-3939-3>
- Bellenger, C. R., Fuller, J. T., Nelson, M. J., Hartland, M., Buckley, J. D., & DeBenedictis, T. A. (2015). Predicting maximal aerobic speed through set distance time-trials. *European Journal of Applied Physiology*, 115(12), 2593–2598. <https://doi.org/10.1007/s00421-015-3233-6>
- Benson, L. C., Clermont, C. A., Bošnjak, E., & Ferber, R. (2018). The use of wearable devices for walking and running gait analysis outside of the lab: A systematic review. *Gait & Posture*, 63, 124–138. <https://doi.org/10.1016/j.gaitpost.2018.04.047>
- Benson, L. C., Räisänen, A. M., Clermont, C. A., & Ferber, R. (2022). Is This the Real Life, or Is This Just Laboratory? A Scoping Review of IMU-Based Running Gait Analysis. *Sensors*, 22(5), 5. <https://doi.org/10.3390/s22051722>
- Bergamini, E., Picerno, P., Pillet, H., Natta, F., Thoreux, P., & Camomilla, V. (2012). Estimation of temporal parameters during sprint running using a trunk-mounted inertial measurement unit. *Journal of Biomechanics*, 45(6), 1123–1126. <https://doi.org/10.1016/j.jbiomech.2011.12.020>
- Bertelsen, M. L., Hulme, A., Petersen, J., Brund, R. K., Sørensen, H., Finch, C. F., Parner, E. T., & Nielsen, R. O. (2017). A framework for the etiology of running-related injuries. *Scandinavian Journal of Medicine & Science in Sports*, 27(11), 1170–1180. <https://doi.org/10.1111/sms.12883>
- Berthoin, S., Gerbeaux, M., Turpin, E., Guerrin, F., Lensele-Corbeil, G., & Vandendorpe, F. (1994). Comparison of two field tests to estimate maximum aerobic speed. *Journal of Sports Sciences*, 12(4), 355–362. <https://doi.org/10.1080/02640419408732181>
- Bertram, J. E. A., & Hasaneini, S. J. (2013). Neglected losses and key costs: Tracking the energetics of walking and running. In *Journal of Experimental Biology* (Vol. 216, Issue 6, pp. 933–938). The Company of Biologists Ltd. <https://doi.org/10.1242/jeb.078543>
- Billat, V. L., Palacin, F., Correa, M., & Pycke, J.-R. (2020). Pacing Strategy Affects the Sub-Elite Marathoner's Cardiac Drift and Performance. *Frontiers in Psychology*, 10. <https://www.frontiersin.org/article/10.3389/fpsyg.2019.03026>
- Birrer, D., & Morgan, G. (2010). Psychological skills training as a way to enhance an athlete's performance in high-intensity sports. *Scandinavian Journal of Medicine & Science in Sports*, 20(s2), 78–87. <https://doi.org/10.1111/j.1600-0838.2010.01188.x>
- Bisiaux, M., & Moretto, P. (2008). The effects of fatigue on plantar pressure distribution in walking. *Gait and Posture*, 28(4), 693–698. <https://doi.org/10.1016/j.gaitpost.2008.05.009>
- Blache, Y., Dumas, R., Lundberg, A., & Begon, M. (2017). Main component of soft tissue artifact of the upper-limbs with respect to different functional, daily life and sports movements. *Journal of Biomechanics*, 62, 39–46. <https://doi.org/10.1016/j.jbiomech.2016.10.019>
- Bland, J. M., & Altman, D. G. (2003). Applying the right statistics: Analyses of measurement studies. *Ultrasound in Obstetrics & Gynecology*, 22(1), 85–93. <https://doi.org/10.1002/uog.122>
- Błażkiewicz, M., Wiszomirska, I., & Wit, A. (2014). Comparison of four methods of calculating the symmetry of spatial-temporal parameters of gait. *Acta of Bioengineering and Biomechanics*, 16(1), 29–35.
- Blickhan, R. (1989). The spring-mass model for running and hopping. *Journal of Biomechanics*, 22(11), 1217–1227. [https://doi.org/10.1016/0021-9290\(89\)90224-8](https://doi.org/10.1016/0021-9290(89)90224-8)
- Bontemps, B., Vercruyssen, F., Gruet, M., & Louis, J. (2020). Downhill Running: What Are The Effects and How Can We Adapt? A Narrative Review. *Sports Medicine*, 50(12), 2083–2110. <https://doi.org/10.1007/s40279-020-01355-z>
- Borg, G. A. (1982). Psychophysical bases of perceived exertion. *Medicine and Science in Sports and Exercise*, 14(5), 377–381.
- Borrani, F., Candau, R., Perrey, S., Millet, G. Y., Millet, G. P., & Rouillon, J. D. (2003). Does the Mechanical Work in Running Change during the $\dot{V}O_2$ slow component? *Medicine and Science in Sports and Exercise*, 35(1), 50–57. <https://doi.org/10.1097/00005768-200301000-00009>
- Borresen, J., & Lambert, M. I. (2009). The Quantification of Training Load, the Training Response and the Effect on Performance. *Sports Medicine*, 39(9), 779–795. <https://doi.org/10.2165/11317780-000000000-00000>
- Bourdon, P. C., Cardinale, M., Murray, A., Gastin, P., Kellmann, M., Varley, M. C., Gabbett, T. J., Coutts, A. J., Burgess, D. J., Gregson, W., & Cable, N. T. (2017). Monitoring Athlete Training Loads: Consensus Statement. *Inter-*

-
- national Journal of Sports Physiology and Performance*, 12(s2), S2-161. <https://doi.org/10.1123/IJSP.2017-0208>
- Bovalino, S. P., Cunningham, N. J., Zordan, R. D., Harkin, S. M., Thies, H. H. G., Graham, C. J., & Kingsley, M. I. C. (2020). Change in foot strike patterns and performance in recreational runners during a road race: A cross-sectional study. *Journal of Science and Medicine in Sport*, 23(6), 621–624. <https://doi.org/10.1016/j.jsams.2019.12.018>
- Bramble, D. M., & Lieberman, D. E. (2004). Endurance running and the evolution of Homo. *Nature*, 432(7015), 7015. <https://doi.org/10.1038/nature03052>
- Braune, W., & Fischer, O. (1895). *Der Gang des Menschen*. B.S. Hirzel.
- Brodie, M., Walmsley, A., & Page, W. (2008). Fusion motion capture: A prototype system using inertial measurement units and GPS for the biomechanical analysis of ski racing. *Sports Technology*, 1(1), 17–28. <https://doi.org/10.1080/19346182.2008.9648447>
- Brooks, V. B., Cooke, J. D., & Thomas, J. S. (1973). The Continuity of Movements. In R. B. Stein, K. G. Pearson, R. S. Smith, & J. B. Redford (Eds.), *Control of Posture and Locomotion* (pp. 257–272). Springer US. https://doi.org/10.1007/978-1-4613-4547-3_22
- Brownstein, C. G., Millet, G. Y., & Thomas, K. (2020). Neuromuscular responses to fatiguing locomotor exercise. *Acta Physiologica*. <https://doi.org/10.1111/apha.13533>
- Bruijn, S. M., Meijer, O. G., Beek, P. J., & van Dieën, J. H. (2013). Assessing the stability of human locomotion: A review of current measures. *Journal of The Royal Society Interface*, 10(83), 20120999. <https://doi.org/10.1098/rsif.2012.0999>
- Buchheit, M., Samozino, P., Glynn, J. A., Michael, B. S., Al Haddad, H., Mendez-Villanueva, A., & Morin, J. B. (2014). Mechanical determinants of acceleration and maximal sprinting speed in highly trained young soccer players. *Journal of Sports Sciences*, 32(20), 1906–1913. <https://doi.org/10.1080/02640414.2014.965191>
- Buckley, C., O'Reilly, M. A., Whelan, D., Farrell, A. V., Clark, L., Longo, V., Gilchrist, M. D., & Caulfield, B. (2017). Binary classification of running fatigue using a single inertial measurement unit. *2017 IEEE 14th International Conference on Wearable and Implantable Body Sensor Networks (BSN)*, 197–201. <https://doi.org/10.1109/BSN.2017.7936040>
- Buckley, C., O'Reilly, M. A., Whelan, D., Vallety Farrell, A., Clark, L., Longo, V., Gilchrist, M. D., & Caulfield, B. (2017). Binary classification of running fatigue using a single inertial measurement unit. *2017 IEEE 14th International Conference on Wearable and Implantable Body Sensor Networks, BSN 2017*, 197–201.
- Budgett, R., Newsholme, E., Lehmann, M., Sharp, C., Jones, D., Jones, T., Peto, T., Collins, D., Nerurkar, R., & White, P. (2000). Redefining the overtraining syndrome as the unexplained underperformance syndrome. *British Journal of Sports Medicine*, 34(1), 67–68. <https://doi.org/10.1136/bjbm.34.1.67>
- Buman, M. P., Brewer, B. W., Cornelius, A. E., Van Raalte, J. L., & Petitpas, A. J. (2008). Hitting the wall in the marathon: Phenomenological characteristics and associations with expectancy, gender, and running history. *Psychology of Sport and Exercise*, 9(2), 177–190. <https://doi.org/10.1016/j.psychsport.2007.03.003>
- Bunc, V., & Heller, J. (1989). Energy cost of running in similarly trained men and women. *European Journal of Applied Physiology and Occupational Physiology*, 59(3), 178–183. <https://doi.org/10.1007/BF02386184>
- Burl, J. B. (1998). *Linear Optimal Control: H(2) and H (Infinity) Methods* (1st ed.). Addison-Wesley Longman Publishing Co., Inc.
- Burns, G. T., Gonzalez, R., Zendler, J. M., & Zernicke, R. F. (2021). Bouncing behavior of sub-four minute milers. *Scientific Reports*, 11(1), 1. <https://doi.org/10.1038/s41598-021-89858-1>
- Busso, T., Candau, R., & Lacour, J.-R. (1994). Fatigue and fitness modelled from the effects of training on performance. *European Journal of Applied Physiology and Occupational Physiology*, 69(1), 50–54. <https://doi.org/10.1007/BF00867927>
- Butler, R. J., Crowell, H. P., & Davis, I. M. (2003). Lower extremity stiffness: Implications for performance and injury. *Clinical Biomechanics (Bristol, Avon)*, 18(6), 511–517. [https://doi.org/10.1016/s0268-0033\(03\)00071-8](https://doi.org/10.1016/s0268-0033(03)00071-8)
- Cajigas, I., Koenig, A., Severini, G., Smith, M., & Bonato, P. (2017). Robot-induced perturbations of human walking reveal a selective generation of motor adaptation. *Science Robotics*, 2(6), eaam7749. <https://doi.org/10.1126/scirobotics.aam7749>
- Calbet, J. A. L. (2006). The rate of fatigue accumulation as a sensed variable. *The Journal of Physiology*, 575(Pt 3), 688. <https://doi.org/10.1113/JPHYSIOL.2006.116087>
- Camomilla, V., Bergamini, E., Fantozzi, S., & Vannozzi, G. (2018). Trends Supporting the In-Field Use of Wearable Inertial Sensors for Sport Performance Evaluation: A Systematic Review. *Sensors*, 18(3), 3. <https://doi.org/10.3390/s18030873>
- Candau, R., Belli, A., Millet, G. Y., Georges, D., Barbier, B., & Rouillon, J. D. (1998). Energy cost and running mechanics during a treadmill run to voluntary exhaustion in humans. *European Journal of Applied Physiology and Occupational Physiology*, 77(6), 479–485. <https://doi.org/10.1007/s004210050363>
- Cao, Z., Hidalgo, G., Simon, T., Wei, S.-E., & Sheikh, Y. (2021). OpenPose: Realtime Multi-Person 2D Pose Estimation Using Part Affinity Fields. *IEEE Transactions on Pattern Analysis and Machine Intelligence*, 43(1), 172–186. <https://doi.org/10.1109/TPAMI.2019.2929257>

- Carey, D. L., Crow, J., Ong, K.-L., Blanch, P., Morris, M. E., Dascombe, B. J., & Crossley, K. M. (2018). Optimizing Pre-season Training Loads in Australian Football. *International Journal of Sports Physiology and Performance*, 13(2), 194–199. <https://doi.org/10.1123/ijsspp.2016-0695>
- Carlet, G. (1892). *Précis de zoologie médicale*. G. Masson, éditeur.
- Carter, J. A., Rivadulla, A. R., & Preatoni, E. (2022). A support vector machine algorithm can successfully classify running ability when trained with wearable sensor data from anatomical locations typical of consumer technology. *Sports Biomechanics*, 0(0), 1–18. <https://doi.org/10.1080/14763141.2022.2027509>
- Caruso, M., Sabatini, A. M., Knaflitz, M., Gazzoni, M., Croce, U. D., & Cereatti, A. (2019). Accuracy of the Orientation Estimate Obtained Using Four Sensor Fusion Filters Applied to Recordings of Magneto-Inertial Sensors Moving at Three Rotation Rates. 2019 41st Annual International Conference of the IEEE Engineering in Medicine and Biology Society (EMBC), 2053–2058. <https://doi.org/10.1109/EMBC.2019.8857655>
- Cavagna, G. A., Heglund, N. C., & Willems, P. A. (2005). Effect of an increase in gravity on the power output and the rebound of the body in human running. *Journal of Experimental Biology*, 208(12), 2333–2346. <https://doi.org/10.1242/jeb.01661>
- Cavagna, G. A., & Kaneko, M. (1977). Mechanical work and efficiency in level walking and running. *The Journal of Physiology*, 268(2), 467–481. <https://doi.org/10.1113/jphysiol.1977.sp011866>
- Cavagna, G. A., Saibene, F. P., & Margaria, R. (1964). Mechanical work in running. *Journal of Applied Physiology*, 19(2), 249–256. <https://doi.org/10.1152/jappl.1964.19.2.249>
- Cerezuela-Espejo, V., Courel-Ibáñez, J., Morán-Navarro, R., Martínez-Cava, A., & Pallarés, J. G. (2018). The Relationship Between Lactate and Ventilatory Thresholds in Runners: Validity and Reliability of Exercise Test Performance Parameters. *Frontiers in Physiology*, 9. <https://www.frontiersin.org/article/10.3389/fphys.2018.01320>
- Ceyssens, L., Vanelderen, R., Barton, C., Malliaras, P., & Dingenen, B. (2019). Biomechanical Risk Factors Associated with Running-Related Injuries: A Systematic Review. *Sports Medicine* 2019 49:7, 49(7), 1095–1115. <https://doi.org/10.1007/S40279-019-01110-Z>
- Chakravarty, P., Cozzi, G., Ozgul, A., & Aminian, K. (2019). A novel biomechanical approach for animal behaviour recognition using accelerometers. *Methods in Ecology and Evolution*, 10(6), 802–814. <https://doi.org/10.1111/2041-210X.13172>
- Challis, J. H. (2001). The Variability in Running Gait Caused by Force Plate Targeting. *Journal of Applied Biomechanics*, 17(1), 77–83. <https://doi.org/10.1123/jab.17.1.77>
- Chan-Roper, M., Hunter, I., Myrer, J. W., Eggett, D. L., & Seeley, M. K. (2012). Kinematic changes during a marathon for fast and slow runners. *Journal of Sports Science and Medicine*, 11(1), 77–82. <https://doi.org/10.1162/qjec.122.2.831>
- Chaouachi, A., Brughelli, M., Chamari, K., Levin, G. T., Abdelkrim, N. B., Laurencelle, L., & Castagna, C. (2009). Lower Limb Maximal Dynamic Strength and Agility Determinants in Elite Basketball Players. *The Journal of Strength & Conditioning Research*, 23(5), 1570–1577. <https://doi.org/10.1519/JSC.0b013e3181a4e7f0>
- Chiu, L., & Bradford, J. (2003). The Fitness-Fatigue Model Revisited: Implications for Planning Short- and Long-Term Training. *Strength & Conditioning Journal*, 25, 42–51. [https://doi.org/10.1519/1533-4295\(2003\)025<0042:TFMRIF>2.0.CO;2](https://doi.org/10.1519/1533-4295(2003)025<0042:TFMRIF>2.0.CO;2)
- Clansey, A. C., Hanlon, M., Wallace, E. S., & Lake, M. J. (2012). Effects of fatigue on running mechanics associated with tibial stress fracture risk. *Medicine and Science in Sports and Exercise*, 44(10), 1917–1923. <https://doi.org/10.1249/MSS.0b013e318259480d>
- Clansey, A. C., Lake, M. J., Wallace, E. S., Feehally, T., & Hanlon, M. (2016). Can Trained Runners Effectively Attenuate Impact Acceleration During Repeated High-Intensity Running Bouts? *Journal of Applied Biomechanics*, 32(3), 261–268.
- Clemente, F. M., Sequeiros, J. B., Correia, A., Silva, F. G. M., & Martins, F. M. L. (2018). *Computational Metrics for Soccer Analysis*. Springer International Publishing. <https://doi.org/10.1007/978-3-319-59029-5>
- Clermont, C. A., Benson, L. C., Edwards, W. B., Hettinga, B. A., & Ferber, R. (2019). New Considerations for Wearable Technology Data: Changes in Running Biomechanics During a Marathon. *Journal of Applied Biomechanics*, 35(6), 1–9. <https://doi.org/10.1123/jab.2018-0453> PM - 31629343
- Clermont, C. A., Benson, L. C., Osis, S. T., Kobsar, D., & Ferber, R. (2019). Running patterns for male and female competitive and recreational runners based on accelerometer data. *Journal of Sports Sciences*, 37(2), 204–211. <https://doi.org/10.1080/02640414.2018.1488518>
- Clermont, C. A., Phinyomark, A., Osis, S. T., & Ferber, R. (2019). Classification of higher- and lower-mileage runners based on running kinematics. *Journal of Sport and Health Science*, 8(3), 249–257. <https://doi.org/10.1016/j.jshs.2017.08.003>
- Cochrum, R. G., Connors, R. T., Caputo, J. L., Coons, J. M., Fuller, D. K., Frame, M. C., & Morgan, D. W. (2021). Visual classification of running economy by distance running coaches. *European Journal of Sport Science*, 21(8), 1111–1118. <https://doi.org/10.1080/17461391.2020.1824020>
- Cooper, K. H. (1968). A Means of Assessing Maximal Oxygen Intake: Correlation Between Field and Treadmill Testing. *JAMA*, 203(3), 201–204. <https://doi.org/10.1001/jama.1968.03140030033008>

- Cormie, P., McGuigan, M. R., & Newton, R. U. (2011). Developing maximal neuromuscular power: Part 2 - training considerations for improving maximal power production. *Sports Medicine (Auckland, N.Z.)*, 41(2), 125–146. <https://doi.org/10.2165/11538500-000000000-00000>
- Coyle, E. F., & González-Alonso, J. (2001). Cardiovascular Drift During Prolonged Exercise: New Perspectives. *Exercise and Sport Sciences Reviews*, 29(2), 88–92.
- Coyne, J. O. C., Gregory Haff, G., Coutts, A. J., Newton, R. U., & Nimphius, S. (2018). The Current State of Subjective Training Load Monitoring—A Practical Perspective and Call to Action. *Sports Medicine - Open*, 4(1), 58. <https://doi.org/10.1186/s40798-018-0172-x>
- Cronin, J. B., & Rumpf, M. C. (2014). Effect of Four Different Step Detection Thresholds on Nonmotorized Treadmill Sprint Measurement. *The Journal of Strength & Conditioning Research*, 28(10), 2996–3000. <https://doi.org/10.1519/JSC.0000000000000497>
- Cronin, J., & Hansen, K. (2005). Strength And Power Predictors Of Sports Speed. *Journal of Strength and Conditioning Research*. <https://doi.org/10.1519/14323.1>
- Cross, M. R., Brughelli, M., Brown, S. R., Samozino, P., Gill, N. D., Cronin, J. B., & Morin, J.-B. (2015). Mechanical Properties of Sprinting in Elite Rugby Union and Rugby League. *International Journal of Sports Physiology and Performance*, 10(6), 695–702. <https://doi.org/10.1123/ijsp.2014-0151>
- Cross, R. (1999). Standing, walking, running, and jumping on a force plate. *American Journal of Physics*, 67(4), 304–309. <https://doi.org/10.1119/1.19253>
- Cummins, C., Orr, R., O'Connor, H., & West, C. (2013). Global positioning systems (GPS) and microtechnology sensors in team sports: A systematic review. *Sports Medicine (Auckland, N.Z.)*, 43(10), 1025–1042. <https://doi.org/10.1007/s40279-013-0069-2>
- Curran, S. L., Andrykowski, M. A., & Studts, J. L. (1995). Short Form of the Profile of Mood States (POMS-SF): Psychometric information. *Psychological Assessment*. <https://doi.org/10.1037/1040-3590.7.1.80>
- Cushman, S. A. (2010). Animal Movement Data: GPS Telemetry, Autocorrelation and the Need for Path-Level Analysis. In S. A. Cushman & F. Huettemann (Eds.), *Spatial Complexity, Informatics, and Wildlife Conservation* (pp. 131–149). Springer Japan. https://doi.org/10.1007/978-4-431-87771-4_7
- da Costa Santos, C. M., de Mattos Pimenta, C. A., & Nobre, M. R. C. (2007). The PICO strategy for the research question construction and evidence search. *Revista Latino-Americana De Enfermagem*, 15(3), 508–511. <https://doi.org/10.1590/s0104-11692007000300023>
- da Rosa, R. G., Oliveira, H. B., Gomeñuka, N. A., Masiero, M. P. B., da Silva, E. S., Zanardi, A. P. J., de Carvalho, A. R., Schons, P., & Peyré-Tartaruga, L. A. (2019). Landing-Takeoff Asymmetries Applied to Running Mechanics: A New Perspective for Performance. *Frontiers in Physiology*, 10. <https://www.frontiersin.org/article/10.3389/fphys.2019.00415>
- Dai, S., Carroll, D. D., Watson, K. B., Paul, P., Carlson, S. A., & Fulton, J. E. (2015). Participation in Types of Physical Activities Among US Adults—National Health and Nutrition Examination Survey 1999–2006. *Journal of Physical Activity & Health*, 12(0 1), S128–S140. <https://doi.org/10.1123/jpah.2015-0038>
- Damouras, S., Chang, M. D., Sejdíć, E., & Chau, T. (2010). An empirical examination of detrended fluctuation analysis for gait data. *Gait & Posture*, 31(3), 336–340. <https://doi.org/10.1016/j.gaitpost.2009.12.002>
- Daniels, J., & Daniels, N. (1992). Running economy of elite male and elite female runners. *Medicine and Science in Sports and Exercise*, 24(4), 483–489.
- Daniels, J. T. (1985). A physiologist's view of running economy. *Medicine & Science in Sports & Exercise*, 17(3), 332–338.
- Darch, L., Chalmers, S., Wiltshire, J., Causby, R., & Arnold, J. (2022). Running-induced fatigue and impact loading in runners: A systematic review and meta-analysis. *Journal of Sports Sciences*, 0(0), 1–20. <https://doi.org/10.1080/02640414.2022.2089803>
- Davey, A., Endres, N. K., Johnson, R. J., & Shealy, J. E. (2019). Alpine skiing injuries. *Sports Health*, 11(1), 18–26.
- Davis, I. S., Bowser, B. J., & Mullineaux, D. R. (2016). Greater vertical impact loading in female runners with medically diagnosed injuries: A prospective investigation. *British Journal of Sports Medicine*, 50(14), 887–892. <https://doi.org/10.1136/bjsports-2015-094579>
- Davis, R. B., Öunpuu, S., Tyburski, D., & Gage, J. R. (1991). A gait analysis data collection and reduction technique. *Human Movement Science*, 10(5), 575–587. [https://doi.org/10.1016/0167-9457\(91\)90046-Z](https://doi.org/10.1016/0167-9457(91)90046-Z)
- Dayakidis, M. K., & Boudolos, K. (2006). Ground reaction force data in functional ankle instability during two cutting movements. *Clinical Biomechanics*, 21(4), 405–411.
- de Siqueira Santos, S., Takahashi, D. Y., Nakata, A., & Fujita, A. (2014). A comparative study of statistical methods used to identify dependencies between gene expression signals. *Briefings in Bioinformatics*, 15(6), 906–918. <https://doi.org/10.1093/bib/bbt051>
- Deelen, I., Janssen, M., Vos, S., Kamphuis, C. B. M., & Ettema, D. (2019). Attractive running environments for all? A cross-sectional study on physical environmental characteristics and runners' motives and attitudes, in relation to the experience of the running environment. *BMC Public Health*, 19(1), 366. <https://doi.org/10.1186/s12889-019-6676-6>
- Degache, F., Morin, J.-B., Oehen, L., Guex, K., Giardini, G., Schena, F., Millet, G. Y., & Millet, G. P. (2016). Running Mechanics During the World's Most Challenging Mountain Ultramarathon. *International Journal of Sports Physiology and Performance*, 11(5), 608–614. <https://doi.org/10.1123/ijsp.2015-0238>

- Degache, F., Van Zaen, J., Oehen, L., Guex, K., & Trabucchi, P. (2014). Alterations in Postural Control during the World's Most Challenging Mountain Ultra-Marathon. *PLoS ONE*, 9(1), 84554. <https://doi.org/10.1371/journal.pone.0084554>
- Delaney, J. A., Scott, T. J., Ballard, D. A., Duthie, G. M., Hickmans, J. A., Lockie, R. G., & Dascombe, B. J. (2015). Contributing Factors to Change-of-Direction Ability in Professional Rugby League Players. *The Journal of Strength & Conditioning Research*, 29(10), 2688–2696. <https://doi.org/10.1519/JSC.0000000000000960>
- Derrick, T. R., Dereu, D., & Mclean, S. P. (2002). Impacts and kinematic adjustments during an exhaustive run. *Medicine and Science in Sports and Exercise*, 34(6), 998–1002. <https://doi.org/10.1097/00005768-200206000-00015>
- Di Michele, R., & Merni, F. (2014). The concurrent effects of strike pattern and ground-contact time on running economy. *Journal of Science and Medicine in Sport*, 17(4), 414–418. <https://doi.org/10.1016/j.jsams.2013.05.012>
- Dierks, T. A., Davis, I. S., & Hamill, J. (2010). The effects of running in an exerted state on lower extremity kinematics and joint timing. *JOURNAL OF BIOMECHANICS*, 43(15), 2993–2998.
- Dittrich, N., de Lucas, R. D., Maioral, M. F., Diefenthaler, F., & Guglielmo, L. G. A. (2013). Continuous and intermittent running to exhaustion at maximal lactate steady state: Neuromuscular, biochemical and endocrinal responses. *Journal of Science and Medicine in Sport*, 16(6), 545–549. <https://doi.org/10.1016/J.JSAMS.2012.12.001>
- Dos' Santos, T., McBurnie, A., Thomas, C., Comfort, P., & Jones, P. A. (2019). Biomechanical comparison of cutting techniques: A review and practical applications. *Strength & Conditioning Journal*, 41(4), 40–54.
- Dos'Santos, T., Thomas, C., Comfort, P., & Jones, P. A. (2018). The effect of angle and velocity on change of direction biomechanics: An angle-velocity trade-off. *Sports Medicine*, 48(10), 2235–2253.
- Drew, M. K., & Finch, C. F. (2016). The Relationship Between Training Load and Injury, Illness and Soreness: A Systematic and Literature Review. *Sports Medicine*, 46(6), 861–883. <https://doi.org/10.1007/s40279-015-0459-8>
- Dugan, S. A., & Bhat, K. P. (2005). Biomechanics and Analysis of Running Gait. *Physical Medicine and Rehabilitation Clinics*, 16(3), 603–621. <https://doi.org/10.1016/j.pmr.2005.02.007>
- Dutto, D. J., & Smith, G. A. (2002). Changes in spring-mass characteristics during treadmill running to exhaustion. *Medicine and Science in Sports and Exercise*, 34(8), 1324–1331.
- Easthope, C. S., Nosaka, K., Caillaud, C., Vercruyssen, F., Louis, J., & Brisswalter, J. (2014). Reproducibility of performance and fatigue in trail running. *Journal of Science and Medicine in Sport*, 17(2), 207–211. <https://doi.org/10.1016/j.jsams.2013.03.009>
- Edwards, R. B., Tofari, P. J., Cormack, S. J., & Whyte, D. G. (2017). Non-motorized Treadmill Running Is Associated with Higher Cardiometabolic Demands Compared with Overground and Motorized Treadmill Running. *Frontiers in Physiology*, 8(NOV), 914. <https://doi.org/10.3389/fphys.2017.00914>
- Eichelberger, P., Ferraro, M., Minder, U., Denton, T., Blasimann, A., Krause, F., & Baur, H. (2016). Analysis of accuracy in optical motion capture – A protocol for laboratory setup evaluation. *Journal of Biomechanics*, 49(10), 2085–2088. <https://doi.org/10.1016/j.jbiomech.2016.05.007>
- Eilers, P. H. C. (2003). A Perfect Smoother. *Analytical Chemistry*, 75(14), 3631–3636. <https://doi.org/10.1021/ac034173t>
- Eisinga, R., Heskes, T., Pelzer, B., & Te Grotenhuis, M. (2017). Exact p-values for pairwise comparison of Friedman rank sums, with application to comparing classifiers. *BMC Bioinformatics*, 18(1), 68. <https://doi.org/10.1186/s12859-017-1486-2> M4 - Citavi
- Emery, C. A., Cassidy, J. D., Klassen, T. P., Rosychuk, R. J., & Rowe, B. H. (2005). Effectiveness of a home-based balance-training program in reducing sports-related injuries among healthy adolescents: A cluster randomized controlled trial. *CMAJ*, 172(6), 749–754. <https://doi.org/10.1503/cmaj.1040805>
- Engelbrechtsen, A. H., Myklebust, G., Holme, I., Engelbrechtsen, L., & Bahr, R. (2008). Prevention of Injuries among Male Soccer Players: A Prospective, Randomized Intervention Study Targeting Players with Previous Injuries or Reduced Function. *The American Journal of Sports Medicine*, 36(6), 1052–1060. <https://doi.org/10.1177/0363546508314432>
- England, S. (2019). *Active Lives data tables*. Sport England. <https://www.sportengland.org/know-your-audience/data/active-lives/active-lives-data-tables>
- Enoka, R. M., & Duchateau, J. (2008). Muscle fatigue: What, why and how it influences muscle function. In *Journal of Physiology* (Vol. 586, Issue 1, pp. 11–23). John Wiley & Sons, Ltd. <https://doi.org/10.1113/jphysiol.2007.139477>
- Enoka, R. M., & Duchateau, J. (2016). Translating Fatigue to Human Performance. *Medicine and Science in Sports and Exercise*, 48(11), 2228–2238. <https://doi.org/10.1249/MSS.0000000000000929> PM - 27015386
- Erdem, N. S., Ersoy, C., & Tunca, C. (2019). Gait Analysis Using Smartwatches. *2019 IEEE 30th International Symposium on Personal, Indoor and Mobile Radio Communications (PIMRC Workshops)*, 1–6. <https://doi.org/10.1109/PIMRCW.2019.8880821>
- Erp, T. van, Sanders, D., & Koning, J. J. de. (2019). Training Characteristics of Male and Female Professional Road Cyclists: A 4-Year Retrospective Analysis. *International Journal of Sports Physiology and Performance*, 15(4), 534–540. <https://doi.org/10.1123/ijspp.2019-0320>

-
- Eskofier, B., Kugler, P., Melzer, D., & Kuehner, P. (2012). Embedded classification of the perceived fatigue state of runners: Towards a body sensor network for assessing the fatigue state during running. *Proceedings - BSN 2012: 9th International Workshop on Wearable and Implantable Body Sensor Networks*, 113–117. <https://doi.org/10.1109/BSN.2012.4>
- Esteve-Lanao, J., Lucia, A., deKoning, J. J., & Foster, C. (2008). How Do Humans Control Physiological Strain during Strenuous Endurance Exercise? *PLOS ONE*, 3(8), e2943. <https://doi.org/10.1371/JOURNAL.PONE.0002943>
- Eston, R. G., Mickleborough, J., & Baltzopoulos, V. (1995). Eccentric activation and muscle damage: Biomechanical and physiological considerations during downhill running. *British Journal of Sports Medicine*, 29(2), 89–94. <https://doi.org/10.1136/bjsm.29.2.89>
- Falbriard, M., Meyer, F., Mariani, B., Millet, G. P., & Aminian, K. (2018). Accurate Estimation of Running Temporal Parameters Using Foot-Worn Inertial Sensors. *Frontiers in Physiology*, 9. <https://www.frontiersin.org/article/10.3389/fphys.2018.00610>
- Falbriard, M., Meyer, F., Mariani, B., Millet, G. P., & Aminian, K. (2020). Drift-Free Foot Orientation Estimation in Running Using Wearable IMU. *Frontiers in Bioengineering and Biotechnology*, 8. <https://www.frontiersin.org/article/10.3389/fbioe.2020.00065>
- Falbriard, M., Soltani, A., & Aminian, K. (2021). Running Speed Estimation Using Shoe-Worn Inertial Sensors: Direct Integration, Linear, and Personalized Model. *Frontiers in Sports and Active Living*, 3. <https://www.frontiersin.org/article/10.3389/fspor.2021.585809>
- Farley, C. T., & Ferris, D. P. (1998). Biomechanics of Walking and Running: Center of Mass Movements to Muscle Action. *Exercise and Sport Sciences Reviews*, 26(1), 253–286.
- Farley, C. T., & González, O. (1996). Leg stiffness and stride frequency in human running. *Journal of Biomechanics*, 29(2), 181–186. [https://doi.org/10.1016/0021-9290\(95\)00029-1](https://doi.org/10.1016/0021-9290(95)00029-1)
- Fasel, B., Sporri, J., Chardonnens, J., Kroll, J., Muller, E., & Aminian, K. (2018). Joint Inertial Sensor Orientation Drift Reduction for Highly Dynamic Movements. *IEEE Journal of Biomedical and Health Informatics*, 22(1), 77–86. <https://doi.org/10.1109/JBHI.2017.2659758>
- Flueck, M., & Eilers, W. (2010). Training Modalities: Impact on Endurance Capacity. *Endocrinology and Metabolism Clinics*, 39(1), 183–200. <https://doi.org/10.1016/j.ecl.2009.10.002>
- Fohrmann, D., Mai, P., Ziolkowski, L., Mählich, D., Kurz, M., & Willwacher, S. (2019). *Estimating Whole-body Mechanical Power In Running By Means Of Simulated Inertial Sensor Signals*. 4.
- Folland, J. P., Allen, S. J., Black, M. I., Handsaker, J. C., & Forrester, S. E. (2017). Running Technique is an Important Component of Running Economy and Performance. *Medicine and Science in Sports and Exercise*, 49(7), 1412–1423. <https://doi.org/10.1249/MSS.0000000000001245>
- Foster, C., & Lucia, A. (2007). Running Economy. *Sports Medicine*, 37(4), 316–319. <https://doi.org/10.2165/00007256-200737040-00011>
- Foster, C., Rodriguez-Marroyo, J. A., & Koning, J. J. de. (2017). Monitoring Training Loads: The Past, the Present, and the Future. *International Journal of Sports Physiology and Performance*, 12(s2), S2–8. <https://doi.org/10.1123/IJSP.2016-0388>
- Francis, P., Whatman, C., Sheerin, K., Hume, P., & Johnson, M. I. (2019). The Proportion of Lower Limb Running Injuries by Gender, Anatomical Location and Specific Pathology: A Systematic Review. *Journal of Sports Science & Medicine*, 18(1), 21–31.
- Fredette, A., Roy, J.-S., Perreault, K., Dupuis, F., Napier, C., & Esculier, J.-F. (2021). The association between running injuries and training parameters: A systematic review. *Journal of Athletic Training*. <https://doi.org/10.4085/1062-6050-0195.21>
- Furusawa, K., Hill, A. V., & Parkinson, J. L. (1927). The dynamics of “sprint” running. *Proceedings of the Royal Society of London. Series B, Containing Papers of a Biological Character*, 102(713), 29–42. <https://doi.org/10.1098/rspb.1927.0035>
- Gabbett, T. J. (2020). Debunking the myths about training load, injury and performance: Empirical evidence, hot topics and recommendations for practitioners. *British Journal of Sports Medicine*, 54(1), 58–66. <https://doi.org/10.1136/bjsports-2018-099784>
- Garcia-Perez, J. A., Perez-Soriano, P., Llana Belloch, S., Lucas-Cuevas, A. G., Sanchez-Zuriaga, D., Antonio Garcia-Perez, J., Perez-Soriano, P., Llana Belloch, S., Gabriel Lucas-Cuevas, A., Sanchez-Zuriaga, D., García-Pérez, J. A., Pérez-Soriano, P., Llana Belloch, S., Lucas-Cuevas, Á. G., & Sánchez-Zuriaga, D. (2014). Effects of treadmill running and fatigue on impact acceleration in distance running. *Sports Biomechanics*, 13(3), 259–266. <https://doi.org/10.1080/14763141.2014.909527>
- García-Pinillos, F., Latorre-Román, P. Á., Roche-Seruendo, L. E., & García-Ramos, A. (2019). Prediction of power output at different running velocities through the two-point method with the Stryd™ power meter. *Gait & Posture*, 68, 238–243. <https://doi.org/10.1016/j.gaitpost.2018.11.037>
- García-Pinillos, F., Párraga-Montilla, J. A., Soto-Hermoso, V. M., & Latorre-Román, P. A. (2016). Changes in balance ability, power output, and stretch-shortening cycle utilisation after two high-intensity intermittent training protocols in endurance runners. *Journal of Sport and Health Science*, 5(4), 430–436. <https://doi.org/10.1016/j.jshs.2015.09.003>

- Garofolini, A., Taylor, S., & Lepine, J. (2019). Evaluating dynamic error of a treadmill and the effect on measured kinetic gait parameters: Implications and possible solutions. *Journal of Biomechanics*, 82, 156–163. <https://doi.org/10.1016/j.jbiomech.2018.10.025>
- Gerlach, K. E., White, S. C., Burton, H. W., Dorn, J. M., Leddy, J. J., & Horvath, P. J. (2005). Kinetic changes with fatigue and relationship to injury in female runners. *Medicine and Science in Sports and Exercise*, 37(4), 657–663. <https://doi.org/10.1249/01.MSS.0000158994.29358.71>
- Giandolini, M., Vernillo, G., Samozino, P., Horvais, N., Edwards, W. B., Morin, J. B., & Millet, G. Y. (2016). Fatigue associated with prolonged graded running. In *European Journal of Applied Physiology* (Vol. 116, Issue 10, pp. 1859–1873). Springer Verlag. <https://doi.org/10.1007/s00421-016-3437-4>
- Gibala, M. J., Little, J. P., Macdonald, M. J., & Hawley, J. A. (2012). Physiological adaptations to low-volume, high-intensity interval training in health and disease. *Journal of Physiology*, 590(5), 1077–1084. <https://doi.org/10.1113/jphysiol.2011.224725>
- Gignac, G. E., & Szodorai, E. T. (2016). Effect size guidelines for individual differences researchers. *Personality and Individual Differences*, 102, 74–78. <https://doi.org/10.1016/j.paid.2016.06.069>
- Gilgen-Ammann, R., Schweizer, T., & Wyss, T. (2020). Accuracy of Distance Recordings in Eight Positioning-Enabled Sport Watches: Instrument Validation Study. *JMIR MHealth and UHealth*, 8(6), e17118. <https://doi.org/10.2196/17118>
- Gindre, C., Lussiana, T., Hebert-Losier, K., & Mourot, L. (2015). Aerial and Terrestrial Patterns: A Novel Approach to Analyzing Human Running. *International Journal of Sports Medicine*, 37(01), 25–26. <https://doi.org/10.1055/s-0035-1555931>
- Girard, O., Brocherie, F., Morin, J.-B., & Millet, G. P. (2017a). Mechanical alterations during interval-training treadmill runs in high-level male team-sport players. *Journal of Science and Medicine in Sport*, 20(1), 87–91. <https://doi.org/10.1016/j.jsams.2016.05.002>
- Girard, O., Brocherie, F., Morin, J.-B., & Millet, G. P. (2017b). Lower limb mechanical asymmetry during repeated treadmill sprints. *Human Movement Science*, 52, 203–214. <https://doi.org/10.1016/j.humov.2017.02.008>
- Girard, O., Brocherie, F., Tomazin, K., Farooq, A., & Morin, J.-B. (2016). Changes in running mechanics over 100-m, 200-m and 400-m treadmill sprints. *Journal of Biomechanics*, 49(9), 1490–1497. <https://doi.org/10.1016/j.jbiomech.2016.03.020>
- Glaister, B. C., Orendurff, M. S., Schoen, J. A., Bernatz, G. C., & Klute, G. K. (2008). Ground reaction forces and impulses during a transient turning maneuver. *Journal of Biomechanics*, 41(14), 3090–3093.
- Glazer, D. D. (2009). Development and Preliminary Validation of the Injury-Psychological Readiness to Return to Sport (I-PRRS) Scale. *Journal of Athletic Training*, 44(2), 185–189. <https://doi.org/10.4085/1062-6050-44.2.185>
- Gleason, B. H., Kramer, J. B., & Stone, M. H. (2015). Agility training for American football. *Strength & Conditioning Journal*, 37(6), 65–71.
- Gløersen, Ø., Kocbach, J., & Gilgien, M. (2018). Tracking Performance in Endurance Racing Sports: Evaluation of the Accuracy Offered by Three Commercial GNSS Receivers Aimed at the Sports Market. *Frontiers in Physiology*, 9. <https://www.frontiersin.org/articles/10.3389/fphys.2018.01425>
- Goffredo, M., Bouchrika, I., Carter, J. N., & Nixon, M. S. (2010). Performance analysis for automated gait extraction and recognition in multi-camera surveillance. *Multimedia Tools and Applications*, 50(1), 75–94. <https://doi.org/10.1007/s11042-009-0378-5>
- Gómez, A. L., Radzwich, R. J., Denegar, C. R., Volek, J. S., Rubin, M. R., Bush, J. A., Doan, B. K., Wickham, R. B., Mazzetti, S. A., Newton, R. U., French, D. N., Häkkinen, K., Ratamess, N. A., & Kraemer, W. J. (2002). The effects of a 10-kilometer run on muscle strength and power. *Journal of Strength and Conditioning Research*, 16(2), 184–191. [https://doi.org/10.1519/1533-4287\(2002\)016<0184:TEOAKR>2.0.CO;2](https://doi.org/10.1519/1533-4287(2002)016<0184:TEOAKR>2.0.CO;2)
- Goodall, S., Charlton, K., Howatson, G., Thomas, K., Long, M. A., Stretesky, P. B., Harms, G., Sollund, R., Macmillan, P., & Chapter, B. (2015). Neuromuscular fatigability during repeated-sprint exercise in male athletes. *Medicine & Science in Sports & Exercise*, 47(3), 528–536.
- Grant, S., Corbett, K., Amjad, A. M., Wilson, J., & Aitchison, T. (1995). A comparison of methods of predicting maximum oxygen uptake. *British Journal of Sports Medicine*, 29(3), 147–152. <https://doi.org/10.1136/bjism.29.3.147>
- Green-Demers, I., Pelletier, L. G., Stewart, D. G., & Gushue, N. R. (1998). Coping With the Less Interesting Aspects of Training: Toward a Model of Interest and Motivation Enhancement in Individual Sports. *Basic and Applied Social Psychology*, 20(4), 251–261. https://doi.org/10.1207/s15324834basps2004_2
- Gronwald, T., Hoos, O., Ludyga, S., & Hottenrott, K. (2018). Non-linear dynamics of heart rate variability during incremental cycling exercise. <https://doi.org/10.1080/15438627.2018.1502182>, 27(1), 88–98.
- Gronwald, T., Rogers, B., & Hoos, O. (2020). Fractal Correlation Properties of Heart Rate Variability: A New Biomarker for Intensity Distribution in Endurance Exercise and Training Prescription? *Frontiers in Physiology*, 11. <https://www.frontiersin.org/article/10.3389/fphys.2020.550572>
- Groves, P. D. (2015). Principles of GNSS, inertial, and multisensor integrated navigation systems, 2nd edition [Book review]. *IEEE Aerospace and Electronic Systems Magazine*, 30(2), 26–27. <https://doi.org/10.1109/MAES.2014.14110>

-
- Gruber, A. H., Edwards, W. B., Hamill, J., Derrick, T. R., & Boyer, K. A. (2017). A comparison of the ground reaction force frequency content during rearfoot and non-rearfoot running patterns. *Gait & Posture*, 56, 54–59. <https://doi.org/10.1016/j.gaitpost.2017.04.037>
- Gruber, A. H., McDonnell, J., Davis, J. J., Vollmar, J. E., Harezlak, J., & Paquette, M. R. (2021). Monitoring Gait Complexity as an Indicator for Running-Related Injury Risk in Collegiate Cross-Country Runners: A Proof-of-Concept Study. *Frontiers in Sports and Active Living*, 3. <https://www.frontiersin.org/article/10.3389/fspor.2021.630975>
- Guerra-filho, G. B. (2005). Optical motion capture: Theory and implementation. *Journal of Theoretical and Applied Informatics (RITA)*, 12, 61–89.
- Gurchiek, R. D., McGinnis, R. S., Needle, A. R., McBride, J. M., & van Werkhoven, H. (2017). The use of a single inertial sensor to estimate 3-dimensional ground reaction force during accelerative running tasks. *Journal of Biomechanics*, 61, 263–268. <https://doi.org/10.1016/j.jbiomech.2017.07.035>
- Gurchiek, R. D., McGinnis, R. S., Needle, A. R., McBride, J. M., & van Werkhoven, H. (2018). An adaptive filtering algorithm to estimate sprint velocity using a single inertial sensor. *Sports Engineering*, 21(4), 389–399. <https://doi.org/10.1007/s12283-018-0285-y>
- Gurchiek, R. D., Rupasinghe Arachchige Don, H. S., Pelawa Watagoda, L. C. R., McGinnis, R. S., van Werkhoven, H., Needle, A. R., McBride, J. M., & Arnholt, A. T. (2019). Sprint Assessment Using Machine Learning and a Wearable Accelerometer. *Journal of Applied Biomechanics*, 35(2), 164–169. <https://doi.org/10.1123/jab.2018-0107>
- Hader, K., Palazzi, D., & Buchheit, M. (2015). Change of direction speed in soccer: How much braking is enough? *Kinesiology*, 47(1.), 67–74.
- Halilaj, E., Rajagopal, A., Fiterau, M., Hicks, J. L., Hastie, T. J., & Delp, S. L. (2018). Machine learning in human movement biomechanics: Best practices, common pitfalls, and new opportunities. *Journal of Biomechanics*, 81, 1–11. <https://doi.org/10.1016/j.jbiomech.2018.09.009>
- Halsen, S. L. (2014). Monitoring Training Load to Understand Fatigue in Athletes. *Sports Medicine*, 44(2), 139–147. <https://doi.org/10.1007/s40279-014-0253-z>
- Hamacher, D., Hamacher, D., Hohnbaum, M., Gerth, K., Schega, L., & Zech, A. (2018). Effects of physical exhaustion on local dynamic stability and automaticity of walking. *Gait & Posture*, 66, 135–138. <https://doi.org/10.1016/J.GAITPOST.2018.08.031>
- Hamidi Rad, M., Gremeaux, V., Dadashi, F., & Aminian, K. (2021). A Novel Macro-Micro Approach for Swimming Analysis in Main Swimming Techniques Using IMU Sensors. *Frontiers in Bioengineering and Biotechnology*, 8. <https://www.frontiersin.org/articles/10.3389/fbioe.2020.597738>
- Hamill, J., Bates, B. T., Knutzen, K. M., & Sawhill, J. A. (1983). Variations in ground reaction force parameters at different running speeds. *Human Movement Science*, 2(1), 47–56. [https://doi.org/10.1016/0167-9457\(83\)90005-2](https://doi.org/10.1016/0167-9457(83)90005-2)
- Hamner, S. R., Seth, A., & Delp, S. L. (2010). Muscle contributions to propulsion and support during running. *Journal of Biomechanics*, 43(14), 2709–2716. <https://doi.org/10.1016/j.jbiomech.2010.06.025>
- Handsaker, J. C., Forrester, S. E., Folland, J. P., Black, M. I., & Allen, S. J. (2016). A kinematic algorithm to identify gait events during running at different speeds and with different footstrike types. *Journal of Biomechanics*, 49(16), 4128–4133. <https://doi.org/10.1016/j.jbiomech.2016.10.013>
- Hanley, B., & Mohan, A. K. (2014). Changes in gait during constant pace treadmill running. *Journal of Strength and Conditioning Research*, 28(5), 1219–1225. <https://doi.org/10.1519/JSC.0b013e3182a38796>
- Harmison, R. J. (2006). Peak performance in sport: Identifying ideal performance states and developing athletes' psychological skills. *Professional Psychology: Research and Practice*, 37(3), 233–243. <https://doi.org/10.1037/0735-7028.37.3.233>
- Hastie, T., Friedman, J., & Tibshirani, R. (2001). Linear Methods for Regression. In T. Hastie, J. Friedman, & R. Tibshirani (Eds.), *The Elements of Statistical Learning: Data Mining, Inference, and Prediction* (pp. 41–78). Springer. https://doi.org/10.1007/978-0-387-21606-5_3
- Hastie, T., Friedman, J., & Tibshirani, R. (2008a). Basis Expansions and Regularization. In T. Hastie, J. Friedman, & R. Tibshirani (Eds.), *The Elements of Statistical Learning: Data Mining, Inference, and Prediction* (pp. 115–163). Springer. https://doi.org/10.1007/978-0-387-21606-5_5
- Hastie, T., Friedman, J., & Tibshirani, R. (2008b). Neural Networks. In T. Hastie, J. Friedman, & R. Tibshirani (Eds.), *The Elements of Statistical Learning: Data Mining, Inference, and Prediction* (pp. 347–369). Springer. https://doi.org/10.1007/978-0-387-21606-5_11
- Haugen, T., & Buchheit, M. (2016). Sprint Running Performance Monitoring: Methodological and Practical Considerations. *Sports Medicine*, 46(5), 641–656. <https://doi.org/10.1007/s40279-015-0446-0>
- Haugen, T., Sandbakk, Ø., Seiler, S., & Tønnessen, E. (2022). The Training Characteristics of World-Class Distance Runners: An Integration of Scientific Literature and Results-Proven Practice. *Sports Medicine - Open*, 8(1), 46. <https://doi.org/10.1186/s40798-022-00438-7>
- Hausdorff, J. M. (2007). Gait dynamics, fractals and falls: Finding meaning in the stride-to-stride fluctuations of human walking. *Human Movement Science*, 26(4), 555–589. <https://doi.org/10.1016/j.humov.2007.05.003>

-
- Hauswirth, C., & Brisswalter, J. (2008). Strategies for Improving Performance in Long Duration Events. *Sports Medicine*, 38(11), 881–891. <https://doi.org/10.2165/00007256-200838110-00001>
- Havens, K. L., & Sigward, S. M. (2015). Whole body mechanics differ among running and cutting maneuvers in skilled athletes. *Gait & Posture*, 42(3), 240–245. <https://doi.org/10.1016/j.gaitpost.2014.07.022>
- Hayes, P., & Caplan, N. (2012). Foot strike patterns and ground contact times during high-calibre middle-distance races. *Journal of Sports Sciences*, 30(12), 1275–1283.
- Heglund, N. C., & Taylor, C. R. (1988). Speed, stride frequency and energy cost per stride: How do they change with body size and gait? *Journal of Experimental Biology*, 138(1), 301–318. <https://doi.org/10.1242/jeb.138.1.301>
- Heiderscheit, B. C., Chumanov, E. S., Michalski, M. P., Wille, C. M., & Ryan, M. B. (2011). Effects of Step Rate Manipulation on Joint Mechanics during Running. *Medicine and Science in Sports and Exercise*, 43(2), 296–302. <https://doi.org/10.1249/MSS.0b013e3181ebedf4>
- Herren, R., Sparti, A., Aminian, K., & Schutz, Y. (1999). The prediction of speed and incline in outdoor running in humans using accelerometry. *Medicine and Science in Sports and Exercise*, 31(7), 1053–1059. <https://doi.org/10.1097/00005768-199907000-00020>
- Higginson, B. K. (2009). Methods of Running Gait Analysis. *Current Sports Medicine Reports*, 8(3), 136–141. <https://doi.org/10.1249/JSR.0b013e3181a6187a>
- Hill, D. W., & Rowell, A. L. (1996). Running velocity at VO₂max. *Medicine and Science in Sports and Exercise*, 28(1), 114–119. <https://doi.org/10.1097/00005768-199601000-00022>
- Hoenig, T., Hamacher, D., Braumann, K.-M., Zech, A., & Hollander, K. (2018). Analysis of running stability during 5000 m running*. *European Journal of Sport Science*. <https://doi.org/10.1080/17461391.2018.1519040>
- Hoenig, T., Rolvien, T., & Hollander, K. (2020). Footstrike patterns in runners: Concepts, classifications, techniques, and implications for running-related injuries. *Deutsche Zeitschrift Für Sportmedizin*, 71(3), 55–61. <https://doi.org/10.5960/dzsm.2020.424>
- Hofmann-Wellenhof, B., Lichtenegger, H., & Collins, J. (2012). *Global Positioning System: Theory and Practice*. Springer Science & Business Media.
- Hopkins, W. G., Marshall, S. W., Batterham, A. M., & Hanin, J. (2009). Progressive statistics for studies in sports medicine and exercise science. *Medicine and Science in Sports and Exercise*, 41(1), 3–13. <https://doi.org/10.1249/MSS.0b013e31818cb278>
- Hreljac, A. (2004). Impact and Overuse Injuries in Runners. *Medicine and Science in Sports and Exercise*, 36(5), 845–849. <https://doi.org/10.1249/01.MSS.0000126803.66636.DD>
- Huang, Y., Xia, H., Chen, G., Cheng, S., Cheung, R. T. H., & Shull, P. B. (2019). Foot strike pattern, step rate, and trunk posture combined gait modifications to reduce impact loading during running. *Journal of Biomechanics*, 86, 102–109. <https://doi.org/10.1016/j.jbiomech.2019.01.058>
- Hübscher, M., Zech, A., Pfeifer, K., Hänsel, F., Vogt, L., & Banzer, W. (2010). Neuromuscular Training for Sports Injury Prevention: A Systematic Review. *Medicine & Science in Sports & Exercise*, 42(3), 413–421. <https://doi.org/10.1249/MSS.0b013e3181b88d37>
- Hulin, B. T., Gabbett, T. J., Lawson, D. W., Caputi, P., & Sampson, J. A. (2016). The acute:chronic workload ratio predicts injury: High chronic workload may decrease injury risk in elite rugby league players. *British Journal of Sports Medicine*, 50(4), 231–236. <https://doi.org/10.1136/bjsports-2015-094817>
- Hunt, K. D. (1991). Mechanical implications of chimpanzee positional behavior. *American Journal of Physical Anthropology*, 86(4), 521–536. <https://doi.org/10.1002/ajpa.1330860408>
- Iaia, F. M., & Bangsbo, J. (2010). Speed endurance training is a powerful stimulus for physiological adaptations and performance improvements of athletes. *Scandinavian Journal of Medicine & Science in Sports*, 20(s2), 11–23. <https://doi.org/10.1111/j.1600-0838.2010.01193.x>
- Imbach, F., Candau, R., Chailan, R., & Perrey, S. (2020). Validity of the Stryd Power Meter in Measuring Running Parameters at Submaximal Speeds. *Sports*, 8(7), 7. <https://doi.org/10.3390/sports8070103>
- Impellizzeri, F. M., Marcora, S. M., & Coutts, A. J. (n.d.). Internal and External Training Load: 15 Years On. *International Journal of Sports Physiology and Performance*, 14(2), 270–273. <https://doi.org/10.1123/ijsspp.2018-0935>
- Jain, A., Nandakumar, K., & Ross, A. (2005). Score normalization in multimodal biometric systems. *Pattern Recognition*, 38(12), 2270–2285. <https://doi.org/10.1016/j.patcog.2005.01.012>
- Jaskólski, A., Veenstra, B., Goossens, P., Jaskólska, A., & Skinner, J. S. (1996). Optimal resistance for maximal power during treadmill running. *Sports Medicine, Training and Rehabilitation*, 7(1), 17–30. <https://doi.org/10.1080/15438629609512067>
- Jenny, D. F., & Jenny, P. (2020). On the mechanical power output required for human running – Insight from an analytical model. *Journal of Biomechanics*, 110, 109948. <https://doi.org/10.1016/j.jbiomech.2020.109948>
- Jewell, C., Boyer, K. A., & Hamill, J. (2017). Do footfall patterns in forefoot runners change over an exhaustive run? *Journal of Sports Sciences*, 35(1), 74–80. <https://doi.org/10.1080/02640414.2016.1156726>
- Johnston, M., Cook, C. J., Crewther, B. T., Drake, D., & Kilduff, L. P. (2015). Neuromuscular, physiological and endocrine responses to a maximal speed training session in elite games players. *European Journal of Sport Science*, 15(6), 550–556. <https://doi.org/10.1080/17461391.2015.1010107>

-
- Johnston, W., O'Reilly, M., Dolan, K., Reid, N., Coughlan, G., & Caulfield, B. (2016). *Objective Classification of Dynamic Balance Using a Single Wearable Sensor*. 15–24. <https://doi.org/10.5220/0006079400150024>
- Jones, C. M., Griffiths, P. C., & Mellalieu, S. D. (2017). Training Load and Fatigue Marker Associations with Injury and Illness: A Systematic Review of Longitudinal Studies. *Sports Medicine*, 47(5), 943–974. <https://doi.org/10.1007/s40279-016-0619-5>
- Jones, P. A., Thomas, C., Dos'Santos, T., McMahon, J. J., & Graham-Smith, P. (2017). The role of eccentric strength in 180 turns in female soccer players. *Sports*, 5(2), 42.
- Kammoun, N., Apte, A., Karami, H., & Aminian, K. (2022). Estimation of temporal parameters during running with a wrist-worn inertial sensor: An in-field validation (accepted). *2022 44th Annual International Conference of the IEEE Engineering in Medicine Biology Society (EMBC)*. 2022 44th Annual International Conference of the IEEE Engineering in Medicine Biology Society (EMBC).
- Kamuk, Y. U. (2020). Reliability and validity of a novel agility measurement device for badminton players. *African Educational Research Journal*, 8(1), 54–61.
- Kasper, K. (2019). Sports Training Principles. *Current Sports Medicine Reports*, 18(4), 95–96. <https://doi.org/10.1249/JSR.0000000000000576>
- Keller, T., Weisberger, A., Ray, J., Hasan, S., Shiavi, R., & Spengler, D. (1996). Relationship between vertical ground reaction force and speed during walking, slow jogging, and running. *Clinical Biomechanics*, 11(5), 253–259. [https://doi.org/10.1016/0268-0033\(95\)00068-2](https://doi.org/10.1016/0268-0033(95)00068-2)
- Kellmann, M., Bertollo, M., Bosquet, L., Brink, M., Coutts, A. J., Duffield, R., Erlacher, D., Halson, S. L., Hecksteden, A., Heidari, J., Wolfgang Kallus, K., Meeusen, R., Mujika, I., Robazza, C., Skorski, S., Venter, R., & Beckmann, J. (2018). Recovery and performance in sport: Consensus statement. *International Journal of Sports Physiology and Performance*, 13(2), 240–245. <https://doi.org/10.1123/ijsp.2017-0759>
- Kendall, A., Grimes, M., & Cipolla, R. (2015). *PoseNet: A convolutional network for real-time 6-dof camera relocation*. IEEE. <https://doi.org/10.17863/CAM.26495>
- Kiely, J., Pickering, C., & Collins, D. J. (2019). Smoothness: An Unexplored Window into Coordinated Running Proficiency. *Sports Medicine - Open*, 5(1), 43. <https://doi.org/10.1186/s40798-019-0215-y>
- Kim, K. J., Gailey, R., Agrawal, V., Gaunaud, I., Feigenbaum, L., Bennett, C., Felt, V., & Best, T. M. (2020). Quantification of Agility Testing with Inertial Sensors after a Knee Injury. *Medicine and Science in Sports and Exercise*, 52(1), 244–251.
- King, A. D. (1998). Inertial Navigation—Forty Years of Evolution. *Undefined*. <https://www.semanticscholar.org/paper/Inertial-Navigation-Forty-Years-of-Evolution-King/b67513d4d222eee35409b8e03d52ae52bc8346b0>
- Kiviniemi, A. M., Hautala, A. J., Kinnunen, H., & Tulppo, M. P. (2007). Endurance training guided individually by daily heart rate variability measurements. *European Journal of Applied Physiology*, 101(6), 743–751. <https://doi.org/10.1007/s00421-007-0552-2>
- Kluitenberg, B., Bredeweg, S. W., Zijlstra, S., Zijlstra, W., & Buist, I. (2012). Comparison of vertical ground reaction forces during overground and treadmill running. A validation study. *BMC Musculoskeletal Disorders*, 13(1), 1–8. <https://doi.org/10.1186/1471-2474-13-235>
- Knicker, A. J., Renshaw, I., Oldham, A. R. H., & Cairns, S. P. (2011). Interactive processes link the multiple symptoms of fatigue in sport competition. *Sports Medicine*, 41(4), 307–328. <https://doi.org/10.2165/11586070-000000000-00000> PM - 21425889
- Koblbauer, I. F., van Schooten, K. S., Verhagen, E. A., & van Dieën, J. H. (2014). Kinematic changes during running-induced fatigue and relations with core endurance in novice runners. *Journal of Science and Medicine in Sport*, 17(4), 419–424. <https://doi.org/10.1016/j.jsams.2013.05.013>
- Kok, M., & Schön, T. B. (2016). Magnetometer Calibration Using Inertial Sensors. *IEEE Sensors Journal*, 16(14), 5679–5689. <https://doi.org/10.1109/JSEN.2016.2569160>
- Kraskov, A., Stögbauer, H., & Grassberger, P. (2004). Estimating mutual information. *Physical Review E*, 69(6), 066138. <https://doi.org/10.1103/PhysRevE.69.066138>
- Kreher, J. B., & Schwartz, J. B. (2012). Overtraining Syndrome. *Sports Health*, 4(2), 128–138. <https://doi.org/10.1177/1941738111434406>
- Kyröläinen, H., Avela, J., & Komi, P. V. (2005). Changes in muscle activity with increasing running speed. *Journal of Sports Sciences*, 23(10), 1101–1109. <https://doi.org/10.1080/02640410400021575>
- Larson, P., Higgins, E., Kaminski, J., Decker, T., Preble, J., Lyons, D., McIntyre, K., & Normile, A. (2011). Foot strike patterns of recreational and sub-elite runners in a long-distance road race. *Journal of Sports Sciences*, 29(15), 1665–1673. <https://doi.org/10.1080/02640414.2011.610347>
- Laursen, P. B. (2010). Training for intense exercise performance: High-intensity or high-volume training? *Scandinavian Journal of Medicine and Science in Sports*, 20(SUPPL. 2), 1–10. <https://doi.org/10.1111/j.1600-0838.2010.01184.x>
- Lee, J. B., James, D. A., Ohgi, Y., & Yamanaka, S. (2012). Monitoring sprinting gait temporal kinematics of an athlete aiming for the 2012 London Paralympics. *Procedia Engineering*, 34, 778–783. <https://doi.org/10.1016/j.proeng.2012.04.133>

- Lee, J. B., Mellifont, R. B., & Burkett, B. J. (2010). The use of a single inertial sensor to identify stride, step, and stance durations of running gait. *Journal of Science and Medicine in Sport*, 13(2), 270–273. <https://doi.org/10.1016/j.jsams.2009.01.005>
- Lee, J. B., Sutter, K. J., Askew, C. D., & Burkett, B. J. (2010). Identifying symmetry in running gait using a single inertial sensor. *Journal of Science and Medicine in Sport*, 13(5), 559–563. <https://doi.org/10.1016/j.jsams.2009.08.004>
- Lees, A. (2002). Technique analysis in sports: A critical review. *Journal of Sports Sciences*, 20(10), 813–828. <https://doi.org/10.1080/026404102320675657>
- Léger, L. A., Mercier, D., Gadoury, C., & Lambert, J. (1988). The multistage 20 metre shuttle run test for aerobic fitness. *Journal of Sports Sciences*, 6(2), 93–101. <https://doi.org/10.1080/02640418808729800>
- Léger, L., & Boucher, R. (1980). An indirect continuous running multistage field test: The Université de Montréal track test. *Canadian Journal of Applied Sport Sciences. Journal Canadien Des Sciences Appliquees Au Sport*, 5(2), 77–84.
- Léger, L., & Mercier, D. (1984). Gross Energy Cost of Horizontal Treadmill and Track Running. *Sports Medicine*, 1(4), 270–277. <https://doi.org/10.2165/00007256-198401040-00003>
- Lehmann, M. J., Lormes, W., Opitz-Gress, A., Steinacker, J. M., Netzer, N., Foster, C., & Gastmann, U. (1997). Training and overtraining: An overview and experimental results in endurance sports. *The Journal of Sports Medicine and Physical Fitness*, 37(1), 7–17.
- Leitch, J., Stebbins, J., Paolini, G., & Zavatsky, A. B. (2011). Identifying gait events without a force plate during running: A comparison of methods. *Gait & Posture*, 33(1), 130–132. <https://doi.org/10.1016/j.gaitpost.2010.06.009>
- Lenhart, R., Thelen, D., & Heiderscheit, B. (2014). Hip Muscle Loads During Running at Various Step Rates. *Journal of Orthopaedic & Sports Physical Therapy*. <https://doi.org/10.2519/jospt.2014.5575>
- Leveritt, M., Abernethy, P. J., Barry, B. K., & Logan, P. A. (1999). Concurrent Strength and Endurance Training. *Sports Medicine*, 28(6), 413–427. <https://doi.org/10.2165/00007256-199928060-00004>
- Li, J., Cheng, K., Wang, S., Morstatter, F., Trevino, R. P., Tang, J., & Liu, H. (2017). Feature Selection: A Data Perspective. *ACM Computing Surveys*, 50(6), 94:1-94:45. <https://doi.org/10.1145/3136625>
- Liberati, A., Altman, D. G., Tetzlaff, J., Mulrow, C., Gøtzsche, P. C., Ioannidis, J. P. A., Clarke, M., Devereaux, P. J., Kleijnen, J., & Moher, D. (2009). The PRISMA Statement for Reporting Systematic Reviews and Meta-Analyses of Studies That Evaluate Health Care Interventions: Explanation and Elaboration. *PLoS Medicine*, 6(7), e1000100. <https://doi.org/10.1371/journal.pmed.1000100>
- Lieberman, D. E., Venkadesan, M., Werbel, W. A., Daoud, A. I., D’Andrea, S., Davis, I. S., Mang’Eni, R. O., & Pitsiladis, Y. (2010). Foot strike patterns and collision forces in habitually barefoot versus shod runners. *Nature*, 463(7280), 7280. <https://doi.org/10.1038/nature08723>
- Lin, L. I.-K. (1989). A Concordance Correlation Coefficient to Evaluate Reproducibility. *Biometrics*, 45(1), 255–268. <https://doi.org/10.2307/2532051>
- Loh, W.-Y. (2011). Classification and regression trees. *WIREs Data Mining and Knowledge Discovery*, 1(1), 14–23. <https://doi.org/10.1002/widm.8>
- Luca, C. J. D. (1997). The Use of Surface Electromyography in Biomechanics. *Journal of Applied Biomechanics*, 13(2), 135–163. <https://doi.org/10.1123/jab.13.2.135>
- Lupo, C., Ungureanu, A. N., Varalda, M., & Brustio, P. R. (2019). Running technique is more effective than soccer-specific training for improving the sprint and agility performances with ball possession of prepubescent soccer players. *Biology of Sport*, 36(3), 249–255. <https://doi.org/10.5114/biolosport.2019.87046>
- Lussiana, T., & Gindre, C. (2015). Feel your stride and find your preferred running speed. *Biology Open*, 5(1), 45–48. <https://doi.org/10.1242/bio.014886>
- Maas, E., De Bie, J., Vanfleteren, R., Hoogkamer, W., & Vanwanseele, B. (2018). Novice runners show greater changes in kinematics with fatigue compared with competitive runners. *Sports Biomechanics*, 17(3), 350–360.
- Madden, C., Putukian, M., McCarty, E., & Young, C. (2013). *Netter’s Sports Medicine E-Book*. Elsevier Health Sciences.
- Madgwick, S. O. H., Harrison, A. J. L., & Vaidyanathan, R. (2011). Estimation of IMU and MARG orientation using a gradient descent algorithm. *2011 IEEE International Conference on Rehabilitation Robotics*, 1–7. <https://doi.org/10.1109/ICORR.2011.5975346>
- Magee, D. J. (2014). *Orthopedic physical assessment*. (Sixth edition). Elsevier Saunders. <http://public.ebookcentral.proquest.com/choice/publicfullrecord.aspx?p=2074410>
- Mai, P., & Willwacher, S. (2019). Effects of low-pass filter combinations on lower extremity joint moments in distance running. *Journal of Biomechanics*, 95, 109311. <https://doi.org/10.1016/j.jbiomech.2019.08.005>
- Maloney, S. J., Richards, J., Nixon, D. G., Harvey, L. J., & Fletcher, I. M. (2017). Do stiffness and asymmetries predict change of direction performance? *Journal of Sports Sciences*, 35(6), 547–556.
- Mann, R. A., & Hagy, J. (1980). Biomechanics of walking, running, and sprinting. *The American Journal of Sports Medicine*, 8(5), 345–350. <https://doi.org/10.1177/036354658000800510>
- Mann, R., Malisoux, L., Brunner, R., Gette, P., Urhausen, A., Statham, A., Meijer, K., & Theisen, D. (2014). Reliability and validity of pressure and temporal parameters recorded using a pressure-sensitive insole during running. *Gait & Posture*, 39(1), 455–459. <https://doi.org/10.1016/j.gaitpost.2013.08.026>

-
- Mann, T., Lamberts, R. P., & Lambert, M. I. (2013). Methods of Prescribing Relative Exercise Intensity: Physiological and Practical Considerations. *Sports Medicine*, 43(7), 613–625. <https://doi.org/10.1007/s40279-013-0045-x>
- Mansfield, E. R., & Helms, B. P. (1982). Detecting Multicollinearity. *The American Statistician*, 36(3a), 158–160. <https://doi.org/10.1080/00031305.1982.10482818>
- Marcora, S. M., & Bosio, A. (2007). Effect of exercise-induced muscle damage on endurance running performance in humans. *Scandinavian Journal of Medicine & Science in Sports*, 17(6), 662–671. <https://doi.org/10.1111/j.1600-0838.2006.00627.x>
- Marey, E.-J. (1890). *Physiologie du mouvement: Vol des oiseaux*. G. Masson.
- Marshall, B. M., Franklyn-Miller, A. D., King, E. A., Moran, K. A., Strike, S. C., & Falvey, É. C. (2014). Biomechanical factors associated with time to complete a change of direction cutting maneuver. *The Journal of Strength & Conditioning Research*, 28(10), 2845–2851.
- Matthews, M. J., Heron, K., Todd, S., Tomlinson, A., Jones, P., Delestrat, A., & Cohen, D. D. (2017). Strength and endurance training reduces the loss of eccentric hamstring torque observed after soccer specific fatigue. *Physical Therapy in Sport*, 25, 39–46.
- Maurer, A. P., Burke, S. N., Lipa, P., Skaggs, W. E., & Barnes, C. A. (2012). Greater running speeds result in altered hippocampal phase sequence dynamics. *Hippocampus*, 22(4), 737–747. <https://doi.org/10.1002/hipo.20936>
- Mayorga-Vega, D., Bocanegra-Parrilla, R., Ornelas, M., & Viciana, J. (2016). Criterion-Related Validity of the Distance- and Time-Based Walk/Run Field Tests for Estimating Cardiorespiratory Fitness: A Systematic Review and Meta-Analysis. *PLOS ONE*, 11(3), e0151671. <https://doi.org/10.1371/journal.pone.0151671>
- McBurnie, A. J., Dos'Santos, T., & Jones, P. A. (2021). Biomechanical Associates of Performance and Knee Joint Loads During A 70–90° Cutting Maneuver in Subelite Soccer Players. *Journal of Strength and Conditioning Research*, 35(11), 3190–3198. <https://doi.org/10.1519/JSC.0000000000003252>
- McGawley, K. (2017). The Reliability and Validity of a Four-Minute Running Time-Trial in Assessing V'O₂max and Performance. *Frontiers in Physiology*, 8. <https://www.frontiersin.org/articles/10.3389/fphys.2017.00270>
- McGinnis, R. S., Cain, S. M., Davidson, S. P., Vitali, R. V., McLean, S. G., & Perkins, N. C. (2017). Inertial sensor and cluster analysis for discriminating agility run technique and quantifying changes across load. *Biomedical Signal Processing and Control*, 32, 150–156. <https://doi.org/10.1016/j.bspc.2016.10.013>
- McLaren, S. J., Macpherson, T. W., Coutts, A. J., Hurst, C., Spears, I. R., & Weston, M. (2018). The Relationships Between Internal and External Measures of Training Load and Intensity in Team Sports: A Meta-Analysis. *Sports Medicine*, 48(3), 641–658. <https://doi.org/10.1007/s40279-017-0830-z>
- McMahon, T. A., & Greene, P. R. (1979). The influence of track compliance on running. *Journal of Biomechanics*, 12(12), 893–904. [https://doi.org/10.1016/0021-9290\(79\)90057-5](https://doi.org/10.1016/0021-9290(79)90057-5)
- McNaughton, L., Hall, P., & Cooley, D. (1998). Validation of Several Methods of Estimating Maximal Oxygen Uptake in Young Men. *Perceptual and Motor Skills*, 87(2), 575–584. <https://doi.org/10.2466/pms.1998.87.2.575>
- Meardon, S. A., Hamill, J., & Derrick, T. R. (2011). Running injury and stride time variability over a prolonged run. *Gait & Posture*, 33(1), 36–40. <https://doi.org/10.1016/j.gaitpost.2010.09.020>
- Meghji, M., Balloch, A., Habibi, D., Ahmad, I., Hart, N., Newton, R., Weber, J., & Waqar, A. (2019). An Algorithm for the Automatic Detection and Quantification of Athletes' Change of Direction Incidents Using IMU Sensor Data. *IEEE Sensors Journal*, 19(12), 4518–4527. <https://doi.org/10.1109/JSEN.2019.2898449>
- Mendiguchia, J., Samozino, P., Martinez-Ruiz, E., Brughelli, M., Schmikli, S., Morin, J.-B., & Mendez-Villanueva, A. (2014). Progression of Mechanical Properties during On-field Sprint Running after Returning to Sports from a Hamstring Muscle Injury in Soccer Players. *International Journal of Sports Medicine*, 35(8), 690–695. <https://doi.org/10.1055/s-0033-1363192>
- Mercer, J. A., Bates, B. T., Dufek, J. S., & Hreljac, A. (2003). Characteristics of shock attenuation during fatigued running. *Journal of Sports Science*, 21(11), 911–919. <https://doi.org/10.1080/0264041031000140383>
- Methods, P. E., Yanci, J., Granados, C., Goosey-, V., Science, S., Sciences, H., & Peter, T. (2015). Note. This article will be published in a forthcoming issue of the International Journal of Sports Physiology and Performance. The article appears here in its accepted , peer-reviewed form , as it was provided by the submitting author. It has not been .
- Meyer, F., Falbriard, M., Mariani, B., Aminian, K., & Millet, G. P. (2021a). Continuous Analysis of Marathon Running Using Inertial Sensors: Hitting Two Walls? *International Journal of Sports Medicine*. <https://doi.org/10.1055/a-1432-2336> PM - 33975367
- Meyer, F., Falbriard, M., Mariani, B., Aminian, K., & Millet, G. P. (2021b). Continuous Analysis of Marathon Running Using Inertial Sensors: Hitting Two Walls? *International Journal of Sports Medicine*, 42(13), 1182–1190. <https://doi.org/10.1055/a-1432-2336>
- Meyer, F., Waegli, A., Ducret, S., Skalous, J., & Pesty, R. (2007, January 1). *Assessment of Timing and Performance based on Trajectories from low-cost GPS/INS Positioning*. International Congress on Science and Skiing, St-Christoph am Aarberg.
- Micklewright, D., St Clair Gibson, A., Gladwell, V., & Al Salman, A. (2017). Development and Validity of the Rating-of-Fatigue Scale. *Sports Medicine*, 47(11), 2375–2393. <https://doi.org/10.1007/s40279-017-0711-5>

-
- Miles, H. C., Pop, S. R., Watt, S. J., Lawrence, G. P., & John, N. W. (2012). A review of virtual environments for training in ball sports. *Computers & Graphics*, 36(6), 714–726. <https://doi.org/10.1016/j.cag.2012.04.007>
- Milgrom, C., Finestone, A., Segev, S., Olin, C., Arndt, T., & Ekenman, I. (2003). Are overground or treadmill runners more likely to sustain tibial stress fracture? *British Journal of Sports Medicine*, 37(2), 160–163. <https://doi.org/10.1136/bjism.37.2.160>
- Millet, G. Y. (2011). Can Neuromuscular Fatigue Explain Running Strategies and Performance in Ultra-Marathons? *Sports Medicine*, 41(6), 489–506. <https://doi.org/10.2165/11588760-000000000-00000>
- Millet, G. Y., & Lepers, R. (2004). Alterations of neuromuscular function after prolonged running, cycling and skiing exercises. *Sports Medicine*, 34(2), 105–116. <https://doi.org/10.2165/00007256-200434020-00004>
- Mitschke, C., Zaumseil, F., & Milani, T. L. (2017). The influence of inertial sensor sampling frequency on the accuracy of measurement parameters in rearfoot running. *Computer Methods in Biomechanics and Biomedical Engineering*, 20(14), 1502–1511. <https://doi.org/10.1080/10255842.2017.1382482>
- Mizrahi, J., Verbitsky, O., & Isakov, E. (2000). *Fatigue-Related Loading Imbalance on the Shank in Running: A Possible Factor in Stress Fractures*. <https://link.springer.com/content/pdf/10.1114%2F1.284.pdf>
- Mizrahi, J., Verbitsky, O., Isakov, E., & Daily, D. (2000). Effect of fatigue on leg kinematics and impact acceleration in long distance running. *Human Movement Science*, 19(2), 139–151. [https://doi.org/10.1016/S0167-9457\(00\)00013-0](https://doi.org/10.1016/S0167-9457(00)00013-0)
- Mo, S., & Chow, D. H. K. (2018a). Stride-to-stride variability and complexity between novice and experienced runners during a prolonged run at anaerobic threshold speed. *Gait & Posture*, 64, 7–11. <https://doi.org/10.1016/j.gaitpost.2018.05.021>
- Mo, S., & Chow, D. H. K. (2018b). Differences in lower-limb coordination and coordination variability between novice and experienced runners during a prolonged treadmill run at anaerobic threshold speed. *Journal of Sports Sciences*, 1–8. <https://doi.org/10.1080/02640414.2018.1539294>
- Möhler, F., Fadilioglu, C., & Stein, T. (2021). Fatigue-Related Changes in Spatiotemporal Parameters, Joint Kinematics and Leg Stiffness in Expert Runners During a Middle-Distance Run. *Frontiers in Sports and Active Living*, 3, 23.
- Moncada-Torres, A., Leuenberger, K., Gonzenbach, R., Luft, A., & Gassert, R. (2014). Activity classification based on inertial and barometric pressure sensors at different anatomical locations. *Physiological Measurement*, 35(7), 1245–1263. <https://doi.org/10.1088/0967-3334/35/7/1245>
- Moore, I. S. (2016). Is There an Economical Running Technique? A Review of Modifiable Biomechanical Factors Affecting Running Economy. *Sports Medicine*, 46(6), 793–807. <https://doi.org/10.1007/s40279-016-0474-4>
- Moore, I. S., Ashford, K. J., Cross, C., Hope, J., Jones, H. S. R., & McCarthy-Ryan, M. (2019). Humans Optimize Ground Contact Time and Leg Stiffness to Minimize the Metabolic Cost of Running. *Frontiers in Sports and Active Living*, 1. <https://www.frontiersin.org/article/10.3389/fspor.2019.00053>
- Moore, I. S., Jones, A. M., & Dixon, S. J. (2016). Reduced oxygen cost of running is related to alignment of the resultant GRF and leg axis vector: A pilot study. *Scandinavian Journal of Medicine & Science in Sports*, 26(7), 809–815. <https://doi.org/10.1111/sms.12514>
- Moore, I. S., & Willy, R. W. (2019). Use of Wearables: Tracking and Retraining in Endurance Runners. *Current Sports Medicine Reports*, 18(12), 437–444. <https://doi.org/10.1249/JSR.0000000000000667>
- Mooses, M., Haile, D. W., Ojiambo, R., Sang, M., Mooses, K., Lane, A. R., & Hackney, A. C. (2021). Shorter Ground Contact Time and Better Running Economy: Evidence From Female Kenyan Runners. *The Journal of Strength & Conditioning Research*, 35(2), 481–486. <https://doi.org/10.1519/JSC.00000000000002669>
- Morel, P. (2018). Gramm: Grammar of graphics plotting in Matlab. *The Journal of Open Source Software*, 3(23), 568. <https://doi.org/10.21105/joss.00568>
- Morgan, D. W., Baldini, F. D., Martin, P. E., & Kohrt, W. M. (1989). Ten kilometer performance and predicted velocity at $\dot{V}O_{2\max}$ among well-trained male runners. *Medicine & Science in Sports & Exercise*, 21(1), 78–83.
- Morgan, D. W., & Daniels, J. T. (1994). Relationship Between $\dot{V}O_{2\max}$ and the Aerobic Demand of Running in Elite Distance Runners. *International Journal of Sports Medicine*, 15(7), 426–429. <https://doi.org/10.1055/s-2007-1021082>
- Morin, J. B., Samozino, P., & Millet, G. Y. (2011). Changes in running kinematics, kinetics, and spring-mass behavior over a 24-h run. *Medicine and Science in Sports and Exercise*. <https://doi.org/10.1249/MSS.0b013e3181fec518>
- Morin, J. B., Tomazin, K., Edouard, P., & Millet, G. Y. (2011). Changes in running mechanics and spring-mass behavior induced by a mountain ultra-marathon race. *Journal of Biomechanics*, 44(6), 1104–1107. <https://doi.org/10.1016/j.jbiomech.2011.01.028>
- Morin, J.-B., Bourdin, M., Edouard, P., Peyrot, N., Samozino, P., & Lacour, J.-R. (2012). Mechanical determinants of 100-m sprint running performance. *European Journal of Applied Physiology*, 112(11), 3921–3930. <https://doi.org/10.1007/s00421-012-2379-8>
- Morin, J.-B., Dalleau, G., Kyröläinen, H., Jeannin, T., & Belli, A. (2005). A Simple Method for Measuring Stiffness during Running. *Journal of Applied Biomechanics*, 21(2), 167–180. <https://doi.org/10.1123/JAB.21.2.167>

-
- Morin, J.-B., Edouard, P., & Samozino, P. (2011). Technical ability of force application as a determinant factor of sprint performance. *Medicine and Science in Sports and Exercise*, 43(9), 1680–1688. <https://doi.org/10.1249/MSS.0b013e318216ea37>
- Morin, J.-B., Jeannin, T., Chevallier, B., & Belli, A. (2006). Spring-Mass Model Characteristics During Sprint Running: Correlation with Performance and Fatigue-Induced Changes. *International Journal of Sports Medicine*, 27(2), 158–165. <https://doi.org/10.1055/s-2005-837569>
- Morin, J.-B., & Samozino, P. (2016). Interpreting Power-Force-Velocity Profiles for Individualized and Specific Training. *International Journal of Sports Physiology and Performance*, 11(2), 267–272. <https://doi.org/10.1123/ijssp.2015-0638>
- Mornieux, G., Gehring, D., Fürst, P., & Gollhofer, A. (2014). Anticipatory postural adjustments during cutting manoeuvres in football and their consequences for knee injury risk. *Journal of Sports Sciences*, 32(13), 1255–1262.
- Morton, R. H. (2006). The critical power and related whole-body bioenergetic models. *European Journal of Applied Physiology*, 96(4), 339–354. <https://doi.org/10.1007/s00421-005-0088-2>
- Mujika, I. (2017). Quantification of Training and Competition Loads in Endurance Sports: Methods and Applications. *International Journal of Sports Physiology and Performance*, 12(s2), S2–17. <https://doi.org/10.1123/ijssp.2016-0403>
- Mulligan, M., Adam, G., & Emig, T. (2018). A minimal power model for human running performance. *PLOS ONE*, 13(11), e0206645. <https://doi.org/10.1371/journal.pone.0206645>
- Muniz-Pardos, B., Sutehall, S., Gellaerts, J., Falbriard, M., Mariani, B., Bosch, A., Asrat, M., Schaible, J., & Pitsiladis, Y. P. (2018). Integration of Wearable Sensors Into the Evaluation of Running Economy and Foot Mechanics in Elite Runners. *Current Sports Medicine Reports*, 17(12), 480–488. <https://doi.org/10.1249/JSR.0000000000000550>
- Muñoz, I., Seiler, S., Bautista, J., España, J., Larumbe, E., & Esteve-Lanao, J. (2014). Does Polarized Training Improve Performance in Recreational Runners? *International Journal of Sports Physiology and Performance*, 9(2), 265–272. <https://doi.org/10.1123/ijssp.2012-0350>
- Muñoz-Jimenez, M., Latorre-Román, P. A., Soto-Hermoso, V. M., & García-Pinillos, F. (2015). Influence of shod/unshod condition and running speed on foot-strike patterns, inversion/eversion, and vertical foot rotation in endurance runners. *Journal of Sports Sciences*, 33(19), 2035–2042. <https://doi.org/10.1080/02640414.2015.1026377>
- Munro, C. F., Miller, D. I., & Fuglevand, A. J. (1987). Ground reaction forces in running: A reexamination. *Journal of Biomechanics*, 20(2), 147–155. [https://doi.org/10.1016/0021-9290\(87\)90306-X](https://doi.org/10.1016/0021-9290(87)90306-X)
- Musgjerd, T., Anason, J., Rutherford, D., & Kernozek, T. W. (n.d.). Effect of Increasing Running Cadence on Peak Impact Force in an Outdoor Environment. *International Journal of Sports Physical Therapy*, 16(4), 1076–1083. <https://doi.org/10.26603/001c.25166>
- Muybridge, J. (1882). The Horse in Motion. *Nature*, 25(652), 652. <https://doi.org/10.1038/025605b0>
- Myer, G. D., Faigenbaum, A. D., Ford, K. R., Best, T. M., Bergeron, M. F., & Hewett, T. E. (2011). When to initiate integrative neuromuscular training to reduce sports-related injuries in youth? *Current Sports Medicine Reports*, 10(3), 155–166. <https://doi.org/10.1249/JSR.0b013e31821b1442>
- Nagahara, R., Botter, A., Rejc, E., Koido, M., Shimizu, T., Samozino, P., & Morin, J.-B. (2017). Concurrent Validity of GPS for Deriving Mechanical Properties of Sprint Acceleration. *International Journal of Sports Physiology and Performance*, 12(1), 129–132. <https://doi.org/10.1123/ijssp.2015-0566>
- Nagel, A., Fernholz, F., Kibele, C., & Rosenbaum, D. (2008). Long distance running increases plantar pressures beneath the metatarsal heads: A barefoot walking investigation of 200 marathon runners. *Gait & Posture*, 27(1), 152–155. <https://doi.org/10.1016/J.GAITPOST.2006.12.012>
- Nakano, N., Sakura, T., Ueda, K., Omura, L., Kimura, A., Iino, Y., Fukushima, S., & Yoshioka, S. (2020). Evaluation of 3D Markerless Motion Capture Accuracy Using OpenPose With Multiple Video Cameras. *Frontiers in Sports and Active Living*, 2. <https://www.frontiersin.org/articles/10.3389/fspor.2020.00050>
- Nakayama, Y., Kudo, K., & Ohtsuki, T. (2010). Variability and fluctuation in running gait cycle of trained runners and non-runners. *Gait & Posture*, 31(3), 331–335. <https://doi.org/10.1016/j.gaitpost.2009.12.003>
- Napier, C., MacLean, C. L., Maurer, J., Taunton, J. E., & Hunt, M. A. (2019). Kinematic Correlates of Kinetic Outcomes Associated With Running-Related Injury. *Journal of Applied Biomechanics*, 35(2), 123–130. <https://doi.org/10.1123/jab.2018-0203>
- Nardone, A., Tarantola, J., Giordano, A., & Schieppati, M. (1997). Fatigue effects on body balance. *Electroencephalography and Clinical Neurophysiology*, 105(4), 309–320. [https://doi.org/10.1016/s0924-980x\(97\)00040-4](https://doi.org/10.1016/s0924-980x(97)00040-4)
- Nedergaard, N. J., Kersting, U., & Lake, M. (2014). Using accelerometry to quantify deceleration during a high-intensity soccer turning manoeuvre. *Journal of Sports Sciences*, 32(20), 1897–1905.
- Nes, B. M., Janszky, I., Wisløff, U., Støylen, A., & Karlsen, T. (2013). Age-predicted maximal heart rate in healthy subjects: The HUNT Fitness Study. *Scandinavian Journal of Medicine & Science in Sports*, 23(6), 697–704. <https://doi.org/10.1111/j.1600-0838.2012.01445.x>
- Neugebauer, J. M., Collins, K. H., & Hawkins, D. A. (2014). Ground Reaction Force Estimates from ActiGraph GT3X+ Hip Accelerations. *PLOS ONE*, 9(6), e99023. <https://doi.org/10.1371/journal.pone.0099023>

-
- Neville, C., Ludlow, C., & Rieger, B. (2015). Measuring postural stability with an inertial sensor: Validity and sensitivity. *Medical Devices: Evidence and Research*, 8, 447–455. <https://doi.org/10.2147/MDER.S91719>
- Newson, R. (2002). Parameters behind “Nonparametric” Statistics: Kendall’s tau, Somers’ D and Median Differences. *The Stata Journal*, 2(1), 45–64. <https://doi.org/10.1177/1536867X0200200103>
- Nicholl, J. P., Coleman, P., & Williams, B. T. (1995). The epidemiology of sports and exercise related injury in the United Kingdom. *British Journal of Sports Medicine*, 29(4), 232–238. <https://doi.org/10.1136/bjism.29.4.232>
- Norris, M., Anderson, R., & Kenny, I. C. (2014). Method analysis of accelerometers and gyroscopes in running gait: A systematic review. *Proceedings of the Institution of Mechanical Engineers, Part P: Journal of Sports Engineering and Technology*, 228(1), 3–15. <https://doi.org/10.1177/1754337113502472>
- Novacheck, T. F. (1998). The biomechanics of running. *Gait & Posture*, 7(1), 77–95. [https://doi.org/10.1016/S0966-6362\(97\)00038-6](https://doi.org/10.1016/S0966-6362(97)00038-6)
- Nummela, A., Keränen, T., & Mikkelsen, L. O. (2007). Factors Related to Top Running Speed and Economy. *International Journal of Sports Medicine*, 28(08), 655–661. <https://doi.org/10.1055/s-2007-964896>
- O’Connor, F. G. (2013). *ACSM’s sports medicine: A comprehensive review*. Wolters Kluwer Health/Lippincott Williams & Wilkins.
- O’gorman, D., Hunter, A., McDONNACHA, C., & Kirwan, J. P. (2000). Validity of Field Tests for Evaluating Endurance Capacity in Competitive and International-Level Sports Participants. *The Journal of Strength & Conditioning Research*, 14(1), 62–67.
- Oh, S. E., Choi, A., & Mun, J. H. (2013). Prediction of ground reaction forces during gait based on kinematics and a neural network model. *Journal of Biomechanics*, 46(14), 2372–2380. <https://doi.org/10.1016/j.jbiomech.2013.07.036>
- Op De Beeck, T., Meert, W., Schutte, K., Vanwanseele, B., & Davis, J. (2018). Fatigue Prediction in Outdoor Runners Via Machine Learning and Sensor Fusion. *KDD’18: PROCEEDINGS OF THE 24TH ACM SIGKDD INTERNATIONAL CONFERENCE ON KNOWLEDGE DISCOVERY & DATA MINING*, 606–615. <https://doi.org/10.1145/3219819.3219864>
- Orendurff, M. S., Kobayashi, T., Tulchin-Francis, K., Tullock, A. M. H., Villarosa, C., Chan, C., Kraus, E., & Strike, S. (2018). A little bit faster: Lower extremity joint kinematics and kinetics as recreational runners achieve faster speeds. *Journal of Biomechanics*, 71, 167–175. <https://doi.org/10.1016/j.jbiomech.2018.02.010>
- Pageaux, B., & Lepers, R. (2016). Fatigue induced by physical and mental exertion increases perception of effort and impairs subsequent endurance performance. *Frontiers in Physiology*, 7(NOV). <https://doi.org/10.3389/fphys.2016.00587>
- Paquette, M. R., Napier, C., Willy, R. W., & Stellingwerff, T. (2020). Moving Beyond Weekly “Distance”: Optimizing Quantification of Training Load in Runners. *Journal of Orthopaedic & Sports Physical Therapy*, 50(10), 564–569. <https://doi.org/10.2519/jospt.2020.9533>
- Paradisi, G. P., Zacharogiannis, E., Mandila, D., Smirtiotou, A., Argeitaki, P., & Cooke, C. B. (2014). Multi-Stage 20-m Shuttle Run Fitness Test, Maximal Oxygen Uptake and Velocity at Maximal Oxygen Uptake. *Journal of Human Kinetics*, 41(1), 81–87. <https://doi.org/10.2478/hukin-2014-0035>
- Passfield, L., Hopker, JG., Jobson, S., Friel, D., & Zabala, M. (2017). Knowledge is power: Issues of measuring training and performance in cycling. *Journal of Sports Sciences*, 35(14), 1426–1434. <https://doi.org/10.1080/02640414.2016.1215504>
- Passfield, L., Murias, J. M., Sacchetti, M., & Nicolò, A. (2022). Validity of the Training-Load Concept. *International Journal of Sports Physiology and Performance*, 17(4), 507–514. <https://doi.org/10.1123/ijsp.2021-0536>
- Paterno, M. V., Schmitt, L. C., Ford, K. R., Rauh, M. J., Myer, G. D., Huang, B., & Hewett, T. E. (2010). Biomechanical Measures during Landing and Postural Stability Predict Second Anterior Cruciate Ligament Injury after Anterior Cruciate Ligament Reconstruction and Return to Sport. *The American Journal of Sports Medicine*, 38(10), 1968–1978. <https://doi.org/10.1177/0363546510376053>
- Pauole, K., Madole, K., Garhammer, J., Lacourse, M., & Rozenek, R. (2000). Reliability and Validity of the T-Test as a Measure of Agility, Leg Power, and Leg Speed in College-Aged Men and Women. *The Journal of Strength & Conditioning Research*, 14(4), 443–450.
- Peltonen, J., Cronin, N. J., Stenroth, L., Finni, T., & Avela, J. (2012). Achilles tendon stiffness is unchanged one hour after a marathon. *Journal of Experimental Biology*, 215(20), 3665–3671. <https://doi.org/10.1242/jeb.068874>
- Peñailillo, L., Silvestre, R., & Nosaka, K. (2013). Changes in surface EMG assessed by discrete wavelet transform during maximal isometric voluntary contractions following supramaximal cycling. *European Journal of Applied Physiology*, 113(4), 895–904. <https://doi.org/10.1007/s00421-012-2499-1>
- Perrey, S., Racinais, S., Saimouaa, K., & Girard, O. (2010). Neural and muscular adjustments following repeated running sprints. *European Journal of Applied Physiology*, 109(6), 1027–1036. <https://doi.org/10.1007/s00421-010-1445-3>
- Pes, B. (2020). Learning From High-Dimensional Biomedical Datasets: The Issue of Class Imbalance. *IEEE Access*, 8, 13527–13540. <https://doi.org/10.1109/ACCESS.2020.2966296>

- Peserico, C. S., & Machado, F. A. (2014). Comparison between running performance in time trials on track and treadmill. *Revista Brasileira de Cineantropometria & Desempenho Humano*, 16, 456–464. <https://doi.org/10.5007/1980-0037.2014v16n4p456>
- Peters, A., Galna, B., Sangeux, M., Morris, M., & Baker, R. (2010). Quantification of soft tissue artifact in lower limb human motion analysis: A systematic review. *Gait & Posture*, 31(1), 1–8. <https://doi.org/10.1016/j.gaitpost.2009.09.004>
- Picerno, P., Camomilla, V., & Capranica, L. (2011). Countermovement jump performance assessment using a wearable 3D inertial measurement unit. *Journal of Sports Sciences*, 29(2), 139–146. <https://doi.org/10.1080/02640414.2010.523089>
- Pickering, C., & Kiely, J. (2019). The Development of a Personalised Training Framework: Implementation of Emerging Technologies for Performance. *Journal of Functional Morphology and Kinesiology*, 4(2), 2. <https://doi.org/10.3390/jfmk4020025>
- Plooi, M., Apte, S., Keller, U., Baines, P., Sterke, B., Asboth, L., Courtine, G., von Zitzewitz, J., & Vallery, H. (2021). Neglected physical human-robot interaction may explain variable outcomes in gait neurorehabilitation research. *Science Robotics*, 6(58), eabf1888. <https://doi.org/10.1126/scirobotics.abf1888>
- Pociello, C. (1999). *La science en mouvements: ??Tienne Marey et Georges Demy : 1870-1920*. Presses universitaires de France.
- Pollard, C. D., Davis, I. M., & Hamill, J. (2004). Influence of gender on hip and knee mechanics during a randomly cued cutting maneuver. *Clinical Biomechanics*, 19(10), 1022–1031. <https://doi.org/10.1016/j.clinbiomech.2004.07.007>
- Pontzer, H., Holloway, J. H., Holloway, J. H., Raichlen, D. A., & Lieberman, D. E. (2009). Control and function of arm swing in human walking and running. *The Journal of Experimental Biology*, 212(Pt 4), 523–534. <https://doi.org/10.1242/jeb.024927>
- Preece, S. J., Bramah, C., & Mason, D. (2019). The biomechanical characteristics of high-performance endurance running. *European Journal of Sport Science*, 19(6), 784–792. <https://doi.org/10.1080/17461391.2018.1554707>
- Prigent, G., Apte, S., Paraschiv-Ionescu, Anisoara, Besson, C., Gremeaux, V., & Aminian, K. (2022). Concurrent evolution of biomechanical and physiological parameters with running-induced acute fatigue. *Frontiers in Physiology*, 74. <https://www.frontiersin.org/articles/10.3389/fphys.2022.814172/abstract>
- Provot, T., Nadjem, A., Valdes-Tamayo, L., Bourgain, M., & Chimentin, X. (2021). Does exhaustion modify acceleration running signature? *Sports Biomechanics*, 0(0), 1–11. <https://doi.org/10.1080/14763141.2021.1974930>
- Quinn, T. J., Dempsey, S. L., LaRoche, D. P., Mackenzie, A. M., & Cook, S. B. (2021). Step Frequency Training Improves Running Economy in Well-Trained Female Runners. *The Journal of Strength & Conditioning Research*, 35(9), 2511–2517. <https://doi.org/10.1519/JSC.0000000000003206>
- Rabita, G., Couturier, A., Dorel, S., Hausswirth, C., & Le Meur, Y. (2013). Changes in spring-mass behavior and muscle activity during an exhaustive run at $\dot{V}O_2\text{max}$. *Journal of Biomechanics*, 46(12), 2011–2017. <https://doi.org/10.1016/j.jbiomech.2013.06.011>
- Rabita, G., Dorel, S., Slawinski, J., Sàez-de-Villarreal, E., Couturier, A., Samozino, P., & Morin, J.-B. (2015). Sprint mechanics in world-class athletes: A new insight into the limits of human locomotion. *Scandinavian Journal of Medicine & Science in Sports*, 25(5), 583–594. <https://doi.org/10.1111/sms.12389>
- Racinais, S., Girard, O., Micallef, J. P., & Perrey, S. (2007). Failed Excitability of Spinal Motoneurons Induced by Prolonged Running Exercise. *J Neuro-Physiol*, 97, 596–603. <https://doi.org/10.1152/jn.00903.2006>
- Radzak, K. N., Putnam, A. M., Tamura, K., Hetzler, R. K., & Stickley, C. D. (2017). Asymmetry between lower limbs during rested and fatigued state running gait in healthy individuals. *Gait & Posture*, 51, 268–274. <https://doi.org/10.1016/j.gaitpost.2016.11.005>
- Raglin, J. S. (2001). Psychological Factors in Sport Performance. *Sports Medicine*, 31(12), 875–890. <https://doi.org/10.2165/00007256-200131120-00004>
- Rajagopal, A., Dembia, C. L., DeMers, M. S., Delp, D. D., Hicks, J. L., & Delp, S. L. (2016). Full-Body Musculoskeletal Model for Muscle-Driven Simulation of Human Gait. *IEEE Transactions on Biomedical Engineering*, 63(10), 2068–2079. <https://doi.org/10.1109/TBME.2016.2586891>
- Ranacher, P., Brunauer, R., Trutschnig, W., Van der Spek, S., & Reich, S. (2016). Why GPS makes distances bigger than they are. *International Journal of Geographical Information Science*, 30(2), 316–333. <https://doi.org/10.1080/13658816.2015.1086924>
- Reilly, T., Morris, T., & Whyte, G. (2009). The specificity of training prescription and physiological assessment: A review. *Journal of Sports Sciences*, 27(6), 575–589. <https://doi.org/10.1080/02640410902729741>
- Rein, R., & Memmert, D. (2016). Big data and tactical analysis in elite soccer: Future challenges and opportunities for sports science. *SpringerPlus*, 5(1), 1410. <https://doi.org/10.1186/s40064-016-3108-2>
- Riazati, S., Caplan, N., Matabuena, M., & Hayes, P. R. (2020). Fatigue Induced Changes in Muscle Strength and Gait Following Two Different Intensity, Energy Expenditure Matched Runs. *FRONTIERS IN BIOENGINEERING AND BIOTECHNOLOGY*, 8. <https://doi.org/10.3389/fbioe.2020.00360>
- Ribeiro, N., Ugrinowitsch, C., Leme, V., Panissa, G., & Tricoli, V. (2018). *European Journal of Sport Science Acute effects of aerobic exercise performed with different volumes on strength performance and neuromuscular*

- parameters Acute effects of aerobic exercise performed with different volumes on strength performance and neurom. <https://doi.org/10.1080/17461391.2018.1500643>
- Riemer, R., Hsiao-Weckler, E. T., & Zhang, X. (2008). Uncertainties in inverse dynamics solutions: A comprehensive analysis and an application to gait. *Gait & Posture*, 27(4), 578–588. <https://doi.org/10.1016/j.gaitpost.2007.07.012>
- Roberts, T. J., & Belliveau, R. A. (2005). Sources of mechanical power for uphill running in humans. *Journal of Experimental Biology*, 208(10), 1963–1970. <https://doi.org/10.1242/jeb.01555>
- Robusto, C. C. (1957). The cosine-haversine formula. *The American Mathematical Monthly*, 64(1), 38–40. <https://doi.org/10.2307/2309088> M4 - Citavi
- Rodrigo-Carranza, V., González-Mohino, F., Turner, A. P., Rodriguez-Barbero, S., & González-Ravé, J. M. (2021). Using a Portable Near-infrared Spectroscopy Device to Estimate The Second Ventilatory Threshold. *International Journal of Sports Medicine*, 42(10), 905–910. <https://doi.org/10.1055/a-1343-2127>
- Roos, L., Taube, W., Brandt, M., Heyer, L., & Wyss, T. (2013). Monitoring of daily training load and training load responses in endurance sports: What do coaches want? *Schweizerische Zeitschrift Fur Sportmedizin Und Sporttraumatologie*, 61, 30–36.
- Rosenbaum, D., Engl, T., & Nagel, A. (2016). Effects of a fatiguing long-distance run on plantar loading during bare-foot walking and shod running. *FOOTWEAR SCIENCE*, 8(3), 129–137.
- Ross, E., Middleton, N., Shave, R., George, K., & Nowicky, A. (2007). Corticomotor excitability contributes to neuromuscular fatigue following marathon running in man. *Experimental Physiology*, 92, 417–426. <https://doi.org/10.1113/expphysiol.2006.035972>
- Ross, M. D., Langford, B., & Whelan, P. J. (2002). Test-retest reliability of 4 single-leg horizontal hop tests. *Journal of Strength and Conditioning Research*, 16(4), 617–622.
- Rosso, S., Del, Barros, E., Tonello, L., Oliveira-Silva, I., Behm, D. G., Foster, C., & Boulosa, D. A. (2016). Can Pacing Be Regulated by Post-Activation Potentiation? Insights from a Self-Paced 30 km Trial in Half-Marathon Runners. <https://doi.org/10.1371/journal.pone.0150679>
- Rothschild, C. E. (2012). Primitive running: A survey analysis of runners' interest, participation, and implementation. *Journal of Strength and Conditioning Research*, 26(8), 2021–2026. <https://doi.org/10.1519/JSC.0b013e31823a3c54> PM - 21997446
- Rousanoglou, E. N., Noutsos, K., Pappas, A., Bogdanis, G., Vagenas, G., Bayios, I. A., & Boudolos, K. D. (2016). Alterations of Vertical Jump Mechanics after a Half-Marathon Mountain Run-ning Race. In *@Journal of Sports Science and Medicine* (Vol. 15).
- Ruder, M., Jamison, S. T., Tenforde, A., Mulloy, F., & Davis, I. S. (2019). Relationship of Foot Strike Pattern and Landing Impacts during a Marathon. *Medicine and Science in Sports and Exercise*, 51(10), 2073–2079. <https://doi.org/10.1249/MSS.0000000000002032> PM - 31525171
- Ruxton, G. D. (2006). The unequal variance t-test is an underused alternative to Student's t-test and the Mann–Whitney U test. *Behavioral Ecology*, 17(4), 688–690. <https://doi.org/10.1093/beheco/ark016>
- Saha, D., Gard, S., & Fatone, S. (2008). The effect of trunk flexion on able-bodied gait. *Gait and Posture*, 27(4), 653–660. <https://doi.org/10.1016/j.gaitpost.2007.08.009>
- Saltin, B., Larsen, H., Terrados, N., Bangsbo, J., Bak, T., Kim, C. K., Svedenhag, J., & Rolf, C. J. (1995). Aerobic exercise capacity at sea level and at altitude in Kenyan boys, junior and senior runners compared with Scandinavian runners. *Scandinavian Journal of Medicine & Science in Sports*, 5(4), 209–221. <https://doi.org/10.1111/j.1600-0838.1995.tb00037.x>
- Samozino, P., Rabita, G., Dorel, S., Slawinski, J., Peyrot, N., Saez de Villarreal, E., & Morin, J. B. (2016). A simple method for measuring power, force, velocity properties, and mechanical effectiveness in sprint running. *Scand J Med Sci Sports*, 26(6), 648–658. <https://doi.org/10.1111/sms.12490>
- Sánchez-Sánchez, J., Bishop, D., García-Unanue, J., Ubago-Guisado, E., Hernando, E., López-Fernández, J., Colino, E., & Gallardo, L. (2018). Effect of a Repeated Sprint Ability test on the muscle contractile properties in elite futsal players. *Scientific Reports*, 8(1), 1–8. <https://doi.org/10.1038/s41598-018-35345-z>
- Sasaki, S., Nagano, Y., Kaneko, S., Sakurai, T., & Fukubayashi, T. (2011). The relationship between performance and trunk movement during change of direction. *Journal of Sports Science & Medicine*, 10(1), 112.
- Sassi, R. H., Dardouri, W., Yahmed, M. H., Gmada, N., Mahfoudhi, M. E., & Gharbi, Z. (2009). Relative and Absolute Reliability of a Modified Agility T-test and Its Relationship With Vertical Jump and Straight Sprint. *The Journal of Strength & Conditioning Research*, 23(6), 1644–1651. <https://doi.org/10.1519/JSC.0b013e3181b425d2>
- Saunders, P. U., Pyne, D. B., Telford, R. D., & Hawley, J. A. (2004). Factors Affecting Running Economy in Trained Distance Runners. *Sports Medicine*, 34(7), 465–485. <https://doi.org/10.2165/00007256-200434070-00005>
- Schache, A. G., Bennell, K. L., Blanch, P. D., & Wrigley, T. V. (1999). The coordinated movement of the lumbo–pelvic–hip complex during running: A literature review. *Gait & Posture*, 10(1), 30–47. [https://doi.org/10.1016/S0966-6362\(99\)00025-9](https://doi.org/10.1016/S0966-6362(99)00025-9)
- Scheerder, J., Breedveld, K., & Borgers, J. (2015). Who Is Doing a Run with the Running Boom? In J. Scheerder, K. Breedveld, & J. Borgers (Eds.), *Running across Europe: The Rise and Size of One of the Largest Sport Markets* (pp. 1–27). Palgrave Macmillan UK. https://doi.org/10.1057/9781137446374_1

- Schmitz, R. J., Cone, J. C., Copple, T. J., Henson, R. A., & Shultz, S. J. (2014). Lower-extremity biomechanics and maintenance of vertical-jump height during prolonged intermittent exercise. *Journal of Sport Rehabilitation*, 23(4), 319–329. <https://doi.org/10.1123/JSR.2013-0065>
- Schütte, K. H., Maas, E. A., Exadaktylos, V., Berckmans, D., Venter, R. E., & Vanwanseele, B. (2015). Wireless Tri-Axial Trunk Accelerometry Detects Deviations in Dynamic Center of Mass Motion Due to Running-Induced Fatigue. *PLOS ONE*, 10(10), e0141957. <https://doi.org/10.1371/journal.pone.0141957>
- Schütte, K. H., Sackey, S., Venter, R., & Vanwanseele, B. (2018). Energy cost of running instability evaluated with wearable trunk accelerometry. *Journal of Applied Physiology*, 124(2), 462–472. <https://doi.org/10.1152/jappphysiol.00429.2017>
- Seiler, K. S., & Kjerland, G. Ø. (2006). Quantifying training intensity distribution in elite endurance athletes: Is there evidence for an “optimal” distribution? *Scandinavian Journal of Medicine & Science in Sports*, 16(1), 49–56. <https://doi.org/10.1111/j.1600-0838.2004.00418.x>
- Seiler, S. (2011). *A Brief History of Endurance Testing in Athletes*. 48.
- Sekulic, D., Uljevic, O., Peric, M., Spasic, M., & Kondric, M. (2017). Reliability and factorial validity of non-specific and tennis-specific pre-planned agility tests; preliminary analysis. *Journal of Human Kinetics*, 55, 107.
- Semaw, S., Rogers, M. J., Quade, J., Renne, P. R., Butler, R. F., Dominguez-Rodrigo, M., Stout, D., Hart, W. S., Pickering, T., & Simpson, S. W. (2003). 2.6-Million-year-old stone tools and associated bones from OGS-6 and OGS-7, Gona, Afar, Ethiopia. *Journal of Human Evolution*, 45(2), 169–177. [https://doi.org/10.1016/s0047-2484\(03\)00093-9](https://doi.org/10.1016/s0047-2484(03)00093-9)
- Semenick, D. (1990). Tests and Measurements: The T-test. *Strength & Conditioning Journal*, 12(1), 36–37.
- Setuain, I., Lecumberri, P., Ahtiainen, J. P., Mero, A. A., Häkkinen, K., & Izquierdo, M. (2018). Sprint mechanics evaluation using inertial sensor-based technology: A laboratory validation study. *Scandinavian Journal of Medicine & Science in Sports*, 28(2), 463–472. <https://doi.org/10.1111/sms.12946>
- Setuain, I., Martinikorena, J., Gonzalez-Izal, M., Martinez-Ramirez, A., Gómez, M., Alfaro-Adrián, J., & Izquierdo, M. (2016). Vertical jumping biomechanical evaluation through the use of an inertial sensor-based technology. *Journal of Sports Sciences*, 34(9), 843–851. <https://doi.org/10.1080/02640414.2015.1075057>
- Shaffer, S. W., Teyhen, D. S., Lorenson, C. L., Warren, R. L., Koreerat, C. M., Straseske, C. A., & Childs, J. D. (2013). Y-Balance Test: A Reliability Study Involving Multiple Raters. *Military Medicine*, 178(11), 1264–1270. <https://doi.org/10.7205/MILMED-D-13-00222>
- Shao, J. (1993). Linear Model Selection by Cross-validation. *Journal of the American Statistical Association*, 88(422), 486–494. <https://doi.org/10.1080/01621459.1993.10476299>
- Sheerin, K. R., Reid, D., & Besier, T. F. (2019). The measurement of tibial acceleration in runners-A review of the factors that can affect tibial acceleration during running and evidence-based guidelines for its use. *Gait & Posture*, 67, 12–24. <https://doi.org/10.1016/j.gaitpost.2018.09.017>
- Sheppard, J. M., & Young, W. B. (2006). Agility literature review: Classifications, training and testing. *Journal of Sports Sciences*, 24(9), 919–932. <https://doi.org/10.1080/02640410500457109>
- Shimokochi, Y., & Shultz, S. J. (2008). Mechanisms of noncontact anterior cruciate ligament injury. *Journal of Athletic Training*, 43(4), 396–408.
- SILER, W. L., & MARTIN, P. E. (1991). CHANGES IN RUNNING PATTERN DURING A TREADMILL RUN TO VOLITIONAL EXHAUSTION - FAST VERSUS SLOWER RUNNERS. *INTERNATIONAL JOURNAL OF SPORT BIOMECHANICS*, 7(1), 12–28. <https://doi.org/10.1123/ijsb.7.1.12>
- Sinclair, J., Richards, J., Taylor, P. J., Edmundson, C. J., Brooks, D., & Hobbs, S. J. (2013). Three-dimensional kinematic comparison of treadmill and overground running. *Sports Biomechanics*, 12(3), 272–282. <https://doi.org/10.1080/14763141.2012.759614>
- Sinex, J. A., & Chapman, R. F. (2015). Hypoxic training methods for improving endurance exercise performance. *Journal of Sport and Health Science*, 4(4), 325–332. <https://doi.org/10.1016/j.jshs.2015.07.005>
- Skals, S., Jung, M. K., Damsgaard, M., & Andersen, M. S. (2017). Prediction of ground reaction forces and moments during sports-related movements. *Multibody System Dynamics*, 39(3), 175–195. <https://doi.org/10.1007/s11044-016-9537-4>
- Skurowski, P., & Pawlyta, M. (2021). Gap Reconstruction in Optical Motion Capture Sequences Using Neural Networks. *Sensors*, 21(18), 18. <https://doi.org/10.3390/s21186115>
- Slade, P., Kochenderfer, M. J., Delp, S. L., & Collins, S. H. (2021). Sensing leg movement enhances wearable monitoring of energy expenditure. *Nature Communications*, 12(1), 1. <https://doi.org/10.1038/s41467-021-24173-x>
- Slaughter, P. R., & Adamczyk, P. G. (2020). Tracking Quantitative Characteristics of Cutting Maneuvers with Wearable Movement Sensors during Competitive Women’s Ultimate Frisbee Games. *Sensors*, 20(22), 6508.
- Slawinski, J., Demarle, A., Koralsztejn, J.-P., & Billat, V. (2001). Effect of Supra-Lactate Threshold Training on the Relationship between Mechanical Stride Descriptors and Aerobic Energy Cost in Trained Runners. *Archives of Physiology and Biochemistry*, 109(2), 110–116. <https://doi.org/10.1076/apab.109.2.110.4270>
- Slim, K., Nini, E., Forestier, D., Kwiatkowski, F., Panis, Y., & Chipponi, J. (2003a). Methodological index for non-randomized studies (MINORS): Development and validation of a new instrument. *ANZ Journal of Surgery*, 73(9), 712–716. <https://doi.org/10.1046/j.1445-2197.2003.02748.x>

-
- Slim, K., Nini, E., Forestier, D., Kwiatkowski, F., Panis, Y., & Chipponi, J. (2003b). Methodological index for non-randomized studies (MINORS): Development and validation of a new instrument. *ANZ Journal of Surgery*, 73(9), 712–716. <https://doi.org/10.1046/j.1445-2197.2003.02748.x>
- Smith, J. A. H., McKerrow, A. D., & Kohn, T. A. (2016). Metabolic cost of running is greater on a treadmill with a stiffer running platform. *Journal of Sports Sciences*, 35(16), 1–6. <https://doi.org/10.1080/02640414.2016.1225974>
- Soligard, T., Schwellnus, M., Alonso, J.-M., Bahr, R., Clarsen, B., Dijkstra, H. P., Gabbett, T., Gleeson, M., Hägg, M., Hutchinson, M. R., Rensburg, C. J. van, Khan, K. M., Meeusen, R., Orchard, J. W., Pluim, B. M., Raftery, M., Budgett, R., & Engebretsen, L. (2016). How much is too much? (Part 1) International Olympic Committee consensus statement on load in sport and risk of injury. *British Journal of Sports Medicine*, 50(17), 1030–1041. <https://doi.org/10.1136/bjsports-2016-096581>
- Soltani, A., Dejnabadi, H., Savary, M., & Aminian, K. (2020). Real-World Gait Speed Estimation Using Wrist Sensor: A Personalized Approach. *IEEE Journal of Biomedical and Health Informatics*, 24(3), 658–668. <https://doi.org/10.1109/JBHI.2019.2914940>
- Souza, R. B. (2016). An Evidence-Based Videotaped Running Biomechanics Analysis. *Physical Medicine and Rehabilitation Clinics of North America*, 27(1), 217–236. <https://doi.org/10.1016/j.pmr.2015.08.006>
- Sperlich, B., Aminian, K., Düking, P., & Holmberg, H.-C. (2020). Editorial: Wearable Sensor Technology for Monitoring Training Load and Health in the Athletic Population. *Frontiers in Physiology*, 10. <https://www.frontiersin.org/articles/10.3389/fphys.2019.01520>
- Spiteri, T., Cochrane, J. L., Hart, N. H., Haff, G. G., & Nimphius, S. (2013). Effect of strength on plant foot kinetics and kinematics during a change of direction task. *European Journal of Sport Science*, 13(6), 646–652. <https://doi.org/10.1080/17461391.2013.774053>
- Sporis, G., Jukic, I., Milanovic, L., & Vucetic, V. (2010). Reliability and factorial validity of agility tests for soccer players. *The Journal of Strength & Conditioning Research*, 24(3), 679–686.
- Stanton, R., Hayman, M., Humphris, N., Borgelt, H., Fox, J., Del Vecchio, L., & Humphries, B. (2016). Validity of a Smartphone-Based Application for Determining Sprinting Performance. *Journal of Sports Medicine*, 2016, e7476820. <https://doi.org/10.1155/2016/7476820>
- Starkes, J. L., Deakin, J. M., Allard, F., Hodges, N. J., & Hayes, A. (2014). Deliberate practice in sports: What is it anyway? In *The road to excellence* (pp. 81–106). Psychology Press.
- Steib, S., Hentschke, C., Welsch, G., Pfeifer, K., & Zech, A. (2013). Effects of fatiguing treadmill running on sensorimotor control in athletes with and without functional ankle instability. *Clinical Biomechanics*, 28(7), 790–795. <https://doi.org/10.1016/j.clinbiomech.2013.07.009>
- Stetter, B. J., Ringhof, S., Krafft, F. C., Sell, S., & Stein, T. (2019). Estimation of Knee Joint Forces in Sport Movements Using Wearable Sensors and Machine Learning. *Sensors*, 19(17), 17. <https://doi.org/10.3390/s19173690>
- Stewart, P. F., Turner, A. N., & Miller, S. C. (2014). Reliability, factorial validity, and interrelationships of five commonly used change of direction speed tests. *Scandinavian Journal of Medicine & Science in Sports*, 24(3), 500–506.
- Stirling, L. M., von Tschanner, V., Fletcher, J. R., & Nigg, B. M. (2012). Quantification of the manifestations of fatigue during treadmill running. *European Journal of Sport Science*, 12(5), 418–424.
- Strang, A. J., Choi, H. J., & Berg, W. P. (2008). The effect of exhausting aerobic exercise on the timing of anticipatory postural adjustments. *Journal of Sports Medicine and Physical Fitness*, 48(1), 9–16.
- Strohrmann, C., Harms, H., Kappeler-Setz, C., & Tröster, G. (2012). Monitoring kinematic changes with fatigue in running using body-worn sensors. *IEEE Transactions on Information Technology in Biomedicine*, 16(5), 983–990. <https://doi.org/10.1109/TITB.2012.2201950>
- Strohrmann, C., Harms, H., Kappeler-Setz, C., & Troster, G. (2012). Monitoring Kinematic Changes With Fatigue in Running Using Body-Worn Sensors. *IEEE Transactions on Information Technology in Biomedicine*, 16(5), 983–990. <https://doi.org/10.1109/TITB.2012.2201950>
- Strohrmann, C., Harms, H., Tröster, G., Hensler, S., & Müller, R. (2011). Out of the lab and into the woods: Kinematic analysis in running using wearable sensors. *Proceedings of the 13th International Conference on Ubiquitous Computing*, 119–122. <https://doi.org/10.1145/2030112.2030129>
- Suchomel, T. J., Nimphius, S., Bellon, C. R., & Stone, M. H. (2018). The Importance of Muscular Strength: Training Considerations. *Sports Medicine*, 48(4), 765–785. <https://doi.org/10.1007/s40279-018-0862-z>
- Taboga, P., Giovanelli, N., Spinazzè, E., Cuzzolin, F., Fedele, G., Zanuso, S., & Lazzer, S. (2021). Running power: Lab based vs. portable devices measurements and its relationship with aerobic power. *European Journal of Sport Science*, 0(0), 1–14. <https://doi.org/10.1080/17461391.2021.1966104>
- Tabor, P., Iwańska, D., Grabowska, O., Karczewska-Lindinger, M., Popieluch, A., & Mastalerz, A. (2021). Evaluation of selected indices of gait asymmetry for the assessment of running asymmetry. *Gait & Posture*, 86, 1–6. <https://doi.org/10.1016/j.gaitpost.2021.02.019>
- Tan, H., Wilson, A. M., & Lowe, J. (2008). Measurement of stride parameters using a wearable GPS and inertial measurement unit. *Journal of Biomechanics*, 41(7), 1398–1406. <https://doi.org/10.1016/j.jbiomech.2008.02.021>

-
- Taylor, J. L., Amann, M., Duchateau, J., Meeusen, R., & Rice, C. L. (2016). Neural contributions to muscle fatigue: From the brain to the muscle and back again. *Medicine and Science in Sports and Exercise*, 48(11), 2294–2306. <https://doi.org/10.1249/MSS.0000000000000923>
- Taylor, K.-L., Chapman, D. W., Cronin, J. B., Newton, M. J., & Gill, N. (2012). Fatigue monitoring in high performance sport: A survey of current trends. In *J. Aust. Strength Cond* (Vol. 20, Issue 1, pp. 12–23).
- Thiel, D. V., Shepherd, J., Espinosa, H. G., Kenny, M., Fischer, K., Worsey, M., Matsuo, A., & Wada, T. (2018). Predicting Ground Reaction Forces in Sprint Running Using a Shank Mounted Inertial Measurement Unit. *Proceedings*, 2(6), 6. <https://doi.org/10.3390/proceedings2060199>
- Thorpe, R. T., Atkinson, G., Drust, B., & Gregson, W. (2017). Monitoring fatigue status in elite team-sport athletes: Implications for practice. *International Journal of Sports Physiology and Performance*, 12(s2), 27–34. <https://doi.org/10.1123/ijsp.2016-0434>
- Thorstensson, A., & Roberthson, H. (1987). Adaptations to changing speed in human locomotion: Speed of transition between walking and running. *Acta Physiologica Scandinavica*, 131(2), 211–214. <https://doi.org/10.1111/j.1748-1716.1987.tb08228.x>
- Tim Op De Beéck, Wannes Meert, K. S. (2018). Fatigue Prediction in Outdoor Runners Via Machine Learning and Sensor Fusion. *KDD*, 57(5), 1184–1192. [https://doi.org/10.1016/0003-4975\(94\)91354-4](https://doi.org/10.1016/0003-4975(94)91354-4)
- Timmins, R. G., Opar, D. A., Williams, M. D., Schache, A. G., Dear, N. M., & Shield, A. J. (2014). Reduced biceps femoris myoelectrical activity influences eccentric knee flexor weakness after repeat sprint running. *Scandinavian Journal of Medicine and Science in Sports*, 24(4), e299–e305. <https://doi.org/10.1111/sms.12171>
- Tomczak, M., & Tomczak, E. (2014). *The need to report effect size estimates revisited. An overview of some recommended measures of effect size*. 21, 19–25.
- Vago, P., Mercier, J., Ramonatxo, M., & Prefaut, C. (1987). Is Ventilatory Anaerobic Threshold a Good Index of Endurance Capacity? *International Journal of Sports Medicine*, 08(3), 190–195. <https://doi.org/10.1055/s-2008-1025654>
- van der Kruk, E., van der Helm, F. C. T., Veeger, H. E. J., & Schwab, A. L. (2018). Power in sports: A literature review on the application, assumptions, and terminology of mechanical power in sport research. *Journal of Biomechanics*, 79, 1–14. <https://doi.org/10.1016/j.jbiomech.2018.08.031>
- Van Hooren, B., Fuller, J. T., Buckley, J. D., Miller, J. R., Sewell, K., Rao, G., Barton, C., Bishop, C., & Willy, R. W. (2020). Is Motorized Treadmill Running Biomechanically Comparable to Overground Running? A Systematic Review and Meta-Analysis of Cross-Over Studies. *Sports Medicine*, 50(4), 785–813. <https://doi.org/10.1007/s40279-019-01237-z>
- Van Hulle, R., Schwartz, C., Denoël, V., Croisier, J.-L., Forthomme, B., & Brûls, O. (2020). A foot/ground contact model for biomechanical inverse dynamics analysis. *Journal of Biomechanics*, 100, 109412. <https://doi.org/10.1016/j.jbiomech.2019.109412>
- van Mastrigt, N. M., Celie, K., Mieremet, A. L., Ruifrok, A. C. C., & Geradts, Z. (2018). Critical review of the use and scientific basis of forensic gait analysis. *Forensic Sciences Research*, 3(3), 183–193. <https://doi.org/10.1080/20961790.2018.1503579>
- van Mechelen, W., Hlobil, H., Kemper, H. C., Voorn, W. J., & de Jongh, H. R. (1993). Prevention of running injuries by warm-up, cool-down, and stretching exercises. *The American Journal of Sports Medicine*, 21(5), 711–719. <https://doi.org/10.1177/036354659302100513>
- van Oeveren, B. T., de Ruiter, C. J., Beek, P. J., & van Dieën, J. H. (2021). The biomechanics of running and running styles: A synthesis. *Sports Biomechanics*, 0(0), 1–39. <https://doi.org/10.1080/14763141.2021.1873411>
- Vanrenterghem, J., Nedergaard, N. J., Robinson, M. A., & Drust, B. (2017). Training Load Monitoring in Team Sports: A Novel Framework Separating Physiological and Biomechanical Load-Adaptation Pathways. *Sports Medicine*, 47(11), 2135–2142. <https://doi.org/10.1007/s40279-017-0714-2>
- Vargas, N. T., & Marino, F. (2014). A neuroinflammatory model for acute fatigue during exercise. *Sports Medicine*, 44(11), 1479–1487. <https://doi.org/10.1007/s40279-014-0232-4> PM - 25164464
- Venhorst, A., Micklewright, D., & Noakes, T. D. (2018). Perceived Fatigability: Utility of a Three-Dimensional Dynamical Systems Framework to Better Understand the Psychophysiological Regulation of Goal-Directed Exercise Behaviour. *Sports Medicine*, 48(11), 2479–2495. <https://doi.org/10.1007/s40279-018-0986-1/FIGURES/2>
- Vergara, J. R., & Estévez, P. A. (2014). A review of feature selection methods based on mutual information. *Neural Computing and Applications*, 24(1), 175–186. <https://doi.org/10.1007/s00521-013-1368-0>
- Verkerke, G. J., Ament, W., Wierenga, R., & Rakhorst, G. (1998). Measuring changes in step parameters during an exhausting running exercise. *Gait and Posture*, 8(1), 37–42. [https://doi.org/10.1016/S0966-6362\(98\)00017-4](https://doi.org/10.1016/S0966-6362(98)00017-4)
- Vernillo, G., Gandolini, M., Edwards, W. B., Morin, J.-B., Samozino, P., Horvais, N., & Millet, G. Y. (2017). Biomechanics and Physiology of Uphill and Downhill Running. *Sports Medicine*, 47(4), 615–629. <https://doi.org/10.1007/s40279-016-0605-y>
- Verschueren, J., Tassignon, B., Pauw, K., Proost, M., Teugels, A., van Cutsem, J., Roelands, B., Verhagen, E., & Meeusen, R. (2020). Does Acute Fatigue Negatively Affect Intrinsic Risk Factors of the Lower Extremity Injury Risk Profile? A Systematic and Critical Review. *Sports Medicine*, 50(4), 767–784. <https://doi.org/10.1007/s40279-019-01235-1> PM - 31782066

- Vigotsky, A. D., Zelik, K. E., Lake, J., & Hinrichs, R. N. (2019). Mechanical misconceptions: Have we lost the “mechanics” in “sports biomechanics”? *Journal of Biomechanics*, 93, 1–5. <https://doi.org/10.1016/j.jbiomech.2019.07.005>
- Vogt, M. (2017). *Swiss-Ski Power Test 2013*.
- Voloshin, A. S., Mizrahi, J., Verbitsky, O., & Isakov, E. (1998). Dynamic loading on the human musculoskeletal system effect of fatigue. *Clinical Biomechanics*, 13(7), 515–520. [https://doi.org/10.1016/S0268-0033\(98\)00030-8](https://doi.org/10.1016/S0268-0033(98)00030-8)
- Warden, S. J., Davis, I. S., & Fredericson, M. (2014). Management and prevention of bone stress injuries in long-distance runners. *Journal of Orthopaedic and Sports Physical Therapy*, 44(10), 749–765. <https://doi.org/10.2519/jospt.2014.5334>
- Wardoyo, S., Hutajulu, P. T., & Togibasa, O. (2016). A Development of Force Plate for Biomechanics Analysis of Standing and Walking. *Journal of Physics: Conference Series*, 739, 012118. <https://doi.org/10.1088/1742-6596/739/1/012118>
- Weinberg, R. S., & Comar, W. (1994). The Effectiveness of Psychological Interventions in Competitive Sport. *Sports Medicine*, 18(6), 406–418. <https://doi.org/10.2165/00007256-199418060-00005>
- Weist, R., Eils, E., & Rosenbaum, D. (2004). The influence of muscle fatigue on electromyogram and plantar pressure patterns as an explanation for the incidence of metatarsal stress fractures. *The American Journal of Sports Medicine*, 32(8), 1893–1898.
- Welch, N., Richter, C., Franklyn-Miller, A., & Moran, K. (2021). Principal component analysis of the biomechanical factors associated with performance during cutting. *The Journal of Strength & Conditioning Research*, 35(6), 1715–1723.
- Weyand, P. G., Sternlight, D. B., Bellizzi, M. J., & Wright, S. (2000). Faster top running speeds are achieved with greater ground forces not more rapid leg movements. *Journal of Applied Physiology*, 89(5), 1991–1999. <https://doi.org/10.1152/jappl.2000.89.5.1991>
- Wickler, S. J., Hoyt, D. F., Cogger, E. A., & Hirschbein, M. H. (2000). Preferred speed and cost of transport: The effect of incline. *Journal of Experimental Biology*, 203(14), 2195–2200. <https://doi.org/10.1242/jeb.203.14.2195>
- Willems, T. M., De Ridder, R., & Roosen, P. (2012). The effect of a long-distance run on plantar pressure distribution during running. *Gait and Posture*, 35(3), 405–409. <https://doi.org/10.1016/j.gaitpost.2011.10.362>
- Williams, K. R. (1985). Biomechanics of Running. *Exercise and Sport Sciences Reviews*, 13(1), 389–442.
- Williams, K. R., & Cavanagh, P. R. (1987). Relationship between distance running mechanics, running economy, and performance. *Journal of Applied Physiology*, 63(3), 1236–1245. <https://doi.org/10.1152/jappl.1987.63.3.1236>
- Willson, J. D., & Kernozek, T. W. (1999). Plantar loading and cadence alterations with fatigue. *Medicine and Science in Sports and Exercise*, 31(12), 1828–1833. <https://doi.org/10.1097/00005768-199912000-00020>
- Willy, R. W. (2018). Innovations and pitfalls in the use of wearable devices in the prevention and rehabilitation of running related injuries. *Physical Therapy in Sport*, 29, 26–33. <https://doi.org/10.1016/j.ptsp.2017.10.003>
- Willy, R. W., Manal, K. T., Witvrouw, E. E., & Davis, I. S. (2012). Are mechanics different between male and female runners with patellofemoral pain? *Medicine and Science in Sports and Exercise*, 44(11), 2165–2171. <https://doi.org/10.1249/MSS.0b013e3182629215>
- Winter, E. M., Abt, G., Brookes, F. B. C., Challis, J. H., Fowler, N. E., Knudson, D. V., Knuttgen, H. G., Kraemer, W. J., Lane, A. M., Mechelen, W. van, Morton, R. H., Newton, R. U., Williams, C., & Yeadon, M. R. (2016). Misuse of “Power” and Other Mechanical Terms in Sport and Exercise Science Research. *The Journal of Strength & Conditioning Research*, 30(1), 292–300. <https://doi.org/10.1519/JSC.0000000000001101>
- Winter, S. C. (2018). Centre of Mass Acceleration-Derived Variables Detects Differences between Runners of Different Abilities and Fatigue-Related Changes during a Long Distance Over ground Run. *Journal of Physical Fitness, Medicine & Treatment in Sports*, 4(2). <https://doi.org/10.19080/JPFMTS.2018.04.555632>
- Winter, S., Gordon, S., & Watt, K. (2017). Effects of fatigue on kinematics and kinetics during overground running: A systematic review. *The Journal of Sports Medicine and Physical Fitness*, 57(6), 887–899. <https://doi.org/10.23736/S0022-4707.16.06339-8>
- Wolpern, A. E., Burgos, D. J., Janot, J. M., & Dalleck, L. C. (2015). Is a threshold-based model a superior method to the relative percent concept for establishing individual exercise intensity? A randomized controlled trial. *BMC Sports Science, Medicine and Rehabilitation*, 7(1), 16. <https://doi.org/10.1186/s13102-015-0011-z>
- Wouda, F. J., Giuberti, M., Bellusci, G., Maartens, E., Reenalda, J., van Beijnum, B.-J. F., & Veltink, P. H. (2018). Estimation of Vertical Ground Reaction Forces and Sagittal Knee Kinematics During Running Using Three Inertial Sensors. *Frontiers in Physiology*, 9. <https://www.frontiersin.org/article/10.3389/fphys.2018.00218>
- Wrangham, R. W., Jones, J. H., Laden, G., Pilbeam, D., & Conklin-Brittain, N. (1999). The Raw and the Stolen: Cooking and the Ecology of Human. *Current Anthropology*, 40(5), 567–594. <https://doi.org/10.1086/300083>
- Wu, W.-L., Chang, J.-J., Wu, J.-H., Guo, L.-Y., & Lin, H.-T. (2008). Emg and Plantar Pressure Patterns After Prolonged Running. *Biomedical Engineering: Applications, Basis and Communications*, 19(06), 383–388. <https://doi.org/10.4015/s1016237207000483>
- Wundersitz, D. W., Netto, K. J., Aisbett, B., & Gastin, P. B. (2013). Validity of an upper-body-mounted accelerometer to measure peak vertical and resultant force during running and change-of-direction tasks. *Sports Biomechanics*, 12(4), 403–412.

-
- Yang, S., Mohr, C., & Li, Q. (2011). Ambulatory running speed estimation using an inertial sensor. *Gait & Posture*, 34(4), 462–466. <https://doi.org/10.1016/j.gaitpost.2011.06.019>
- Ye, H., Dong, K., & Gu, T. (2018). HiMeter: Telling You the Height Rather than the Altitude. *Sensors (Basel, Switzerland)*, 18(6), 1712. <https://doi.org/10.3390/s18061712>
- Young, W. B., Dawson, B., & Henry, G. J. (2015). Agility and Change-of-Direction Speed are Independent Skills: Implications for Training for Agility in Invasion Sports. *International Journal of Sports Science & Coaching*, 10(1), 159–169. <https://doi.org/10.1260/1747-9541.10.1.159>
- Yu, H., & Wilamowski, B. M. (2011). Levenberg–Marquardt Training. In *Intelligent Systems*. CRC Press.
- Yu, P., Gong, Z., Meng, Y., Baker, J. S., Istvan, B., Gu, Y., István, B., & Gu, Y. (2020). The Acute Influence of Running-Induced Fatigue on the Performance and Biomechanics of a Countermovement Jump. *APPLIED SCIENCES-BASEL*, 10(12), 1–13. <https://doi.org/10.3390/app10124319>
- Yu, P., Liang, M., Fekete, G. G., Baker, J. S., & Gu, Y. (2021). Effect of running-induced fatigue on lower limb mechanics in novice runners. *TECHNOLOGY AND HEALTH CARE*, 29(2), 231–242. <https://doi.org/10.3233/THC-202195>
- Zago, M., Sforza, C., Dolci, C., Tarabini, M., & Galli, M. (2019). Use of machine learning and wearable sensors to predict energetics and kinematics of cutting maneuvers. *Sensors*, 19(14), 3094.
- Zandbergen, M. A., Reenalda, J., van Middelaar, R. P., Ferla, R. I., Buurke, J. H., & Veltink, P. H. (2022). Drift-Free 3D Orientation and Displacement Estimation for Quasi-Cyclical Movements Using One Inertial Measurement Unit: Application to Running. *Sensors*, 22(3), 3. <https://doi.org/10.3390/s22030956>
- Zeni, J. A., Richards, J. G., & Higginson, J. S. (2008). Two simple methods for determining gait events during treadmill and overground walking using kinematic data. *Gait & Posture*, 27(4), 710–714. <https://doi.org/10.1016/j.gaitpost.2007.07.007>
- Zhang, J. H., Chan, Z. Y. S., Lau, F. O. Y., Huang, M., Wang, A. C., Wang, S., Au, I. P. H., Wang, S., Lam, B. M. F., An, W. W., & Cheung, R. T. H. (2021). How do training experience and geographical origin of a runner affect running biomechanics? *Gait & Posture*, 84, 209–214. <https://doi.org/10.1016/j.gaitpost.2020.12.003>
- Zihajehzadeh, S., Loh, D., Lee, T. J., Hoskinson, R., & Park, E. J. (2015). A cascaded Kalman filter-based GPS/MEMS-IMU integration for sports applications. *Measurement*, 73, 200–210. <https://doi.org/10.1016/j.measurement.2015.05.023>
- Zou, H., & Hastie, T. (2005). Regularization and variable selection via the elastic net. *Journal of the Royal Statistical Society: Series B (Statistical Methodology)*, 67(2), 301–320. <https://doi.org/10.1111/j.1467-9868.2005.00503.x>

Salil Apte

☎ +41 789067459 | ✉ sal1l@protonmail.com | 🏠 22, Rue des Terreaux, Lausanne 1003 CH | 🌐 sal1l

Education

Doctoral candidate at EPFL

EDRS - ROBOTICS, CONTROL, AND INTELLIGENT SYSTEMS

Topics: sensor fusion, body motion tracking, machine learning, wearable sensors, digital health

Lausanne, Switzerland

Aug 2018 – ongoing

Master of Science (cum laude, hons.) at TU Delft

MECHANICAL ENGINEERING WITH BIOMECHANICAL DESIGN TRACK & BIOBOTICS SPECIALIZATION

Topics: gait analysis, dynamical simulations, robot-assisted rehabilitation, compliant actuation

Delft, Netherlands

Sept 2015 – Nov 2017

Bachelor of Technology (hons.) at IIT Kharagpur

MECHANICAL ENGINEERING

Topics: mechanical design & prototyping, CAD/FEA, design optimization, system integration

Kharagpur, India

Jul 2009 – Jul 2013

Professional Experience

Doctoral assistant & EPFLinnovators fellow | LMAM, EPFL

Aug 2018 – Ongoing | Lausanne, CH

- Aim: Measurement of running biomechanics and performance using wearable sensors to personalize training and reduce injuries
- Competence with data pipelines: development of protocols to collect high quality real-world data, design of algorithms for movement analysis, validation using statistical methods, performance modelling using supervised or unsupervised learning, and dissemination
- Coordination of an interdisciplinary collaboration across clinicians, scientists, athletes, and coaches
- Teaching assistant for master's and doctoral courses, and mentoring of 1 master project and 4 semester project students
- Training in business development, policymaking, and communication as a part of the industry-oriented EPFLinnovators fellowship

Algorithm researcher | Gaitup S.A.

Jan 2019 – June 22 | Lausanne, CH

- 6 months secondment at Gaitup S.A. as a part of the EPFLinnovators fellowship
- Interfacing with coaches and elite athletes to conduct customer needs analysis for wearable motion tracking solutions
- Algorithm development based on sensor fusion and machine learning for in-field measurement of sprint velocity and running power
- Filed an international patent (n° PCT/IB2021/054045) for the speed measurement algorithm along with the EPFL TTO

Research engineer | Delft Biorobotics Lab, TU Delft

Jan 2018 – Sept 2021 | Delft, NL

- Developed an user interface to enable experiment design for the RYSEN body weight support (BWS) system
- Implemented and tested BWS strategies using the RYSEN device and experimentally assessed walking of healthy people and patients with a gait analysis system comprising of motion capture cameras, force plates, and eletromyography sensors
- Managed a collaboration of clinicians, neuroscientists, and roboticists, and published in the prestigious Science Robotics journal ([link](#))

Biomechanical Researcher | Motek Medical BV

Aug – Oct 2016 | Amsterdam, NL

- Developed a proof-of-concept model of a spring-based body weight support system for over-ground rehabilitation
- Designed a motion-capture-based gait analysis experiment to investigate the effects of this device on human locomotion

Researcher | Dynamics & Control Lab, SUTD-MIT IDC

Nov 2014 – June 2015 | Singapore

- Conceptualized and designed a lightweight compliant actuator for energy efficient impedance modulation
- Designed an EMG-based experiment to test the efficacy of the actuator in a human-machine cooperation task

Design engineer | Future Factory LLP

Jan – May 2014 | Mumbai, India

- Co-Developed a sound-tube of a hearing aid device for a Fortune 500 firm to achieve a 50% reduction in the necessary inventory
- Core responsibilities included technology validation and prototype development for mechanisms and medical devices

System engineer | Energo Engineering Projects Ltd

Aug – Dec 2013 | Delhi, India

- Control and operation of the Ash Handling System for the commissioning of a 660 MW thermal power plant unit at Kawai, Rajasthan
- Managed a team of 15 site supervisors, mechanics, and electricians for site inspection and troubleshooting

Research intern | LBNL, UC Berkeley

May – July 2012 | Berkeley, USA

- Developed the first TEM-based biomechanically functional 3D graphical model of Arabidopsis plant cell wall in Solidworks
- Introduced the concepts of mechanical design to 20+ researchers from bioimaging and microbiology background

Skills

- **Softwares:** Matlab, Python, Simulink, OpenSim, Solidworks, Ansys APDL, V-REP
- **Prototyping Tools:** Arduino, 3D Printing, Rapid Prototyping, Wire EDM, Lathe, Milling, CMM
- **Publishing softwares:** Microsoft Office, Adobe Photoshop & Illustrator, LaTeX
- **Languages:** English (fluent), Marathi (mother tongue), Hindi (fluent), French (A1)

Publications

JOURNAL ARTICLES

- **Apte, S.**, Troxler, S., Besson, C., Gremeaux, V., & Aminian, K. Augmented Cooper test: biomechanical contributions to endurance performance. *Frontiers in Sports and Active Living*, 337.
- Prigent, G.[†], **Apte, S.[†]**, Paraschiv-Ionescu, A., Besson, C., Gremeaux, V., & Aminian, K. (2022). Concurrent Evolution of Biomechanical and Physiological Parameters With Running-Induced Acute Fatigue. *Frontiers in Physiology*, 74.
- Plooi, M.[†], **Apte, S.[†]**, Keller, U., Baines, P., Sterke, B., Asboth, L., ... & Vallery, H. (2021). Neglected physical human-robot interaction may explain variable outcomes in gait neurorehabilitation research. *Science Robotics*, 6(58), eabf1888.
- **Apte, S.[†]**, Prigent, G.[†], Stöggel, T., Martínez, A., Snyder, C., Gremeaux-Bader, V., & Aminian, K. (2021). Biomechanical response of the lower extremity to running-induced acute fatigue: a systematic review. *Frontiers in physiology*, 1076.
- **Apte, S.**, Plooi, M., & Vallery, H. (2020). Simulation of human gait with body weight support: benchmarking models and unloading strategies. *Journal of NeuroEngineering and Rehabilitation*, 17(1), 1-16.
- **Apte, S.**, Meyer, F., Gremeaux, V., Dadashi, F., & Aminian, K. (2020). A sensor fusion approach to the estimation of instantaneous velocity using single wearable sensor during sprint. *Frontiers in Bioengineering and Biotechnology*, 8, 838.
- Braun, D. J., Chalvet, V., Chong, T. H., **Apte, S.**, & Hogan, N. (2019). Variable stiffness spring actuators for low-energy-cost human augmentation. *IEEE Transactions on Robotics*, 35(6), 1435-1449.
- **Apte, S.**, Plooi, M., & Vallery, H. (2018). Influence of body weight unloading on human gait characteristics: a systematic review. *Journal of neuroengineering and rehabilitation*, 15(1), 1-18.
- Sarkar, P., Kowalczyk, M., **Apte, S.**, Yap, E. G., Das, J., Adams, P. D., ... & Auer, M. (2018). Cryo-electron tomography 3D structure and nanoscale model of Arabidopsis thaliana cell wall. *bioRxiv*, 492140.

Projects

Start-up training: Business Concept | Innosuisse

Sept 2020 – Jan 2021

- Conducted market analysis to understand customer needs and created a value proposition canvas
- Undertook training in financial planning, funding instruments, and designed a business plan
- Created and presented an award-winning business pitch to independent investors and coaches from Innosuisse

Master's thesis on neurorehabilitation | Advisor: Prof. Heike Vallery

Jan – Nov 2017

- Undertook a systematic review and meta-analysis of the experiments on walking using body weight support (BWS) systems
- Conducted dynamical modelling and simulation of human locomotion under unloading forces using Matlab/Simulink
- Bench-marked gait models for their use in BWS simulations and compared BWS strategies based on their influence on gait models

Bachelor's thesis on electric vehicles | Advisor: Prof. C. S. Kumar

2013

- Development of electric vehicle for testing vehicle-control scheme
- Designed the wheel assembly with the aim of reducing wheel scrub radius and optimizing weight
- Designed and implemented a steering system for improving the neutral steer response

Formula Student racing team, IIT Kharagpur

Dec. 2009 – Apr. 2013

- Designed and fabricated the throttle assembly and the entire brake system including a custom-made bias bar
- Designed a unique adjustable differential mounting system which compensated for the chain elongation, leading to a combined weight reduction of 39% and a 10% higher factor of safety over previous design
- Identified the opportunities and proposed changes in the team structure, documentation, and information flow; following year, the team was nominated among the final 6 (out of 105 participants) for the Airbus Teamwork Award at the Formula Student event

Volunteer positions

Formula Student racing team, IIT Kharagpur

Aug 2010 – Apr 2013

- **Design team head:** Led a team of four students to strategize and develop the branding campaign for the 2012 Formula Student Competition and public displays for the car. Conceptualized the website for the team.
- **Transmission team lead:** Led a team of five students for the design and manufacturing of transmission system

Non-technical domains

July 2012 – ongoing

- **Fundraising and Communication, Humane Warriors:** Raised more than 100k CHF through crowdfunding campaigns and grant applications for providing access to education and Covid relief in India
- **Treasurer, VOX Delft:** VOX is a student organization that facilitates and promotes discussions about society, philosophy and culture
- **Captain, Quiz Team, R.P. Hall of Residence:** Led a team of 4 in the Technology General Championship from the year 2012 to 2014 which won an unprecedented 2 silver medals and 1 gold medal at the championships

Honours

- **Winner, Innosuisse Business Concept course:** As a member of the project Smart Helmet, now Bearmind
- **EPFLinnovators fellowship:** Among the 36 fellows to be selected from over 1800 applicants
- **UC Berkeley - IIT Kharagpur fellowship:** Among the 5 students selected from over 1000 applicants
- **All India Rank 939 in IIT-JEE 2009:** Achieved a 99.8 percentile among 500000 applicants
- **Nationwide top 1%:** Indian National Chemistry Olympiad, Indian National Astronomy Olympiad
- **Scholarship recipient:** National Talent Search Scholarship (NTSE)